Physiological function of phosphatidylethanolamine *N*-methyltransferase

by

Xia Gao

A thesis submitted in partial fulfillment of the requirements for the degree of

Doctor of Philosophy

Department of Biochemistry
University of Alberta

Abstract

Phosphatidylethanolamine *N*-methyltransferase (PEMT), a liver enriched enzyme, is responsible for approximately one third of hepatic phosphatidylcholine (PC) biosynthesis via three sequential methylations of phosphatidylethanolamine (PE). PEMT is also expressed in white adipose tissue (WAT). When fed a high-fat diet (HF), *Pemt*$^{-/-}$mice are protected from diet-induced obesity (DIO), but develop steatohepatitis. This thesis is endeavored to seek the underlying mechanisms for the resistance to DIO and the development of steatohepatitis in HF-fed *Pemt*$^{-/-}$ mice, mainly focusing on the liver, WAT and brown adipose tissue (BAT).

The vagus nerve relays signals between the liver and brain, regulating energy metabolism. Thus, a possible role of the hepatic branch of the vagus nerve in the resistance to DIO and the development of steatohepatitis in *Pemt*$^{-/-}$ mice was first explored. *Pemt*$^{-/-}$ and *Pemt*$^{+/+}$ mice were subjected to hepatic vagotomy (HV), compared with sham operation; or subjected to capsaicin treatment, which selectively disrupts the afferent nerve, versus vehicle-treated mice. After surgery, mice were fed the HF for 10 weeks. HV abolished the protection against DIO and prevented the development of steatohepatitis in *Pemt*$^{-/-}$ mice. However, disruption of the hepatic afferent vagus nerve by capsaicin failed to reverse either the protection against DIO or the development of HF-induced steatohepatitis in *Pemt*$^{-/-}$ mice. Thus, neuronal signals, relayed particularly via the efferent

vagus nerve, contribute to the development of steatohepatitis and protection against obesity in HF-fed *Pemt*$^{-/-}$ mice.

Endoplasmic reticulum (ER) stress is associated with the development and progression of steatohepatitis. PEMT is located on the ER and mitochondrial-associated membranes. Thus, we proposed that PEMT deficiency might cause aberrant composition of PC and PE in the ER and consequently ER stress, which sensitized mice to HF-induced steatohepatitis. Indeed, chow-fed *Pemt*$^{-/-}$ mice had reduced PC and increased PE in hepatic ER fractions. Chow-fed *Pemt*$^{-/-}$ mice presented ER stress in the livers with higher expression of CHOP and BIP compared to *Pemt*$^{+/+}$ mice, without activating the unfolded protein response (UPR). HF led to more severe ER stress and activated UPR including all three branches PERK-eIF2α, IRE1α-XBP1s and ATF6, in the livers from *Pemt*$^{-/-}$ mice than *Pemt*$^{+/+}$ mice. Similarly, McArdle cells without PEMT activity exhibited ER stress and activated UPR compared with McArdle cells expressing PEMT. Furthermore, the chemical chaperone 4-phenyl butyric acid (PBA) reversed the activation of UPR and ER stress caused by PEMT deficiency in McArdle cells. PBA had a minor impact on hepatic ER stress or the development of steatohepatisis in HF-fed *Pemt*$^{-/-}$ mice. However, PBA decreased triglyceride accumulation and alleviated apoptotic signaling in the livers from these mice. Together, PEMT deficiency leads to hepatic ER stress and sensitizes mice to HF-induced steatohepatitis.

The contribution of WAT and BAT to the protection against DIO in *Pemt*$^{-/-}$ mice has also been studied. PEMT deficiency had no effect on adipocyte differentiation or lipolysis in WAT, but resulted in a decreased lipogenesis in WAT, which at least partially contributes to the lower weight gain in HF-fed *Pemt*$^{-/-}$ mice. Contrary to WAT, BAT is a highly oxidative tissue, responsible for non-shivering thermogenesis. In BAT, the protein and enzyme activity of PEMT was not detectable, compared to that in the liver or WAT. The capability for thermogenesis in mice was evaluated by cold exposure at 4˚C. When fed standard chow diet, both *Pemt*$^{+/+}$ and *Pemt*$^{-/-}$ mice were able to maintain their body temperature above 33˚C for up to 4 h upon cold exposure. However, after fed the HF diet for 2 weeks, *Pemt*$^{-/-}$ mice developed hypothermia, whereas *Pemt*$^{+/+}$ mice maintained their body temperature throughout the 4 h cold challenge. However, thermogenic capacity in BAT remained intact in HF-fed *Pemt*$^{-/-}$ mice. Dietary choline supplementation prevented the cold-induced hypothermia in *Pemt*$^{-/-}$ mice, coinciding with restoration of lower plasma glucose and increased expression of hepatic gluconeogenesis-related genes. Thus, cold-induced hypothermia in HF-fed *Pemt*$^{-/-}$ mice is likely due to an insufficient glucose supply caused by impaired hepatic gluconeogenesis, highlighting the importance of glucose as a substrate for thermogenesis.

Preface

Contents in Chapter 2 of this thesis were published in *Journal of Hepatology* in 2015, entitled “Vagus nerve contributes to the development of steatohepatitis and obesity in phosphatidylethanolamine *N*-methyltransferase deficient mice”. [*Journal of Hepatology*. 62 (2015) 913-920]

Contents in Chapter 4 of this thesis have been accepted by *Biochimica et Biophysica Acta (BBA)-molecular and cell biology of lipid* in 2015, entitled “Decreased lipogenesis in white adipose tissue contributes to the resistance to high fat diet-induced obesity in phosphatidylethanolamine N-methyltransferase-deficient mice”. [*Biochimica et Biophysica Acta (BBA)-molecular and cell biology of lipids*. 1851 (2015) 152–162]

All procedures regarding animal handling, feeding and surgeries were approved by the University of Alberta’s Institutional Animal Care Committee in accordance with guidelines of the Canadian Council on Animal Care.

Dedication

This thesis is dedicated to my beloved parents who I missed so much, to my grandparents and to my little brother.

Acknowledgements

First, I want to express my sincere gratitude and appreciation to my supervisor, Dr. Dennis E Vance, for kindly recruiting me into his laboratory, for his guidance, advice, encouragement and support throughout my graduate studies, and for providing such a positive and pleasant training environment. I would like to thank my supervisor, Dr. René L. Jacobs for his support, kindness and advice. I would also like to show my great gratitude to Dr. Carlos Fernandez-Patron for serving in my supervisory committee, for his brilliant suggestions and great support on my project throughout my training. Moreover, I would like to extend my gratitude to Dr. Joanne Lemieux in Department of Biochemistry for being the examiners of my candidacy exam and my thesis defense, and Dr. Andrew Mason in Department of Medicine for being the examiners of my candidacy exam. I thank Dr. Khosrow Adeli from the University of Toronto for serving as the external examiner for my thesis defense.

Second, I am thankful to the current lab members, Dr. Jelske N. van der Veen, Susanne Lingrell and Randal Nelson, for the daily discussion and technical support. I would also like to thank the past lab member Dr. Martin Hermansson for being such a nice friend and help with my writing and collaboration on my project, and other former lab members Guergana Tasseva and Zhuo (Bill) Li. Special acknowledgement should be delivered to Dr. Jean Vance for her comments and support in my studies. I am also

in great debt to all the other members of Group on the Molecular and Cell Biology of Lipids (MCBL) for the exciting discussion, technical support for my research in weekly journal club and advice on my presenting skills.

Third, special acknowledgements should be extended to the following persons for their contribution and cooperation throughout my graduate study. I am very grateful to Dr. Linfu Zhu for his talented surgical operation on mice for the study of the hepatic branch of the vagus nerve; pathologist Drs. Todd Chaba and Aducio Thiesen for scoring the histological slides of mouse livers; Dr. Xuejun Sun and his lab member Ms. Pinzhang Gao for their technical support on electron microscopy analysis of the vagus nerve; Marta Ordoñez and Antonio Gomez-Muñoz from University of the Basque Country, Spain for the collaboration on the analysis of cytokines and chemokines in the liver and white adipose tissue for chapter 2 and 4; Dr. Howard Young and his lab members Dr. Catharine A. Trieber for their technical support on the ER project. Regarding to the studies on adipose tissue, I need to extend my gratitude to Martin Hermansson for analyzing lipid species in adipose tissue using mass spectrometry, Drs. Carlos Fernandez-Patron, Gary D. Lopaschuk and their lab members for their collaboration and technical support on the analysis and interpretation of data on blood pressure and cardiac function; Ms Donna Beker for her analysis of cardiac function by echocardiography.

Fourth, I am very thankful to the following awards and funding agencies, which have graciously supported my graduate studies here: the

studentship from Alberta Innovates-Health Solutions, the Motyl Graduate Scholarship in Cardiac Sciences, the Mazankowski Alberta Heart Institute Graduate Studentship, 75th Anniversary Scholarship, Medical Sciences Graduate Program Graduate Research Assistantship and the FoMD/AHS Graduate Student Recruitment Studentship.

Finally, I want to thank my teachers at senior high school, who are also my life-long friends, Yalin Sun, Zhongming Wang and Tingyong Ma. Without your guidance at high school, I could never make to this far. I am also grateful to other family members and family friends for being there and helping my brother and myself getting through the tough time in our lives.

Table of Contents

Chapter 1: Introduction

Lists of Tables

Lists of Figures

List of Abbreviations

ACC	acetyl-CoA carboxylase
ACLY	ATP citrate lyase
AdoHcy	*S*-adenosylhomocysterine
AdoMet	*S*-adenosylmethionine
ATF	activating transcription factor
ATG7	autophagy-related protein 7
ATGL	adipose triglyceride lipase
ATP	adenosine triphosphate
BAT	brown adipose tissue
BiP	glucose-regulated protein 78
BMP	bone morphogenetic protein
cAMP	cyclic AMP
CD	cluster of differentiation
CDD	choline-deficient diet
CDP	cytidine diphosphate
CHOP	C/EBP–homologous protein
CRE	cAMP response elements
CREB	CRE binding protein
CT	CTP:phosphocholine cytidylyltransferase
CTP	cytidine triphosphate
C/EBP	CCAAT/enhancer-binding protein

DG	diacylglycerol
DGAT	acyl CoA:diacylglycerol acyltransferase
DIO	diet induced obesity
DNL	*de novo* lipogenesis
eIF2α	the eukaryotic initiation factor 2α
ER	endoplasmic reticulum
ERAD	ER-associated protein degradation
FABP4	fatty acid binding protein 4
FAO	fatty acid oxidation
FAS	fatty acid synthase
GAPDH	glyceraldehyde 3-phosphate dehydrogenase
GPAT	glycerol-3-phosphate acyltransferase
Hcy	Homocysteine
HDL	high density lipoprotein
HF	high-fat
HFCS	HF choline-supplementation
HSL	hormone-sensitive lipase
HV	hepatic vagotomy
IL	interleukin
IR	insulin resistance
IRE1	inositol-requiring enzyme-1
LC3	light chain protein 3
LDL	low density lipoprotein

lyso-PC	lysophosphatidylcholine
JNK	c-Jun N-terminal kinase
MCP	monocyte chemoattractant protein
MCD	methionine and choline deficient
MGAT	acyl CoA:monoacylglycerol acyltransferase
MYF	myogenic factor
nAChR	nicotinic acetylcholine receptor
NAFLD	nonalcoholic fatty liver disease
NASH	non-alcoholic steatohepatitis
NEFA	non-esterified fatty acids
NF-κB	nuclear factor kappa β
PBA	4-phenyl butyric acid
PC	phosphatidylcholine
PDI	protein disulfide isomerase
PE	phosphatidylethanolamine
PEMT	phosphatidylethanolamine *N*-methyltransferase
PEPCK	phosphoenolpyruvate carboxykinase
PERK	protein kinase-like ER kinase
PGC1α	PPARγ coactivator 1α
PKA	protein kinase A
PPAR	peroxisome proliferator-activated receptor
PS	phosphatidylserine
SCD	stearoyl-CoA desaturase

SREBP	sterol regulatory element binding protein
TG	triacylglycerol
TGF	transforming growth factor
TGH	triacylglycerol hydrolase
TR	thyroid hormone receptor
TNF	tumor necrosis factor
UCP	uncoupling protein
UPR	unfolded protein response
VLDL	very low density lipoprotein
WAT	white adipose tissue
XBP1	X-box binding protein-1
XBP1s	the spliced form of XBP1.

Chapter 1

Introduction

1.1 phosphatidylcholine (PC) and phosphatidylethanolamine (PE)

1.1.1 PC

Phosphatidylcholine (PC) was first described in 1847 as a constituent of egg yolk and named as lecithin based on the Greek equivalent *lekythos* (1). PC contains two fatty acids esterified to a glycerol backbone and a phosphodiester linkage connecting to choline (Figure 1.1) (2). The diversity of PC molecules relies on the differences in the length, number and position of double bonds in the two fatty acids (3). There are more than 20 different PC species in mammalian cells (3). PC in the liver typically contains a saturated fatty acid (e.g., palmitic acid) at the sn-1 position and a polyunsaturated fatty acid (e.g., arachidonic acid) at the sn-2 position (3).

1.1.2 Function of PC

PC primarily functions as a structural component of eukaryotic cellular membranes (4). PC is the major lipid component of eukaryotic transport pathways, facilitating and maintaining the intracellular distribution of PC (5,6). Presumably, the appropriate distribution of PC has important consequences for cellular and organelle function (7). Physical properties of the membrane such as fluidity and permeability (integrity) are altered by phospholipid composition (8,9). It is becoming clear that a direct link exists between the lipid environment and the function of some integral membrane proteins (10).

PC in cellular membranes also serves as a precursor for essential signalling molecules. In response to physiological and pathophysiological stimuli such as hormones and cytokines, second messengers derived from membrane lipids are rapidly

released due to the presence of phospholipases (11,12) (Figure 1.2). PC-derived signals include lysophosphatidylcholine (lyso-PC), lysophosphatic acid, phosphatidic acid, diacylglycerol (DG), and eicosanoids produced from long chain fatty acids (13). The generation of specific lipid signalling molecules is dependent on the extracellular stimuli and cell type. Metabolites derived from PC are implicated in a wide range of cellular events and provide targets for seeking potential treatments for immune diseases, post-ischemic brain injury and cancer (14-16).

Beyond being the membrane component, PC in the liver is also an essential component for bile and lipoprotein particles. Bile secreted from the liver contains bile acids, cholesterol, and phospholipids, and facilitates the digestion and absorption of lipids and fat soluble vitamins in the intestinal tract (17). The majority (~95%) of phospholipid in bile is PC (18). PC is required to neutralize bile acids and maintain the solubility of cholesterol (17). In mice, the amount of PC secreted from the liver into bile within 24 h is equivalent to the total pool of hepatic PC (19). Hepatic PC actively translocates across the hepatocyte canalicular membrane into bile by a PC-specific transport protein (flippase), multiple-drug resistance protein 2 (MDR2, which is called ABCB4/MDR3 in humans) (20). In humans, mutations in MDR3 gene were associated with progressive familial intrahepatic cholestasis 3 (21), a rare disease characterized by persistent blockage of bile ducts, which can progress to irreversible liver damage (22).

PC is the major phospholipid in all the lipoprotein classes with levels ranging from 60-80% (23). In addition to PC, lipoprotein particles also contain other phospholipids including sphingomyelin, lyso-PC, phosphotidylethanolamine (PE), phosphatidylserine (PS), and phosphatidylinositol (23). Lipoproteins are responsible for transporting the

hydrophobic lipids in the hydrophilic circulatory system (24). Structurally on the surface of lipoproteins, phospholipids and cholesterol form a monolayer surrounding the hydrophobic core containing triacylglycerol (25) and cholesteryl esters (24). Based on the density, lipoproteins are classified into chylomicrons, very low density lipoproteins (VLDL), low density lipoproteins (LDL) and high density lipoproteins (HDL). Compared to VLDL with a TG-rich core, LDL and HDL are denser and have a relatively higher proportion of cholesterol (24). Moreover, different lipoprotein classes carry distinctive proteins referred to as apolipoproteins; for instance, apolipoprotein B is mainly found in VLDL and LDL (24). In general, the higher the total phospholipid component of lipoproteins, the greater density and surface area; in HDL, up to 40% of the total lipoprotein lipid is composed of PC (23).

Notably, PC is also an important component of pulmonary surfactant. Surfactant is predominately composed of PC (~70%) and surfactant proteins (26,27). A specific PC specie dipalmitoylphophatidylcholine is the major PC in pulmonary surfactant (26,27). In addition to its immune function, which mainly depends on surfactant proteins, surfactant that coats alveoli is critical for lung function as it intersperses between water and air to reduce the surface tension (26,27). Moreover, most recent studies have confirmed that PC can be a source of TG in hepatocyte (28,29) and in the liver (30). It is estimated that ~ 50% of hepatic PC is taken up from plasma lipoproteins, and remarkably that 30% of lipoprotein-derived hepatic PC is converted into TG (30).

1.1.3 PC biosynthesis: CDP-choline pathway

In mammals, there are two pathways for *de novo* PC synthesis: the cytidine diphosphate (CDP)-choline pathway and the phosphatidylethanolamine *N*-

methyltransferase (PEMT) pathway. In all nucleated cells, the major pathway for PC production is the CDP-choline pathway (Figure 1.2), whereas the PEMT pathway (will be discussed in section 1.3) is only quantitatively significant in the liver. The CDP-choline pathway was first characterized by Eugene Kennedy in the 1950s (31); therefore, it is occasionally referred to as the Kennedy pathway (4). PC may also be generated through base-exchange of the choline head group (4) or by the reacylation of lyso-PC (32).

The CDP-choline pathway requires dietary choline as substrate and generates PC via three enzymatic reactions (Figure 1.3). First, choline, an important essential nutrient, is phosphorylated to phosphocholine by choline kinase using adenosine triphosphate (ATP). Second, in the presence of cytidine triphosphate (CTP), phosphocholine is converted into CDP-choline by CTP:phosphocholine cytidylyltransferase (33). CT is the rate-limiting enzyme in the CDP-choline pathway (4). CT is encoded by two genes, *Pcyt1a* and *Pcyt1b*, and CTα (the product of *Pcyt1a*) is the predominant isoform in the liver (34,35). Whole body deletion of CTα in mice is embryonic lethal at day 3.5, indicating a critical role of the CDP-pathway in embryogenesis (36). Mice with liver-specific deletion of CTα have been generated and exhibit compromised lipoprotein secretion (37). The final reaction is catalyzed by CDP-choline:1,2-diacylglycerol cholinephosphotransferase, which exchanges cytidine monophosphate for DG to generate PC (4).

1.1.4 PE and its function

Historically, PE was first described as a nitrogen- and phosphorus-containing lipid in 1884 (4). The first pure preparation of PE was isolated by Rudy and Page in 1930

and following that, its structure was demonstrated in 1952 by Baer and et al (4). PE is different from PC, with ethanolamine replacing the choline group (Figure 1.1).

Similar to PC, one major function of PE is to act as a primary structural component of cellular membranes. Typically, PE is the second most abundant phospholipid in mammalian cells, comprising of ~ 20% of total phospholipids (4). One exception is in the brain, where ~ 45% of total phospholipids are PE (38). The PE content is different among cellular organelles. For example, mitochondria contain higher amounts of PE than other organelles; the inner mitochondrial membrane is more enriched in PE than the outer mitochondrial membrane (4). Convincing *in vitro* evidence shows that PE is involved in membrane fusion (38). Consistent with this notion, PE is required during cytokinesis of mammalian cells for the disassembly of contractile ring at the cleavage furrow (39). PE also regulates the fusion of mitotic Golgi membranes (40). Lack of PE in the parasite *T. brucei* impairs membrane fusion, alters mitochondrial morphology and inhibits progression of the cell cycle (41).

Other than its structural role in membranes, PE also performs numerous additional functions. PE acts as a substrate for PC production via the PEMT pathway (Figure 1.3). PE is the precursor for N-acylethanolamine, a neurotransmitter in the brain (42) and for the synthesis of *N*-arachidonoylethanolamine, the ligand for cannabinoid receptors in the brain (38,43). PE also provides the ethanolamine moiety that covalently modifies several proteins including the glycosylphosphatidylinositol anchors, which attach many signaling proteins to the plasma membrane (44). Recently, PE has been demonstrated to play a role in autophagy, a “self-eating” process defined as a lysosome-dependent cytoplasm turnover mechanism (45). Autophagy relies on the formation of

autophagosomes before their final fusion with lysosomes for the degradation of the encapsulated cellular components (45). The formation of autophagosomes in mammalian cells requires the lipid modification of ubiquitin-like light chain protein 3 (LC3), specifically the covalent association of PE with LC3 (46). The origin of PE in autophagosomes is still under debate, although some evidence supports PE derived from mitochondria and endoplasmic reticulum (ER)/mitochondria connections are used for attachment to LC3 (38). Moreover, PE appears to be essential for heart function, since a decreased PE content in cardiac myocytes results in cell damage, and during ischemia, the asymmetrical distribution of PE in sarcolemmal membranes is altered (47). Most recently, PE, rather than PC or PS, was unexpectedly identified as the single endogenous factor that is able to facilitate the formation of prion proteins (48).

In *Drosophila*, PE is the major membrane phospholipid (4). In contrast to mammalian cells where cholesterol is the master regulator of cellular cholesterol homeostasis, in *Drosophila,* PE regulates the processing of sterol regulatory element binding protein (SREBP) (49), the key transcription factor for cholesterol synthesis in mammalians (44). In *E. coli,* PE functions as a “lipid chaperone”, regulating protein folding and the topology of integral membrane proteins such as lactose permease (4,50).

1.1.5 PE biosynthesis

In eukaryotic cells, PE can be synthesized through four pathways: two major pathways and two minor pathways (Figure 1.4). The CDP-ethanolamine pathway and the PS decarboxylase (PSD)-mediated PSD pathway are the two major routes for PE production, which are discussed in more details below. PE can also be generated via

two quantitatively minor pathways: the acylation of lyso-PE and a base-exchange reaction catalyzed by PS synthase (PSS)2, where the serine group of PS is replaced by ethanolamine (4). The acylation of lyso-PE pathway is active in yeast, which has the majority of lyso-PE acyltransferase activity in the mitochondria-associated membranes (MAM), and might also be important in mammals (38,51). The base-exchange reaction takes place in the ER in a calcium-dependent manner (38). The relative contribution of the four pathways to PE synthesis appears to be cell type dependent (4). In rat liver/hepatocytes, the CDP-ethanolamine pathway contributes to the majority of PE production, and particularly in *Trypanosoma brucei,* it is the sole pathway (4,52). Whereas, in many other types of cells such as baby hamster kidney cells, over 80% of PE is generated from the PSD pathway even when additional ethanolamine is provided (53). It should be noted that the quantitative contribution of each pathway to PE production in each cell type is complex and difficult to determine due to the limitation of methodology (38). Moreover, the CDP-ethanolamine pathway is the *de novo* pathway for PE production, since all the remaining pathways rely on the pre-existing phospholipids (4).

The CDP-ethanolamine pathway was first described by Kennedy and Weiss in 1956 (31). Parallel with the CDP-choline pathway, the CDP-ethanolamine pathway also consists of three sequential enzymatic reactions (Figure 1.4). First, phosphorylation of ethanolamine is catabolized by ethanolamine kinases. Ethanolamine in mammalian cells derives from diet or breakdown of PE or sphingosine phosphate (38). Two ethanolamine kinases have been characterized: one isoform (ethanolamine kinase-1) phosphorylates both ethanolamine and choline, whereas the other isoform

ethanolamine kinase-2 is ethanolamine-specific (38). Mice with deletion of ethanolamine kinase-2 show a comparable amount of hepatic PE compared to control mice, although fewer pups are born and have a lower survival rate (54). Second, the rate limiting reaction is catalyzed by CTP:phosphoethanolamine cytidylyltransferase, forming CDP-ethanolamine from phosphoethanolamine and CTP (4). In mice, CTP:phosphoethanolamine cytidylyltransferase is encoded by the *Pcyt2* gene and its global deletion is embryonic lethal (55). The reaction is completed by CDP--ethanolamine:1,2-diacylglycerol ethanolamine phosphotransferase residing primarily in the ER (4).

In mammalian cells, the other major pathway for PE production is the decarboxylation of PS by PSD that is located on mitochondrial inner membranes (56). The substrate PS is synthesized in the ER/MAM from PC via PSS1 or PE by PSS2 (Figure 1.4). It remains inconclusive regarding which pool of PS is preferably used for PE production, the PS from PC or that from PE (38). Disruption of PSD in mice is embryonic lethal at day 9.5, supporting its major contribution for PE production and embryogenesis (57). It should be noted that embryonic fibroblasts in PSD-deficient mice exhibit profoundly altered mitochondrial morphology and extensively fragmented mitochondria (57). Reducing the expression of PSD by silencing mRNA in CHO cells also results in morphological alteration in mitochondria and defects in mitochondrial functions (38). The underlying mechanism for changes in mitochondrial morphology and function caused by loss of mitochondrial PE is still an open question (38), although PE is known to be implicated in membrane fusion as aforementioned.

Thus, there are at least two spatially distinct pools of PE synthesized in mammalian cells: one in the ER by the CDP-ethanolamine pathway and the other in the mitochondria via PSD (4). Notably, the PE species generated by these two pathways are distinct in their acyl-chain compositions. PE derived from the CDP-ethanolamine pathway preferentially contains mono- or di-unsaturated acyl chains, such as 18:2, at the *sn-2* position; whereas PE derived from the PSD pathway preferentially has polyunsaturated acyl chains, such as 20:4, at the *sn-2* position (58).

1.2 Phosphatidylethanolamine *N*-methyltransferase (PEMT)

PEMT catalyzes the production of PC by three sequential methylations of PE using *S*-adenosylmethionine (AdoMet) as the methyl-donor, resulting in its conversion into *S*-adenosylhomocysterine (AdoHcy). In 1941, the methyl groups from methionine were first shown to be utilized for the generation of choline, which was then incorporated into PC (59). It was until 1960s that Bremer and Greenberg demonstrated that PE acted as the methyl group acceptor (60,61). Soon after that, PEMT activity was discovered and characterized mainly in rat liver (62). Due to the presence of phospholipase D (Figure 1.2) (63), PC can be converted into choline, which provides substrate for PC production via the CDP-choline pathway. Therefore, PEMT is the only known endogenous pathway for choline synthesis (4).

1.2.1 Purification and characterization of PEMT

PEMT is a membrane-associated enzyme. It was only in 1987 that the PEMT protein was purified by Neale Ridgway and Dennis E. Vance from rat liver (64). PEMT

solubilized in Triton X-100 shows enzyme activity with substrates PE, phosphatidyl-*N*-monomethylethanolamine and phosphatidyl-*N,N*-dimethylethanolamine (64,65). Kinetic studies suggest that the purified enzyme has a common substrate binding site for these 3 substrates and the enzyme activity is optimized at pH 10.5 (64,66). The physiological relevance of the high pH optimum for PEMT is unclear (67). The pure PEMT protein has a molecular weight of 18.3 kDa determined by SDS-polyacrylamide gel electrophoresis (64). This is similar to the calculated molecular weight from the cDNA sequence of PEMT (22.3 kDa) (68).

With the availability of the purified rat PEMT, oligonucleotide probes were designed and used to screen for the PEMT cDNA from a rat liver cDNA library (68). One cDNA identified was cloned and expressed in COS-1 cells, McArdle RH7777 rat hepatoma (McA-RH7777) cells, and Sf9 insect cells (68). The enzyme activity and molecular weight of the expressed protein matched with the purified PEMT enzyme (68). Subsequently, the rat *PEMT* cDNA was used to probe for *PEMT* from a mouse genomic DNA library (69) and a human liver cDNA library (70). In human livers, three forms of *PEMT* mRNA have been identified and they are distinctive from each other in the 5′-region with or without the presence of 15 nucleotides upstream of the codon for initiation of translation (70,71). *PEMT* from rat, mouse and human, encodes a 199-amino acid protein with a molecular weight of 22 kDa (68,70,72). The rat PEMT protein shares 93.5% and 80.4% similarity with mouse and human PEMT, respectively (70,72).

1.2.2 Location and structure

Subsequent to the cloning of *PEMT*, a specific antibody against PEMT was raised in rats using a synthetic peptide encoding the 12 carboxyl terminal amino acids of

PEMT (68). The protein expression of PEMT is significantly higher in the liver than in other tested tissues in mice, possessing less than 0.5% immunoreactivity of hepatic PEMT (73). Among all the non-hepatic tissues examined, the immunoreactivity is only relatively high in the white adipose tissue (WAT) and testes (73). Consistently, the PEMT activity is high in the liver (74), although low activity, less than 1% of that in the liver, is also present in other tissues such as the heart and adipocytes (73,75), where the functional significance has not been well characterized. Moreover, PEMT activity was also reported in rat brains, with 4-fold higher enzyme activity in neonatal brains than in adult brains (76). PEMT deficiency in mice showed altered fetal brain development (77).

The protein expression and enzyme activity have also been determined in subcellular fractions of rat liver (68). The majority (70%) of PEMT activity was found in the ER fractions and MAM (68,78). The MAM are defined as a specific region of the ER that transiently tethered to mitochondria (79). They are implicated in phospholipid translocation from the ER to mitochondria (80) and in various cellular functions such as regulation of calcium homeostasis (73). A surprising finding is that the specific antibody raised against PEMT did not recognize PEMT in purified ER fractions from rat livers, where the highest enzyme activity was detected (68). However, this antibody is able to detect PEMT in both ER fractions and MAM in human livers (78). The potential difference in PEMT detection in purified ER fractions and MAM remains to be determined.

The structure of PEMT has not been characterized by X-ray crystallography or NMR (nuclear magnetic resonance spectroscopy) (73). A topological model has been

proposed based on studies of endoproteinase digestion of epitope-tagged PEMT (78). In this model, PEMT contains 4 transmembrane regions spanning the ER membrane, with both the N- and C- terminal residues in the cytosol (78). Additional studies have identified two separate AdoMet binding motifs, which are located on the 3rd and 4th transmembrane domains in proximity to the cytosolic surface of the ER (81). Mutagenesis studies show that residues Gly^{100} and Glu^{180} are involved in the regulation of AdoMet binding (81). The C-terminal residue Lys^{197} is essential for localizing PEMT to the ER, as PEMT was directed to the Golgi when Lys^{197} was mutated to Cys^{197} (82). However, the activity of PEMT was not affected by this mutation (82).

1.2.3 Regulation of PEMT activity

Substrate Supply

PEMT activity is regulated by the availability of substrates and final products. In primary cultured hepatocytes, the conversion of PE to PC is doubled in the presence of 0.2 mM methionine (83,84) and addition of ethanolamine causes 50% increase of PE and doubles the rate of PC conversion from PE (85). Similarly, increased availability of phosphatidyl-*N*-monomethylethanolamine and phosphatidyl-*N,N*-dimethylethanolamine by providing *N*-monomethylethanolamine or *N,N*–dimethylethanolamine stimulates the formation of PC (84). An increased concentration of PE stimulates PE methylation using rat liver microsomes (86). In addition, only newly formed PE generated via the CDP-ethanolamine pathway seems to be methylated into PC in rat hepatocytes (87).

Increased intracellular level of AdoMet by exogenous L-methionine also raises the rate of PC formation (88). On the contrary, an elevated cellular AdoHcy concentration by 3-deazaadenosine, an AdoHcy hydrolase inhibitor, reduces the cellular

AdoMet/AdoHcy ratio and inhibits PEMT activity (89,90). The ratio of AdoMet to AdoHcy regulates cellular methylation reactions including PE methylation by PEMT (88-90).

Hormonal regulation

In the 1980s, numerous studies have shown that various hormones were involved in the regulation of PEMT activity (91-95). Preliminary reports indicate that vasopressin, angiotensin (96), epidermal growth factor (91), estradiol (97), and calmodulin (98) increased PEMT activity. Glucagon is another hormone extensively studied in the regulation of PEMT. However, conclusive statements are difficult to reach due to either the small effects of hormones or conflicting published results. In one study, 100 nM glucagon showed an inhibitory effect on the conversion of PE to PC by 25% (94) in isolated rat hepatocytes, whereas, it activated the methylation of PE by 1-fold in another study (99). *In vitro* studies with purified enzyme showed that PEMT was phosphorylated by glucagon-activated cyclic AMP (100)-dependent protein kinase (92). However, addition of exogenous cAMP to intact hepatocytes failed to promote phosphorylation of PEMT (92).

Estrogen is a well characterized hormonal regulator of PEMT. The first evidence comes from studies on mice, where the expression of PEMT is higher in female mice than in male mice (101). Consequently, deletion of *PEMT* results in reduced plasma PC in chow-fed female mice but not in male mice (101). When fed a high fat/high cholesterol diet, only female *Pemt*$^{-/-}$ mice exhibit a significant reduction in the level of hepatic PC (101). In humans, postmenopausal women and men are more likely to develop muscle and liver damage under choline-restricted condition (102). Subsequent analysis implies that PEMT is regulated by estrogen in an isoform-specific fashion

(103,104). A common genetic polymorphism (rs12325817) in the PEMT transcript has been identified to be associated with increased risk of organ dysfunction in response to a choline-deficient diet (CDD) (104). This is likely related to the ablation of the binding between the risk allele and estrogen receptor (103). Furthermore, PEMT transcription has been shown to be increased by estrogen in a dose-dependent manner in primary cultured mouse and human hepatocytes (105). However, it is not clear at the moment that the observed induction of *Pemt* mRNA levels is due to altered regulation of gene transcription or increased stability of mRNA (67).

Transcriptional Regulation

The transcriptional regulation has not been well characterized. Human active *PEMT* transcripts share 50% similarity of the promoter region with mouse *PEMT* (69,71). In both mice and humans, a TATA box is not present in the proximal promoter region for *PEMT* (69,71). Further analysis of the promoter region reveals potential transcription factor binding sites including hepatic nuclear factor, activating factor-1, yin yang protein 1, GATA and Sp1 (69,71). The regulatory role of majority of these factors has not been examined until recently when a suitable cell model was identified. *PEMT* mRNA is low in several immortalized cell lines, including the monkey kidney cell line COS-7, the mouse hepatoma cell lines H2.35, McA-RH7777and Hepa-1c1c7, and the mouse embryonic fibroblast cell line C3H10T1/2 (106). Although primary hepatocytes have high expression of *PEMT* initially, the mRNA levels of *PEMT* drop rapidly within 16 h of isolation and are undetectable with extended culture, which is likely related to the de-differentiation of hepatocytes during the primary culture (19,106,107).

Lately, the discovery that the expression of PEMT protein was significantly increased during the differentiation of 3T3-L1 cells solves this problem (75). Using 3T3-L1 cells, a regulatory region is identified by *PEMT* promoter-luciferase assay between − 471 and − 371 bp relative to the transcription start site (106). Sp1 protein binds to this GC-rich region and the amount of Sp1 decreases just before the protein level of PEMT increases. Furthermore, tamoxifen, a drug commonly prescribed for breast cancer treatment, inhibits the expression of *PEMT* by manipulating the binding of Sp1 to the promoter region (108). Thus, Sp1 is suggested to be a negative transcriptional regulator of *PEMT* (106). Additionally, Sp3 and yin yang protein 1 also binds to the promoter region of *PEMT* in 3T3-L1 cells, but neither protein has effect on the protein levels of PEMT during cell differentiation (106). Interestingly, Sp1 acts as a positive regulator of the expression of CT, the rate-limiting enzyme in the CDP-choline pathway (109-111). The CDP-choline pathway is inversely up-regulated in the liver when PEMT expression is decreased during hepatic regeneration and growth (112-114). Therefore, Sp1 might play an important role in the reciprocal regulation of the PEMT and CDP-choline pathways.

Other regulation

PEMT is inversely correlated with liver cell growth. PEMT expression is negatively correlated with the liver growth in rats (112). In rats, the activity of hepatic PEMT is very low (0.03 nmol/min/mg protein) before birth, but rapidly increases after birth, peaking at 10 days (0.45 nmol/min/mg protein), and maintains into adulthood (115). After a partial hepatectomy, when two-thirds of the liver is removed, the remaining hepatocytes de-differentiate and proliferate to recover the liver mass (116,117). The mRNA and protein

levels of PEMT were reduced by 90% and the hepatic PEMT activity was decreased by 45% 24 h after partial hepatectomy in rats (114), whereas the CDP-choline pathway was reciprocally activated (118). As the liver size was restored (~48 h post hepatectomy), the protein level of PEMT increased and the reduced PEMT activity was restored 3–4 days after the partial hepatectomy (114). Furthermore, *Pemt*$^{-/-}$ mice fed *a* high fat (119) diet had only a 32% survival rate of that in *Pemt*$^{+/+}$ mice after the partial hepatectomy (120). Even to date, the regulatory mechanisms for PEMT in these observations are still lacking.

The above inverse correlation between PEMT and cell growth is also present in cell models. As cultured primary hepatocytes de-differented, the expression of PEMT was decreased (107), which is consistent with a previous report where the *PEMT* mRNA was undetectable in primary rat hepatocytes after 50 h of culture (*19*). Moreover, PEMT activity is negligible in immortalized hepatoma cell lines, which typically have increased expression of genes for cell growth (68,121-123). In contrast, expression of PEMT in McA-RH7777 cells stalled cell growth (121).

PEMT catalyzes reactions responsible for the production for PC and endogenous choline. Thus, it is not surprising that PEMT activity is altered by the availability of choline or the presence of CTα, the key enzyme in CDP-choline pathway. Rats fed a CDD for 3 weeks had 2-fold increase of PEMT activity, concomitant with the increased levels of mRNA and protein (124). Likewise, PC production was doubled via the PEMT-mediated PE methylation in *LCTα*$^{-/-}$ mice (125). However, the mechanisms underlying these alterations have not been determined.

1.3 Physiological function of PEMT

The knowledge on the physiological importance of PEMT was limited until generation of PEMT knockout mice by C. Walkey (72). A vector was constructed, specifically targeting exon 2 of *PEMT*, and introducing the vector into mice generated mice lacking PEMT enzyme activity (*Pemt*$^{-/-}$ mice) (72). The *Pemt*$^{-/-}$ mouse is the very first mouse model generated with deletion of an enzyme in phospholipid biosynthesis (73). *Pemt*$^{-/-}$ mice appear overly normal with minimal effect on the levels of PC and PE in the liver. This is not too surprising since the enzyme is only quantitatively significant in the liver (72). In addition, a 60% increase in CT activity in the livers of *Pemt*$^{-/-}$ mice likely minimizes the effect of PEMT elimination on the production of hepatic PC (72). Insights into the physiological relevance of PEMT have been gained since mice were specially treated with a CDD. We and others have uncovered the physiological importance of PEMT in fatty liver, cardiovascular diseases, and obesity and type 2 diabetes.

1.3.1 PEMT and non-alcoholic fatty liver

Non-alcoholic fatty liver disease (NAFLD) is rapidly rising throughout the world with the epidemic of obesity and diabetes (126-128). NAFLD includes a wide spectrum of hepatic diseases, from steatosis to non-alcoholic steatohepatitis (NASH) and more advanced stages of liver failure (129-132). It is unclear how steatosis progresses into NASH. The significance of PEMT in NAFLD has been shown in mice fed the CDD or the HF diet and in humans.

The first and critical evidence linking PEMT to NAFLD comes from studies on *Pemt*$^{-/-}$ mice fed the CDD. CDD-fed *Pemt*$^{-/-}$ mice develop severe liver failure with highly

elevated plasma alanine aminotransferase, an indicator of liver pathology and typically die within 5 days (133). This lethal effect is mainly caused by reduced PC production and removal of PC via biliary excretion (73). With depletion of dietary choline, PC production via the CDP-choline pathway is essentially attenuated and *Pemt*$^{-/-}$ mice show only 50% hepatic PC compared to control mice (133). The importance of hepatic PC is further supported by deletion of MDR2 in *Pemt*$^{-/-}$ mice, which is a PC-specific flippase, responsible for the secretion of PC into bile (20,133). Quantitatively significant amounts of hepatic PC are secreted into bile as shown in a 20 g mouse, the liver of which contains ~ 20 mg of PC and secretes ~ 23 mg of PC each day into the bile (134). When fed the CDD for three days, *Pemt*$^{-/-}$/*Mdr2*$^{-/-}$ mice show only ~20% reduction in hepatic total choline-metabolites compared with over 50% decrease in *Pemt*$^{-/-}$ mice and have an negligible level of biliary PC (133). As expected, *Pemt*$^{-/-}$/*Mdr2*$^{-/-}$ mice are able to survive over 90 days when placed on the CDD (133). A surprising finding in *Pemt*$^{-/-}$/*Mdr2*$^{-/-}$ mice is that hepatic PC is also decreased by 50% as in *Pemt*$^{-/-}$ mice, which is not concomitant with the decrease of other phospholipids such as PE (135).

Membranes are constituted of various lipids with distinct physical properties and plays different functional roles (136). PC is one major component of lipid bilayer, mainly residing in the outer monolayer of the plasma membrane; PE, on the other hand, is concentrated on the inner layer of the plasma membrane (137). This leads to the speculation that the decreased hepatic PC in *Pemt*$^{-/-}$ mice might cause redistribution of PE on plasma membrane, which consequently affects membrane permeability (73). Indeed, a striking correlation was found between hepatic PC/PE ratio in *Pemt*$^{-/-}$/*Mdr2*$^{-/-}$ and *Pemt*$^{-/-}$ mice and plasma alanine aminotransferase (135).

Manipulating PC/PE ratio using large unilamellar vesicles also supports the idea that a decreased PC/PE ratio induces membrane permeability (135). Furthermore, this PC/PE ratio shows clinical relevance, as a decreased ratio has been observed in NASH patients compared to control livers (135). Thus, the liver failure in CDD-fed *Pemt*$^{-/-}$ mice is caused by the deprivation of PC and the loss of membrane integrity, resulting from a decreased hepatic PC/PE ratio (135).

When fed the HF diet, *Pemt*$^{-/-}$ mice develop NASH quickly within two weeks (120). It has been shown that HF-induced NASH in *Pemt*$^{-/-}$ mice is likely due to both increased steatosis and decreased hepatic PC/PE. The steatosis in HF-fed *Pemt*$^{-/-}$ mice is largely caused by an impaired VLDL secretion. Inadequate amount of hepatic PC reduces the secretion of TG-rich VLDL particles (138-140). Disruption of either the CDP-choline pathway or the PEMT pathway, results in TG accumulation in cells and animal models (37,101,141-144). When fed a HF/high cholesterol diet for 3 weeks, *Pemt*$^{-/-}$ mice accumulate ~5-fold more hepatic TG compared to wild-type mice (101). When fed the HF diet for 10 weeks, *Pemt*$^{-/-}$ mice have ~3-fold more hepatic TG than control mice (33). The hepatic TG accumulation in *Pemt*$^{-/-}$ mice could be also attributed to PC derived from plasma lipoprotein particles (29). PC derived from plasma lipoprotein particles has been shown to be a significant source of hepatic TG in mice, ~ 50% of hepatic PC is estimated to be from plasma lipoproteins, and among them, 30% is converted into hepatic TG (30). Particularly in *Pemt*$^{-/-}$ mice, a relatively larger portion (49%) of hepatic PC is converted to TG versus control mice, which is not observed in *LCTα*$^{-/-}$ mice (30). Furthermore, HF-fed *Pemt*$^{-/-}$ mice also exhibit a reduced PC/PE ratio, which is associated with the survival rate after partial hepatectomy (120).

Additionally, hepatic PC/PE ratio appears to be increased in *ob/ob* mice (a genetic mouse model lacking the functional hormone leptin) compared to control mice, concomitant with hepatic ER stress and impaired calcium homeostasis (145). Attenuating the PEMT activity by 50–70% in *ob/ob* mice alleviates hepatic ER stress and improves calcium homeostasis (145). Together, the HF diet also induces the occurrence of NASH in *Pemt*$^{-/-}$ mice.

In humans, there is evidence for a correlation between PEMT and NAFLD. Zeisel's group first reported the polymorphism at residue 175 of PEMT, at which, a Val-to-Met substitution led to ~ 40% reduction of enzyme activity (146). Studies from 59 control subjects and 28 humans with non-alcoholic liver disease showed that Met/Met at residue 175 occurred in 68% of the subjects with non-alcoholic liver disease but in only 41% of control subjects (146). The V175M polymorphism was then suspected to confer susceptibility to non-alcoholic liver disease in humans (146). This concept was again supported from a later study carried out in Japan on 107 NASH patients and 150 healthy volunteers (147). This association between the V175M polymorphism and steatosis did not appear in the Dallas Heart study (148), but was detected when only Caucasians were considered. One possible explanation could be that the V175M polymorphism is associated with fatty liver on the condition that the secretion of TG into plasma VLDL is decreased and/or TG synthesis is increased (149). Another polymorphism was identified with the substitution of G to C in the promoter region of the *PEMT* gene (150). This G to C polymorphism is likely associated with the development of organ dysfunction in humans consuming a low choline diet (104).

Moreover, the C allele in the PEMT gene increased the requirement for choline in both post-menopausal and pre-menopausal women (104).

1.3.2 PEMT and cardiovascular disease

A possible relationship between methylation of ethanolamine to PC and atherosclerosis was reported in 1954 (151). C57BL/6 mice are protected against diet-induced atherosclerosis (73). To date, there are two commonly used mouse models for atherosclerosis: LDL receptor-deficient (*Ldlr*$^{-/-}$) mice and mice lacking apolipoprotein E (*Apoe*$^{-/-}$) (152). *Ldlr*$^{-/-}$ mice develop atherosclerosis when fed a HF, high-cholesterol diet, whereas *Apoe*$^{-/-}$ mice present atherosclerosis spontaneously with chow-feeding (152). The protective role of PEMT against atherosclerosis has been examined in both genetic backgrounds (153,154). When fed the HF, high-cholesterol diet for 16 weeks, deletion of *PEMT* in *Ldlr*$^{-/-}$ mice (*Pemt*$^{-/-}$/*Ldlr*$^{-/-}$) decreased the atherosclerotic lesions by ~ 80% (154). When fed the chow diet for 1 year, *Pemt*$^{-/-}$/*Apoe*$^{-/-}$ mice also showed ~30% reduction of atherosclerotic lesions compared to *Pemt*$^{+/+}$/*Apoe*$^{-/-}$ mice (153). Moreover, deletion of *PEMT* in *Apoe*$^{-/-}$ mice improved systolic function examined by echocardiography and decreased the accumulation of TG in the heart by 34% (153), indicating a beneficial effect of PEMT deficiency in cardiac function. Taken together, the lack of PEMT protects mice (*Ldlr*$^{-/-}$ and *Apoe*$^{-/-}$) against the development of atherosclerosis.

The beneficial effect of PEMT deficiency in atherosclerosis mainly is attributed to an improved plasma lipoprotein profile. The VLDL/LDL lipids in *Pemt*$^{-/-}$/*Ldlr*$^{-/-}$ mice was significantly lower than that in *Ldlr*$^{-/-}$ mice, with ~ 70%, 56% and 34% reduction for plasma TG, cholesterol and cholesteryl esters respectively (154). Consistently, the

levels of plasma apoB100 and apoB48 were also decreased by 30% and 60% in *Pemt*$^{-/-}$/*Ldlr*$^{-/-}$ mice (154). Additionally, VLDL from *Pemt*$^{-/-}$/*Ldlr*$^{-/-}$ mice was more rapidly cleared from plasma than that from *Pemt*$^{+/+}$/*Ldlr*$^{-/-}$ mice, which is possibly due to alterations in lipid content and structure of VLDL (154). Similarly, *Pemt*$^{-/-}$/*Apoe*$^{-/-}$ mice also showed a 45% reduction in the level of TG and a 25% decrease in cholesterol in plasma VLDL/LDL fractions (153).

The improved plasma lipid profile is closely related to the requirement of PEMT in VLDL secretion. This notion was first demonstrated in primary rat hepatocytes: when cultured in medium lacking both methionine and choline, hepatocytes had increased cellular TG accumulation, but decreased VLDL secretion (143). Both methionine and choline are relevant to PC biosynthesis: choline is a precursor in the CDP-choline pathway, whereas methionine, once converted to AdoMet, acts as the methyl donor for PC production via PEMT-mediated methylation of PE (73). Supplementation of either methionine or choline normalized VLDL secretion in hepatocytes, suggesting an active synthesis of PC via either the PEMT pathway or the CDP-choline pathway satisfies the demand of PC for secretion of VLDL in cultured rodent hepatocytes (73,143). Indeed, VLDL secretion was defective in *Pemt*$^{-/-}$ mice, despite an intact CDP-choline pathway (101,142). Similarly in *LCTα*$^{-/-}$ mice, VLDL secretion was decreased even though the activity of PEMT was increased by 2-fold in the liver (37). Thus, it seems that both the PEMT and CDP-choline pathways are required for normal hepatic VLDL secretion. It is still not clear why both pathways are needed. An early study from rat hepatocytes showed that VLDL secretion might require specific pools of PC (155). Compared to PC made from PE via the CDP-ethanolamine pathway, PC generated

from PE originating from PS decarboxylation is preferable for VLDL secretion (73). Future studies are required to shed light on this puzzle. It is noteworthy to mention that PEMT deficiency decreased hepatic secretion of VLDL in a gender specific manner, in male but not female *Pemt*$^{-/-}$ mice (101).

The beneficial effect of PEMT deficiency in atherosclerosis is also associated with decreased plasma homocysteine (Hcy). Hcy is a non-protein amino acid. Hyperhomocysteinemia, denoted by elevated level of total Hcy in the blood, is an independent risk factor for cardiovascular diseases such as atherosclerotic vascular disease in the coronary artery (156,157). In the liver, PEMT-mediated methylation of PE to PC is a significant contributor of plasma Hcy. Through the complete methylation of 1 molecule of PE, 3 molecules of AdoHcy are generated (Figure 1.3). In *Pemt*$^{-/-}$ mice, the plasma levels of Hcy were decreased by 50% in comparison to those in *Pemt*$^{+/+}$ mice (158). Hepatocytes Isolated from *Pemt*$^{-/-}$ mice also showed 50% reduction in the secreted Hcy than hepatocytes from *Pemt*$^{+/+}$ mice (158). In McA-RH7777 cells, expression of human *PEMT* caused close to a 3-fold increase in the levels of Hcy in medium after 24 h of culture compared to control cells (158). Furthermore, in *LCTα*$^{-/-}$ mice, where PEMT activity was doubled, plasma Hcy was elevated by 20–40% compared to control mice (125). Consistently, hepatocytes from *LCTα*$^{-/-}$ mice secreted 40% more Hcy into medium than did control hepatocytes (125). In addition, PEMT-mediated hepatic methylation of PE could be a major source of plasma Hcy. Mammals are estimated to have at least 50 AdoMet-dependent methylation reactions (159). Earlier report showed that in humans, ~ 70% of AdoMet was consumed for the biosynthesis of creatine (160). However, with the latest studies

on the significance of PEMT in the utilization of AdoMet, the methyl balance in humans may need to be re-evaluated and the contribution of creatine biosynthesis in the utilization of AdoMet is likely less than the previous estimation (161,162).

1.3.3 PEMT and obesity

It is unexpected that *Pemt*$^{-/-}$ mice are resistant to weight gain and protected from insulin resistance when fed a HF diet. Over 10 weeks of HF feeding, *Pemt*$^{-/-}$ mice maintain constant body weight, whereas *Pemt*$^{+/+}$ mice gain over 10 g of weight and show significant WAT hypertrophy (33). Unfortunately, *Pemt*$^{-/-}$ mice also develop NASH (33,120). The subsequent journey to explore the potential mechanisms for the resistance to diet-induced obesity (DIO) in *Pemt*$^{-/-}$ mice has been exciting.

Due to its quantitative relevance to hepatic PC production, insufficient PC might lead to the resistance to DIO in *Pemt*$^{-/-}$ mice. However, HF-fed *LCTα*$^{-/-}$ mice become as obese and insulin resistant as the control mice (33). *LCTα*$^{-/-}$ mice also swiftly develop NASH when fed the HF diet (33). Thus, the resistance to DIO in *Pemt*$^{-/-}$ mice is due to factors beyond a compromised PC production and VLDL secretion, which have been characterized in both *Pemt*$^{-/-}$ and *LCTα*$^{-/-}$ mice (73). Interestingly, dietary choline supplementation (2.7 g of choline/kg diet) to HF, which contains 1.3 g of choline/kg diet, completely prevents the resistance to DIO in *Pemt*$^{-/-}$ mice (33). Concomitant with the effect on insulin resistance in *Pemt*$^{-/-}$ mice, choline increases the expression of hepatic glucagon receptor, phosphorylated cAMP-activated protein kinase and serine-307-phosphorylated insulin receptor substrate 1 (163). Thus, choline might regulate hepatic gluconeogenesis via increasing glucagon action (163). The insufficiency of dietary choline likely causes reduced weight gain, as *Pemt*$^{+/+}$ mice demonstrate significant less

weight gain and improved insulin sensitivity when fed the choline-deficient HF diet for 12 weeks (33). Moreover, *ob/ob* mice fed a choline-deficient HF diet also gain less weight and exhibit improved insulin and glucose tolerance compared to mice fed the choline-supplemented diet (163).

Choline insufficiency in HF-fed *Pemt*$^{-/-}$ mice leads to the protection against DIO, but it remains unclear which choline metabolite(s) is (are) relevant. Betaine, the oxidized form of choline, is an important methyl-group donor and osmolyte. Oral addition of betaine has shown a beneficial effect on fatty liver conditions caused by alcohol, sucrose or others (164,165). But, dietary betaine supplementation has no effect on body weight gain or insulin sensitivity in HF-fed *Pemt*$^{-/-}$ mice (33).

The resistance to DIO in *Pemt*$^{-/-}$ mice could also be attributed to aberrant energy homeostasis. One possibility is that lack of PEMT affects adipogenesis or lipid hydrolysis in adipose tissue, since PEMT is present in the WAT (75). Most recently, an increased mitochondrial PE level caused by PEMT deficiency in mice was shown to modulate ATP production and decrease hepatic gluconeogenesis, which contributed to the regulation of whole body glucose metabolism (166). Moreover, HF-fed *Pemt*$^{-/-}$ mice exhibit increased oxygen consumption and elevated respiratory exchange ratio examined by indirect calorimetry in metabolic cages (33), suggesting an increase of energy expenditure and a preference of glucose over lipids as fuel respectively.

1.4 Vagus nerve and metabolism

1.4.1 Vagus nerve

The vagus nerve, also known as the cranial nerve X, is different from all the other cranial nerves due to its most extensive distribution (167). It wanders along the esophagus and major arteries, and predominantly innervates the thoracic and abdominal cavities (167). The vagus nerve is responsible for the parasympathetic innervation of the upper abdominal organs (167,168). It originates from four nuclei in the medulla oblongata: dorsal nucleus, nucleus ambiguus, nucleus of tractus solitarius (NTS) and spinal nucleus of trigeminal nerve (169). Axons in the dorsal nucleus generate the pre-ganglionic parasympathetic visceral efferent (motor) fibers of the vagus nerve (169). The motor neurons in the nucleus ambiguus, together with cranial nerves IX, X, and XI, give rise to parasympathetic nerve fibers innervating the heart (169). The NTS receives signals derived from the respiratory system, the taste buds and the visceral gastrointestinal tract via the afferent (sensory) fibers (169). In addition, the spinal nucleus of trigeminal nerve obtains general somatic information via afferent nerve fibers from the external auditory meatus and the ear (169). The majority (80%) of vagus nerve fibers are afferent fibers, which relay neuronal signals to the NTS (167). From the NTS, the vagus nerve projects to different aspects of the brain including the dorsal raphe nuclei in the brain stem and hypothalamus (167).

The understanding of the distribution of the vagal afferent nerve has been largely obtained from the retrograde tracing (tracer injected into peripheral organs) and anterograde tracing (tracer injected into the nodose ganglia) studies (167). In the earliest tracing studies, tritiated amino acids were injected into the nodose ganglia and later, DiI (1,1′-dioleyl-3,3,3′,3′-tetramethylindo-carbocyanine), an intensely orange fluorescent carbocyanine dye and wheat germ agglutinin-horseradish

peroxidase (WGA-HRP) have been widely used for tracing afferent nerve fibers (167). The labeling materials have been evolving with the availability of other dyes such as diaminobenzidine (DAB) and fluorescently labeled streptavidin (167). Several other experimental approaches can also be used to explore the function and anatomy of the vagus nerve including immunohistochemistry, electrophysiological recording and selective ablation (170). Unlike the sympathetic postganglionics and dorsal root afferents, which can be traced by immunohistochemical analysis of their specific neurochemical markers such as calcitonin gene-related peptide and tyrosine hydroxylase, there are no generally unique neurochemical markers known that are exclusively expressed in the vagal nerve (170). However, certain markers may reasonably predict the presence of the vagal afferent nerve and its terminal structure in specific regions. For instance, calretinin, a calcium binding protein, is a fairly good marker for vagal afferent innervation of the esophagus (171) and might be a relatively specific marker for vagal afferentation in the liver (170). This is mainly due to the fact that the distribution of calretinin-immunoreactive fibers in the liver, portal vein, bile ducts and paraganglia is similar to the pattern gained from DiI-tracing study, as well as the absence of calretinin in the dorsal root afferent nerve fibers (170). In addition, the central terminal of vagal afferent nerve is partly determined by electrophysiological recording and c-Fos studies, in addition to the retrograde and anterograde tracing studies (170).

The left and right cervical vagus nerve is formed as the afferent and efferent rootlets converge and leave the cranium through the jugular foramen (167). They run through the nodose ganglia, where the afferent neurons are located (167). These

neurons contain axonal projections to the periphery and central projections into the NTS and other compartments of the dorsal vagal complex (170). They possess a variety of transmitters and receptors, and generally release glutamate at the central terminals (170). The cervical vagus nerve runs in parallel with the carotid artery (167). The first branches, namely the auricular and meningeal branches, leave the cervical vagus at the level of the jugular ganglion, and project to the skin of the external acoustic meatus and the dura of the posterior cranial fossa, respectively. The pharyngeal branches splitting off at the level of the nodose ganglion innervate the larynx, caudal pharynx and upper esophagus (167). The cardiac branches mainly contain afferent fibers from barosensors of the aortic arch. The recurrent laryngeal nerve, given off from the vagus nerve at the level of the subclavian artery (the right side) and the aortic arch (the left side), is closely attached to and innervates the trachea and esophagus (167). Overall in the upper mediastinum, the vagal branches innervate the main bronchi, lungs, and heart.

Passing through the diaphragm along with the esophagus, the left and right cervical vagus nerves contiguously become the anterior and posterior vagal trunks, respectively in the abdomen (167). The branching and distribution pattern of the abdominal vagus nerve has been well characterized in rats, with large similarity to that in humans (167,172). The anterior vagal trunk branches into the common hepatic, anterior gastric and anterior celiac branches (167). The vagal afferent innervation is predominantly wired through the left nodose ganglion and the common hepatic branch of the vagus nerve, with minor portions through the right nodose ganglion and the celiac branch (170). Based on studies using electron microscopy, subdiaphragmatic vagal trunks in rats are estimated to contain about 11,000 nerve fibers, among which ~8000

are afferent and the remaining ~3000 are efferent (167). The myelinated nerve fibers compose less than 1% of the total fibers. The common hepatic branch is given off typically at about one third the distance between the diaphragm and gastric cardia (172). It contains about 3000 fibers in total, among which, 2200 are afferent, 200 are efferent, and 600 are non-vagal fibers (173). The name of this branch is somewhat misleading since the major portion of this branch does not serve the liver, portal vein, and bile ducts; instead it innervates the proximal duodenum, pancreas, pylorus, and distal gastric antrum (167,170).

Vagal preganglionic efferent neurons reside in the dorsal motor nucleus of the vagus, projecting to the abdominal organs where they are called postganglionic neurons. In the gut, the efferent neurons are located in the enteric plexuses (170). In the pancreas, they are present in the interlobular pancreatic ganglia (174). However, the location of these parasympathetic ganglia in the liver is still unclear (170). The majority of the efferent neurons are cholinergic, whereas up to 10% are catecholaminergic (170). The preganglionic neurons are generally cholinergic, whereas the postganglionic neurons are catecholaminergic (170). Some postganglionic neurons also contain nitric oxide, vasoactive intestinal peptide, gastrin-releasing peptide, neuropeptide Y, and other transmitters (170). Notably, in addition to axons and glial cells, the vagal trunks also contain dendritic cells, important in the immune defense system, and paraganglia, which are demonstrated to be in the major trunks adjacent to branch points (167).

The knowledge regarding the function of the vagus nerve has been largely gained from disruption of the nerve (167). Vagal rhizotomy is a procedure that selectively interrupts the efferent or afferent nerve fibers at an easily accessible level. This

technique can be easily applied to cats, where the vagal efferent fibers are relatively well separated from the afferent fibers, but not in rats (167). Pharmacologically, capsaicin destroys a class of thin, unmyelinated primary afferent nerve fibers (167). Due to the presence of the vanilloid receptor on the afferent neurons, binding of capsaicin to these receptor causes apoptotic cell death and neurotoxicity (167). Therefore, application of capsaicin to the vagal nerve results in non-functional afferent nerve fibers and is the best procedure for selective vagal deafferentation (167). However, it should be noted that not all vagal afferent nerve fibers are capsaicin-sensitive. Histologically, hepatic branch vagotomy has been extensively used to denervate the liver. As aforementioned, the common hepatic branch innervates the stomach, pancreas and proximal duodenum, in addition to the liver (167,170). This makes it extremely difficult to selectively transect the hepatic branch of the vagus nerve (the only vagal fibers that terminate in the liver). Herein, cutting the gastroduodenal vagal branch has been suggested to be applied as a control procedure for vagotomy studies on the common hepatic branch of vagus nerve (167). Extra caution should be taken to interpret the data from such studies.

1.4.2 Vagus nerve and obesity

The vagus nerve is a major component in the parasympathetic autonomic nervous system. In addition to its regulatory role in the cardiovascular and respiratory function, the vagus nerve is implicated in a variety of visceral functions including gastrointestinal motility and hormonal secretion, pancreatic secretion, hepatic glucose production, and others. Extensive studies over the past decade have unravelled a significant role of the vagus nerve in obesity. In humans, obese subjects show reduced activity of the vagus

nerve (175-177). Vagus nerve stimulation, a FDA approved approach for the treatment of epilepsy and depression, has been demonstrated to inhibit appetite and cause weight loss (169,178,179). The amount of weight loss was suggested to be proportional to the status of obesity (179). This likely explains a preliminary observation that no significant body weight change was observed in 21 patients receiving vagus nerve stimulation for the treatment of epilepsy (180). Furthermore, bariatric surgery, currently the most efficient approach for treating obesity, is also involved in denervation of the vagus nerve (168). The vagus nerve regulates food intake and energy metabolism requiring the sensory signals derived from the gastrointestinal tract and other abdominal organs, and the efferent motion projecting from the central to the visceral organs. Moreover, it is a major constituent of a neural inflammatory reflex—cholinergic anti-inflammatory pathway, which is associated with energy homeostasis (181,182).

The sensory signals transmitted via the vagus nerve primarily derive from the gastrointestinal tract (168,183). The gastrointestinal tract senses all macronutrients absorbed from intestinal digestion and regulates food intake and energy balance through distinctive mechanisms (183). In the oral cavity, food intake is directly monitored via the afferent input from the taste receptors on the tongue and palate (184). Additional contribution comes from the trigeminal somatosensory system (168), which is composed of a variety of receptors including thermoreceptors, mechanoreceptors and chemoreceptors. In the stomach, the vagal nerve senses the ingested food via the mechanical touch in the mucosa and the stretch and tension in the external muscle layers, the latter of which is also present throughout the esophagus and gastrointestinal tract (168). The afferent vagus nerve also innervates the gastric mucosa, where it likely

senses hormones locally released from the stomach. Leptin production is rapidly motivated by food intake in the mucosa of stomach and this hormone appears to activate the vagal afferent nerve (185). Ghrelin, on the other hand, is mainly secreted from the mucosa of an empty stomach and its production is rapidly suppressed by food ingestion (186). Ghrelin stimulates appetite via the afferent vagus nerve, and this effect is abolished in rats with subdiaphragmatic vagotomy or with capsaicin-induced vagal deafferentation (187), and in human patients through surgical procedures involving vagotomy (188). In the upper small intestine, the vagal afferent nerve does not sense luminal nutrients directly, but the locally secreted hormones such as cholecystokinin. It is notable to mention that in response to glucose, glucose-dependent insulinotropic polypeptide, secreted from K-cells concentrated in the upper small intestine, is not sensed by the vagal afferent nerve due to the absence of its receptor (168,189). Consistently, the production of this polypeptide is not affected by vagotomy or vagal stimulation (168). Moreover, all macronutrients in the gut lumen are able to stimulate the secretion of polypeptide YY and glucagon-like peptide-1 mainly from the L-cells in the lower gut (168,190). These two orexigenic hormones could function through firing the vagal afferent nerve, as well as acting directly on the brain though the circulation (189,191). Together, the vagal afferent nerve detects the luminal contents in the gastrointestinal tract via direct mechanical touch such as distension and stretch, and indirect detection mediated by the released peptides and transmitters, which interact with the brain and the peripheral organs through the circulation system.

In addition to the gastrointestinal tract, the vagal afferent nerve also innervates other abdominal organs including the liver, pancreas and adipose tissue. In the liver, the

major and possibly only neural route is through the liver hilus, along the hepatic artery, portal vein, and bile ducts (170). There is no neuroanatomical evidence supporting the direct sensory innervation in the hepatic parenchyma (170). Interestingly, hepatic over-expression of peroxisome proliferator-activated receptor (PPAR)γ2 in mice increases blood pressure, decreases peripheral adiposity and improves insulin sensitivity, and these effects require an intact hepatic afferent vagus nerve (192,193). Similarly, the hepatic afferent vagus nerve is also essential for the effect of hepatic PPARα activation on glucocorticoid-mediated insulin resistance and hypertension (194). The pancreas is sparsely innervated by the vagal afferent fibers (195). Thus, it mainly sends metabolic signals to the brain via the hormonal route mediated by the pancreatic hormones including insulin, amylin, and glucagon, although glucagon also suppresses food intake in a vagal afferent nerve-dependent manner (196). As for WAT, its vagal innervation status remains inconclusive based on the limited experimental data (197,198).

The brain integrates the afferent signals and projects to the gastrointestinal tract, pancreas and liver via the vagus efferent nerve (168,183). This vagal efferent outflow can affect energy expenditure through several ways. It controls the levels of gastrointestinal and pancreatic hormones involved in satiation and hunger through regulating the intestinal motility and absorption rate of nutrients, as well as the exposure of nutrients to the enteroendocrine cells (168). It also affects pancreatic hormone secretion (168). In particular, lesions in the ventromedial hypothalamus cause an acute elevation of plasma insulin in a vagal efferent-dependent manner (199). Furthermore, vagal efferent innervation to the liver is implicated in glucose and lipid metabolism. Central inhibition of fatty acid oxidation suppresses hepatic glucose production via

activating the ATP-sensitive potassium channels in the hypothalamus (200,201). Similarly, selective increase of glucose in the hypothalamus also curtails hepatic VLDL secretion and this effect of glucose is lost in rats with DIO (202). These central regulations of hepatic glucose and lipid metabolism are mediated by vagal efferent fibers running through the common hepatic branch (200-202). Additional other studies have also highlighted a role of neuronal circuits via the vagus nerve, particularly the efferent nerve, in the regulation of metabolism. Activation of extracellular regulated kinase signaling in the liver is able to induce the proliferation of pancreatic β-cell through the vagus nerve (203). The accumulation of lipid in the upper intestine and the secretion of intestinal cholecystokinin suppress hepatic glucose generation via triggering the gut-brain-liver circuit (204,205).

The vagus nerve mediated cholinergic anti-inflammatory reflex can suppress obesity associated inflammation, which in turn counteracts obesity and its complications (206). Obesity is an inflammation associated metabolic disorder (207,208). Adipose tissue is one major origin of pro-inflammatory factors in obese individuals (discussed later in section 1.6). The inflammatory pathways are also activated in various other tissues including the liver, brain and skeletal muscle (207,208). Recent studies show that the onset of inflammation in obese individuals also attributes to gut microbiota (209,210).

The inflammatory reflex, which is activated by cytokines or pathogen-derived products, is integrated by the afferent vagus nerve signalling, the central control of the brain and the functional output mediated by the efferent vagus nerve (181,206). It regulates the production of cytokines. The absence of this neuronal-inflammatory reflex

leads to cytokine toxicity and extensive immune response (206,211). Intraperitoneal injection of bacterial endotoxins such as lipopolysaccharide or inflammatory factor such as interleukin(IL)-1β activates the vagal afferent nerve with enhanced electrical discharge and induces fever, hyperalgesia and other behavior changes (170). These reactions could be interrupted by subdiaphragmatic vagotomy or selective vagotomy of the common hepatic vagal branch in some cases (170,206). On the other hand, activating this inflammatory reflex attenuates the production of proinflammatory cytokines and the systematic effect to endotoxin (211).

The vagal efferent effect is regulated mainly by the release of acetylcholine in the central and the peripheral tissues (212). In the brain, muscarinic acetylcholine receptors are expressed and implicated in this regulation of systematic cytokine production (212,213). An insufficient supply of acetylcholine impairs the central nervous system through muscarinic acetylcholine receptors, which are required for the development of DIO (214,215). Central control of the acetylcholinesterase activity can activate the efferent cholinergic arm of the inflammatory reflex through the muscarinic receptor (212). Additionally, vagus nerve-derived cholinergic signalling through the M3 muscarinic receptor in the pancreas has been well documented to be implicated in promoting insulin release (216,217). In the peripheral tissues, the α7 nicotinic acetylcholine receptor (nAChR) plays a principle role in the relay of this inflammatory process (211,218). Other than in macrophages, α7nAChR is also expressed in monocytes, T cells, dendritic cells, endothelial and other non-neuronal cells (206,219). When fed a HF diet, mice lacking α7nAChR develop greater impairment in glucose homeostasis, insulin sensitivity and insulin signaling in the muscle and liver than control

mice (220). In humans, the expression of α7nAChR in adipocytes is significantly reduced in obese individuals, whereas this decrease is restored partially with weight loss (221). Administration of nicotine significantly improves glucose homeostasis and insulin signalling in the liver, adipose tissue and skeletal muscle in HF-fed mice (220). Several selective α7nAChR agonists such as TC-7020 and GTS-21 show anti-inflammatory properties (206). Application of TC-7020 to *db/db* mice reduces weight gain and food intake, and improves the blood hyperlipidemia and hyperglycemia (222). A selective α7nAChR agonist TC-6987 has also been tested in a phase II clinical trial on patients with type 2 diabetes mellitus (223). Taken together, activating the vagus nerve-mediated cholinergic anti-inflammatory pathway provides a potential avenue for attenuating the inflammation, insulin resistance and other obesity-related metabolic complications.

1.5 ER stress and metabolic syndrome

1.5.1 ER structure and function

In eukaryotic cells, the ER is a main membrane-bound subcellular organelle that is implicated in various cellular functions. The ER membrane accounts for over 50% of the total cellular membranes (224). The ER, stretching from the nuclear envelope to the plasma membrane, is composed of cisternae and microtubules (224). It plays a crucial role in protein synthesis, folding and maturation, and presumably it produces around one-third of the total proteome (225). It is the main site for protein sorting and trafficking (225,226). ER chaperones such as binding immunoglobulin protein (BiP, also known as 78 kDa glucose-regulated protein or heat shock protein 5), calnexin and calreticulin bind

to the hydrophobic domains of proteins, inhibit protein aggregation and facilitate the folding of newly synthesized proteins (225). Protein posttranslational modifications including the formation of disulfide bond and N-linked glycosylation in the ER are important for protein folding (227). The ER is also the major intracellular reservoir for Ca^{2+} (227). The Ca^{2+}concentration in the ER lumen is normally maintained at around 1–2 mM, whereas the cytosolic concentration is around 0.1 μM (227). The ER Ca^{2+} homeostasis is maintained by the ryanodine receptors and inositol-1,4,5-triphosphate receptors mediated efflux and via the ATP-dependent sarco/ER Ca^{2+}-ATPase regulated influx (224,227). The ER regulates cellular signaling, metabolism and survival particularly via ER Ca^{2+} through the elaborative communication between the ER and other organelles, including the plasma membrane, nucleus, mitochondria and Golgi apparatus (227). In addition, several ER chaperones are Ca^{2+} dependent (227). Moreover, the ER is also involved in the biosynthesis of lipid such as sterols and phospholipids (4,228).

The function of ER can be disturbed by various factors such as altered protein glycosylation, disrupted Ca^{2+} homeostasis, cellular oxidative stress, energy deprivation or overload, and inflammatory stimuli (225,226). In particular, the accumulation of unfolded and misfolded proteins in the ER lumen is referred to as ER stress (225,226). ER stress initiates a series of intracellular signaling pathways known as the unfolded protein response (229) to resolve the defect in protein folding and to restore protein homeostasis (230). Activated UPR signals increase the ER capacity for protein folding and modification, reduce protein synthesis and increase ER-associated protein degradation (ERAD). In the case where ER stress is too severe and/or the UPR is not

able to restore protein homeostasis, the UPR may also activate numerous apoptotic signaling pathways leading to apoptotic cell death (231). ER stress can also be caused by impaired lipid homeostasis. Overload of palmitate and cholesterol increases their incorporation into the ER and induces ER stress (232,233). Palmitate may also evoke ER stress via elevating intracellular reactive oxygen species (232). In contrast, polyunsaturated fatty acids suppress ER stress (234). Moreover, in the liver of *ob/ob* mice, reducing the PC/PE ratio by silencing PEMT alleviates ER stress and restore Ca^{2+} equilibrium caused by a long-term feeding of a HF diet (145).

1.5.2 The unfolded protein response

In mammalian cells, the UPR is composed of three canonical branches mediated by three ER membrane transducer proteins (Figure 1.5): protein kinase-like ER kinase (235), inositol-requiring enzyme-1 (IRE1), and activating transcription factor (ATF)6α (226,230). Binding of the ER chaperone BiP inactivates signaling through these transducers (230). Upon ER stress, BiP released from the UPR transducers activates the UPR and binds to increased cellular unfolded/misfolded proteins (225,230). Three branches of the UPR trigger distinct and overlapping pathways to re-establish ER homeostasis.

Activation of PERK, a transmembrane protein with a cytosolic Ser/Thr kinase domain, requires dimerization and *trans*-autophosphorylation (230). Activated PERK phosphorylates the α subunit of eukaryotic translation initiation factor 2 (eIF2α) at Ser51, which in turn attenuates translation initiation of global protein synthesis and reduces the ER protein folding load (236,237). In addition to PERK, eIF2α can also be phosphorylated by three other kinases: double-stranded RNA-activated protein kinase,

general control non-derepressible kinase 2 and heme-regulated inhibitor kinase in mammals (226). Double-stranded RNA-activated protein kinase has recently been shown to be activated during ER stress and involved with the UPR (238). However, the relative contribution of these three kinases in ER stress and the UPR is largely unknown (226). On the other hand, protein phosphatase PPP1 directly dephosphorylates eIF2α (239). Upon ER stress, eIF2α phosphorylation-mediated translation attenuation is reversible by growth arrest and DNA damage-inducible protein 34 (GADD34) and CReP (the product of *Ppp1r5a* and *Ppp1r5b* respectively), two regulatory targeting subunits of protein phosphatase PPP1 (239). In addition to global inhibition of protein translation, phosphorylated eIF2α is broadly involved in transcriptional regulation (226). Through the transcriptional regulation of ribosomal RNA, eIF2α selectively elevates the translation of ATF4, Nrf2 (nuclear erythroid 2 p45-related factor 2), and NF-κB (nuclear factor kappa β), a master transcription factor in the cellular inflammatory response (226). ATF4 promotes expression of numerous genes including GADD34, a negative regulator of eIF2α, and C/EBP homologous protein (229), a transcription factor crucial in ER stress-induced apoptosis (230,240,241). Notably, ATF4 also activates genes in glucose metabolism such as glucokinase and phosphoenolpyruvate carboxykinase (240,241). Moreover, through activation of Nrf2 and ATF4, the PERK signaling pathway is engaged in anti-oxidative stress program, regulating the expression of heme oxygenase-1, thioredoxin reductase 1, and the glutathione *S*-transferases (242)

IRE1 is a transmembrane protein containing an endoribonuclease domain and a Ser/Thr kinase domain in the cytoplasm. The IRE1-mediated UPR branch is the most conserved in the evolutionary sense, and one of the major pathways involved in

enhancing the protein folding capacity in the ER in response to ER stress (226). In mammals, there are two isoforms of IRE1, IRE1α and IRE1β (239). IRE1α is ubiquitously expressed, whereas IRE1β is primarily expressed in the intestinal epithelium (239). Similar to PERK, IRE1α activation depends on its dimerization and *trans*-autophosphorylation (239). The endoribonuclease activity of IRE1α cleaves a 26 base-pair intron from the mRNA of the *X-box binding protein-1 (XBP1)*, causing a translational frameshift, which is translated into the spliced (active) form of XBP1 (XBP1s) (243). XBP1s transcriptionally activates a number of genes crucial in protein folding such as protein disulfide isomerase and BiP and proteins associated with ERAD (for example, ER degradation-enhancing α-mannosidase-like protein). Moreover, the IRE1α-XBP1s axis also regulats ER biogenesis and phospholipid synthesis (226). In addition to XBP1, IRE1 also degrades a subset of mRNAs in a stress-dependent manner (226), and microRNAs, which results in activation of apoptotic and inflammatory pathways (244). As a protein kinase, IRE1 interacts with tumour necrosis factor (TNF)α receptor-associated factor 2 and activates the c-Jun N-terminal kinase (JNK) and NF-κB pathways independent of XBP1s (225,239).

The last canonical arm of UPR is mediated by ATF6α (230). In response to ER stress, ATF6α translocates to the Golgi, where it is cleaved by the serine protease site-1 protease and the metalloprotease site-2 protease generating the active form of the transcription factor (245). Activated ATF6α proceeds into the nucleus and enhances the expression of genes containing ER stress elements, UPR elements and cAMP response elements (CRE) in their promoters (230). As a result, ATF6α increases the production of chaperones such as BiP and proteins involved in ERAD such as the ER

degradation-enhancing α-mannosidase-like protein (230). ATF6α also regulates the mRNA expression of *XBP1* and directly interacts with the XBP1 protein, targeting proteins in the UPR as discussed in the IRE1 branch of the UPR (230). In mammals, other proteins including CRE binding protein (CREB) 3, OASIS (CREB3 like-protein1), CREB3L2 (CREB3 like-protein2), CREBH (CREB3 like-protein 3) and Tisp40 (CREB4), share sequence similarity with ATF6α, a conserved bZIP region adjacent to a transmembrane domain, and have been shown to be implicated in the ER stress response (246). These ATF6α-like proteins exhibit distinct tissue distribution patterns and respond to different stimuli (246). The evolutionary and functional significance of these protein remains to be determined (226).

When the UPR is insufficient to alleviate ER stress or the stress is excessive or prolonged, the UPR can induce apoptosis and cause cell death (230). The signaling pathways involved in apoptosis are tightly regulated, although the mechanisms by which the UPR leads to cell survival or death remain to be unravelled (230). Activation of the PERK and ATF6α pathways induces the expression of CHOP, the master regulator of ER stress induced apoptosis (231,239). Activation of the IRE pathway promotes the caspase-12 and JNK signaling and activates the proapoptotic Bcl-2 proteins BAX and BAK (231,247). Activated IRE1α also recruits TNF receptor-associated factor 2 and apoptosis signal-regulating kinase 1 to the cytosolic leaflet of the ER membrane (231). All three branches of the UPR are involved in the regulation of the NF-κB signaling pathway during ER stress. In addition, ER stress-evoked mitochondrial dysfunction contributes to apoptosis (239). In response to ER stress, the ER releases Ca^{2+}, which can be taken up by mitochondria via the MAM (248).

1.5.3 ER stress and metabolic diseases

ER stress and the activated UPR have shown a wide impact on diverse pathological conditions including neurodegenerative disorders, cancer, and various inflammatory disorders (239,249). Recent studies also suggest a significant contribution of ER stress and the UPR to metabolic diseases, including insulin resistance, diabetes, obesity, non-alcoholic fatty liver and atherosclerosis (226,239). In particular, the association of ER stress with obesity and NAFLD will be briefly overviewed here. Targeting ER stress and the UPR provides another avenue for drug design or discovery and for seeking potential treatment strategies for the above pathological conditions (225,239).

The ER stress in the liver and WAT was first described in mice fed a HF diet and in *ob/ob* mice (250). The mechanisms for the emergence of ER stress in various tissues including the liver, adipose tissue, and pancreas from obese mice remain inconclusive (226). One theory is that ER stress is driven by increased demand of synthesis in response to the excessive energy supply. The liver has the highest protein synthesis rate and the majority of proteins are generated in the ER (226). Parallel with this notion, the adipose tissue, which has a significant endocrine function, also faces high requirement for protein synthesis (226). A second possibility derives from the increased free fatty acids. Excessive free fatty acids cause ER stress in hepatocytes, pancreatic β cells, and macrophages and certain free fatty acids also induce cellular inflammatory response (226). However, it should be noted that some fatty acids exhibit beneficial effects, for example, C16:1n7-palmitoleate suppresses lipid accumulation in the liver

(251,252). Additionally, ER stress could be also linked to other stimuli such as inflammatory mediators, reactive oxygen species, nitric oxide and hypoxia (226).

ER stress and the UPR are involved in metabolism. Overexpression of BiP in the liver of *ob/ob* mice reduces hepatic ER stress, attenuates hepatic TG and cholesterol accumulation and improves insulin sensitivity (253). Similarly, overexpression of ER chaperone oxygen-regulated protein 150 in *db/db* mice (diabetic mouse model lacking leptin receptor) significantly ameliorates insulin resistance and glucose tolerance (254). In mice, XBP1s is elevated in the liver coinciding with increased hepatic lipogenesis, whereas selective deletion of XBP1s in the liver reduces hepatic lipid production (255). Recent studies suggest that XBP1s is also involved with regulating hepatic gluconeogenesis via interacting with the transcription factor forkhead box O1 and the regulatory subunits of phosphoinositide 3-kinase, p85α, and p85β (256,257). Moreover, ATF6α inhibits hepatic glucose production, whereas a reduced level of ATF6α contributes at least partially to the enhanced hepatic gluconeogenesis in obese mice (258). The role of ER stress in adipogenesis remains inconclusive due to the conflicting results from the limited available data (249).

ER stress is also linked with lipotoxicity, inflammation, apoptosis and steatosis in the liver (259). ER stress and activation of the UPR have been described in the livers from patients with NAFLD or NASH (260). Reducing phosphorylation of eIF2α by overexpressing GADD34 in the liver reduces hepatic glycogen levels in lean mice and prevents steatosis when mice are fed a HF diet (261). Mice with hepatocyte-specific deletion of IRE1α demonstrate impaired VLDL assembly and secretion due to reduced activity of microsomal triglyceride-transfer protein (262). When challenged with a high

fructose diet, these mice develop more severe steatosis compared to control mice (262). In addition to its central regulatory role in the acute phase response (263), CREBH, a liver-specific transcription factor in the UPR, regulates hepatic lipid homeostasis via regulating lipogenesis and lipolysis (264). CREBH is also involved in plasma TG metabolism via regulating the activity of lipoprotein lipase (265). Mice with deletion of CREBH are sensitive to HF-induced steatosis and are hyperlipidemia (264,265).

Extensive studies are ongoing seeking potential drugs to modulate the UPR and ER stress (225,239). Notably, chemical chaperones, a group of compounds with low-molecular mass, are able to facilitate protein folding, reduce ER stress and improve ER function. 4-phenylbutyrate (PBA) and tauroursodeoxycholic acid are two widely studied chemical chaperones in a disease setting and have been approved by FDA for the treatment of primary biliary cirrhosis and urea cycle disorders respectively. PBA improves ER stress in the livers from obese mouse models, and exhibits a beneficial impact on insulin sensitivity, leptin sensitivity and glucose homeostasis (266,267). PBA also improves the insulin resistance and β-cell dysfunction in obese patients (268). Consistently, tauroursodeoxycholic acid alleviates insulin resistance in the liver and muscle from obese humans with no significant effect observed in adipose tissue (269). Furthermore, administration of PBA or tauroursodeoxycholic acid protects the liver from injury caused by ischemia–reperfusion and improves liver regeneration after partial hepatectomy (270,271). Due to the significant presence of ER among organs in the body, chemical chaperones and other modulators targeting ER stress and the UPR might provide potential treatments for diseases beyond obesity and fatty liver (225,239).

1.6 Adipose tissue

1.6.1 Overview of adipose tissue

Obesity increases the risk for the development of many other metabolic conditions such as hyperinsulinemia, dyslipidemia, NAFLD and cardiovascular diseases. One major feature of obesity is the increased fat mass, particularly the visceral fat. The epidemic of obesity worldwide has greatly accelerated the understanding of adipose tissue. Adipose tissue is an organ with multiple depots, subcutaneous (under the skin) depots and visceral (surrounding the internal organs) depots (272,273). In rodents, there are two main subcutaneous depots, anterior and posterior, and several visceral depots including the mediastinal, mesenteric, retroperitoneal, omental, and abdomino-pelvic depot (in females) and the epididymal depot (or gonadal depot in males) (274). Adipose tissue is divided into two types: WAT and brown adipose tissue (BAT) (275). In rodents, most of the anterior subcutaneous depots are composed of BAT, and particularly the interscapular region is considered as the classic BAT depot, whereas the posterior subcutaneous depots are mostly white (274). For visceral depots, the mediastinal is mostly brown, the abdomino-pelvic depot is composed of BAT and WAT equally, whereas the omental, mesenteric and epididymal are predominantly white (273,276). The composition of BAT and WAT in each depot varies depending on the genetic background, age, gender and environmental conditions such as temperature, diet, and exercise (273).

Both WAT and BAT contribute to balancing energy store and expenditure, and serve as therapeutic targets for the treatment of metabolic syndrome (277). WAT used

to be classified as an inert storage tissue for excessive energy, but has since emerged to be an endocrine organ (277,278). BAT, on the other hand, is distinguished in energy expenditure and functions to maintain core body temperature by non-shivering thermogenesis through uncoupling protein (UCP)1 (279). In humans, BAT has long been assumed to be present in new born babies and disappears in adults (273). BAT has now been detected in adult humans by ^{18}F-fluordeoxyglucose positron emission tomography/computed tomography (280-282). In addition, both WAT and BAT are vascularized and innervated, although BAT is more enriched with vessels and nerves than WAT (273,283,284). The nerves are predominantly adrenergic (284,285).

Adipose tissue is mainly composed of adipocytes, including white, brown and beige adipocytes (277). Other than mature adipocytes, which have high physiological adipocyte plasticity, adipose tissue also contains stromal vascular fraction cells, including preadipocytes, fibroblasts, endothelial cells and immune cells (273,275). Morphologically, white adipocytes are unilocular and contain one single large lipid droplet, which counts for 90% of total cell volume (286). The nucleus, usually under-developed Golgi apparatus, and other cellular organelles such as ER and elongated mitochondria with randomly oriented cristae are squeezed by the lipid droplet in the thin cytoplasm (274,286). By contrast, brown adipocytes are multilocular and consist of many small lipid droplets and dense spherical or ovoid mitochondria, which are enriched with laminar cristae (274). The rich mitochondria and the dense vascularity in BAT are two major causes of its “brown” colour (274,286). In addition, the nucleus is usually spherical and centrally located in brown adipocytes (274). Beige (or “brite”) adipocytes are newly defined inducible brown adipocytes, residing in WAT, primarily the

supraclavicular region (286,287) and muscle (288,289). Similar to classical brown adipocytes, beige cells are multilocular and rich in lipid droplets and mitochondrial contents (287). They express markers of the classical brown adipocytes and the beige-specific genes (286,287).

Both WAT and BAT go through active remodeling after establishment in early life (289). The capability of adipose expansion and activation in response to environmental changes including excessive food and cold environment relies on the presence of adipogenic precursor cells in adulthood and adipogenesis. Understanding the lineage origin of adipocytes and the process of adipogenesis is essential for seeking potential therapeutic treatment by targeting adipose tissue.

1.6.2 Adipocytes

It is generally accepted that mature adipocytes, both brown and white, derive from the embryonic mesoderm (289). Thus, they share the same developmental origin as other mesodermal tissues such as the skeletal muscle and bone (275,289). The only known exception is adipocytes in the skull, which derive from the stem cells residing in the ectodermal neural crest (289,290). It has only been recently established that adipogenic progenitor cells for both brown and white adipocytes are located within the vasculature of the adipose tissue anatomically (291,292). Adipogenic progenitor cells residing in other tissues appear to exhibit similar surface marker properties, such as PDGFR*α* (platelet-derived growth factor receptor *α*), cluster of differentiation (CD)29 and CD34, with adipose-residing progenitor cells (293,294). However, it is still an open question whether they share the functional similarity (289).

Brown adipocyte precursors express muscle-specific microRNAs and transcription factors (295,296). Lineage-tracing studies have demonstrated that brown adipocytes can derive from myogenic factor *(MYF)5*$^{+}$ and *PAX7* (paired box 7)$^{+}$ progenitors in the mesoderm as myocytes and also from skeletal muscle satellite cells in adulthood (277,297,298). However, white adipocytes and their precursors can derive from both *MYF5*$^{+}$ and *MYF5*$^{-}$ lineage (277). White adipocytes would preferentially originate from a *MYF5*$^{-}$ lineage, since they generally lack the characteristics of the myogenic gene expression (277,296,298). However, conditional depletion of phosphatase and tensin homolog, an ubiquitously expressed protein involved in regulation of cell cycle, driven by *MYF5*-Cre in mice causes a paradoxical overgrowth of specific WAT depots (299). Subsequent lineage-tracing studies confirm that some *MYF5*$^{+}$ adipocyte precursors are also present in WAT (299,300). Unexpectedly, some brown and white adipocytes also show endothelial origins in the lineage-tracing studies using an endothelial marker such as vascular endothelial cadherin, although not all endothelial markers are expressed in adipocytes (292,301).

Depending on the fat depots, beige adipocytes arise via two distinctive pathways: direct differentiation of brown adipogenic progenitors and transdifferentiation of mature white to brown adipocytes (274,289). It has been shown over a decade ago by Himms-Hagen *et al.* that beige cells derive from pre-existing adipocytes, which were presumed to be mature adipocytes (302). This transformation change from unilocular white adipocyte to beige adipocytes is inducible by cold or β3-adrenergic agonists (303). Cold stimulates the formation of beige cells from both adipogenic progenitors and mature white adipocytes (304,305). A recent study using a pulse-chase fat-mapping technique

by Wang *et al.* show that in responding to cold or β_3-adrenergic agonists, the majority of newly acquired beige cells arise from precursors rather than pre-existing adipocytes, at least in the subcutaneous depot (305). It is noteworthy to mention that the thermogenic features of beige cells are reversible: the expression of UCP1 is induced when exposed to cold, and is lost after mice are moved to a warm condition (304). Regarding the origin, beige adipocytes likely share the *MYF5*$^-$ lineage origin with white adipocytes, since they can arise from white adipocyte precursors *in vitro* when treated with PPARγ agonists (306,307). Following this, Spiegelman's group has cloned preadipocytes from the stromal vascular fractions of subcutaneous (inguinal) WAT using limited dilutions and identified specific markers, namely CD137 and TMEM26 (transmembrane protein 26), for beige precursors (308). Maintaining the thermogenic feature of *CD137*$^+$*TMEM26*$^+$ beige precursors requires constant stimulation (308). In another lineage tracing study, *PDGFR-α*$^+$ precursors are identified as a significant source of newly formed beige adipocytes upon adrenergic stimulation, and these precursors preserve 'bipotential' features because they can generate both beige and white adipocytes in *in vitro* culture (309). Thus, beige cells may arise from different adipocyte precursors in WAT.

The differentiation process from adipocyte precursors to mature adipocytes has been extensively studied (310,311). Briefly, the PPARγ and CCAAT/enhancer-binding protein(C/EBP)s (C/EBPα/β/δ) are the most well established transcription factors in directing the differentiation of both brown and white adipocytes (310,311). The brown adipogenic program is regulated by PPARγ coactivator (PGC)1α and transcription cofactor PRDM16 (PR domain containing 16), the latter of which interacts with C/EBPβ

(312). Recent evidence suggests that modulators of PPARγ binding activity may specify brown adipogenic lineage transcriptional activity. Deacetylation of PPARγ by NAD-dependent deacetylase SirT1, which is essential for the recruitment of PRDM16 to PPARγ, promotes the browning of white fat (313). Transcription factor EBF2 (early B-cell factor 2) acts as a transcriptional regulator and is also required for the brown adipogenic process via the recruitment and binding of PPARγ to its target genes (314). Moreover, SREBPs are a family of well-known transcription factors regulating cellular lipogenesis and lipid homeostasis (315). Finally, adipogenesis is also affected by other factors such as adipokines, cell cycle regulating proteins and age (119).

1.6.3 WAT, an energy storage tissue

One main function of WAT is to control energy balance between storing fatty acids in the form of TG and mobilization of TG (272). TG storage is augmented in postprandial state and stimulated by insulin. Under energy surplus, the expansion of WAT largely depends on an increase in adipocyte volume, as well as adipocyte number (305). The number of adipocytes remains constant in adult humans, with an estimated 10% yearly turnover rate (316). Consistently, obese patients after bypass surgery demonstrate significant weight loss and decrease in adipocyte size, but the quantity of adipocytes is not affected (316). In times of energy deprivation such as cold exposure, exercise or fasting, stored TG is mobilized, releasing energy substrates glycerol and free fatty acids into the circulation for other tissues.

In principle, lipid deposition in WAT arises from net uptake from circulation and *de novo* lipogenesis (DNL) locally. The main source of fatty acids in WAT is from lipoproteins in the blood, in particular chylomicrons via lipoprotein lipase mediated

hydrolysis of TG (317). WAT shows clear preference for the uptake of fatty acids from lipoproteins versus non-esterified fatty acids (NEFA), another source of fatty acids in the blood. After uptake, re-esterification of fatty acids is required for energy storage in the form of TG. WAT contains enzymes such as fatty acid synthase (FAS) and acetyl-CoA carboxylase (ACC), which are required for DNL, although DNL only contributes to a small portion of fat deposition under most conditions (318). Insulin stimulates fatty acid uptake via increasing lipoprotein lipase activity and the translocation of fatty acid transporter CD36 and fatty acid transport protein FATP1 (319). Insulin also dephosphorylates and activates ACC, resulting in increased malonyl-CoA production, dephosphorylates FAS, and eventually promotes DNL (319). In addition, lipogenesis in WAT is regulated by transcription factors PPARγ, SREBP1c and carbohydrate response element binding protein (319). Meanwhile, insulin increases glucose uptake into adipocyte via stimulating the translocation of glucose transporter GLUT4 to the plasma membrane (319). This increase of glucose uptake and glyceroneogenesis, namely the conversion of pyruvate to glycerol 3-phosphate, act in concert providing substrate glycerol 3-phosphate for esterification of fatty acids into TG (319,320). Notably, the glyceroneogenesis process could be the limiting step for the esterification of fatty acids (320).

Intracellular lipolysis in WAT is regulated by a complex enzyme system (Figure 1.6) (321). It is initiated by adipose triglyceride lipase (ATGL), which specifically hydrolyzes TGs to DGs (322). The activity of ATGL is demonstrated to be largely dependent on its association with comparative gene identification-58 (322). The DGs are then either re-esterified by a DG acyltransferases or hydrolyzed by hormone-

sensitive lipase (HSL) into monoacylglycerol and free fatty acids. HSL shows substrate preference for DG, but possesses a broad substrate specificity, hydrolyzing monoacylglycerol, cholesteryl ester, retinyl ester and other ester substrates (321). The final step is catalyzed by a monoacylglycerol specific enzyme MGL (monoacylglycerol lipase), generating fatty acids and glycerol. ATGL, HSL and MGL work consecutively and are responsible for over 95% lipolytic capacity in WAT (321,323). Inactivation of ATGL in mice leads to adipose hypertrophy and TG deposition in multiple tissues, in particular the heart, resulting in cardiac dysfunction and premature death (324). HSL-deficient mice have normal body weight, but demonstrate DG accumulation in various tissues including WAT, BAT, skeletal muscle and cardiac muscle (321,325). The physiological function of MGL is not clear at the moment (321). Other lipases such as TG hydrolase might contribute to TG mobilization under certain physiological conditions, but play only a quantitatively minor role (321,323,326).

Lipolysis is controlled by a complex network composed of hormones, cytokines and adipokines (321). The most well characterized stimulators are catecholamines acting on adrenergic receptors on white adipocytes (Figure 1.6). In mice, WAT expresses all three types of β-adrenergic receptors (β_1, β_2, and β_3), whereas in humans, only β_1- and β_2-adrenergic receptors stimulate lipolysis (327). Catecholamines bind to β-adrenergic receptors, activate adenylyl cyclase via stimulatory G_s protein-coupled receptors to increase the concentration of cytoplasmic cAMP, which further enhances protein kinase A (PKA) activity (321). PKA enhances lipolysis by phosphorylating lipid droplet protein perilipin and lipolytic enzymes including HSL. Other hormones such as glucagon, thyroid hormones and adrenocorticotropin also activate PKA. In contrast,

antilipolytic effectors act through their corresponding receptors (e.g. catecholamine through α_2-adrenergic receptor, prostaglandin through E2 receptor) on their associated inhibitory G_i protein-coupled receptors. Herein, the relative distribution of α- and β-adrenergic receptors determines the lipolytic effect (321). Insulin and insulin-like growth factor are the two most potent inhibitory hormones for lipolysis. They act on insulin receptors, phosphorylate insulin receptor substrates 1-4, and activate phosphatidylinositol-3 kinase and protein kinase B. Their signaling cascade interacts with cytokine and extracellular signal-regulated kinase (ERK) signaling (321). Moreover, lipolysis is also regulated by other factors including TNFα, growth hormone and the Cide domain-containing proteins (CIDEA, -B, and -C), although the mechanisms for these regulators remain to be characterized (321).

1.6.4 WAT, an endocrine organ

WAT has also emerged as an important regulator of energy metabolism and inflammation via secretion of a number of adipokines, cytokines secreted from adipose tissue (328). In the mid-1980s, the Spiegelman laboratory demonstrated for the first time that adipocytes were an important source of a specific secretory protein, called adipsin (328,329). In 1995, leptin was identified as a protein secreted from adipocytes (330). Another protein initially termed Acrp30, which is now known as adiponectin, was reported at around the same time (331). Since then, the family of adipokines, has largely expanded including prostaglandins, resistin, TNFα, retinol binding protein-4, IL-6, IL-8, IL-10, monocyte chemoattractant protein (MCP)-1, interferon-γ-inducible protein 10, macrophage inflammatory protein-1β, granulocyte colony stimulating factor and others (119,328). Adipokines play a fundamental role in the regulation of energy

metabolism. For example, leptin, one of the most well characterized adipokines, is a 16 kDa cytokine, (278). The circulating level of leptin is positively correlated with total body fat mass and the secretion of leptin per gram adipose is two times more in obese than in lean subjects (332,333). Leptin acts through the leptin receptor centrally in the hypothalamus and peripherally as well in the ovary, testis, prostate, and placenta (278,334). Leptin deficiency in mice (*ob/ob*) results in hyperphagia, hypothermia, early onset morbid obesity and insulin resistance (330). Leptin deficiency in humans also leads to childhood morbid obesity (335).

The secretion of adipokines is mainly determined by the adipocyte size or volume and the location of adipose tissue (336,337). Large adipocytes generate significantly more proinflammatory adipokines than small or medium sized adipocytes (337). In both humans and rodents, the onset of obesity and adipocyte hypertrophy are accompanied by the macrophage infiltration and tissue inflammation (338,339). The proportion of macrophages in normal visceral adipose tissue was estimated to be 15%, which was elevated to 45-60% in case of obesity (340). The mechanisms underlying the macrophage infiltration have been under intensive investigation. A pivotal event is the recruitment of bone marrow derived $CD11c^+$ macrophages, which are stimulated by adipocyte-derived MCP-1 (341). Based on the expression of antigens, WAT macrophages can be broadly divided into two classes: the M1 population, expressing F4/80, IL-6, CD11c and TNFα, and the M2 population, expressing F4/80, CD301, IL-10, and arginase 1 (342). Obesity is associated with the transformation of the anti-inflammatory M2 population to the pro-inflammatory M1 population (342,343). Activated M1 macrophages generate pro-inflammatory factors, including MCP-1, IL-6 and TNFα,

which likely contribute to obesity associated insulin resistance and inflammation (344). The relative contribution of macrophages and adipocytes to production of adipokines, insulin resistance and WAT inflammation is still unknown (342).

Due to its function in energy storage and endocrinology, WAT appears to be a target for the treatment of obesity and its associated metabolic syndrome. Potential strategies include direct fat removal, reducing fat overload by limiting food intake, promoting “safe” fat storage and modulating adipokines (345). Surgical removal of visceral WAT in mice improves glucose homeostasis (345,346). Thiazolidinediones, synthetic PPARγ agonists, can stimulate adipocyte differentiation and increase adipose tissue mass without adipocyte hypertrophy (347). Consequently, they reduce tissue inflammation, normalize adipokine levels and improve insulin sensitivity (347). Modulating the levels of adipokines could be an effective approach for treating patients with obesity and other associated metabolic conditions. For patients with a mutation in leptin, leptin replacement is a beneficial treatment (345). Application of antibodies generated against TNFα to patients with metabolic syndrome reduces the inflammatory parameters in circulation, but it has no improvement in insulin sensitivity (348). In addition, anti-inflammatory drugs such as aspirin can lower the fasting glucose level in diabetic patients (349).

1.6.5 BAT-mediated thermogenesis

BAT is a highly oxidative and vascularized tissue, specialized for heat production via dissipation of chemical proton gradients generated in the mitochondria (279). This process is mediated by a unique inner mitochondrial membrane protein UCP1 (Figure 1.7), which uncouples the proton gradient generated via mitochondrial oxidative

phosphorylation from ATP synthesis to heat generation (279). Thus, beige cells, which occur in the “browning” WAT and are featured with UCP1 expression, also possess the capability for heat generation. UCP1 activity is constitutively inhibited by purine di- and triphosphate nucleotides (350), but activated by cold (351). Cold also stimulates the mobilization of free fatty acids from stored TG in lipid droplets via lipolysis, which not only provides substrates for BAT mitochondria, but also directly activates UCP1 activity (351,352). With cold being the major environmental regulator of BAT-mediated thermogenesis, high caloric diet might also activate BAT (353). However, this diet-induced thermogenesis is highly controversial (354).

The sympathetic nervous system is an essential regulator of thermogenesis in BAT. In response to cold temperatures, sensory signals from thermoreceptors in the peripheral tissues increase the sympathetic tone and the release of the catecholamine norepinephrine, initiating a thermogenic program via adrenergic receptors in adipocytes (279). Additional to this central neuronal relay, adipocytes can sense the cold via other pathways such as transient receptor potential cation channels in brown adipocytes (355). Cold activates macrophages in WAT and BAT, which also generate catecholamines (356). As discussed earlier in WAT, BAT also expresses all three types of β-adrenergic receptors (β_1, β_2, and β_3), among which, the β_3- adrenergic receptor is most abundant in mature brown adipocytes (279). Mice lacking all three adrenergic receptors are cold sensitive (357). Norepinephrine binds to β-adrenergic receptors, increases cytoplasmic cAMP concentrations and further enhances PKA activity (Figure 1.7). PKA drives the thermogenic program including stimulating the expression of UCP1 in adipocytes via phosphorylation of CREB, a transcription factor, and of p38 mitogen-

activated protein kinase (279). PKA also stimulates lipolysis via activation (phosphorylation) of HSL and deactivation of perilipin, a lipid droplet residing protein (279). Ultimately, lipolysis of TG in lipid droplets results in the release of glycerol and free fatty acids within the cytosol and most of the released fatty acids are channelled into the mitochondria for β-oxidation (279). The generated electrons following the respiratory chain are uncoupled by UCP1 for heat production (Figure 1.7) (279). Apart from the aforementioned thermogenic and lipolytic effects in brown adipocytes, prolonged cold exposure also enhances the browning of WAT and BAT expansion (286,287)

The thyroid hormones are well-defined regulators of BAT activity. Production of triiodothyronine (T3) is tightly controlled by the central nervous system, the so-called hypothalamic-pituitary-thyroid axis (358). Hypothyroidism reduces thermogenesis in BAT (359), whereas hyperthyroidism increases BAT activity (358,360). Thyroxine T4 can be taken up by brown adipocytes and converted into the most active thyroid hormone T3 by type 2 deiodinase (358). Mice lacking type 2 deiodinase have impaired lipolysis and lipogenesis in BAT and are cold-sensitive (358,359). Thyroid hormones are essential for the adrenergic activation of BAT (358). BAT presents α1 and β1 thyroid hormone receptor (TR)s and the TRα1 isoform is required for normal adrenergic response in brown adipocytes (358). Mice with global deficiency of TRα1, TR-α1/β, or with deletion of all isoforms of TRα are cold intolerant due to reduced BAT thermogenesis, which is caused by the blunted response to norepinephrine, rather than the development and recruitment of BAT morphology (100,358,361,362).

Several other neuropeptides and hormones have also been shown to regulate the activity of BAT. Brain-derived neurotrophic factors are implicated in the hypothalamic control of energy expenditure, which is attributed at least partially to the increased activity of BAT (289). Orexin induces sympathetic activation of BAT (363), whereas loss of orexin inhibits the proliferation of brown pre-adipocytes and induces the expression of PRDM16 and PGC1α (289). Melanocortin in the central nervous system is especially important for BAT-mediated thermogenesis via the melanocortin receptor type 4, and deletion of this receptor results in abrogating the induction of UCP1 (364,365). The transforming growth factor-β family members, notably the bone morphogenetic protein (BMP)s, also play critical roles in adipogenesis (366). In line with this function, a few BMPs have been identified to regulate BAT activity. In brief, central administration of BMP8b results in systemic activation of BAT (367). BMP2 and BMP4 promote the browning within WAT depots (368). BMP7 is crucial to reduce body weight via increasing energy expenditure and reducing food intake (369). Moreover, cardiac natriuretic peptides, both the atrial and ventricular, can induce the browning of WAT, and their levels in circulation are enhanced by cold (370). Direct infusion of ventricular natriuretic peptide increases energy expenditure in BAT and WAT. Furthermore, myokine irisin, inducible by exercise, is an important mediator in the browning of WAT in mice, although its physiological relevance in humans is controversial (287,371). In line with the contribution of prostaglandins in activation of BAT and the browning of WAT, cyclooxygenase-2, a key enzyme in prostaglandin biosynthesis, is also critical in these processes (372,373). In addition, fibroblast growth factor 21, generated in the liver and BAT, stimulates the browning of WAT in a PGC1α-dependent manner (374). Fibroblast

growth factor 19 also appears to regulate BAT, as its administration or overexpression in mice increases BAT mass and energy expenditure (25,375).

1.6.6 BAT and energy metabolism

In rodents, it has been well-established that BAT-mediated thermogenesis plays a significant role in energy metabolism. Three decades ago, Rothwell and Stock first reported that BAT was activated to limit weight gain during voluntary overeating (353). Consistently, mice with genetic ablation of BAT develop obesity (376). Mice lacking all three known β-adrenergic receptors are cold-sensitive, and develop adipose hypertrophy and obesity (357,377). Mice with UCP1-deficiency are cold-sensitive, although the effect of UCP1-deficiency on obesity has been controversial for many years: it either has no effect or increases susceptibility to DIO (378,379) or even causes resistance to the development of obesity (380). Recently, this was clarified by the Cannon and Nedergaard group (381), who showed that UCP1-deficient mice gained more weight than control mice when housed under thermoneutral conditions (28–30°C) *versus* mice housed at room temperature (20–22°C). When housed at room temperature, mice are under constant cold stress, which activates BAT, and consume extra energy to maintain body temperature. In UCP1-deficient mice, alternative thermogenic mechanisms are activated to defend their body temperature (382,383). The significant effect of environmental temperature on physiological energy metabolism has been overlooked particularly in rodent models. Regardless, targeting UCP1-mediated thermogenesis in BAT or beige cells could provide a potential strategy to combat obesity and its associated metabolic syndrome. Experimentally expanding BAT activity or beige fat or both in mice via various approaches including genetic

manipulation, drugs or transplantation has shown beneficial effect on certain metabolic diseases (287,371,384-386).

BAT consumes both glucose and lipids for thermogenesis (387). Acute exposure to cold is a high energy-consuming process, evidenced by the depletion of lipid in the adrenal gland and of glycogen in the liver (388,389). When exposed to cold (5°C) for 7 days, mice fed a HF diet exhibited a 55% loss of body fat mass, even though they ate 50% more food (390). Short-term cold exposure also increased the clearance rate of TG-enriched lipoproteins from plasma largely due to increased uptake in the BAT, which was higher than that in the muscle, liver, and WAT (391). BAT is also a glucose consumer, although the exact contribution of glucose for thermogenesis is debatable (287). The glucose uptake in BAT is under sympathetic regulation in a UCP1-dependent manner (392-395). In responding to norepinephrine or insulin, BAT exhibits high rates of glucose uptake (395). Insulin stimulates glucose uptake in BAT independent of its thermogenic function (287). Cold exposure further increases the rate of glucose disposal in BAT responding to insulin (392). Furthermore, mice with increased BAT or beige fat activity exhibit improvement in glucose tolerance and insulin sensitivity (287,370,371,386). A most recent study showed that transplantation of BAT into the visceral cavity in mice resulted in a marked improvement in glucose homeostasis, which was cytokine IL-6 dependent (385)

In humans, BAT has long been presumed to function only in infants, until recent studies demonstrated that BAT is also metabolically active in adults by ^{18}F-fluordeoxyglucose positron emission tomography/computed tomography (280-282,396-398). This expensive technique provides a useful tool for studying human BAT, although

there are limitations in terms of sensitivity and particularly accuracy for monitoring BAT activity (289). Other approaches such as magnetic resonance imaging may be helpful in charactering human BAT (235). Human BAT is composed of both brown and white adipocytes (289). It is highly innervated and vascularized as in rodents. Cold stimulates the uptake of glucose and NEFA into BAT, and increases the oxidative capacity, confirming its functional role in thermogenesis in humans (396,398,399). Notably, cold-induced BAT activity is significantly higher in lean subjects versus overweight or obese subjects and the percentage of body fat and body mass index is negatively correlated with BAT activity (398,400). It was suggested that fully activated BAT in humans could utilize an equivalent amount of energy to ~4.1 kg WAT over one year (280). Under physiological condition, human BAT exhibits differential rates of glucose uptake in response to cold versus insulin stimulation (401). Most recent studies highlight its contribution in regulating whole body glucose homeostasis, insulin sensitivity and body fat (400,402). Furthermore, brown adipocytes present in the interscapular region in human infants vanish with aging (287,403), while a significant portion of recruited beige adipocytes are found in the supraclavicular depots in adult humans and some children (308,404). Overall, targeting BAT-mediated energy expenditure in humans could have physiological benefits for the treatment of obesity and its associated conditions.

1.7 Thesis objectives

PEMT is functionally significant in the liver, responsible for ~30% of hepatic PC production, whereas the remaining ~70% of hepatic PC is made via the CDP-choline pathway (405,406). Inhibition of either the CDP-choline pathway in the liver or the

PEMT pathway results in steatosis (407), which is mainly due to decreased hepatic PC production and VLDL secretion. Both *LCTα*$^{-/-}$ and *Pemt*$^{-/-}$ mice develop severe NASH upon HF feeding (33). However, while HF-fed *LCTα*$^{-/-}$ mice develop obesity, HF-fed *Pemt*$^{-/-}$ mice are protected from DIO (33). Thus, the reason for the resistance to DIO in *Pemt*$^{-/-}$ mice is not simply due to either reduced PC synthesis or decreased VLDL secretion (33). The resistance to DIO and the development of NASH in HF-fed *Pemt*$^{-/-}$ mice is prevented and improved by dietary choline supplementation, respectively (33,120), indicating a role for choline insufficiency in these phenotypes. I endeavored to seek the underlying mechanisms for the resistance to DIO and the development of NASH in HF-fed *Pemt*$^{-/-}$ mice, mainly focusing on the liver, WAT and BAT.

Thesis objective #1:

The vagus nerve, containing sensor (afferent) and motor (efferent) nerve fibers, plays an essential role in regulating energy metabolism (408). It relays signals involved in satiety, hormonal secretion and response to hormones (168,170). The hepatic vagus nerve is a mixed nerve, carrying both afferent fibers from the liver hilus to the NTS in the brain stem, and efferent fibers from the dorsal motor vagal nucleus of the brain stem to the liver. Afferent vagus nerve fibers originating from the liver are key for regulation of energy metabolism under both pathological (192,194,203) and physiological conditions (409). Long-term stimulation of the hepatic vagus nerve in rats results in reduced body weight gain (410). Hepatic vagotomy (HV) is a surgical procedure used for the treatment of peptic ulcers (411,412), and has recently been applied for the treatment of obesity (413). We hypothesized that neuronal signals relayed through the hepatic branch of vagus nerve were implicated in the resistance to DIO and the development of NASH in

HF-fed *Pemt*$^{-/-}$ mice. **Thus, the first objective was to explore a possible role of the hepatic branch of the vagus nerve in the resistance to DIO and the development of NASH in HF-fed *Pemt*$^{-/-}$ mice.** The hepatic branch of the vagus nerve in *Pemt*$^{-/-}$ and *Pemt*$^{+/+}$ mice were subjected to HV, compared with sham operation; or subjected to capsaicin treatment, which selectively disrupts the afferent nerve, versus vehicle-treated mice. After surgery, mice were fed the HF diet for 10 weeks. Body weight gain, glucose and insulin sensitivity were examined, and the development of HF-induced NASH was also evaluated.

Thesis objective #2:

The ER is an intracellular organelle with various cellular functions (259,414). ER stress is associated with metabolic syndrome such as obesity and fatty liver diseases (226,250,414,415). In responding to stress caused by aberrant protein metabolism, cells activate the UPR to restore the homeostatic equilibrium (230). PEMT is located in the ER and MAM (68). Thus, we proposed that PEMT deficiency might lead to aberrant composition of PC and PE in the ER and consequently ER stress, which sensitizes the liver to HF-induced NASH in *Pemt*$^{-/-}$ mice. **The second objective was to test this hypothesis and elucidate a possible role of ER stress in the development of NASH in *Pemt*$^{-/-}$ mice**. PC and PE mass in the ER fractions isolated from mouse livers were determined in chow- and HF-fed *Pemt*$^{-/-}$ and *Pemt*$^{+/+}$ mice. The expression of proteins in ER stress and the UPR pathway was measured in the livers from these mice and in McA-RH7777 cells with or without *PEMT* expression. The chemical chaperone PBA was administered to McA-RH7777 cells and HF-fed *Pemt*$^{-/-}$ mice to alleviate ER stress.

Thesis objective #3:

PEMT is present at low levels in WAT and 3T3-L1 adipocytes (75,106). The expression of PEMT is concomitantly and strongly induced during differentiation of 3T3-L1 adipocytes. Along with this increase, the levels of PC and PE are greatly increased while the PC/PE ratio is reduced (75). Attenuation of *PEMT* in 3T3-L1 adipocytes increases basal TG lipolysis, which leads to a proposed role for PE in lipid droplet formation and stability (75). However, it is unclear whether WAT contributes to the protection against DIO in *Pemt*$^{-/-}$ mice. **Thus, the third objective was to evaluate the contribution of WAT to the protection against DIO in *Pemt*$^{-/-}$ mice.** *Pemt*$^{-/-}$ and *Pemt*$^{+/+}$ mice were fed the HF diet for 2 weeks. Adipocyte differentiation and adipogenesis in (gonadal) WAT were evaluated. The lipolytic capability was evaluated by immunoblotting the lipolytic enzymes using WAT homogenates and by examining the release of glycerol and free fatty acids from WAT explants in the absence or presence of isoproterenol. Furthermore, the endocrine function of WAT was determined by assaying the levels of cytokines and chemokines in WAT.

Thesis objective #4:

Contrary to WAT, BAT is a highly oxidative tissue, enriched with mitochondria and nerve fibers (279). BAT is responsible for non-shivering thermogenesis via UCP1 (279). BAT-mediated thermogenesis plays a critical role in regulating the whole body energy metabolism (279,400,402). The evidence for PEMT in BAT is limited to the presence of PEMT mRNA in BAT from five-day-old *Pemt*$^{+/+}$ mice (75). We proposed that a higher amount of energy might be used for BAT-mediated thermogenesis in HF-fed *Pemt*$^{-/-}$ mice, which might contribute to the resistance to DIO in these mice. **Thus, the fourth**

objective was to unravel the contribution of BAT (interscapular depot) to the resistance to DIO in *Pemt*$^{-/-}$ mice. The presence of PEMT protein and enzyme activity in BAT was first determined. The capacity of thermogenesis was evaluated in both chow- and HF-fed *Pemt*$^{+/+}$ and *Pemt*$^{-/-}$ mice by cold exposure at 4˚C. Unexpectedly, we found *Pemt*$^{-/-}$ mice fed the HF diet for 2 weeks were hypothermic upon cold exposure. To explore the potential mechanisms for this hypothermia, the thermogenic capacity of BAT, cardiac function and hepatic gluconeogenesis were evaluated.

The outcomes of these studies will greatly enhance understanding the physiological functions of PEMT and provide potential therapeutic strategies for the treatment of obesity and fatty liver diseases.

Figure 1.1 Structure of phosphatidylcholine and phosphatidylethanolamine

(A) The typical molecular structure of phosphatidylcholine: 1-palmitoyl-2-arachidonyl-phosphatidylcholine. (B) The typical molecular structure of phosphatidylethanolamine: 1, 2-dipalmitolylphosphatdylethanomaine.

Figure 1.1

(A) Phosphatidylcholine

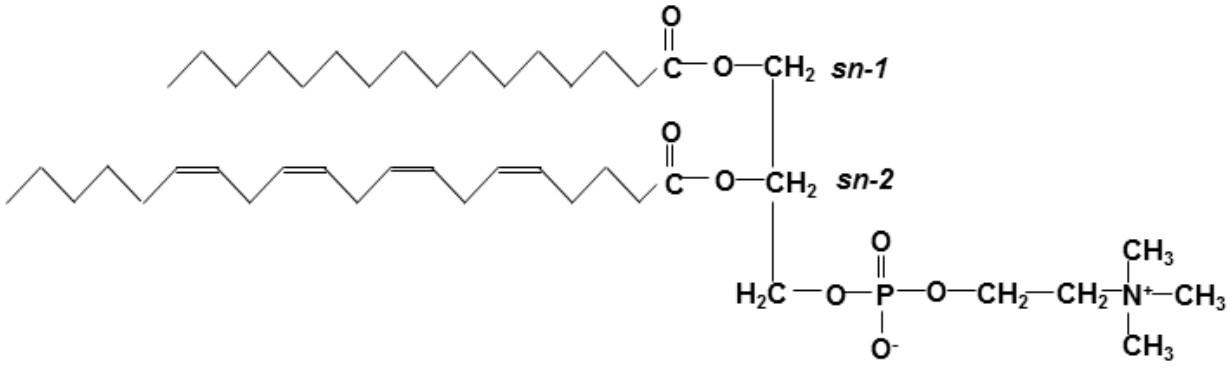

(B) Phosphatidylethanolamine

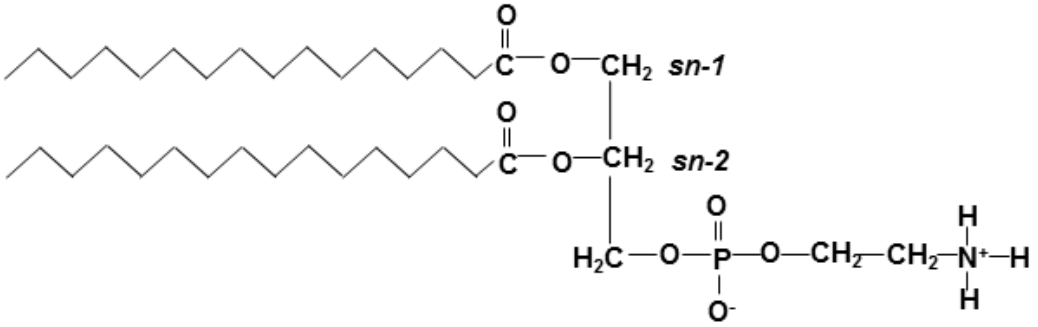

Figure 1.2 Signalling molecules derived from PC

Phosphatidylcholine (PC) can be hydrolyzed by different phospholipases, generating diverse second messengers. Phospholipase A (PLA) hydrolyses the acyl ester bond at the *sn-1* (PLA1) or *sn-2* (PLA2) position, producing lyso-PC and free fatty acids such as arachidonic acid. Phospholipase C (PLC) converts PC into diacylglycerol and phosphocholine. Phospholipase D (PLD) catalyzes the release of phosphatidic acid and choline.

Figure 1.2

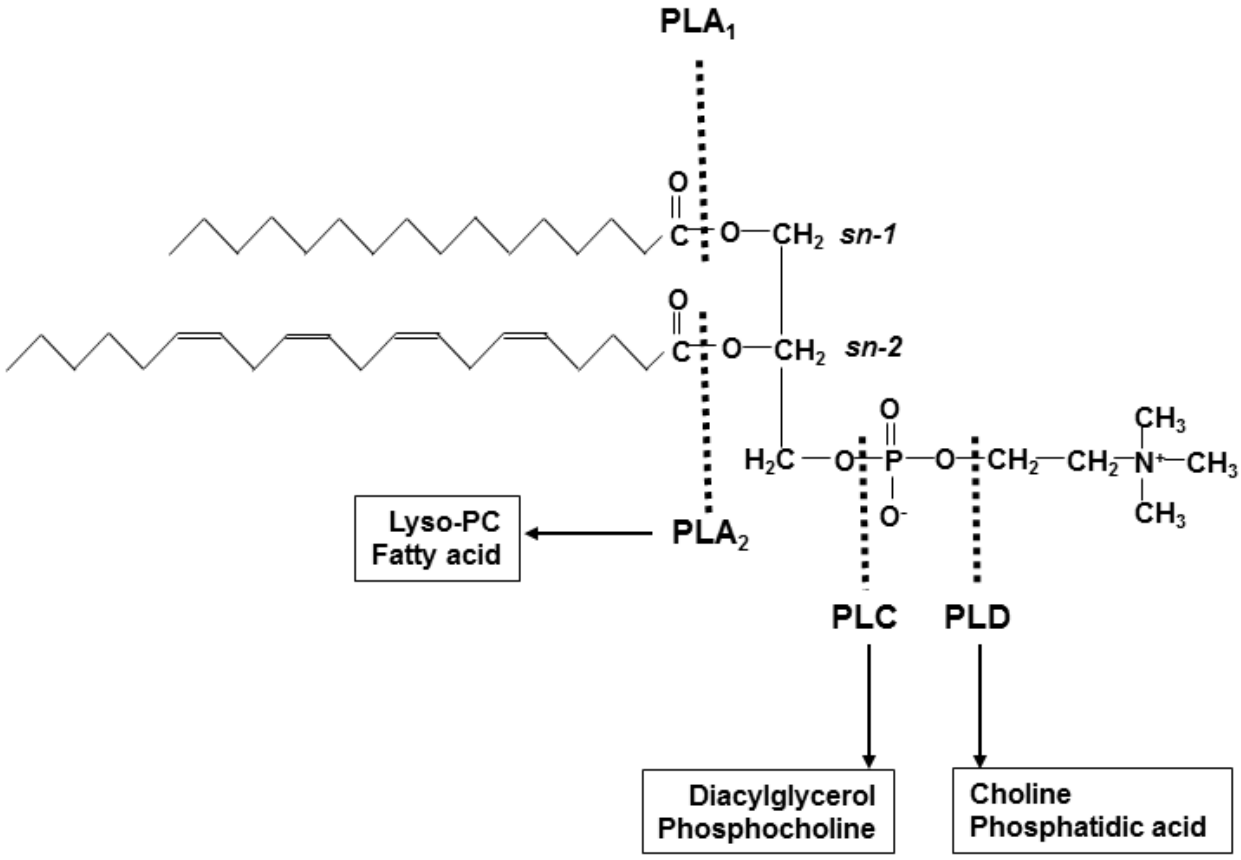
PLA1
sn-1
sn-2
PLA2
Lyso-PC
Fatty acid
PLC
PLD
Diacylglycerol
Phosphocholine
Choline
Phosphatidic acid

Figure 1.3 Pathways involved in PC biosynthesis

In all nucleated cells, the major pathway for phosphatidylcholine (PC) production is the CDP-choline pathway. PC can also be produced via the PEMT pathway, which is only quantitatively significant in the liver. In the CDP-choline pathway, choline is first phosphorylated by choline kinase. Phosphocholine is then converted into CDP-choline, and this step is mediated by the rate-limiting enzyme CTP:phosphocholine cytidylyltransferase. The final step is completed by CDP-choline:1,2-diacylglycerol cholinephosphotransferase, which substitutes diacylglycerol (DG) for cytidine monophosphate (CMP) generating PC. Particularly in the liver, PC can also be generated by phosphatidylethanolamine *N*-methyltransferase (PEMT), which mediates three sequential methylation reactions of phosphatidylethanolamine (PE), using *S*-adenosylmethionine (AdoMet) as the methyl-donor. Other abbreviations include: ATP, adenosine triphosphate; ADP, adenosine diphosphate; CTP, cytidine triphosphate; CDP, cytidine diphosphate; PPi, pyrophosphate; Phosphatidylmonomethylethanolamine (PMME); phosphatidyldimethylethanolamine (PDME); AdoHcy, *S*-adenosylhomocysteine; Hcy, homocysteine.

Figure 1.3

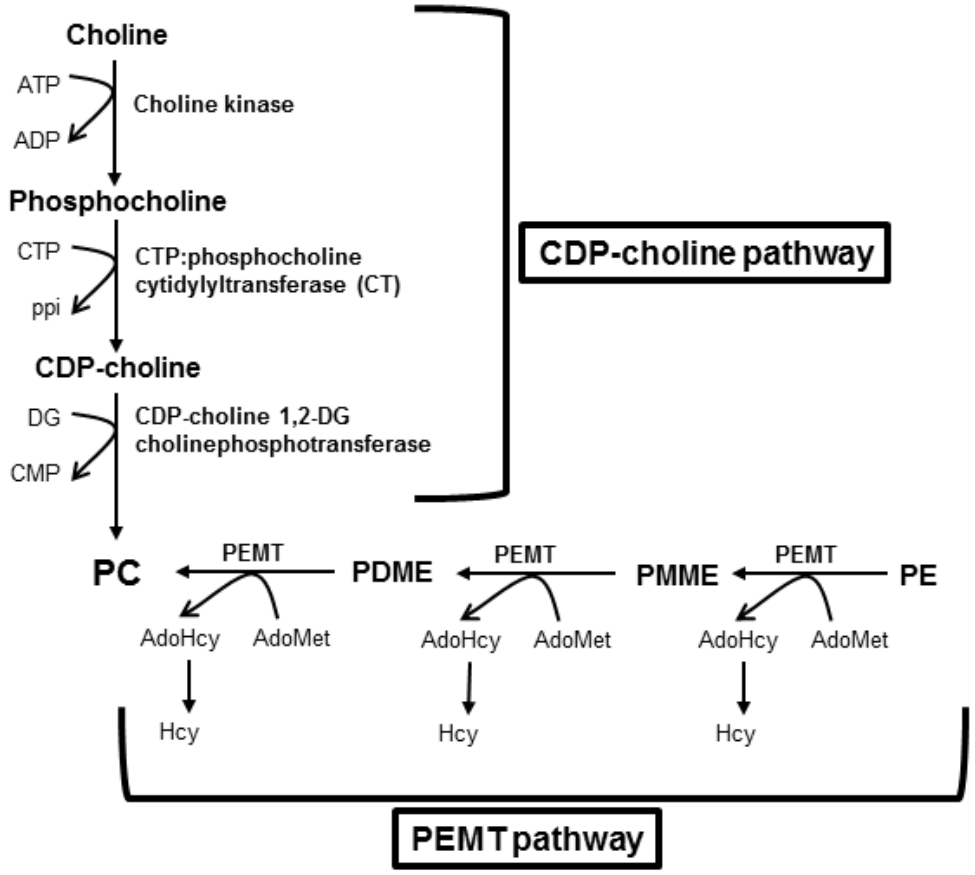
Choline
ATP
ADP
Choline kinase
Phosphocholine
CTP
ppi
CTP:phosphocholine cytidylyltransferase (CT)
CDP-choline
DG
CMP
CDP-choline 1,2-DG cholinephosphotransferase
CDP-choline pathway
PC
PEMT
AdoHcy
AdoMet
Hcy
PDME
PEMT
AdoHcy
AdoMet
Hcy
PMME
PEMT
AdoHcy
AdoMet
Hcy
PE
PEMT pathway

Figure 1.4 Pathways involved in PE biosynthesis

In eukaryotic cells, phosphatidylethanolamine (PE) can be synthesized through four pathways, two major pathways including the CDP-ethanolamine pathway and the decarboxylation of PS mediated by PS decarboxylase (PSD) and two other minor pathways. The CDP-ethanolamine pathway is parallel with the CDP-choline pathway, using ethanolamine as substrate. In the PSD pathway, substrate PS can derive from either phosphatidylcholine (PC) or PE through head group exchange reactions mediated by PS synthase (PSS)1 and PSS2 respectively. PE can also be generated via two quantitatively minor pathways: the acylation of lyso-PE catalyzed by lyso-PE acyltransferase and a base-exchange reaction catalyzed by PSS2 where the serine group of PS is replaced by ethanolamine. Other abbreviations include: ATP, adenosine triphosphate; ADP, adenosine diphosphate; CTP, cytidine triphosphate; CDP, cytidine diphosphate; PPi, pyrophosphate; DG, diacylglycerol; CMP, cytidine monophosphate.

Figure 1.4

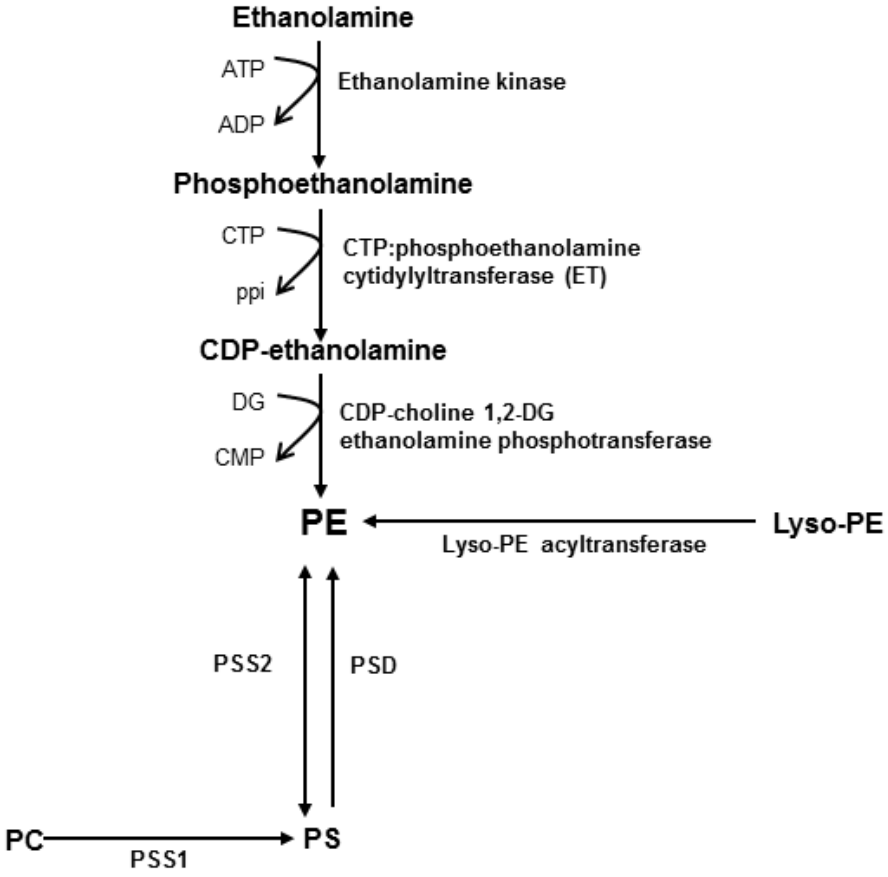
Ethanolamine
ATP
ADP
Ethanolamine kinase
Phosphoethanolamine
CTP
ppi
CTP:phosphoethanolamine
cytidylyltransferase (ET)
CDP-ethanolamine
DG
CMP
CDP-choline 1,2-DG
ethanolamine phosphotransferase
PE
Lyso-PE
Lyso-PE acyltransferase
PSS2
PSD
PC
PS
PSS1

Figure 1.5 The unfolded protein response

In response to stress, the endoplasmic reticulum (ER) initiates a series of intracellular signaling pathways known as the unfolded protein response (229) to restore protein homeostasis. The UPR is composed of three canonical branches mediated by three ER membrane transducer proteins: protein kinase-like ER kinase (235), inositol-requiring enzyme-1 (IRE1), and activating transcription factor (ATF) 6α. PERK activation requires its *trans*-phosphorylation and dimerization. Activated PERK phosphorylates eukaryotic translation initiation factor 2α (eIF2α), which in turn attenuates translation initiation of global protein synthesis and reduces the ER protein folding load. Phosphorylated eIF2α (p-eIF2α) can be dephosphorylated by protein phosphatase PPP1. p-eIF2α also selectively elevates the translation of ATF4, which further regulates expression of genes encoding ER chaperones and genes involved in antioxidant responses, amino acid metabolism, and apoptosis. IRE1 contains an endoribonuclease domain and a Ser/Thr kinase domain in the cytoplasm. Similar to PERK, IRE1α activation depends on its dimerization and *trans*-autophosphorylation. The endoribonuclease activity of IRE1 causes cleavage of the mRNA encoding the X-box binding protein-1 (XBP1), which leads to the translation of the spliced (active) form of XBP1. The spliced XBP1 upregulates a subset of UPR target genes related to protein folding, ER-associated protein degradation (ERAD), ER biogenesis and phospholipid synthesis. In addition to XBP1 processing, IRE1 also degrades a subset of mRNAs in a stress-dependent manner. In response to ER stress, ATF6α translocates to the Golgi apparatus, where it is processed by proteases releasing its cytosolic domain. This cleaved form of ATF6α regulates the UPR target genes including ER chaperone and ERAD proteins.

Figure 1.5

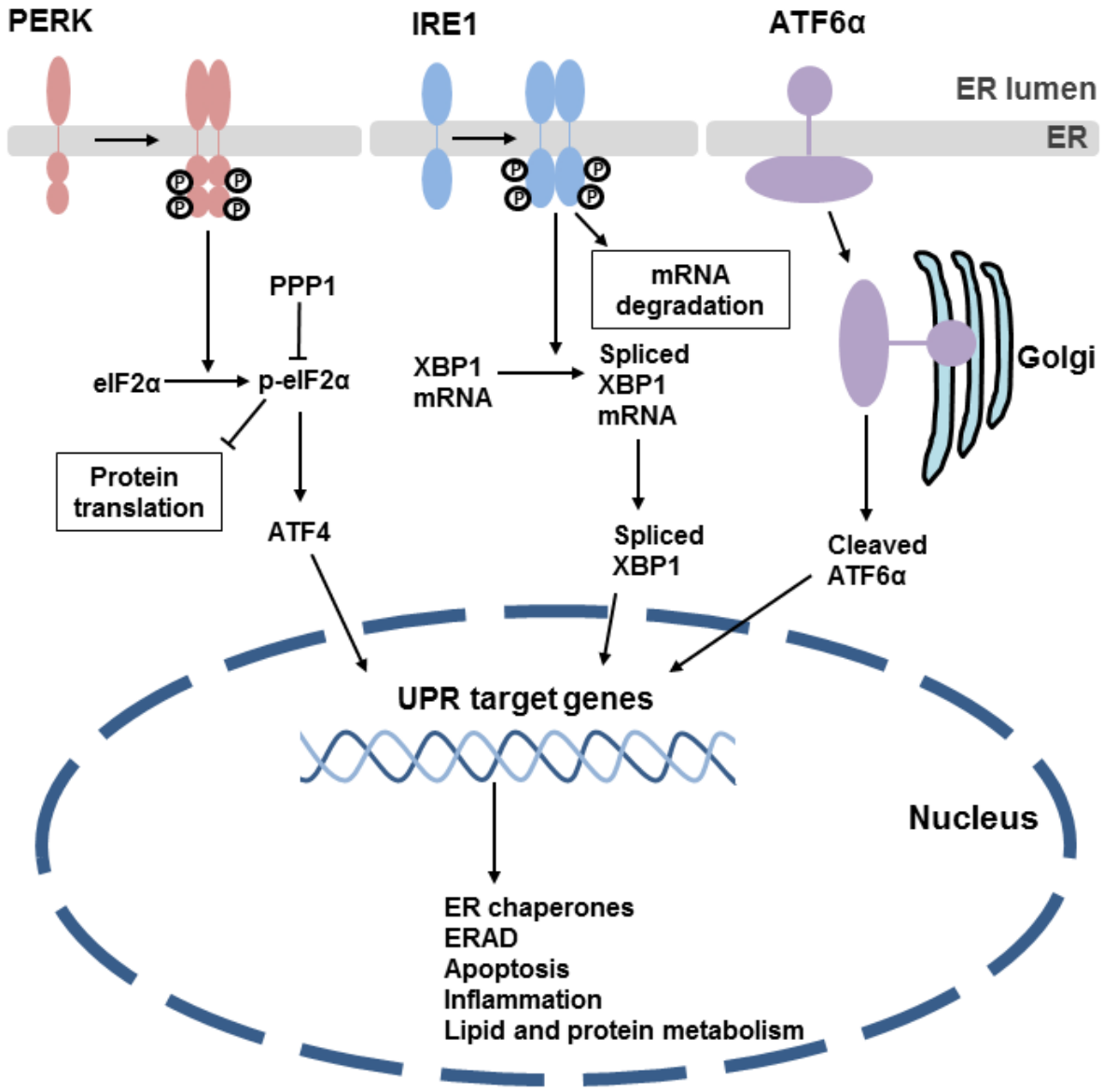
PERK
IRE1
ATF6α
ER lumen
ER
PPP1
eIF2α
p-eIF2α
Protein translation
ATF4
XBP1 mRNA
Spliced XBP1 mRNA
mRNA degradation
Spliced XBP1
Golgi
Cleaved ATF6α
UPR target genes
Nucleus
ER chaperones
ERAD
Apoptosis
Inflammation
Lipid and protein metabolism

Figure 1.6 Simplified lipolysis in adipocytes

Intracellular lipolysis in adipocytes is controlled by extracellular hormones. The catecholamine norepinephrine (NE) binds to β-adrenergic receptor (β-AR)s, activates adenylyl cyclase (AC) via stimulatory G_s protein-coupled receptors and increases the concentration of cytoplasmic cyclic AMP (100), which enhances protein kinase A (PKA) activity. PKA enhances lipolysis via phosphorylating proteins including the lipolytic enzyme hormone-sensitive lipase (HSL). Catecholamines also play an antilipolytic role through α_2-adrenergic receptor and their associated inhibitory G_i protein-coupled receptors. The relative distribution of α- and β-adrenergic receptors on the adipocytes determines the lipolytic effect of catecholamines. Intracellular lipolysis in lipid droplet (LD)s is regulated by a complex enzyme system. Adipose triglyceride lipase (ATGL) initiates lipolysis via specifically hydrolyzing triglyceride (25) to diacylglycerol (DG) and free fatty acids (375). The released DG can be either re-esterified by a DG acyltransferase (DGAT) into TGs or further hydrolyzed by the rate limiting enzyme HSL into monoacylglycerol (MG)s and FFA. MG are then specifically catabolized by enzyme MG lipase (MGL), generating FFA and glycerol. The released FFA and glycerol will be either exported for energy utilization or re-incorporated as TG. FFA can also be converted into CoA molecules (FA-CoA), which provide substrates for mitochondrial fatty acid oxidation.

Figure 1.6

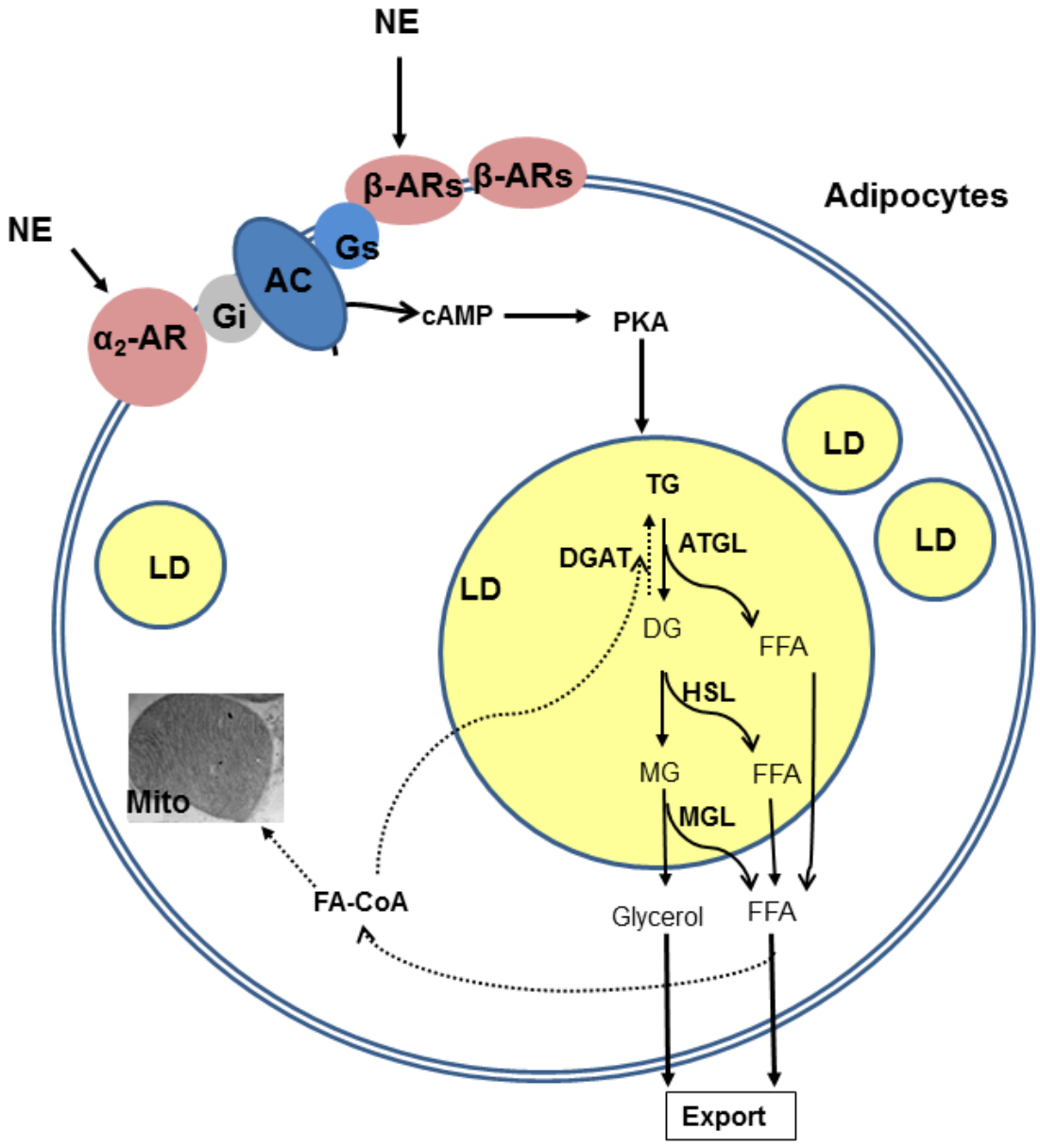
NE
β-ARs
β-ARs
Adipocytes
NE
Gs
AC
Gi
α2-AR
cAMP
PKA
LD
LD
LD
LD
TG
DGAT
ATGL
DG
FFA
HSL
MG
FFA
MGL
Mito
FA-CoA
Glycerol
FFA
Export

Figure 1.7 Uncoupling protein UCP1 mediated thermogenesis

Cold environment increases the sympathetic tone, causing the release of norepinephrine (NE). NE, acting through the β-adrenergic receptors (β-ARs) expressed in mature brown or beige adipocytes, causes increased cytoplasmic cyclic AMP (100) concentrations, which further enhances protein kinase A (PKA) activity. PKA drives the thermogenic program including stimulating the expression of uncoupling protein 1 (UCP1) in adipocytes and promoting lipolysis in lipid droplets. The increased lipolysis results in the release of free fatty acids (375), which provide substrates for mitochondrial fatty acid oxidation. The mitochondrial electron transport chain complexes (I, II, III, IV and V) create a proton gradient crossing the inner mitochondrial membrane. This proton gradient is the driving force for ATP synthesis via complex V, and specifically in mature brown or beige adipocytes, it can also be uncoupled by UCP1, generating heat.

Figure 1.7

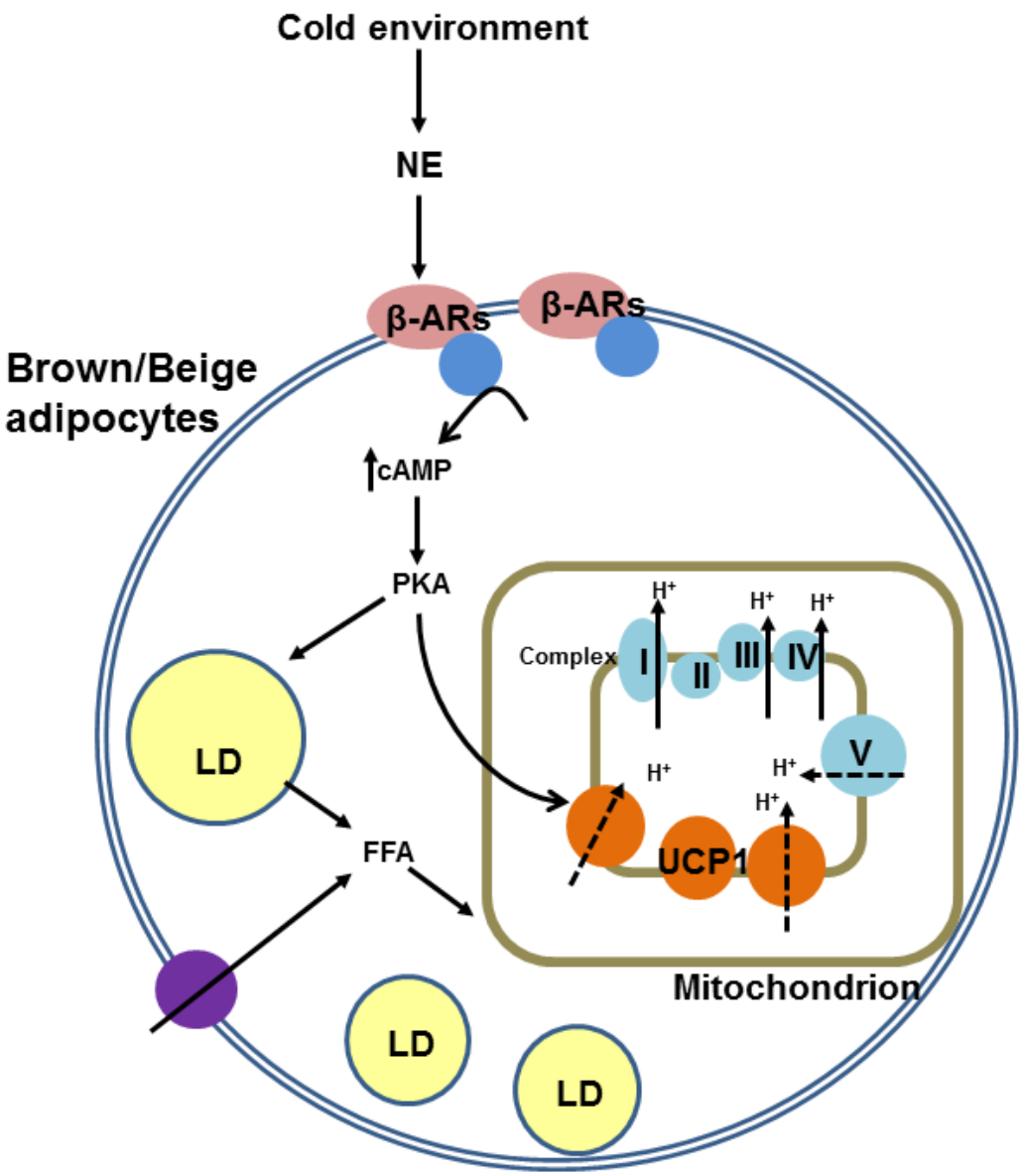
Cold environment
NE
β-ARs
β-ARs
Brown/Beige adipocytes
cAMP
PKA
LD
FFA
Complex
I
II
III
IV
V
H+
UCP1
Mitochondrion
LD
LD

1.8 References

1. Gobley, M. (1847) *J. Pharm. Chim.* **11**, 409
2. Rock, C. O. (2008) Fatty acid and phospholipid metabolism in prokaryotes. in *Biochemistry of Lipids, Lipoproteins and Membranes* (Vance, D. E. V. a. J. E. ed.), 5th Ed., Amsterdam. pp 59-96
3. Yamashita, A., Sugiura, T., and Waku, K. (1997) *J Biochem* **122**, 1-16
4. Vance, D. E., and Vance, J. E. (2008) Phospholipid biosynthesis in eukaryotes. in *Biochemistry of Lipids, Lipoproteins and Membranes* (Vance, D. E., and Vance, J. E., ed.), 5th Ed., Elsevier, Amsterdam. pp 213–244
5. Kanno, K., Wu, M. K., Scapa, E. F., Roderick, S. L., and Cohen, D. E. (2007) *Biochim Biophys Acta* **1771**, 654-662
6. van Helvoort, A., Smith, A. J., Sprong, H., Fritzsche, I., Schinkel, A. H., Borst, P., and van Meer, G. (1996) *Cell* **87**, 507-517
7. Testerink, N., van der Sanden, M. H., Houweling, M., Helms, J. B., and Vaandrager, A. B. (2009) *J Lipid Res* **50**, 2182-2192
8. Cribier, S., Morrot, G., Neumann, J. M., and Devaux, P. F. (1990) *Eur Biophys J* **18**, 33-41
9. Kumar, V. V. (1991) *Proc Natl Acad Sci U S A* **88**, 444-448
10. Phillips, R., Ursell, T., Wiggins, P., and Sens, P. (2009) *Nature* **459**, 379-385
11. Jenkins, G. M., and Frohman, M. A. (2005) *Cell Mol Life Sci* **62**, 2305-2316
12. Shimizu, T., Ohto, T., and Kita, Y. (2006) *IUBMB Life* **58**, 328-333
13. van Meer, G., Voelker, D. R., and Feigenson, G. W. (2008) *Nat Rev Mol Cell Biol* **9**, 112-124

14. Toschi, A., Lee, E., Xu, L., Garcia, A., Gadir, N., and Foster, D. A. (2009) *Mol Cell Biol* **29**, 1411-1420

15. Saleem, S., Kim, Y. T., Maruyama, T., Narumiya, S., and Dore, S. (2009) *J Neuroimmunol* **208**, 87-93

16. Yao, C., Sakata, D., Esaki, Y., Li, Y., Matsuoka, T., Kuroiwa, K., Sugimoto, Y., and Narumiya, S. (2009) *Nat Med* **15**, 633-640

17. M., G. (1847) *J Pharm. Chim.* **11**, 409

18. Alvaro, D., Cantafora, A., Attili, A. F., Ginanni Corradini, S., De Luca, C., Minervini, G., Di Biase, A., and Angelico, M. (1986) *Comp Biochem Physiol B* **83**, 551-554

19. Walkey, C. J., Yu, L., Agellon, L. B., and Vance, D. E. (1998) *J Biol Chem* **273**, 27043-27046

20. Smit, J. J., Schinkel, A. H., Oude Elferink, R. P., Groen, A. K., Wagenaar, E., van Deemter, L., Mol, C. A., Ottenhoff, R., van der Lugt, N. M., van Roon, M. A., and et al. (1993) *Cell* **75**, 451-462

21. de Vree, J. M., Jacquemin, E., Sturm, E., Cresteil, D., Bosma, P. J., Aten, J., Deleuze, J. F., Desrochers, M., Burdelski, M., Bernard, O., Oude Elferink, R. P., and Hadchouel, M. (1998) *Proc Natl Acad Sci U S A* **95**, 282-287

22. Jacquemin, E., De Vree, J. M., Cresteil, D., Sokal, E. M., Sturm, E., Dumont, M., Scheffer, G. L., Paul, M., Burdelski, M., Bosma, P. J., Bernard, O., Hadchouel, M., and Elferink, R. P. (2001) *Gastroenterology* **120**, 1448-1458

23. Skipski, V. P., Barclay, M., Barclay, R. K., Fetzer, V. A., Good, J. J., and Archibald, F. M. (1967) *Biochem J* **104**, 340-352

24. Jonas, A., Phillips, M.A.,. (2008) Lipoprotein structure. in *Biochemistry of Lipids, Lipoproteins and Membranes* (Vance, D. E., and Vance, J.E. ed.), 5 Ed., Elsevier, New York. pp 485-506

25. Perez-Gil, J. (2008) *Biophys J* **94**, 1542-1543; discussion 1544

26. Goerke, J. (1998) *Biochim Biophys Acta* **1408**, 79-89

27. Minahk, C., Kim, K. W., Nelson, R., Trigatti, B., Lehner, R., and Vance, D. E. (2008) *J Biol Chem* **283**, 6449-6458

28. Wiggins, D., and Gibbons, G. F. (1996) *Biochem J* **320 (Pt 2)**, 673-679

29. van der Veen, J. N., Lingrell, S., and Vance, D. E. (2012) *J Biol Chem* **287**, 23418-23426

30. Kennedy, E. P., and Weiss, S. B. (1956) *J Biol Chem* **222**, 193-214

31. Shindou, H., and Shimizu, T. (2009) *J Biol Chem* **284**, 1-5

32. Karim, M., Jackson, P., and Jackowski, S. (2003) *Biochim Biophys Acta* **1633**, 1-12

33. Tang, W., Keesler, G. A., and Tabas, I. (1997) *J Biol Chem* **272**, 13146-13151

34. Wang, L., Magdaleno, S., Tabas, I., and Jackowski, S. (2005) *Mol Cell Biol* **25**, 3357-3363

35. Jacobs, R. L., Devlin, C., Tabas, I., and Vance, D. E. (2004) *J Biol Chem* **279**, 47402-47410

36. Vance, J. E., and Tasseva, G. (2013) *Biochim Biophys Acta* **1831**, 543-554

37. Emoto, K., and Umeda, M. (2000) *J Cell Biol* **149**, 1215-1224

38. Pecheur, E. I., Martin, I., Maier, O., Bakowsky, U., Ruysschaert, J. M., and Hoekstra, D. (2002) *Biochemistry* **41**, 9813-9823

39. Signorell, A., Gluenz, E., Rettig, J., Schneider, A., Shaw, M. K., Gull, K., and Butikofer, P. (2009) *Mol Microbiol* **72**, 1068-1079

40. Hansen, H. S., Lauritzen, L., Strand, A. M., Moesgaard, B., and Frandsen, A. (1995) *Biochim Biophys Acta* **1258**, 303-308

41. Jin, X. H., Okamoto, Y., Morishita, J., Tsuboi, K., Tonai, T., and Ueda, N. (2007) *J Biol Chem* **282**, 3614-3623

42. Brown, M. S., Ye, J., Rawson, R. B., and Goldstein, J. L. (2000) *Cell* **100**, 391-398

43. Mizushima, N., Levine, B., Cuervo, A. M., and Klionsky, D. J. (2008) *Nature* **451**, 1069-1075

44. Mizushima, N., and Yoshimori, T. (2007) *Autophagy* **3**, 542-545

45. Post, J. A., Bijvelt, J. J., and Verkleij, A. J. (1995) *Am J Physiol* **268**, H773-780

46. Deleault, N. R., Piro, J. R., Walsh, D. J., Wang, F., Ma, J., Geoghegan, J. C., and Supattapone, S. (2012) *Proc Natl Acad Sci U S A* **109**, 8546-8551

47. Dobrosotskaya, I. Y., Seegmiller, A. C., Brown, M. S., Goldstein, J. L., and Rawson, R. B. (2002) *Science* **296**, 879-883

48. Dowhan, W., and Bogdanov, M. (2012) *Biochim Biophys Acta* **1818**, 1097-1107

49. Riekhof, W. R., Wu, J., Jones, J. L., and Voelker, D. R. (2007) *J Biol Chem* **282**, 28344-28352

50. Signorell, A., Rauch, M., Jelk, J., Ferguson, M. A., and Butikofer, P. (2008) *J Biol Chem* **283**, 23636-23644

51. Voelker, D. R. (1984) *Proc Natl Acad Sci U S A* **81**, 2669-2673

52. Tian, Y., Jackson, P., Gunter, C., Wang, J., Rock, C. O., and Jackowski, S. (2006) *J Biol Chem* **281**, 28438-28449

53. Fullerton, M. D., Hakimuddin, F., and Bakovic, M. (2007) *Mol Cell Biol* **27**, 3327-3336

54. Zborowski, J., Dygas, A., and Wojtczak, L. (1983) *FEBS Lett* **157**, 179-182

55. Steenbergen, R., Nanowski, T. S., Beigneux, A., Kulinski, A., Young, S. G., and Vance, J. E. (2005) *J Biol Chem* **280**, 40032-40040

56. Bleijerveld, O. B., Brouwers, J. F., Vaandrager, A. B., Helms, J. B., and Houweling, M. (2007) *J Biol Chem* **282**, 28362-28372

57. Du Vigneaud, V., Cohn, M., Chandler, J. P., Schenck, J. R., and Simmonds, S. (1974) *Nutr Rev* **32**, 144-146

58. Bremer, J., and Greenberg, D. M. (1960) *Biochim Biophys Acta* **37**, 173-175

59. Bremer, J., Figard, P. H., and Greenberg, D. M. (1960) *Biochimica Et Biophysica Acta* **43**, 477-488

60. Bremer, J., and Greenberg, D. M. (1961) *Biochimica Et Biophysica Acta* **46**, 205-&

61. Wilton, D. C. (2008) Phospholipases. in *Biochemistry of Lipids, Lipoproteins and Membranes* (Vance, D. E. V. a. J. E. ed.), Elsevier, Amsterdam. pp 305-329

62. Ridgway, N. D., and Vance, D. E. (1987) *J Biol Chem* **262**, 17231-17239

63. Ridgway, N. D., and Vance, D. E. (1988) *J Biol Chem* **263**, 16856-16863

64. Ridgway, N. D., and Vance, D. E. (1988) *J Biol Chem* **263**, 16864-16871

65. Vance, D. E. (2013) *Biochim Biophys Acta* **1831**, 626-632

66. Cui, Z., Vance, J. E., Chen, M. H., Voelker, D. R., and Vance, D. E. (1993) *J Biol Chem* **268**, 16655-16663

67. Walkey, C. J., Cui, Z., Agellon, L. B., and Vance, D. E. (1996) *J Lipid Res* **37**, 2341-2350

68. Walkey, C. J., Shields, D. J., and Vance, D. E. (1999) *Biochim Biophys Acta* **1436**, 405-412

69. Shields, D. J., Agellon, L. B., and Vance, D. E. (2001) *Biochim Biophys Acta* **1532**, 105-114

70. Walkey, C. J., Donohue, L. R., Bronson, R., Agellon, L. B., and Vance, D. E. (1997) *Proc Natl Acad Sci U S A* **94**, 12880-12885

71. Vance, D. E. (2014) *Biochim Biophys Acta* **1838**, 1477-1487

72. Vance, D. E., and Ridgway, N. D. (1988) *Prog Lipid Res* **27**, 61-79

73. Horl, G., Wagner, A., Cole, L. K., Malli, R., Reicher, H., Kotzbeck, P., Kofeler, H., Hofler, G., Frank, S., Bogner-Strauss, J. G., Sattler, W., Vance, D. E., and Steyrer, E. (2011) *J Biol Chem* **286**, 17338-17350

74. Blusztajn, J. K., Zeisel, S. H., and Wurtman, R. J. (1985) *Biochem J* **232**, 505-511

75. Zhu, X., Mar, M. H., Song, J., and Zeisel, S. H. (2004) *Brain Res Dev Brain Res* **149**, 121-129

76. Shields, D. J., Lehner, R., Agellon, L. B., and Vance, D. E. (2003) *J Biol Chem* **278**, 2956-2962

77. Vance, J. E. (1990) *J Biol Chem* **265**, 7248-7256

78. Shiao, Y. J., Balcerzak, B., and Vance, J. E. (1998) *Biochem J* **331 (Pt 1)**, 217-223

79. Shields, D. J., Altarejos, J. Y., Wang, X., Agellon, L. B., and Vance, D. E. (2003) *J Biol Chem* **278**, 35826-35836

80. Shields, D. J., Lingrell, S., Agellon, L. B., Brosnan, J. T., and Vance, D. E. (2005) *J Biol Chem* **280**, 27339-27344

81. Sundler, R., and Akesson, B. (1975) *Biochem J* **146**, 309-315

82. Sundler, R., and Akesson, B. (1975) *J Biol Chem* **250**, 3359-3367

83. Akesson, B. (1978) *FEBS Lett* **92**, 177-180

84. Ridgway, N. D., Yao, Z., and Vance, D. E. (1989) *J Biol Chem* **264**, 1203-1207

85. Samborski, R. W., Ridgway, N. D., and Vance, D. E. (1990) *J Biol Chem* **265**, 18322-18329

86. Hoffman, D. R., Marion, D. W., Cornatzer, W. E., and Duerre, J. A. (1980) *J Biol Chem* **255**, 10822-10827

87. Chiang, P. K., and Cantoni, G. L. (1979) *Biochem Pharmacol* **28**, 1897-1902

88. Pritchard, P. H., Chiang, P. K., Cantoni, G. L., and Vance, D. E. (1982) *J Biol Chem* **257**, 6362-6367

89. Chiva, V. A., Cao, D. M., and Mato, J. M. (1983) *FEBS Lett* **160**, 101-104

90. Ridgway, N. D., and Vance, D. E. (1989) *Biochim Biophys Acta* **1004**, 261-270

91. Merida, I., and Mato, J. M. (1987) *Biochim Biophys Acta* **928**, 92-97

92. Pelech, S. L., Pritchard, P. H., Sommerman, E. F., Percival-Smith, A., and Vance, D. E. (1984) *Can J Biochem Cell Biol* **62**, 196-202

93. Marin-Cao, D., Alvarez Chiva, V., and Mato, J. M. (1983) *Biochem J* **216**, 675-680

94. Alemany, S., Varela, I., and Mato, J. M. (1981) *FEBS Lett* **135**, 111-114

95. Young, D. L. (1971) *J Lipid Res* **12**, 590-595

96. Alemany, S., Varela, I., Harper, J. F., and Mato, J. M. (1982) *J Biol Chem* **257**, 9249-9251

97. Castano, J. G., Alemany, S., Nieto, A., and Mato, J. M. (1980) *J Biol Chem* **255**, 9041-9043

98. Noga, A. A., and Vance, D. E. (2003) *J Biol Chem* **278**, 21851-21859

99. Fischer, L. M., daCosta, K. A., Kwock, L., Stewart, P. W., Lu, T. S., Stabler, S. P., Allen, R. H., and Zeisel, S. H. (2007) *Am J Clin Nutr* **85**, 1275-1285

100. Resseguie, M. E., da Costa, K. A., Galanko, J. A., Patel, M., Davis, I. J., and Zeisel, S. H. (2011) *J Biol Chem* **286**, 1649-1658

101. Fischer, L. M., da Costa, K. A., Kwock, L., Galanko, J., and Zeisel, S. H. (2010) *Am J Clin Nutr* **92**, 1113-1119

102. Resseguie, M., Song, J., Niculescu, M. D., da Costa, K. A., Randall, T. A., and Zeisel, S. H. (2007) *FASEB J* **21**, 2622-2632

103. Cole, L. K., and Vance, D. E. (2010) *J Biol Chem* **285**, 11880-11891

104. Baker, T. K., Carfagna, M. A., Gao, H., Dow, E. R., Li, Q., Searfoss, G. H., and Ryan, T. P. (2001) *Chem Res Toxicol* **14**, 1218-1231

105. Cole, L. K., Jacobs, R. L., and Vance, D. E. (2010) *Hepatology* **52**, 1258-1265

106. Banchio, C., Schang, L. M., and Vance, D. E. (2003) *J Biol Chem* **278**, 32457-32464

107. Banchio, C., Schang, L. M., and Vance, D. E. (2004) *J Biol Chem* **279**, 40220-40226

108. Banchio, C., Lingrell, S., and Vance, D. E. (2007) *J Biol Chem* **282**, 14827-14835

109. Cui, Z., Shen, Y. J., and Vance, D. E. (1997) *Biochim Biophys Acta* **1346**, 10-16

110. Sesca, E., Perletti, G. P., Binasco, V., Chiara, M., and Tessitore, L. (1996) *Biochem Biophys Res Commun* **229**, 158-162

111. Houweling, M., Cui, Z., Tessitore, L., and Vance, D. E. (1997) *Biochim Biophys Acta* **1346**, 1-9

112. Pelech, S. L., Power, E., and Vance, D. E. (1983) *Can J Biochem Cell Biol* **61**, 1147-1152

113. Taub, R. (2004) *Nat Rev Mol Cell Biol* **5**, 836-847

114. Michalopoulos, G. K. (2007) *J Cell Physiol* **213**, 286-300

115. Houweling, M., Tijburg, L. B., Jamil, H., Vance, D. E., Nyathi, C. B., Vaartjes, W. J., and van Golde, L. M. (1991) *Biochem J* **278 (Pt 2)**, 347-351

116. Ling, J., Chaba, T., Zhu, L. F., Jacobs, R. L., and Vance, D. E. (2012) *Hepatology* **55**, 1094-1102

117. Cui, Z., Houweling, M., and Vance, D. E. (1994) *J Biol Chem* **269**, 24531-24533

118. Boess, F., Kamber, M., Romer, S., Gasser, R., Muller, D., Albertini, S., and Suter, L. (2003) *Toxicol Sci* **73**, 386-402

119. Guillouzo, A., Corlu, A., Aninat, C., Glaise, D., Morel, F., and Guguen-Guillouzo, C. (2007) *Chem Biol Interact* **168**, 66-73

120. Cui, Z., and Vance, D. E. (1996) *J Biol Chem* **271**, 2839-2843

121. Jacobs, R. L., Stead, L. M., Devlin, C., Tabas, I., Brosnan, M. E., Brosnan, J. T., and Vance, D. E. (2005) *J Biol Chem* **280**, 28299-28305

122. Moore, J. B. (2010) *Proc Nutr Soc* **69**, 211-220

123. Williams, C. D., Stengel, J., Asike, M. I., Torres, D. M., Shaw, J., Contreras, M., Landt, C. L., and Harrison, S. A. (2011) *Gastroenterology* **140**, 124-131

124. Ogden, C. L., Carroll, M. D., Curtin, L. R., McDowell, M. A., Tabak, C. J., and Flegal, K. M. (2006) *JAMA* **295**, 1549-1555

125. Matteoni, C. A., Younossi, Z. M., Gramlich, T., Boparai, N., Liu, Y. C., and McCullough, A. J. (1999) *Gastroenterology* **116**, 1413-1419

126. Vetelainen, R., van Vliet, A., Gouma, D. J., and van Gulik, T. M. (2007) *Annals of Surgery* **245**, 20-30

127. Angulo, P. (2006) *Liver Transpl* **12**, 523-534

128. Cohen, J. C., Horton, J. D., and Hobbs, H. H. (2011) *Science* **332**, 1519-1523

129. Li, Z., Agellon, L. B., and Vance, D. E. (2005) *J Biol Chem* **280**, 37798-37802

130. Kuipers, F., Oude Elferink, R. P., Verkade, H. J., and Groen, A. K. (1997) *Subcell Biochem* **28**, 295-318

131. Li, Z., Agellon, L. B., Allen, T. M., Umeda, M., Jewell, L., Mason, A., and Vance, D. E. (2006) *Cell Metab* **3**, 321-331

132. Cullis, P. R., Fenske, D. B., and Hope, M. J. (1996) Physical properties and functional roles of lipids in membranes. in *Biochemsitry of Lipids, Lipoproteins and Membranes* (D.E.a.V, J. E. V. ed.), Elsevier Sciences B.V, Amsterdam. pp 1-33

133. Op den Kamp, J. A. (1979) *Annu Rev Biochem* **48**, 47-71

134. Vermeulen, P. S., Lingrell, S., Yao, Z., and Vance, D. E. (1997) *J Lipid Res* **38**, 447-458

135. Verkade, H. J., Fast, D. G., Rusinol, A. E., Scraba, D. G., and Vance, D. E. (1993) *J Biol Chem* **268**, 24990-24996

136. Fast, D. G., and Vance, D. E. (1995) *Biochim Biophys Acta* **1258**, 159-168

137. Jacobs, R. L., Lingrell, S., Zhao, Y., Francis, G. A., and Vance, D. E. (2008) *J Biol Chem* **283**, 2147-2155

138. Noga, A. A., Zhao, Y., and Vance, D. E. (2002) *J Biol Chem* **277**, 42358-42365

139. Yao, Z. M., and Vance, D. E. (1988) *J Biol Chem* **263**, 2998-3004

140. Yao, Z. M., and Vance, D. E. (1990) *Biochem Cell Biol* **68**, 552-558

141. Jacobs, R. L., Zhao, Y., Koonen, D. P., Sletten, T., Su, B., Lingrell, S., Cao, G., Peake, D. A., Kuo, M. S., Proctor, S. D., Kennedy, B. P., Dyck, J. R., and Vance, D. E. (2010) *J Biol Chem* **285**, 22403-22413

142. Fu, S., Yang, L., Li, P., Hofmann, O., Dicker, L., Hide, W., Lin, X., Watkins, S. M., Ivanov, A. R., and Hotamisligil, G. S. (2011) *Nature* **473**, 528-531

143. Song, J., da Costa, K. A., Fischer, L. M., Kohlmeier, M., Kwock, L., Wang, S., and Zeisel, S. H. (2005) *FASEB J* **19**, 1266-1271

144. Dong, H., Wang, J., Li, C., Hirose, A., Nozaki, Y., Takahashi, M., Ono, M., Akisawa, N., Iwasaki, S., Saibara, T., and Onishi, S. (2007) *J Hepatol* **46**, 915-920

145. Romeo, S., Cohen, J. C., and Hobbs, H. H. (2006) No association between polymorphism in PEMT (V175M) and hepatic triglyceride content in the Dallas Heart Study. in *FASEB J*, 2006/10/03 Ed.

146. Zeisel, S. H. (2006) *The FASEB Journal* **20**, 2181-2182

147. da Costa, K. A., Kozyreva, O. G., Song, J., Galanko, J. A., Fischer, L. M., and Zeisel, S. H. (2006) *FASEB J* **20**, 1336-1344

148. Pilgeram, L. O., and Greenberg, D. M. (1954) *Science* **120**, 760-761

149. Moore, K. J., Sheedy, F. J., and Fisher, E. A. (2013) *Nat Rev Immunol* **13**, 709-721

150. Cole, L. K., Dolinsky, V. W., Dyck, J. R., and Vance, D. E. (2011) *Circ Res* **108**, 686-694

151. Zhao, Y., Su, B., Jacobs, R. L., Kennedy, B., Francis, G. A., Waddington, E., Brosnan, J. T., Vance, J. E., and Vance, D. E. (2009) *Arterioscler Thromb Vasc Biol* **29**, 1349-1355

152. Vance, J. E., and Vance, D. E. (1986) *J Biol Chem* **261**, 4486-4491

153. Refsum, H., Ueland, P. M., Nygard, O., and Vollset, S. E. (1998) *Annu Rev Med* **49**, 31-62

154. Robinson, K. (2001) Homocysteine and coronary artery disease. in *Homocysteine in Health and Disease* (R. Carmel, D. W. J. ed., Cambridge University Pres, Cambridge

155. Noga, A. A., Stead, L. M., Zhao, Y., Brosnan, M. E., Brosnan, J. T., and Vance, D. E. (2003) *J Biol Chem* **278**, 5952-5955

156. Katz, J. E., Dlakic, M., and Clarke, S. (2003) *Mol Cell Proteomics* **2**, 525-540

157. Mudd, S. H., and Poole, J. R. (1975) *Metabolism* **24**, 721-735

158. Mudd, S. H., Brosnan, J. T., Brosnan, M. E., Jacobs, R. L., Stabler, S. P., Allen, R. H., Vance, D. E., and Wagner, C. (2007) *Am J Clin Nutr* **85**, 19-25

159. Stead, L. M., Brosnan, J. T., Brosnan, M. E., Vance, D. E., and Jacobs, R. L. (2006) *Am J Clin Nutr* **83**, 5-10

160. Wu, G., Zhang, L., Li, T., Lopaschuk, G., Vance, D. E., and Jacobs, R. L. (2012) *J Obes* **2012**, 319172

161. Kharbanda, K. K., Mailliard, M. E., Baldwin, C. R., Beckenhauer, H. C., Sorrell, M. F., and Tuma, D. J. (2007) *J Hepatol* **46**, 314-321

162. Kathirvel, E., Morgan, K., Nandgiri, G., Sandoval, B. C., Caudill, M. A., Bottiglieri, T., French, S. W., and Morgan, T. R. (2010) *Am J Physiol Gastrointest Liver Physiol* **299**, G1068-1077

163. van der Veen, J. N., Lingrell, S., da Silva, R. P., Jacobs, R. L., and Vance, D. E. (2014) *Diabetes* **63**, 2620-2630

164. Berthoud, H. R., and Neuhuber, W. L. (2000) *Auton Neurosci* **85**, 1-17

165. Berthoud, H. R. (2008) *Regulatory Peptides* **149**, 15-25

166. Ogbonnaya, S., and Kaliaperumal, C. (2013) *J Nat Sci Biol Med* **4**, 8-13

167. Berthoud, H. R. (2004) *Anat Rec A Discov Mol Cell Evol Biol* **280**, 827-835

168. Dutsch, M., Eichhorn, U., Worl, J., Wank, M., Berthoud, H. R., and Neuhuber, W. L. (1998) *J Comp Neurol* **398**, 289-307

169. Prechtl, J. C., and Powley, T. L. (1985) *J Comp Neurol* **235**, 182-195

170. Prechtl, J. C., and Powley, T. L. (1990) *Anat Embryol (Berl)* **181**, 101-115

171. Berthoud, H. R., Patterson, L. M., and Zheng, H. (2001) *Anat Rec* **262**, 29-40

172. Ziegler, D., Zentai, C., Perz, S., Rathmann, W., Haastert, B., Meisinger, C., and Lowel, H. (2006) *Exp Clin Endocrinol Diabetes* **114**, 153-159

173. Richter, W. O., Geiss, H. C., Aleksic, S., and Schwandt, P. (1996) *Int J Obes Relat Metab Disord* **20**, 966-969

174. Carnethon, M. R., Jacobs, D. R., Jr., Sidney, S., and Liu, K. (2003) *Diabetes Care* **26**, 3035-3041

175. Bodenlos, J. S., Kose, S., Borckardt, J. J., Nahas, Z., Shaw, D., O'Neil, P. M., and George, M. S. (2007) *Appetite* **48**, 145-153

176. Pardo, J. V., Sheikh, S. A., Kuskowski, M. A., Surerus-Johnson, C., Hagen, M. C., Lee, J. T., Rittberg, B. R., and Adson, D. E. (2007) *Int J Obes (Lond)* **31**, 1756-1759

177. Koren, M. S., and Holmes, M. D. (2006) *Epilepsy Behav* **8**, 246-249

178. Tracey, K. J. (2002) *Nature* **420**, 853-859

179. Tracey, K. J. (2005) *J Exp Med* **202**, 1017-1021

180. Yi, C. X., la Fleur, S. E., Fliers, E., and Kalsbeek, A. (2010) *Biochim Biophys Acta* **1802**, 416-431

181. Sugita, M. (2006) *Cell Mol Life Sci* **63**, 2000-2015

182. Peters, J. H., Ritter, R. C., and Simasko, S. M. (2006) *Am J Physiol Regul Integr Comp Physiol* **290**, R1544-1549

183. Cummings, D. E., Purnell, J. Q., Frayo, R. S., Schmidova, K., Wisse, B. E., and Weigle, D. S. (2001) *Diabetes* **50**, 1714-1719

184. Date, Y., Murakami, N., Toshinai, K., Matsukura, S., Niijima, A., Matsuo, H., Kangawa, K., and Nakazato, M. (2002) *Gastroenterology* **123**, 1120-1128

185. le Roux, C. W., Neary, N. M., Halsey, T. J., Small, C. J., Martinez-Isla, A. M., Ghatei, M. A., Theodorou, N. A., and Bloom, S. R. (2005) *J Clin Endocrinol Metab* **90**, 4521-4524

186. Nakagawa, A., Satake, H., Nakabayashi, H., Nishizawa, M., Furuya, K., Nakano, S., Kigoshi, T., Nakayama, K., and Uchida, K. (2004) *Auton Neurosci* **110**, 36-43

187. Batterham, R. L., Heffron, H., Kapoor, S., Chivers, J. E., Chandarana, K., Herzog, H., Le Roux, C. W., Thomas, E. L., Bell, J. D., and Withers, D. J. (2006) *Cell Metab* **4**, 223-233

188. Koda, S., Date, Y., Murakami, N., Shimbara, T., Hanada, T., Toshinai, K., Niijima, A., Furuya, M., Inomata, N., Osuye, K., and Nakazato, M. (2005) *Endocrinology* **146**, 2369-2375

189. Uno, K., Katagiri, H., Yamada, T., Ishigaki, Y., Ogihara, T., Imai, J., Hasegawa, Y., Gao, J., Kaneko, K., Iwasaki, H., Ishihara, H., Sasano, H., Inukai, K., Mizuguchi, H., Asano, T., Shiota, M., Nakazato, M., and Oka, Y. (2006) *Science* **312**, 1656-1659

190. Uno, K., Yamada, T., Ishigaki, Y., Imai, J., Hasegawa, Y., Gao, J., Kaneko, K., Matsusue, K., Yamazaki, T., Oka, Y., and Katagiri, H. (2012) *Eur Heart J* **33**, 1279-1289

191. Bernal-Mizrachi, C., Xiaozhong, L., Yin, L., Knutsen, R. H., Howard, M. J., Arends, J. J., Desantis, P., Coleman, T., and Semenkovich, C. F. (2007) *Cell Metab* **5**, 91-102

192. Neuhuber, W. L. (1989) *J Auton Nerv Syst* **29**, 13-18

193. Woods, S. C., Lutz, T. A., Geary, N., and Langhans, W. (2006) *Philos Trans R Soc Lond B Biol Sci* **361**, 1219-1235

194. Kreier, F., Fliers, E., Voshol, P. J., Van Eden, C. G., Havekes, L. M., Kalsbeek, A., Van Heijningen, C. L., Sluiter, A. A., Mettenleiter, T. C., Romijn, J. A., Sauerwein, H. P., and Buijs, R. M. (2002) *J Clin Invest* **110**, 1243-1250

195. Giordano, A., Song, C. K., Bowers, R. R., Ehlen, J. C., Frontini, A., Cinti, S., and Bartness, T. J. (2006) *Am J Physiol Regul Integr Comp Physiol* **291**, R1243-1255

196. Berthoud, H. R., and Jeanrenaud, B. (1979) *Endocrinology* **105**, 146-151

197. Pocai, A., Obici, S., Schwartz, G. J., and Rossetti, L. (2005) *Cell Metab* **1**, 53-61

198. Pocai, A., Lam, T. K., Gutierrez-Juarez, R., Obici, S., Schwartz, G. J., Bryan, J., Aguilar-Bryan, L., and Rossetti, L. (2005) *Nature* **434**, 1026-1031

199. Lam, T. K., Gutierrez-Juarez, R., Pocai, A., Bhanot, S., Tso, P., Schwartz, G. J., and Rossetti, L. (2007) *Nat Med* **13**, 171-180

200. Imai, J., Katagiri, H., Yamada, T., Ishigaki, Y., Suzuki, T., Kudo, H., Uno, K., Hasegawa, Y., Gao, J., Kaneko, K., Ishihara, H., Niijima, A., Nakazato, M., Asano, T., Minokoshi, Y., and Oka, Y. (2008) *Science* **322**, 1250-1254

201. Wang, P. Y., Caspi, L., Lam, C. K., Chari, M., Li, X., Light, P. E., Gutierrez-Juarez, R., Ang, M., Schwartz, G. J., and Lam, T. K. (2008) *Nature* **452**, 1012-1016

202. Cheung, G. W., Kokorovic, A., Lam, C. K., Chari, M., and Lam, T. K. (2009) *Cell Metab* **10**, 99-109

203. Pavlov, V. A., and Tracey, K. J. (2012) *Nat Rev Endocrinol* **8**, 743-754

204. Gregor, M. F., and Hotamisligil, G. S. (2011) *Annu Rev Immunol* **29**, 415-445

205. Donath, M. Y., and Shoelson, S. E. (2011) *Nat Rev Immunol* **11**, 98-107

206. Delzenne, N. M., Neyrinck, A. M., Backhed, F., and Cani, P. D. (2011) *Nat Rev Endocrinol* **7**, 639-646

207. Musso, G., Gambino, R., and Cassader, M. (2011) *Annu Rev Med* **62**, 361-380

208. Borovikova, L. V., Ivanova, S., Zhang, M., Yang, H., Botchkina, G. I., Watkins, L. R., Wang, H., Abumrad, N., Eaton, J. W., and Tracey, K. J. (2000) *Nature* **405**, 458-462

209. Pavlov, V. A., Parrish, W. R., Rosas-Ballina, M., Ochani, M., Puerta, M., Ochani, K., Chavan, S., Al-Abed, Y., and Tracey, K. J. (2009) *Brain Behav Immun* **23**, 41-45

210. Pavlov, V. A., Ochani, M., Gallowitsch-Puerta, M., Ochani, K., Huston, J. M., Czura, C. J., Al-Abed, Y., and Tracey, K. J. (2006) *Proc Natl Acad Sci U S A* **103**, 5219-5223

211. Gautam, D., Gavrilova, O., Jeon, J., Pack, S., Jou, W., Cui, Y., Li, J. H., and Wess, J. (2006) *Cell Metab* **4**, 363-375

212. Maresca, A., and Supuran, C. T. (2008) *Expert Opinion on Therapeutic Targets* **12**, 1167-1175

213. Ruiz de Azua, I., Gautam, D., Guettier, J. M., and Wess, J. (2011) *Trends Endocrinol Metab* **22**, 74-80

214. Gautam, D., Han, S. J., Hamdan, F. F., Jeon, J., Li, B., Li, J. H., Cui, Y., Mears, D., Lu, H., Deng, C., Heard, T., and Wess, J. (2006) *Cell Metab* **3**, 449-461

215. Wang, H., Yu, M., Ochani, M., Amella, C. A., Tanovic, M., Susarla, S., Li, J. H., Yang, H., Ulloa, L., Al-Abed, Y., Czura, C. J., and Tracey, K. J. (2003) *Nature* **421**, 384-388

216. Tracey, K. J. (2009) *Nat Rev Immunol* **9**, 418-428

217. Wang, X., Yang, Z., Xue, B., and Shi, H. (2011) *Endocrinology* **152**, 836-846

218. Cancello, R., Zulian, A., Maestrini, S., Mencarelli, M., Della Barba, A., Invitti, C., Liuzzi, A., and Di Blasio, A. M. (2012) *Int J Obes (Lond)* **36**, 1552-1557

219. Marrero, M. B., Lucas, R., Salet, C., Hauser, T. A., Mazurov, A., Lippiello, P. M., and Bencherif, M. (2010) *J Pharmacol Exp Ther* **332**, 173-180

220. ClinicalTrials.gov. (2012) US National Library of Medicine.

221. Giorgi, C., De Stefani, D., Bononi, A., Rizzuto, R., and Pinton, P. (2009) *Int J Biochem Cell Biol* **41**, 1817-1827

222. Hetz, C., Chevet, E., and Harding, H. P. (2013) *Nat Rev Drug Discov* **12**, 703-719

223. Hotamisligil, G. S. (2010) *Cell* **140**, 900-917

224. Schroder, M. (2008) *Cell Mol Life Sci* **65**, 862-894

225. Chang, T. Y., Chang, C. C., Ohgami, N., and Yamauchi, Y. (2006) *Annu Rev Cell Dev Biol* **22**, 129-157

226. Ron, D., and Walter, P. (2007) *Nat Rev Mol Cell Biol* **8**, 519-529

227. Tabas, I., and Ron, D. (2011) *Nat Cell Biol* **13**, 184-190

228. Borradaile, N. M., Han, X., Harp, J. D., Gale, S. E., Ory, D. S., and Schaffer, J. E. (2006) *J Lipid Res* **47**, 2726-2737

229. Li, Y., Ge, M., Ciani, L., Kuriakose, G., Westover, E. J., Dura, M., Covey, D. F., Freed, J. H., Maxfield, F. R., Lytton, J., and Tabas, I. (2004) *J Biol Chem* **279**, 37030-37039

230. Kim, S. J., Zhang, Z., Saha, A., Sarkar, C., Zhao, Z., Xu, Y., and Mukherjee, A. B. (2010) *Neurosci Lett* **479**, 292-296

231. Harding, H. P., Zhang, Y., and Ron, D. (1999) *Nature* **397**, 271-274

232. Shi, Y., Vattem, K. M., Sood, R., An, J., Liang, J., Stramm, L., and Wek, R. C. (1998) *Mol Cell Biol* **18**, 7499-7509

233. Nakamura, T., Furuhashi, M., Li, P., Cao, H., Tuncman, G., Sonenberg, N., Gorgun, C. Z., and Hotamisligil, G. S. (2010) *Cell* **140**, 338-348

234. Cao, S. S., and Kaufman, R. J. (2013) *Expert Opin Ther Targets* **17**, 437-448

235. Harding, H. P., Zhang, Y., Bertolotti, A., Zeng, H., and Ron, D. (2000) *Mol Cell* **5**, 897-904

236. Ma, Y., Brewer, J. W., Diehl, J. A., and Hendershot, L. M. (2002) *J Mol Biol* **318**, 1351-1365

237. Cullinan, S. B., and Diehl, J. A. (2006) *Int J Biochem Cell Biol* **38**, 317-332

238. Sidrauski, C., and Walter, P. (1997) *Cell* **90**, 1031-1039

239. Upton, J. P., Wang, L., Han, D., Wang, E. S., Huskey, N. E., Lim, L., Truitt, M., McManus, M. T., Ruggero, D., Goga, A., Papa, F. R., and Oakes, S. A. (2012) *Science* **338**, 818-822

240. Chen, X., Shen, J., and Prywes, R. (2002) *J Biol Chem* **277**, 13045-13052

241. Bailey, D., and O'Hare, P. (2007) *Antioxid Redox Signal* **9**, 2305-2321

242. Hetz, C., Bernasconi, P., Fisher, J., Lee, A. H., Bassik, M. C., Antonsson, B., Brandt, G. S., Iwakoshi, N. N., Schinzel, A., Glimcher, L. H., and Korsmeyer, S. J. (2006) *Science* **312**, 572-576

243. Bravo, R., Gutierrez, T., Paredes, F., Gatica, D., Rodriguez, A. E., Pedrozo, Z., Chiong, M., Parra, V., Quest, A. F., Rothermel, B. A., and Lavandero, S. (2012) *Int J Biochem Cell Biol* **44**, 16-20

244. Wang, S., and Kaufman, R. J. (2012) *J Cell Biol* **197**, 857-867

245. Ozcan, U., Cao, Q., Yilmaz, E., Lee, A. H., Iwakoshi, N. N., Ozdelen, E., Tuncman, G., Gorgun, C., Glimcher, L. H., and Hotamisligil, G. S. (2004) *Science* **306**, 457-461

246. Cao, H., Gerhold, K., Mayers, J. R., Wiest, M. M., Watkins, S. M., and Hotamisligil, G. S. (2008) *Cell* **134**, 933-944

247. Yore, M. M., Syed, I., Moraes-Vieira, P. M., Zhang, T., Herman, M. A., Homan, E. A., Patel, R. T., Lee, J., Chen, S., Peroni, O. D., Dhaneshwar, A. S., Hammarstedt, A., Smith, U., McGraw, T. E., Saghatelian, A., and Kahn, B. B. (2014) *Cell* **159**, 318-332

248. Kammoun, H. L., Chabanon, H., Hainault, I., Luquet, S., Magnan, C., Koike, T., Ferre, P., and Foufelle, F. (2009) *J Clin Invest* **119**, 1201-1215

249. Nakatani, Y., Kaneto, H., Kawamori, D., Yoshiuchi, K., Hatazaki, M., Matsuoka, T. A., Ozawa, K., Ogawa, S., Hori, M., Yamasaki, Y., and Matsuhisa, M. (2005) *J Biol Chem* **280**, 847-851

250. Lee, A. H., Scapa, E. F., Cohen, D. E., and Glimcher, L. H. (2008) *Science* **320**, 1492-1496

251. Park, S. W., Zhou, Y., Lee, J., Lu, A., Sun, C., Chung, J., Ueki, K., and Ozcan, U. (2010) *Nat Med* **16**, 429-437

252. Zhou, Y., Lee, J., Reno, C. M., Sun, C., Park, S. W., Chung, J., Fisher, S. J., White, M. F., Biddinger, S. B., and Ozcan, U. (2011) *Nat Med* **17**, 356-365

253. Wang, Y., Vera, L., Fischer, W. H., and Montminy, M. (2009) *Nature* **460**, 534-537

254. Pagliassotti, M. J. (2012) *Annu Rev Nutr* **32**, 17-33

255. Puri, P., Mirshahi, F., Cheung, O., Natarajan, R., Maher, J. W., Kellum, J. M., and Sanyal, A. J. (2008) *Gastroenterology* **134**, 568-576

256. Oyadomari, S., Harding, H. P., Zhang, Y., Oyadomari, M., and Ron, D. (2008) *Cell Metab* **7**, 520-532

257. Wang, S., Chen, Z., Lam, V., Han, J., Hassler, J., Finck, B. N., Davidson, N. O., and Kaufman, R. J. (2012) *Cell Metab* **16**, 473-486

258. Zhang, K., Shen, X., Wu, J., Sakaki, K., Saunders, T., Rutkowski, D. T., Back, S. H., and Kaufman, R. J. (2006) *Cell* **124**, 587-599

259. Zhang, C., Wang, G., Zheng, Z., Maddipati, K. R., Zhang, X., Dyson, G., Williams, P., Duncan, S. A., Kaufman, R. J., and Zhang, K. (2012) *Hepatology* **55**, 1070-1082

260. Lee, J. H., Giannikopoulos, P., Duncan, S. A., Wang, J., Johansen, C. T., Brown, J. D., Plutzky, J., Hegele, R. A., Glimcher, L. H., and Lee, A. H. (2011) *Nat Med* **17**, 812-815

261. Ozcan, U., Yilmaz, E., Ozcan, L., Furuhashi, M., Vaillancourt, E., Smith, R. O., Gorgun, C. Z., and Hotamisligil, G. S. (2006) *Science* **313**, 1137-1140

262. Ozcan, L., Ergin, A. S., Lu, A., Chung, J., Sarkar, S., Nie, D., Myers, M. G., Jr., and Ozcan, U. (2009) *Cell Metab* **9**, 35-51

263. Xiao, C., Giacca, A., and Lewis, G. F. (2011) *Diabetes* **60**, 918-924

264. Kars, M., Yang, L., Gregor, M. F., Mohammed, B. S., Pietka, T. A., Finck, B. N., Patterson, B. W., Horton, J. D., Mittendorfer, B., Hotamisligil, G. S., and Klein, S. (2010) *Diabetes* **59**, 1899-1905

265. Ben Mosbah, I., Alfany-Fernandez, I., Martel, C., Zaouali, M. A., Bintanel-Morcillo, M., Rimola, A., Rodes, J., Brenner, C., Rosello-Catafau, J., and Peralta, C. (2010) *Cell Death Dis* **1**, e52

266. Vilatoba, M., Eckstein, C., Bilbao, G., Smyth, C. A., Jenkins, S., Thompson, J. A., Eckhoff, D. E., and Contreras, J. L. (2005) *Surgery* **138**, 342-351

267. Cinti, S. (2005) *Prostaglandins Leukot Essent Fatty Acids* **73**, 9-15

268. Cinti, S. (2012) *Dis Model Mech* **5**, 588-594

269. Cinti, S. (2011) *Ann Med* **43**, 104-115

270. Gesta, S., Tseng, Y. H., and Kahn, C. R. (2007) *Cell* **131**, 242-256

271. Murano, I., Barbatelli, G., Giordano, A., and Cinti, S. (2009) *J Anat* **214**, 171-178

272. Peirce, V., Carobbio, S., and Vidal-Puig, A. (2014) *Nature* **510**, 76-83

273. Kershaw, E. E., and Flier, J. S. (2004) *J Clin Endocrinol Metab* **89**, 2548-2556

274. Cannon, B., and Nedergaard, J. (2004) *Physiol Rev* **84**, 277-359

275. Virtanen, K. A., Lidell, M. E., Orava, J., Heglind, M., Westergren, R., Niemi, T., Taittonen, M., Laine, J., Savisto, N. J., Enerback, S., and Nuutila, P. (2009) *N Engl J Med* **360**, 1518-1525

276. Cypess, A. M., Lehman, S., Williams, G., Tal, I., Rodman, D., Goldfine, A. B., Kuo, F. C., Palmer, E. L., Tseng, Y. H., Doria, A., Kolodny, G. M., and Kahn, C. R. (2009) *N Engl J Med* **360**, 1509-1517

277. Zingaretti, M. C., Crosta, F., Vitali, A., Guerrieri, M., Frontini, A., Cannon, B., Nedergaard, J., and Cinti, S. (2009) *FASEB J* **23**, 3113-3120

278. Giordano, A., Frontini, A., and Cinti, S. (2008) *Methods Mol Biol* **456**, 83-95

279. Bartness, T. J., Vaughan, C. H., and Song, C. K. (2010) *Int J Obes (Lond)* **34 Suppl 1**, S36-42

280. Bartness, T. J., and Song, C. K. (2007) *J Lipid Res* **48**, 1655-1672

281. Devlin, M. J. (2014) *Am J Phys Anthropol*

282. Harms, M., and Seale, P. (2013) *Nat Med* **19**, 1252-1263

283. Almind, K., Manieri, M., Sivitz, W. I., Cinti, S., and Kahn, C. R. (2007) *Proc Natl Acad Sci U S A* **104**, 2366-2371

284. Schulz, T. J., and Tseng, Y. H. (2013) *Biochem J* **453**, 167-178

285. Bronner-Fraser, M. (1994) *FASEB J* **8**, 699-706

286. Tang, W., Zeve, D., Suh, J. M., Bosnakovski, D., Kyba, M., Hammer, R. E., Tallquist, M. D., and Graff, J. M. (2008) *Science* **322**, 583-586

287. Tran, K. V., Gealekman, O., Frontini, A., Zingaretti, M. C., Morroni, M., Giordano, A., Smorlesi, A., Perugini, J., De Matteis, R., Sbarbati, A., Corvera, S., and Cinti, S. (2012) *Cell Metab* **15**, 222-229

288. Schulz, T. J., Huang, T. L., Tran, T. T., Zhang, H., Townsend, K. L., Shadrach, J. L., Cerletti, M., McDougall, L. E., Giorgadze, N., Tchkonia, T., Schrier, D., Falb,

D., Kirkland, J. L., Wagers, A. J., and Tseng, Y. H. (2011) *Proc Natl Acad Sci U S A* **108**, 143-148

289. Rodeheffer, M. S., Birsoy, K., and Friedman, J. M. (2008) *Cell* **135**, 240-249

290. Walden, T. B., Timmons, J. A., Keller, P., Nedergaard, J., and Cannon, B. (2009) *J Cell Physiol* **218**, 444-449

291. Timmons, J. A., Wennmalm, K., Larsson, O., Walden, T. B., Lassmann, T., Petrovic, N., Hamilton, D. L., Gimeno, R. E., Wahlestedt, C., Baar, K., Nedergaard, J., and Cannon, B. (2007) *Proc Natl Acad Sci U S A* **104**, 4401-4406

292. Seale, P., Bjork, B., Yang, W., Kajimura, S., Chin, S., Kuang, S., Scime, A., Devarakonda, S., Conroe, H. M., Erdjument-Bromage, H., Tempst, P., Rudnicki, M. A., Beier, D. R., and Spiegelman, B. M. (2008) *Nature* **454**, 961-967

293. Yin, H., Pasut, A., Soleimani, V. D., Bentzinger, C. F., Antoun, G., Thorn, S., Seale, P., Fernando, P., van Ijcken, W., Grosveld, F., Dekemp, R. A., Boushel, R., Harper, M. E., and Rudnicki, M. A. (2013) *Cell Metab* **17**, 210-224

294. Sanchez-Gurmaches, J., Hung, C. M., Sparks, C. A., Tang, Y., Li, H., and Guertin, D. A. (2012) *Cell Metab* **16**, 348-362

295. Shan, T., Liang, X., Bi, P., Zhang, P., Liu, W., and Kuang, S. (2013) *J Lipid Res* **54**, 2214-2224

296. Berry, R., and Rodeheffer, M. S. (2013) *Nat Cell Biol* **15**, 302-308

297. Himms-Hagen, J., Melnyk, A., Zingaretti, M. C., Ceresi, E., Barbatelli, G., and Cinti, S. (2000) *Am J Physiol Cell Physiol* **279**, C670-681

298. Vitali, A., Murano, I., Zingaretti, M. C., Frontini, A., Ricquier, D., and Cinti, S. (2012) *J Lipid Res* **53**, 619-629

299. Rosenwald, M., Perdikari, A., Rulicke, T., and Wolfrum, C. (2013) *Nat Cell Biol* **15**, 659-667

300. Wang, Q. A., Tao, C., Gupta, R. K., and Scherer, P. E. (2013) *Nat Med* **19**, 1338-1344

301. Petrovic, N., Walden, T. B., Shabalina, I. G., Timmons, J. A., Cannon, B., and Nedergaard, J. (2010) *J Biol Chem* **285**, 7153-7164

302. Petrovic, N., Shabalina, I. G., Timmons, J. A., Cannon, B., and Nedergaard, J. (2008) *Am J Physiol Endocrinol Metab* **295**, E287-296

303. Wu, J., Bostrom, P., Sparks, L. M., Ye, L., Choi, J. H., Giang, A. H., Khandekar, M., Virtanen, K. A., Nuutila, P., Schaart, G., Huang, K., Tu, H., van Marken Lichtenbelt, W. D., Hoeks, J., Enerback, S., Schrauwen, P., and Spiegelman, B. M. (2012) *Cell* **150**, 366-376

304. Lee, Y. H., Petkova, A. P., Mottillo, E. P., and Granneman, J. G. (2012) *Cell Metab* **15**, 480-491

305. Farmer, S. R. (2006) *Cell Metab* **4**, 263-273

306. Kajimura, S., Seale, P., and Spiegelman, B. M. (2010) *Cell Metab* **11**, 257-262

307. Kajimura, S., Seale, P., Kubota, K., Lunsford, E., Frangioni, J. V., Gygi, S. P., and Spiegelman, B. M. (2009) *Nature* **460**, 1154-1158

308. Qiang, L., Wang, L., Kon, N., Zhao, W., Lee, S., Zhang, Y., Rosenbaum, M., Zhao, Y., Gu, W., Farmer, S. R., and Accili, D. (2012) *Cell* **150**, 620-632

309. Rajakumari, S., Wu, J., Ishibashi, J., Lim, H. W., Giang, A. H., Won, K. J., Reed, R. R., and Seale, P. (2013) *Cell Metab* **17**, 562-574

310. Eberle, D., Hegarty, B., Bossard, P., Ferre, P., and Foufelle, F. (2004) *Biochimie* **86**, 839-848

311. Ali, A. T., Hochfeld, W. E., Myburgh, R., and Pepper, M. S. (2013) *Eur J Cell Biol* **92**, 229-236

312. Spalding, K. L., Arner, E., Westermark, P. O., Bernard, S., Buchholz, B. A., Bergmann, O., Blomqvist, L., Hoffstedt, J., Naslund, E., Britton, T., Concha, H., Hassan, M., Ryden, M., Frisen, J., and Arner, P. (2008) *Nature* **453**, 783-787

313. Zechner, R., Strauss, J., Frank, S., Wagner, E., Hofmann, W., Kratky, D., Hiden, M., and Levak-Frank, S. (2000) *Int J Obes Relat Metab Disord* **24 Suppl 4**, S53-56

314. Chong, M. F., Fielding, B. A., and Frayn, K. N. (2007) *Proc Nutr Soc* **66**, 52-59

315. Czech, M. P., Tencerova, M., Pedersen, D. J., and Aouadi, M. (2013) *Diabetologia* **56**, 949-964

316. Nye, C., Kim, J., Kalhan, S. C., and Hanson, R. W. (2008) *Trends Endocrinol Metab* **19**, 356-361

317. Zechner, R., Kienesberger, P. C., Haemmerle, G., Zimmermann, R., and Lass, A. (2009) *J Lipid Res* **50**, 3-21

318. Zimmermann, R., Strauss, J. G., Haemmerle, G., Schoiswohl, G., Birner-Gruenberger, R., Riederer, M., Lass, A., Neuberger, G., Eisenhaber, F., Hermetter, A., and Zechner, R. (2004) *Science* **306**, 1383-1386

319. Schweiger, M., Schreiber, R., Haemmerle, G., Lass, A., Fledelius, C., Jacobsen, P., Tornqvist, H., Zechner, R., and Zimmermann, R. (2006) *J Biol Chem* **281**, 40236-40241

320. Haemmerle, G., Lass, A., Zimmermann, R., Gorkiewicz, G., Meyer, C., Rozman, J., Heldmaier, G., Maier, R., Theussl, C., Eder, S., Kratky, D., Wagner, E. F., Klingenspor, M., Hoefler, G., and Zechner, R. (2006) *Science* **312**, 734-737

321. Haemmerle, G., Zimmermann, R., Hayn, M., Theussl, C., Waeg, G., Wagner, E., Sattler, W., Magin, T. M., Wagner, E. F., and Zechner, R. (2002) *J Biol Chem* **277**, 4806-4815

322. Okazaki, H., Igarashi, M., Nishi, M., Tajima, M., Sekiya, M., Okazaki, S., Yahagi, N., Ohashi, K., Tsukamoto, K., Amemiya-Kudo, M., Matsuzaka, T., Shimano, H., Yamada, N., Aoki, J., Morikawa, R., Takanezawa, Y., Arai, H., Nagai, R., Kadowaki, T., Osuga, J., and Ishibashi, S. (2006) *Diabetes* **55**, 2091-2097

323. Lafontan, M., and Berlan, M. (1993) *J Lipid Res* **34**, 1057-1091

324. Scherer, P. E. (2006) *Diabetes* **55**, 1537-1545

325. Cook, K. S., Min, H. Y., Johnson, D., Chaplinsky, R. J., Flier, J. S., Hunt, C. R., and Spiegelman, B. M. (1987) *Science* **237**, 402-405

326. Zhang, Y., Proenca, R., Maffei, M., Barone, M., Leopold, L., and Friedman, J. M. (1994) *Nature* **372**, 425-432

327. Scherer, P. E., Williams, S., Fogliano, M., Baldini, G., and Lodish, H. F. (1995) *J Biol Chem* **270**, 26746-26749

328. Galic, S., Oakhill, J. S., and Steinberg, G. R. (2010) *Mol Cell Endocrinol* **316**, 129-139

329. Lonnqvist, F., Nordfors, L., Jansson, M., Thorne, A., Schalling, M., and Arner, P. (1997) *J Clin Invest* **99**, 2398-2404

330. Margetic, S., Gazzola, C., Pegg, G. G., and Hill, R. A. (2002) *Int J Obes Relat Metab Disord* **26**, 1407-1433

331. Fatima, W., Shahid, A., Imran, M., Manzoor, J., Hasnain, S., Rana, S., and Mahmood, S. (2011) *Int J Pediatr Obes* **6**, 419-427

332. Bahceci, M., Gokalp, D., Bahceci, S., Tuzcu, A., Atmaca, S., and Arikan, S. (2007) *J Endocrinol Invest* **30**, 210-214

333. Skurk, T., Alberti-Huber, C., Herder, C., and Hauner, H. (2007) *J Clin Endocrinol Metab* **92**, 1023-1033

334. Xu, H., Barnes, G. T., Yang, Q., Tan, G., Yang, D., Chou, C. J., Sole, J., Nichols, A., Ross, J. S., Tartaglia, L. A., and Chen, H. (2003) *J Clin Invest* **112**, 1821-1830

335. Weisberg, S. P., McCann, D., Desai, M., Rosenbaum, M., Leibel, R. L., and Ferrante, A. W., Jr. (2003) *J Clin Invest* **112**, 1796-1808

336. Odegaard, J. I., and Chawla, A. (2012) *Cold Spring Harb Perspect Med* **2**, a007724

337. Kanda, H., Tateya, S., Tamori, Y., Kotani, K., Hiasa, K., Kitazawa, R., Kitazawa, S., Miyachi, H., Maeda, S., Egashira, K., and Kasuga, M. (2006) *J Clin Invest* **116**, 1494-1505

338. Sun, K., Kusminski, C. M., and Scherer, P. E. (2011) *J Clin Invest* **121**, 2094-2101

339. Lumeng, C. N., Bodzin, J. L., and Saltiel, A. R. (2007) *J Clin Invest* **117**, 175-184

340. Wellen, K. E., and Hotamisligil, G. S. (2003) *J Clin Invest* **112**, 1785-1788

341. Lanthier, N., and Leclercq, I. A. (2014) *Best Pract Res Clin Gastroenterol* **28**, 545-558

342. Pitombo, C., Araujo, E. P., De Souza, C. T., Pareja, J. C., Geloneze, B., and Velloso, L. A. (2006) *J Endocrinol* **191**, 699-706

343. Michalik, L., Auwerx, J., Berger, J. P., Chatterjee, V. K., Glass, C. K., Gonzalez, F. J., Grimaldi, P. A., Kadowaki, T., Lazar, M. A., O'Rahilly, S., Palmer, C. N., Plutzky, J., Reddy, J. K., Spiegelman, B. M., Staels, B., and Wahli, W. (2006) *Pharmacol Rev* **58**, 726-741

344. Bernstein, L. E., Berry, J., Kim, S., Canavan, B., and Grinspoon, S. K. (2006) *Arch Intern Med* **166**, 902-908

345. Hundal, R. S., Petersen, K. F., Mayerson, A. B., Randhawa, P. S., Inzucchi, S., Shoelson, S. E., and Shulman, G. I. (2002) *J Clin Invest* **109**, 1321-1326

346. Kajimura, S., and Saito, M. (2014) *Annu Rev Physiol* **76**, 225-249

347. Pfeifer, A., and Hoffmann, L. S. (2015) *Annu Rev Pharmacol Toxicol* **55**, 207-227

348. Fedorenko, A., Lishko, P. V., and Kirichok, Y. (2012) *Cell* **151**, 400-413

349. Rothwell, N. J., and Stock, M. J. (1979) *Nature* **281**, 31-35

350. Kozak, L. P. (2010) *Cell Metab* **11**, 263-267

351. Bautista, D. M., Siemens, J., Glazer, J. M., Tsuruda, P. R., Basbaum, A. I., Stucky, C. L., Jordt, S. E., and Julius, D. (2007) *Nature* **448**, 204-208

352. Nguyen, K. D., Qiu, Y., Cui, X., Goh, Y. P., Mwangi, J., David, T., Mukundan, L., Brombacher, F., Locksley, R. M., and Chawla, A. (2011) *Nature* **480**, 104-108

353. Bachman, E. S., Dhillon, H., Zhang, C. Y., Cinti, S., Bianco, A. C., Kobilka, B. K., and Lowell, B. B. (2002) *Science* **297**, 843-845

354. Lopez, M., Alvarez, C. V., Nogueiras, R., and Dieguez, C. (2013) *Trends Mol Med* **19**, 418-427

355. de Jesus, L. A., Carvalho, S. D., Ribeiro, M. O., Schneider, M., Kim, S. W., Harney, J. W., Larsen, P. R., and Bianco, A. C. (2001) *J Clin Invest* **108**, 1379-1385

356. Lahesmaa, M., Orava, J., Schalin-Jantti, C., Soinio, M., Hannukainen, J. C., Noponen, T., Kirjavainen, A., Iida, H., Kudomi, N., Enerback, S., Virtanen, K. A., and Nuutila, P. (2014) *J Clin Endocrinol Metab* **99**, E28-35

357. Wikstrom, L., Johansson, C., Salto, C., Barlow, C., Campos Barros, A., Baas, F., Forrest, D., Thoren, P., and Vennstrom, B. (1998) *EMBO J* **17**, 455-461

358. Marrif, H., Schifman, A., Stepanyan, Z., Gillis, M. A., Calderone, A., Weiss, R. E., Samarut, J., and Silva, J. E. (2005) *Endocrinology* **146**, 2872-2884

359. Golozoubova, V., Gullberg, H., Matthias, A., Cannon, B., Vennstrom, B., and Nedergaard, J. (2004) *Mol Endocrinol* **18**, 384-401

360. Sellayah, D., Bharaj, P., and Sikder, D. (2011) *Cell Metab* **14**, 478-490

361. Voss-Andreae, A., Murphy, J. G., Ellacott, K. L., Stuart, R. C., Nillni, E. A., Cone, R. D., and Fan, W. (2007) *Endocrinology* **148**, 1550-1560

362. Vaughan, C. H., Shrestha, Y. B., and Bartness, T. J. (2011) *Brain Res* **1411**, 17-27

363. Margoni, A., Fotis, L., and Papavassiliou, A. G. (2012) *Int J Biochem Cell Biol* **44**, 475-479

364. Whittle, A. J., Carobbio, S., Martins, L., Slawik, M., Hondares, E., Vazquez, M. J., Morgan, D., Csikasz, R. I., Gallego, R., Rodriguez-Cuenca, S., Dale, M., Virtue, S., Villarroya, F., Cannon, B., Rahmouni, K., Lopez, M., and Vidal-Puig, A. (2012) *Cell* **149**, 871-885

365. Qian, S. W., Tang, Y., Li, X., Liu, Y., Zhang, Y. Y., Huang, H. Y., Xue, R. D., Yu, H. Y., Guo, L., Gao, H. D., Sun, X., Li, Y. M., Jia, W. P., and Tang, Q. Q. (2013) *Proc Natl Acad Sci U S A* **110**, E798-807

366. Townsend, K. L., Suzuki, R., Huang, T. L., Jing, E., Schulz, T. J., Lee, K., Taniguchi, C. M., Espinoza, D. O., McDougall, L. E., Zhang, H., He, T. C., Kokkotou, E., and Tseng, Y. H. (2012) *FASEB J* **26**, 2187-2196

367. Bordicchia, M., Liu, D., Amri, E. Z., Ailhaud, G., Dessi-Fulgheri, P., Zhang, C., Takahashi, N., Sarzani, R., and Collins, S. (2012) *J Clin Invest* **122**, 1022-1036

368. Bostrom, P., Wu, J., Jedrychowski, M. P., Korde, A., Ye, L., Lo, J. C., Rasbach, K. A., Bostrom, E. A., Choi, J. H., Long, J. Z., Kajimura, S., Zingaretti, M. C., Vind, B. F., Tu, H., Cinti, S., Hojlund, K., Gygi, S. P., and Spiegelman, B. M. (2012) *Nature* **481**, 463-468

369. Madsen, L., Pedersen, L. M., Lillefosse, H. H., Fjaere, E., Bronstad, I., Hao, Q., Petersen, R. K., Hallenborg, P., Ma, T., De Matteis, R., Araujo, P., Mercader, J., Bonet, M. L., Hansen, J. B., Cannon, B., Nedergaard, J., Wang, J., Cinti, S., Voshol, P., Doskeland, S. O., and Kristiansen, K. (2010) *PLoS One* **5**, e11391

370. Vegiopoulos, A., Muller-Decker, K., Strzoda, D., Schmitt, I., Chichelnitskiy, E., Ostertag, A., Berriel Diaz, M., Rozman, J., Hrabe de Angelis, M., Nusing, R. M.,

Meyer, C. W., Wahli, W., Klingenspor, M., and Herzig, S. (2010) *Science* **328**, 1158-1161

371. Fisher, F. M., Kleiner, S., Douris, N., Fox, E. C., Mepani, R. J., Verdeguer, F., Wu, J., Kharitonenkov, A., Flier, J. S., Maratos-Flier, E., and Spiegelman, B. M. (2012) *Genes Dev* **26**, 271-281

372. Tomlinson, E., Fu, L., John, L., Hultgren, B., Huang, X., Renz, M., Stephan, J. P., Tsai, S. P., Powell-Braxton, L., French, D., and Stewart, T. A. (2002) *Endocrinology* **143**, 1741-1747

373. Fu, L., John, L. M., Adams, S. H., Yu, X. X., Tomlinson, E., Renz, M., Williams, P. M., Soriano, R., Corpuz, R., Moffat, B., Vandlen, R., Simmons, L., Foster, J., Stephan, J. P., Tsai, S. P., and Stewart, T. A. (2004) *Endocrinology* **145**, 2594-2603

374. Lowell, B. B., V, S. S., Hamann, A., Lawitts, J. A., Himms-Hagen, J., Boyer, B. B., Kozak, L. P., and Flier, J. S. (1993) *Nature* **366**, 740-742

375. Jimenez, M., Leger, B., Canola, K., Lehr, L., Arboit, P., Seydoux, J., Russell, A. P., Giacobino, J. P., Muzzin, P., and Preitner, F. (2002) *FEBS Lett* **530**, 37-40

376. Kontani, Y., Wang, Y., Kimura, K., Inokuma, K. I., Saito, M., Suzuki-Miura, T., Wang, Z., Sato, Y., Mori, N., and Yamashita, H. (2005) *Aging Cell* **4**, 147-155

377. Liu, X., Rossmeisl, M., McClaine, J., Riachi, M., Harper, M. E., and Kozak, L. P. (2003) *J Clin Invest* **111**, 399-407

378. Enerback, S., Jacobsson, A., Simpson, E. M., Guerra, C., Yamashita, H., Harper, M. E., and Kozak, L. P. (1997) *Nature* **387**, 90-94

379. Feldmann, H. M., Golozoubova, V., Cannon, B., and Nedergaard, J. (2009) *Cell Metab* **9**, 203-209

380. Anunciado-Koza, R. P., Zhang, J., Ukropec, J., Bajpeyi, S., Koza, R. A., Rogers, R. C., Cefalu, W. T., Mynatt, R. L., and Kozak, L. P. (2011) *J Biol Chem* **286**, 11659-11671

381. Bal, N. C., Maurya, S. K., Sopariwala, D. H., Sahoo, S. K., Gupta, S. C., Shaikh, S. A., Pant, M., Rowland, L. A., Bombardier, E., Goonasekera, S. A., Tupling, A. R., Molkentin, J. D., and Periasamy, M. (2012) *Nat Med* **18**, 1575-1579

382. Guerra, C., Koza, R. A., Yamashita, H., Walsh, K., and Kozak, L. P. (1998) *J Clin Invest* **102**, 412-420

383. Stanford, K. I., Middelbeek, R. J., Townsend, K. L., An, D., Nygaard, E. B., Hitchcox, K. M., Markan, K. R., Nakano, K., Hirshman, M. F., Tseng, Y. H., and Goodyear, L. J. (2013) *J Clin Invest* **123**, 215-223

384. Seale, P., Conroe, H. M., Estall, J., Kajimura, S., Frontini, A., Ishibashi, J., Cohen, P., Cinti, S., and Spiegelman, B. M. (2011) *J Clin Invest* **121**, 96-105

385. Townsend, K. L., and Tseng, Y. H. (2014) *Trends Endocrinol Metab* **25**, 168-177

386. Barnett, S. A., Coleman, E. M., and Manly, B. M. (1960) *Q J Exp Physiol Cogn Med Sci* **45**, 40-49

387. Meneghini, A., Ferreira, C., Abreu, L. C., Valenti, V. E., Ferreira, M., C, F. F., and Murad, N. (2009) *Clinics (Sao Paulo)* **64**, 921-926

388. Nikonova, L., Koza, R. A., Mendoza, T., Chao, P. M., Curley, J. P., and Kozak, L. P. (2008) *FASEB J* **22**, 3925-3937

389. Bartelt, A., Bruns, O. T., Reimer, R., Hohenberg, H., Ittrich, H., Peldschus, K., Kaul, M. G., Tromsdorf, U. I., Weller, H., Waurisch, C., Eychmuller, A., Gordts, P. L., Rinninger, F., Bruegelmann, K., Freund, B., Nielsen, P., Merkel, M., and Heeren, J. (2011) *Nat Med* **17**, 200-205

390. Vallerand, A. L., Perusse, F., and Bukowiecki, L. J. (1990) *Am J Physiol* **259**, R1043-1049

391. Inokuma, K., Ogura-Okamatsu, Y., Toda, C., Kimura, K., Yamashita, H., and Saito, M. (2005) *Diabetes* **54**, 1385-1391

392. Gasparetti, A. L., de Souza, C. T., Pereira-da-Silva, M., Oliveira, R. L., Saad, M. J., Carneiro, E. M., and Velloso, L. A. (2003) *J Physiol* **552**, 149-162

393. Cannon, B., and Nedergaard, J. (2010) *Int J Obes (Lond)* **34 Suppl 1**, S7-16

394. Saito, M., Okamatsu-Ogura, Y., Matsushita, M., Watanabe, K., Yoneshiro, T., Nio-Kobayashi, J., Iwanaga, T., Miyagawa, M., Kameya, T., Nakada, K., Kawai, Y., and Tsujisaki, M. (2009) *Diabetes* **58**, 1526-1531

395. Nedergaard, J., Bengtsson, T., and Cannon, B. (2007) *Am J Physiol Endocrinol Metab* **293**, E444-452

396. van Marken Lichtenbelt, W. D., Vanhommerig, J. W., Smulders, N. M., Drossaerts, J. M., Kemerink, G. J., Bouvy, N. D., Schrauwen, P., and Teule, G. J. (2009) *N Engl J Med* **360**, 1500-1508

397. Hu, H. H., Perkins, T. G., Chia, J. M., and Gilsanz, V. (2013) *AJR Am J Roentgenol* **200**, 177-183

398. Ouellet, V., Labbe, S. M., Blondin, D. P., Phoenix, S., Guerin, B., Haman, F., Turcotte, E. E., Richard, D., and Carpentier, A. C. (2012) *J Clin Invest* **122**, 545-552

399. Matsushita, M., Yoneshiro, T., Aita, S., Kameya, T., Sugie, H., and Saito, M. (2014) *Int J Obes (Lond)* **38**, 812-817

400. Orava, J., Nuutila, P., Lidell, M. E., Oikonen, V., Noponen, T., Viljanen, T., Scheinin, M., Taittonen, M., Niemi, T., Enerback, S., and Virtanen, K. A. (2011) *Cell Metab* **14**, 272-279

401. Chondronikola, M., Volpi, E., Borsheim, E., Porter, C., Annamalai, P., Enerback, S., Lidell, M. E., Saraf, M. K., Labbe, S. M., Hurren, N. M., Yfanti, C., Chao, T., Andersen, C. R., Cesani, F., Hawkins, H., and Sidossis, L. S. (2014) *Diabetes* **63**, 4089-4099

402. Lidell, M. E., Betz, M. J., Dahlqvist Leinhard, O., Heglind, M., Elander, L., Slawik, M., Mussack, T., Nilsson, D., Romu, T., Nuutila, P., Virtanen, K. A., Beuschlein, F., Persson, A., Borga, M., and Enerback, S. (2013) *Nat Med* **19**, 631-634

403. Sharp, L. Z., Shinoda, K., Ohno, H., Scheel, D. W., Tomoda, E., Ruiz, L., Hu, H., Wang, L., Pavlova, Z., Gilsanz, V., and Kajimura, S. (2012) *PLoS One* **7**, e49452

404. Reo, N. V., Adinehzadeh, M., and Foy, B. D. (2002) *Biochim Biophys Acta* **1580**, 171-188

405. DeLong, C. J., Shen, Y. J., Thomas, M. J., and Cui, Z. (1999) *J Biol Chem* **274**, 29683-29688

406. Niebergall, L. J., Jacobs, R. L., Chaba, T., and Vance, D. E. (2011) *Biochim Biophys Acta* **1811**, 1177-1185

407. Katagiri, H., Yamada, T., and Oka, Y. (2007) *Circ Res* **101**, 27-39

408. Izumida, Y., Yahagi, N., Takeuchi, Y., Nishi, M., Shikama, A., Takarada, A., Masuda, Y., Kubota, M., Matsuzaka, T., Nakagawa, Y., Iizuka, Y., Itaka, K., Kataoka, K., Shioda, S., Niijima, A., Yamada, T., Katagiri, H., Nagai, R., Yamada, N., Kadowaki, T., and Shimano, H. (2013) *Nat Commun* **4**, 2316

409. Banni, S., Carta, G., Murru, E., Cordeddu, L., Giordano, E., Marrosu, F., Puligheddu, M., Floris, G., Asuni, G. P., Cappai, A. L., Deriu, S., and Follesa, P. (2012) *PLoS One* **7**, e44813

410. Sachdeva, A. K., Zaren, H. A., and Sigel, B. (1991) *Med Clin North Am* **75**, 999-1012

411. Chang, T. M., Chan, D. C., Liu, Y. C., Tsou, S. S., and Chen, T. H. (2001) *Am J Surg* **181**, 372-376

412. Boss, T., Peters, J., Patti, M., Lustig, R., and Kral, J. (2007) Laparoscopic truncal vagotomy for weight-loss: initial experience in 15 patients from a prospective, multi-center study [Abstract]. in *Scientific Session of the Society of American Gastrointestinal and Endoscopic Surgeons*, Las Vegas, Nevada, USA

413. Hummasti, S., and Hotamisligil, G. S. (2010) *Circ Res* **107**, 579-591

414. Fu, S., Watkins, S. M., and Hotamisligil, G. S. (2012) *Cell Metab* **15**, 623-634

Chapter 2

Vagus Nerve Contributes to the Development of Steatohepatitis and Obesity in Phosphatidylethanolamine *N*-methyltransferase Deficient Mice

2.1 Introduction

The prevalence of non-alcoholic fatty liver disease (NAFLD) is rapidly rising throughout the world. In the United States, it is estimated that 70% of obese and diabetic patients have NAFLD (1). NAFLD includes a wide spectrum of hepatic diseases, from steatosis (lipid accumulation) to non-alcoholic steatohepatitis (NASH; steatosis with inflammation) and eventually end-stage liver failure (2,3). Currently, it is unclear how steatosis progresses into NASH. Recent studies (4,5) by us and others have linked NAFLD with aberrant hepatic phospholipid levels. The amount and ratio of phosphatidylcholine (PC) and phosphatidylethanolamine (PE) are essential for membrane integrity. Decreased hepatic PC and decreased ratio of hepatic PC/PE induces steatosis in mice and has been observed in NASH patients (5). In mice, the PC/PE ratio is a strong predictor of liver function and survival rate after partial hepatectomy (6).

In the liver, PC is synthesized via both the CDP-choline pathway and the PEMT pathway (7,8). Under normal conditions, the CDP-choline pathway accounts for ~70% hepatic PC biosynthesis, and the remaining 30% is synthesized via the PEMT pathway (8). The rate-limiting reaction in the CDP-choline pathway is catalyzed by CTP:phosphocholine cytidylyltransferase (9,10). CT is encoded by two genes, *Pcyt1a* and *Pcyt1b*, and CTα (the product of *Pcyt1a*) is the predominant isoform in the liver (11,12). Inhibition of either the CDP-choline (by liver-specific deletion of CTα) or PEMT pathway results in steatosis (13). This is mainly due to decreased hepatic PC production resulting in impaired very low density lipoprotein (VLDL) secretion. When fed a HF (14) diet for 10 weeks, mice lacking PEMT (*Pemt*$^{-/-}$ mice) are resistant to diet-

induced obesity (DIO) but develop severe NASH (9). The reason for the resistance to DIO in *Pemt*$^{-/-}$ mice is not simply due to either reduced PC synthesis or VLDL secretion, as the liver specific CTα knockout mice (*LCTα*$^{-/-}$ mice) are not protected from DIO (9).

The inter-organ communication through the autonomic nervous system is an essential regulator of metabolism (15). The vagus nerve is an important collection of nerve fibers, including sensor (afferent) and motor (efferent) nerves (16). Selective vagotomy has uncovered a role of vagus nerve in regulating satiety, hormonal secretion (insulin) and response to hormones (ghrelin) (16,17). Adenoviral expression of peroxisome proliferator-activated receptor (PPAR)γ2 in the livers of wild-type mice increases energy expenditure, decreases adiposity and improves insulin sensitivity, all of which are prevented by hepatic vagotomy (HV) (18). Similarly, the vagus nerve is involved in linking lower hepatic PPARα expression to insulin resistance (19). Consequently, long-term stimulation of hepatic vagus nerve in rats results in reduced body weight gain (20). Thus, we hypothesized that neuronal signals relayed via the hepatic branch of vagus nerve are implicated in the resistance to DIO and the development of NASH in *Pemt*$^{-/-}$ mice.

Here, we performed HV on both *Pemt*$^{+/+}$ and *Pemt*$^{-/-}$ mice to investigate whether signals through hepatic vagus nerve contribute to the protection of obesity in *Pemt*$^{-/-}$ mice. Our data show that neuronal signals through hepatic vagus nerve are critical for the resistance to DIO in *Pemt*$^{-/-}$ mice. Surprisingly, HV also completely abolished HF-induced NASH in these mice. To further examine the contribution of afferent hepatic branch of vagus nerve alone, we blunted the afferent nerve with capsaicin. Capsaicin did not reverse the protection against DIO, nor improve the HF-induced NASH in *Pemt*$^{-/-}$

mice. The current study highlights a fundamental role of hepatic vagus nerve in the development of adiposity and NASH in *Pemt*$^{-/-}$ mice.

2.2 Materials and methods

2.2.1 Animal handling, diets and surgery

All procedures were approved by the University of Alberta's Institutional Animal Care Committee in accordance with guidelines of the Canadian Council on Animal Care. Male C57BL/6 (backcrossed >7 generations) *Pemt*$^{+/+}$ and *Pemt*$^{-/-}$ mice were exposed to a 12 h light-dark cycle and housed with free access to water and standard chow diet (LabDiet, #5001) with 58% calories from carbohydrate and 13% from fat, before surgery.

For HV, the common hepatic-branch of the vagus nerve (both afferent and efferent nerves) of 8-week-old *Pemt*$^{+/+}$ and *Pemt*$^{-/-}$ mice was cut and control mice were subjected to sham operation, as described (21). All the procedures were performed using aseptic microvascular technique. The animals had ophthalmic ointment applied to the eyes and were anaesthetized with inhalation of 1.5% isoflurane. After the abdomen was opened by a long midline incision, the anterior vagal trunk along the esophagus was exposed. Then, the common hepatic vagal branch was freed from surrounding tissue and transected. The abdominal incision was closed with 5-0 absorbable vicryl suture. For deafferentation study, the hepatic vagal branch was freed from the surrounding tissues by paraffin paper and then wrapped with gauze soaked with vehicle (Tween 80: olive oil =1:9) alone or 10 mg/ml capsaicin dissolved in the vehicle solution

for 30 min as described (19). All surgeries were performed by Dr. Linfu Zhu (department of surgery, University of Alberta) between 9:00 a.m.-12:00 p.m. under isofluorane anesthesia. For the first 24 h post-surgery, the mice recovered in a warmed nursery incubator in a small animal intensive unit of University of Alberta's Microsurgery Transplantation Laboratory with unrestricted access to food and water. The criteria for euthanasia included lethargy and dehydration. However, all mice survived the surgery and were allowed to recover for a week with free access to water and standard chow diet. After the recovery, mice were fed the HF diet (Bio-Serv, #F3282), in which 60% calories derive from fat, for 10 weeks. Mice were fasted for 12 h before sacrifice. Tissues were collected and stored at -80 °C until analysis or preserved in 10% phosphate-buffered formalin for histology.

2.2.2 *In vivo* metabolic analysis

Metabolic measurements (O_2 consumption, CO_2 production and heat production) were obtained using a Comprehensive Lab Animal Monitoring System (Columbus Instruments, OH). Mice were housed individually for 3 days before being placed in metabolic cages. Following an initial 24 h acclimatization period, measurements were taken every 13 min for 24 h. Mice were fasted for 12 h before a glucose tolerance test. Briefly, mice were administered glucose (2 g/kg body weight) by i.p. injection. Blood glucose was measured by a glucometer prior to injection and at indicated times afterwards.

2.2.3 Analytical procedures

The mass of cholesterol-and cholesteryl ester was measured by gas-liquid chromatography (22). The mass of triacylglycerol (23) was either measured by gas-

liquid chromatography or commercially available kit according to the manufacturer's protocols from Roche Diagnostics. Plasma alanine aminotransferase was measured using commercially available kit (Biotron Diagnostics) according to the manufacturer's protocols. Hepatic cytokines and chemokines were quantified using ELISA kits from eBioscience or Preprotech. Protein concentrations were determined by the Bradford assay (Bio-Rad). Lipid analysis using gas-liquid chromatography was performed by Audric Moses (University of Alberta) and the hepatic cytokines and chemokines were measured by Marta Ordoñez and Antonio Gomez-Muñoz (University of the Basque Country, Spain).

Hepatic PC and PE were quantified as previously described by a phosphorus assay (24). Hepatic lipids were first extracted from liver homogenate (1 mg of protein in 1 ml of PBS) with 4 ml of chloroform/methanol (2/1, v/v). The mixture was vortexed vigorously for 1 min and then centrifuged for 10 min at 1800 rpm. The lower organic phase was collected and dried down under nitrogen. The dried lipids were re-suspended in 200 µl of chloroform/methanol (2/1; v/v) and 50% of each sample was then subjected to lipid separation by thin-layer chromatography. The PC and PE were resolved in the solvent system chloroform/methanol/acetic acid/water (50/30/8/4; v/v). Bands corresponding to PC and PE loading standards (Avanti) were visualized by iodine vapor and scraped for a phosphorus assay in a glass tube. In this assay, phosphate standards (sodium phosphate, 0-200 nmol) were first dried at 180°C. When the standards were cooled to room temperature, 450 µl of 70% perchloric acid was added to each unknown sample or standard. Each tube was covered with a marble on the top and then heated at 180°C for 1 h. Following the heating, all tubes were cooled to

room temperature before the marbles were removed. 2.5 ml of deionized water was added to each tube, followed by 0.5 ml of ammonium molybydate (2.5%, w/v). The mixture was vortexed immediately. Then, 0.5 ml of ascorbic acid (10%, w/v) was added to each tube. The mixture was vortexed immediately before the colour development step by incubation in hot water (90-95°C) for 15 min. Next, samples were centrifuged for 5 min at 2000 rpm to pellet the silica. The absorbance of the supernatant was read at 820 nm and the concentration of PC or PE was calculated from the standard curve.

2.2.4 Histology

A portion of the liver and gonadal white adipose tissue (WAT) was subjected to hematoxylin and eosin (H&E) staining. Tissue was first fixed in 10% buffered formalin for at least 24 hours. Then, tissue was embedded in paraffin, sectioned, and stained with H&E by the Histocore of Alberta Diabetes Institute (University of Alberta). Liver slides were scored for steatosis, hepatocellular ballooning, and portal inflammation and lobular inflammation, using a modified NAFLD activity score system (25). The histological analysis of liver slides was performed by pathologist Dr. Todd Chaba (University of Alberta). All slides were visualized by a dissecting light microscope (40x objective magnification) and images were captured by the ZEISS AxioCam MRc**.** The size of individual adipocytes was quantified using ImageJ software from the National Institutes of Health.

2.2.5 Electron microscopy

The common truncal vagus nerve and the hepatic branch of the vagus nerve were collected from mice with no treatment and from mice 7 days post-surgically treated with or without capsaicin. Samples were processed as described before (9). All samples

were first fixed in fixation buffer (2.5% (v/v) glutaraldehyde in 0.1 M sodium cacodylate buffer, pH 7.2) for 2 h at room temperature and then for overnight at 4°C. The samples were washed three times (20 min each wash) in the same buffer (0.1 M sodium cacodylate, pH 7.2) and were then fixed in 0.1% osmium tetroxide in the same buffer for 2 h at room temperature. These samples were briefly washed in distilled water and dehydrated in a graded series of ethanol solutions (30%, 50%, 70%, 90 and 100%; 15 min each grade) before two 15-min washes with 100% ethanol. The samples were placed in two changes of propylene oxide and embedded in araldite. Blocks were cut at Leica EM UC6 ultramicrotome with DiATOME diamond knife. Ultrathin sections (80-100 nm) were stained with 2% uranyl acetate and 1% lead citrate. Electron micrographs were taken with a Jeol JEM-2100 transmission electron microscope.

2.2.6 Real-time quantitative PCR

Total RNA was isolated from snap-frozen liver tissue using TRIzol reagent (Invitrogen). Total RNA was treated with DNase I (Invitrogen) to degrade genomic DNA, then reverse-transcribed using an oligo(dT)12–18 primer and Superscript II reverse transcriptase (Invitrogen). Real-time quantitative PCR was performed using a Rotor-Gene 3000 instrument (Montreal Biotech). mRNA levels were normalized to cyclophilin mRNA using a standard curve. Primers for real-time quantitative PCR were purchased from the Institute of Biomolecular Design at the University of Alberta and are listed in Table 2.1.

2.2.7 Immunoblotting

Tissues were homogenized in buffer (100 mM Tris–HCl, 150 mM NaCl, 1 mM EDTA, 1 mM dithiothreitol, and 0.1 mM phenylmethylsulfonyl fluoride, pH 7.4) with

addition of protease inhibitor cocktail (Sigma #P8340) and phosphatase inhibitor cocktail 3 (Sigma #P0044), followed by sonication for 10 sec. Twenty micrograms of protein were generally heated for 10 min at 95°C in sample buffer (125 mM Tris-HCl, 25% glycerol, 2% SDS, 0.25% 2-mercaptoethanol, 0.025% bromophenol blue, pH 6.8) and then electrophoresed on a SDS-polyacrylamide gel in electrophoresis buffer (25 mM Tris-HCl, 192 mM glycine, 0.1% SDS buffer, pH 8.5). One exception is for detecting OXPHOS complexes, for which protein samples were brought up to room temperature without heating for 10 min before the electrophoresis. Proteins were transferred to a polyvinylidene fluoride membrane in transfer buffer (25 mM Tris-HCl, 192 mM glycine, 10% (v/v) methanol) for 2 h at 100 V. The membrane was then blocked with 5% (w/v) skim milk in T-TBS buffer (20 mM Tris-HCl, 150 mM NaCl, 0.1% Tween 20, pH 7.4) for 1 h. Following the blocking, membrane was then probed with primary antibodies against OXPHOS complexes (1:1000 dilution, Abcam ab110413), uncoupling protein 2 (UCP2, 1:1000 dilution, Abcam ab67241), porin (VDAC, 1:1000 dilution, Abcam ab14734), C/EBP homologous protein (CHOP, 1:1000 dilution, Cell signaling #2895), total acetyl-CoA carboxylase (ACC, 1:1000 dilution, Cell signaling #3662), phospho-ACC (Ser79, 1:1000 dilution, Cell signaling #3661), fatty acid synthase (FAS, 1:1000 dilution, Cell signaling #3189), and protein disulfide isomerase (PDI, 1:1000 dilution, Enzo Life Sciences SPA-890) for overnight at 4°C. Primary antibodies were diluted with 5% (w/v) bovine serum albumin in T-TBS buffer. Secondary antibodies were goat anti-mouse and goat anti-rabbit IgG-horse radish peroxidase conjugate (Bio-Rad) and were diluted 1:5,000-1:10,000 with 1% (w/v) skim milk in T-TBS buffer. The immunoreactive bands

were visualized by enhanced chemiluminescence system (Amersham Biosciences) according to the manufacturer's instructions.

2.2.8 Statistical analysis

Data are presented as mean values ± SEM. Comparisons between groups for body weight gain, glucose tolerance test and *in vivo* metabolic data were performed using an analysis of variance. For all other comparisons, a two-way ANOVA, followed by post hoc Bonferroni's test of individual group differences was used. $P < 0.05$ was considered significant. Unless otherwise indicated, six to eight animals were used per experimental group.

2.3 Results

2.3.1 HV abolishes the protection against DIO in *Pemt*$^{-/-}$ mice

Pemt$^{+/+}$ and *Pemt*$^{-/-}$ mice were subjected to HV or sham operation, followed with a 10-week HF feeding. HV reduced weight gain in *Pemt*$^{+/+}$ mice (Figure 2.1A). In contrast, HV stimulated weight gain in *Pemt*$^{-/-}$ mice throughout the 10-week HF feeding (Figure 2.1A), although HV-operated *Pemt*$^{+/+}$ mice still gained more weight than that of HV-operated *Pemt*$^{-/-}$ mice. Similar to our previous observation (9), sham-operated *Pemt*$^{-/-}$ mice had lower fasting plasma glucose than *Pemt*$^{+/+}$ mice (Figure 2.1B). A minor but significant decrease of plasma glucose was observed in HV-operated *Pemt*$^{+/+}$ mice compared to sham-operated mice. In accordance with the body weight gain, HV reversed glucose tolerance in the *Pemt*$^{-/-}$ sham group mice (Figure 2.1C). Consistent with our previously report (9), *Pemt*$^{-/-}$ mice had smaller visceral adipocytes than *Pemt*$^{+/+}$

mice following sham operation (Figure 2.1D&E). HV increased the size of adipocytes in *Pemt*$^{-/-}$ mice to that of *Pemt*$^{+/+}$ mice. In addition, macrophage infiltration was observed in *Pemt*$^{+/+}$ and HV-operated *Pemt*$^{-/-}$ mice, but not in sham-operated *Pemt*$^{-/-}$ mice (Figure 2.1D, lower panel). Clearly, HV reverses the protection against DIO and glucose tolerance in *Pemt*$^{-/-}$ mice.

2.3.2 HV reduces whole body energy expenditure in *Pemt*$^{-/-}$ mice

To explain the metabolic changes following hepatic vagotomy, we examined whole body energy utilization in mice fed the HF diet for 8 weeks. Consistent with our previous data (15), sham-*Pemt*$^{-/-}$ mice displayed higher oxygen consumption than *Pemt*$^{+/+}$ mice throughout the light and dark cycles (Figure 2.2A), indicating higher energy expenditure. HV reduced oxygen consumption in *Pemt*$^{-/-}$ mice; however, in *Pemt*$^{+/+}$ mice, HV led to a slight but significant increase in oxygen consumption through the dark cycle only (Figure 2.2A). Sham-*Pemt*$^{-/-}$ mice had an elevated respiratory exchange ratio that was reduced by HV (Figure 2.2B). Heat production was higher in sham-operated *Pemt*$^{-/-}$ mice during both the light and dark cycles; and this increase was normalized by HV (Figure 2.2C). As previously reported, there was no difference in physical activity between genotypes (data not shown). Together, HV decreases energy expenditure in *Pemt*$^{-/-}$ mice.

2.3.3 HV protects *Pemt*$^{-/-}$ mice from HF-induced steatohepatitis

Pemt$^{-/-}$ mice develop steatohepatitis when fed a HF diet (6). The livers of sham-operated *Pemt*$^{-/-}$ mice were 2.5-fold larger than those from *Pemt*$^{+/+}$ mice (Table 2.2). Hepatic cholesteryl ester and TG were elevated 3-fold in sham-operated *Pemt*$^{-/-}$ mice compared to *Pemt*$^{+/+}$ mice (Table 2.2); HV normalized hepatic cholesteryl ester and TG in *Pemt*$^{-/-}$ mice. As previously reported (6), sham-operated *Pemt*$^{-/-}$ mice had lower

hepatic PC when challenged with HF diet (Table 2.2); HV increased PC in *Pemt*$^{-/-}$ mice to wild-type levels. Hepatic PE levels were not different among groups (Table 2.2). Sham-operated *Pemt*$^{-/-}$ mice had low levels of plasma cholesterol and TG as compared to *Pemt*$^{+/+}$ mice. Plasma cholesterol, but not TG, was normalized in HV *Pemt*$^{-/-}$ mice (Table 2.2).

Histopathological analysis revealed the presence of small lipid droplets in the livers from *Pemt*$^{+/+}$ mice (Figure 2.3A, upper left). In comparison, liver sections from sham-operated *Pemt*$^{-/-}$ mice were filled with large lipid droplets (Figure 2.3A, upper right). Accordingly, *Pemt*$^{-/-}$ mice exhibited severe steatosis, inflammation and hepatocellular ballooning; and all these measurements were reversed by HV (Figure 2.3A&C). Plasma alanine aminotransferase, a marker of liver damage, was elevated 4-fold in sham-operated *Pemt*$^{-/-}$ mice compared to wild-type controls and HV-*Pemt*$^{-/-}$ mice (Figure 2.3B). Hepatic mRNA levels of inflammatory genes, *tumor necrosis factor (TNF)α*, *F4/80* and *cluster of differentiation (CD)68*, were elevated in *Pemt*$^{-/-}$ mice; HV normalized the expression of these genes (Figure 2.3D). Moreover, the higher amount of hepatic chemokine monocyte chemotactic protein (MCP)-1 in sham-operated *Pemt*$^{-/-}$ mice was dramatically decreased by HV (Figure 2.4). A similar reduction was observed for chemokine RANTES and pro-inflammatory cytokine interleukin (IL)-1α, although this did not reach significant difference. On the other hand, the low level of the anti-inflammatory cytokine IL-10 in *Pemt*$^{-/-}$ mice was increased by HV (Figure 2.4). Together, HV protects *Pemt*$^{-/-}$ mice from HF-induced NASH.

2.3.4 HV improves hepatic energy metabolism

To examine the mechanism by which HV alters hepatic lipid metabolism, we first examined the expression of mitochondrial proteins. Sham-operated *Pemt*$^{-/-}$ mice had low levels of electron transport chain proteins, including complex I, complex II, complex III and complex V, and elevated UCP2 as compared to *Pemt*$^{+/+}$ mice. The mitochondrial marker VDAC was not different among groups (Figure 2.5A &B). HV had no effect on the expression of these mitochondrial proteins in *Pemt*$^{+/+}$ mice, but prevented the abnormal expression in *Pemt*$^{-/-}$ mice (Figure 2.5A). HV also prevented the increased expression of CHOP, a pro-apoptotic ER stress responsive protein, in *Pemt*$^{-/-}$ mice (Figure 2.5C).

Sham-operated *Pemt*$^{-/-}$ mice exhibited low protein expression of ACC and FAS, indicating a potential impairment in *de novo* lipogenesis; the levels of these proteins were restored by HV (Figure 2.5D&E). Low levels of *malonyl-CoA decarboxylase (MCD)*, *microsomal triglyceride transfer protein (MTTP)*, *glucose-6-P phosphatase (G6P)*, *PPARα*, *sterol regulatory element-binding protein (SREBP)1c* and *PPARγ coactivator (PGC)1α*, and elevated *PPARγ* and *cluster of differentiation (CD)36* mRNA were observed in sham-operated *Pemt*$^{-/-}$ mice (Figure 2.6). The expression of these genes was normalized in HV-*Pemt*$^{-/-}$ mice. In combination, HV improves the expression genes involved in energy metabolism in the liver.

2.3.5 Capsaicin does not reverse the protection against DIO or the development of NASH in HF-fed *Pemt*$^{-/-}$ mice

HV is involved in dissection of both afferent and efferent vagus nerve between the liver and brain. Afferent nerve fibers composed of 80-90% of vagus nerve (26), and the majority of the afferent nerve fibers are unmyelinated and sensitive to capsaicin, which

is toxic to the afferent nerve (16). To further explore whether the afferent hepatic branch of vagus nerve alone is critical to the protection against DIO and the development of HF-induced NASH in *Pemt*$^{-/-}$ mice, hepatic branch of vagus nerve from both *Pemt*$^{+/+}$ mice and *Pemt*$^{-/-}$ mice were treated with capsaicin or vehicle as control. Capsaicin disrupted the unmyelinated fibers, but not the myelinated fibers in the hepatic branch of the vagus nerve as examined by electron microscopy (Figure 2.7A). As control, the unmyelinated and myelinated fibers were intact in the hepatic branch of the vagus nerve from vehicle treated mice and in the common vagal trunk from all mice (Figure 2.7A). There was no difference in the food intake among all four groups of mice over the first two weeks of HF feeding (data not shown). Capsaicin did not change the body weight gain in either *Pemt*$^{+/+}$ mice or *Pemt*$^{-/-}$ mice throughout the 10-week of HF feeding (Figure 2.7B). Accordingly, capsaicin did not reverse the glucose tolerance in *Pemt*$^{-/-}$ mice (Figure 2.7C). Capsaicin did not reverse HF-induced NASH in *Pemt*$^{-/-}$ mice, and this was supported by histological data (Figure 2.7D) and the biochemical measurement of hepatic TG levels (Figure 2.7E). Plasma ALT levels remained high in capsaicin-treated *Pemt*$^{-/-}$ mice (Figure 2.7F). Plasma TG levels showed a trend toward increase in the capsaicin-treated *Pemt*$^{-/-}$ mice (Figure 2.7G). On the other hand, capsaicin-treated *Pemt*$^{+/+}$ mice showed an increased amount of lipid droplets examined by histological analysis (Figure 2.7D) and 42.1% increase in the hepatic TG levels (Figure 2.7E), compared to vehicle-treated *Pemt*$^{+/+}$ mice. Plasma TG levels was greatly decreased in the capsaicin-treated *Pemt*$^{+/+}$ mice (Figure 2.7G). Overall, capsaicin-caused disruption of the afferent nerve fibers does not reverse the protection against DIO or the development of HF-induced NASH in *Pemt*$^{-/-}$ mice.

2.4 Discussion

The current study supports a role for the vagus nerve in the development of DIO and NASH. HV reduced weight gain and increased oxygen consumption in *Pemt*$^{+/+}$ mice, but failed to prevent glucose intolerance. HV led to white adipocyte hypertrophy, reduced oxygen consumption and partially reversed the protection against DIO in *Pemt*$^{-/-}$ mice. Moreover, HV prevented hepatic lipid accumulation and progression into NASH in HF-fed *Pemt*$^{-/-}$ mice. However, capsaicin-mediated disruption of the afferent nerve alone failed to reverse the protection against DIO or the development of HF-induced NASH in *Pemt*$^{-/-}$ mice. Together, the hepatic branch of the vagus nerve, particularly the efferent hepatic vagus nerve, is of great importance in the protection against DIO and the development of NASH in *Pemt*$^{-/-}$ mice.

2.4.1 HV abolishes the protection against DIO in *Pemt*$^{-/-}$ mice

In our previous studies, we demonstrated that choline, but not PC or betaine, deficiency plays a role in protecting *Pemt*$^{-/-}$ mice from obesity (9). Insufficient dietary choline supply also attenuates weight gain in *ob/ob* mice (27), a genetic model of obesity. Choline, in addition to being a substrate for PC biosynthesis, acts as precursor for acetylcholine (a neuronal transmitter). In the present study, HV partially reversed the protection against HF-induced weight gain in *Pemt*$^{-/-}$ mice (Figure 2.1A) and attenuated glucose tolerance (Figure 2.1C). Apparently, neuronal signals through hepatic vagus nerve are also involved in the protection against DIO in *Pemt*$^{-/-}$ mice.

The inter-organ communication among the liver, muscle, brain and adipose tissue, through the autonomic nervous system is an essential component for energy metabolism (15). *Pemt*$^{-/-}$ mice displayed higher oxygen consumption and heat production, and adipocyte hypotrophy; these phenotypes depended on an intact hepatic vagus nerve. *Pemt*$^{-/-}$ mice showed higher hepatic levels of *CD36* mRNA and UCP2 protein, and lower mitochondrial electron transport chain proteins (Figure 2.5 and Figure 2.6), indicating higher fatty acid uptake and dysfunctional mitochondria in the liver. HV reduced levels of *CD36* mRNA and UCP2 protein, restored the expression of mitochondrial electron transport chain proteins (Figure 2.5), and completely abolished NASH development in *Pemt*$^{-/-}$ mice. Thus, HV seems to divert the flow of dietary fat from the liver to adipose tissue in *Pemt*$^{-/-}$ mice, promotes energy store in the adipose tissue and alleviates the burden of excess fat to the liver.

Hypothalamic sensing of circulating fatty acid has been shown to regulate hepatic glucose production (28). Central inhibition of fat oxidation alters hepatic gluconeogenesis through the descending fibers within the vagus nerve (29). In addition, the vagus nerve has been shown to be important in the regulation of satiety (30), mainly through the secretion of hormones, such as insulin, ghrelin and glucose-dependent insulinotropic polypeptide (16,17). However, food intake cannot explain the resistance to DIO in *Pemt*$^{-/-}$ mice, since we observed no difference in food intake after 10 days of the HF feeding (9). HV did not alter physical activity in *Pemt*$^{+/+}$ mice, but increased oxygen consumption during the dark cycle that may account for the reduction in weight gain. This is consistent with the recent report that subdiaphragmatic vagotomy exerts resistance to DIO in rats (31). In contrast, HV reduced oxygen consumption, promoted

diet-induced weight gain and glucose intolerance in *Pemt*$^{-/-}$ mice. It is unclear why *Pemt*$^{+/+}$ and *Pemt*$^{-/-}$ mice responded differently to the HF diet following HV.

2.4.2 HV attenuates the NASH development in *Pemt*$^{-/-}$ mice

The *Pemt*$^{-/-}$ mice and *LCTα*$^{-/-}$ mice develop NASH when fed a HF diet (13) primarily due to a reduction in VLDL assembly and secretion (9). Interestingly, normalization of hepatic TG or PC in *LCTα*$^{-/-}$ mice was not sufficient to prevent liver dysfunction (13), indicating other factor(s) may be involved in NASH development. It has been reported that HF diet feeding activates a cholinergic anti-inflammatory pathway (32), controlled by the vagus nerve, to prevent systematic inflammatory damage from cytokines and inflammatory diseases (33). Furthermore, acetylcholine attenuates the release of cytokines in cultured human macrophages stimulated by lipopolysaccharide (34). Thus, insufficient choline in *Pemt*$^{-/-}$ mice (35) may impair the cholinergic neuronal pathway, blunt protection from cytokines, and eventually result in the development of NASH. Indeed, mRNA levels for proinflammatory marker *TNFα* and macrophage markers (*CD68* and *F4/80*) were higher in *Pemt*$^{-/-}$ mice (Figure 2.3C), along with the ER stress marker CHOP (Figure 2.5C). The hepatic chemokine MCP-1 was significantly increased, while the hepatic IL-10 and IL-6 was dramatically reduced in *Pemt*$^{-/-}$ mice (Figure 2.4). The tissue levels of TNFα were much lower than IL-10, and there was no difference between *Pemt*$^{+/+}$ mice and *Pemt*$^{-/-}$ mice (Figure 2.4). We observed no significant changes in hepatic lipid accumulation or inflammation in *Pemt*$^{+/+}$ mice after HV. However, hepatomegaly, hepatic lipid accumulation and inflammation were rescued in the HV-operated *Pemt*$^{-/-}$ mice. Taken Together, we speculate that an intact cholinergic neuronal system protects *Pemt*$^{+/+}$ mice from NAFLD, however, choline

deficiency impairs this mechanism in *Pemt*$^{-/-}$ mice. The lack of choline (or acetylcholine) may cause systematic inflammation in *Pemt*$^{-/-}$ mice through hepatic vagus nerve signals, leading to the development of NASH.

2.4.3 Deafferentation by Capsaicin does not reverse the protection against DIO or the development of HF-induced NASH in *Pemt*$^{-/-}$ mice

Afferent vagus nerve originating from the liver is a neuronal pathway of key regulation in energy metabolism under both pathological (18,30) and physiological conditions (36). Hepatic over-expression of PPARγ2 in mice promotes HF-induced steatosis, increases peripheral lipolysis, decreases peripheral adiposity and improves insulin sensitivity in the muscle and WAT via the hepatic afferent vagus nerve (18,37). Ironically, afferent vagus nerve also relays signals of key importance in the development of obesity related hypertension (37) and glucocorticoid induced metabolic dysfunction (19). We observed increased hepatic PPARγ2 in *Pemt*$^{-/-}$ mice; however, this increase in PPARγ2 is unlikely the key player regulating peripheral energy metabolism. This is because denervating the afferent vagus nerve from the liver by capsaicin did not change the body weight gain, WAT mass, insulin sensitivity (data not shown) or glucose intolerance in *Pemt*$^{-/-}$ mice (Figure 2.7). The HF-induced NASH was not alleviated neither, judging by the hepatic TG levels and the histological staining of the liver sections (Figure 2.7 D & E). These data clearly highlight the importance of the efferent hepatic branch of vagus nerve in both protection against DIO and the development of HF-induced NASH in *Pemt*$^{-/-}$ mice. They are consistent with previous report that responding to the increased availability of lipids, the efferent hepatic vagus nerve, rather than the afferent flow to the brain is required for hepatic autoregulation (28).

Hepatic afferent nerve is involved in hepatic lipid metabolism in *Pemt*$^{+/+}$ mice. Upon the 10-week HF feeding, capsaicin-treated *Pemt*$^{+/+}$ mice showed a significant increase in the hepatic lipid accumulation compared to vehicle-treated *Pemt*$^{+/+}$ mice (Figure 2.7 D&E). Plasma TG was greatly reduced in these mice (Figure 2.7G). These data suggest that hepatic afferent vagus nerve also contributes to the regulation of hepatic lipid metabolism in responding to increased availability of dietary fat. As in *Pemt*$^{-/-}$ mice, the relevance of the afferent hepatic vagus nerve in the HF-induced NASH development is difficult to judge. But in the case of the hypothesis that the impaired cholinergic anti-inflammatory pathway in *Pemt*$^{-/-}$ mice caused by choline deficiency results in NASH development is valid, both afferent and efferent hepatic branch of vagus nerve will be required for the HF-induced NASH in *Pemt*$^{-/-}$ mice.

In summary, the protection from obesity and insulin resistance in the HF-fed *Pemt*$^{-/-}$ mice is eliminated by HV. HV also protects *Pemt*$^{-/-}$ mice from HF diet-induced inflammation and NASH in *Pemt*$^{-/-}$ mice. Deafferentation of hepatic vagus nerve by capsaicin fails to revers either the protection from DIO or the development of HF-induced NASH in *Pemt*$^{-/-}$ mice. Collectively, the data highlight a role for the hepatic branch of the vagus nerve, particularly the efferent hepatic vagus nerve, in regulating energy metabolism and liver function in *Pemt*$^{-/-}$ mice.

Table 2.1 Primers for real-time quantitative PCR

Abbreviations are: *Cd*, cluster of differentiation; *Tnf*, tumor necrosis factor, *Pepck*, phosphoenolpyruvate carboxykinase; *Mttp*, microsomal triglyceride transfer protein; *G6p*, glucose 6-phosphatase; *Mcd*, malonyl-CoA decarboxylase; *Ppar*, peroxisome proliferator activated receptor; *Pgc*, PPARγ co-activator; *Srebp*, sterol regulatory element binding protein.

gene	forward primer (5' -> 3')	reverse primer (5' -> 3')
Cyclophilin	TCC AAA GAC AGC AGA AAA CTT TCG	TCT TCT TGC TGG TCT TGC CAT TCC
Cd68	GCG GCT CCC TGT GTG TCT GAT	GGG CCT GTG GCT GGT CGT AG
F4/80	CCC TCG GGC TGT GAG ATT GTG	TGG CCA AGG CAA GAC ATA CCA G
Tnfα	GTC TAC TGA ACT TCG GGG TGA	CAC CAC TTG GTG GTT TGC TAC GAC
Pepck	GAA CTG ACA GAC TCG CCC TAT	TTC CCA CCA TAT CCG CTT C
Mttp	TGA GCG GTC TGG ATT TAC AAC	CAA GCA CAG CGG TGA CA
G6p	GGA TTC CGG TGT TTG AAC GTC	CGG AGG CTG GCA TTG TAG ATG
Cd36	TGG CTA AAT GAG ACT GGG ACC	ACA TCA CCA CTC CAA TCC CAA G
Mcd	TTC TGC ATG TGG CTC TGA CTG GT	GGG TCA GGC TGA TGG AGT AGA AG
Pparγ	TTG ACA TCA AGC CCT TTA CCA	GGT TCT ACT TTG ATC GCA CTT T
Pgc1α	ATA CCG CAA AGA GCA CGA GAA G	CTC AAG AGC AGC GAA AGC GTC ACA G
Pparα	GAC CTG AAA GAT TCG GAA ACT	CGT CTT CTC GGC CAT ACA C
Srebp1c	ATG GAT TGC ACA TTT GAA GAC	CTC TCA GGA GAG TTG GCA CC

Table 2.2 Plasma and liver parameters in HV- and sham-operated mice

8-week-old male *Pemt*$^{-/-}$ and *Pemt*$^{+/+}$ mice were subjected to hepatic vagotomy (HV) and sham operation. After surgery, mice were fed the HF diet for 10 weeks. Data are presented as mean values ± SEM. (n = 5-7). **P* < 0.05, versus *Pemt*$^{+/+}$ mice on the same surgery; #*p* < 0.05, sham-operated mice vs HV-operated mice of the same genotype. Abbreviations are: B.W., body weight; C, cholesterol; CE, cholesteryl ester; TG, triacylglycerol; PC, phosphatidylcholine; PE, phosphatidylethanolamine.

Operation	Sham		HV	
PEMT genotype	*Pemt*$^{+/+}$	*Pemt*$^{-/-}$	*Pemt*$^{+/+}$	*Pemt*$^{-/-}$
Liver (% B.W.)	4.2 ± 0.3	10.1 ± 0.3*	3.3 ± 0.2	4.7 ± 0.7$^{\#}$
Plasma C (mg/l)	15.7 ± 0.6	6.7 ± 1.0*	11.1 ± 0.9	12.2 ± 2.5$^{\#}$
Plasma CE (mg/l)	23.7 ± 3.8	2.3 ± 0.3*	16.7 ± 3.1	15.9 ± 4.3$^{\#}$
Plasma TG (mg/l)	18.4 ± 2.2	10.8 ± 2.5*	18.8 ± 2.5	12.7 ± 2.1
Hepatic C (μg/mg)	7.09 ± 0.74	7.73 ± 0.68	6.52 ± 0.55	7.13 ± 0.49
Hepatic CE (μg/mg)	1.73 ± 0.31	5.26 ± 1.24*	1.58 ± 0.19	2.58 ± 0.25$^{\#}$
Hepatic TG (μg/mg)	86.4 ± 34.4	326.0 ± 85.7*	88.7 ± 14.6	112.1 ± 21.0$^{\#}$
Hepatic PC (nmol/mg)	87 ± 3	73 ± 1*	86 ± 4	86 ± 1$^{\#}$
Hepatic PE (nmol/mg)	64 ± 8	55 ± 1	40 ± 1	47 ± 1

Figure 2.1 HV abolishes the protection against HF-induced obesity in *Pemt*$^{-/-}$ mice

8-week-old male *Pemt*$^{-/-}$ and *Pemt*$^{+/+}$ mice were subjected to hepatic vagotomy (HV) and sham operation. After surgery, mice were fed the HF diet for 10 weeks. (A) Body weight gain. (B) Blood glucose. (C) Glucose tolerance test. (D) Visceral fat histology (macrophage infiltration indicated by arrows). (E) Adipocyte size. For panels A and C, data were analyzed by a one-way ANOVA analysis of variance. For panels B and E, data were analyzed by a two-way ANOVA, followed by post hoc Bonferroni's test. *P < 0.05, versus *Pemt*$^{+/+}$ mice on the same surgery; #p < 0.05, sham-operated mice vs HV-operated mice of the same genotype.

Figure 2.1

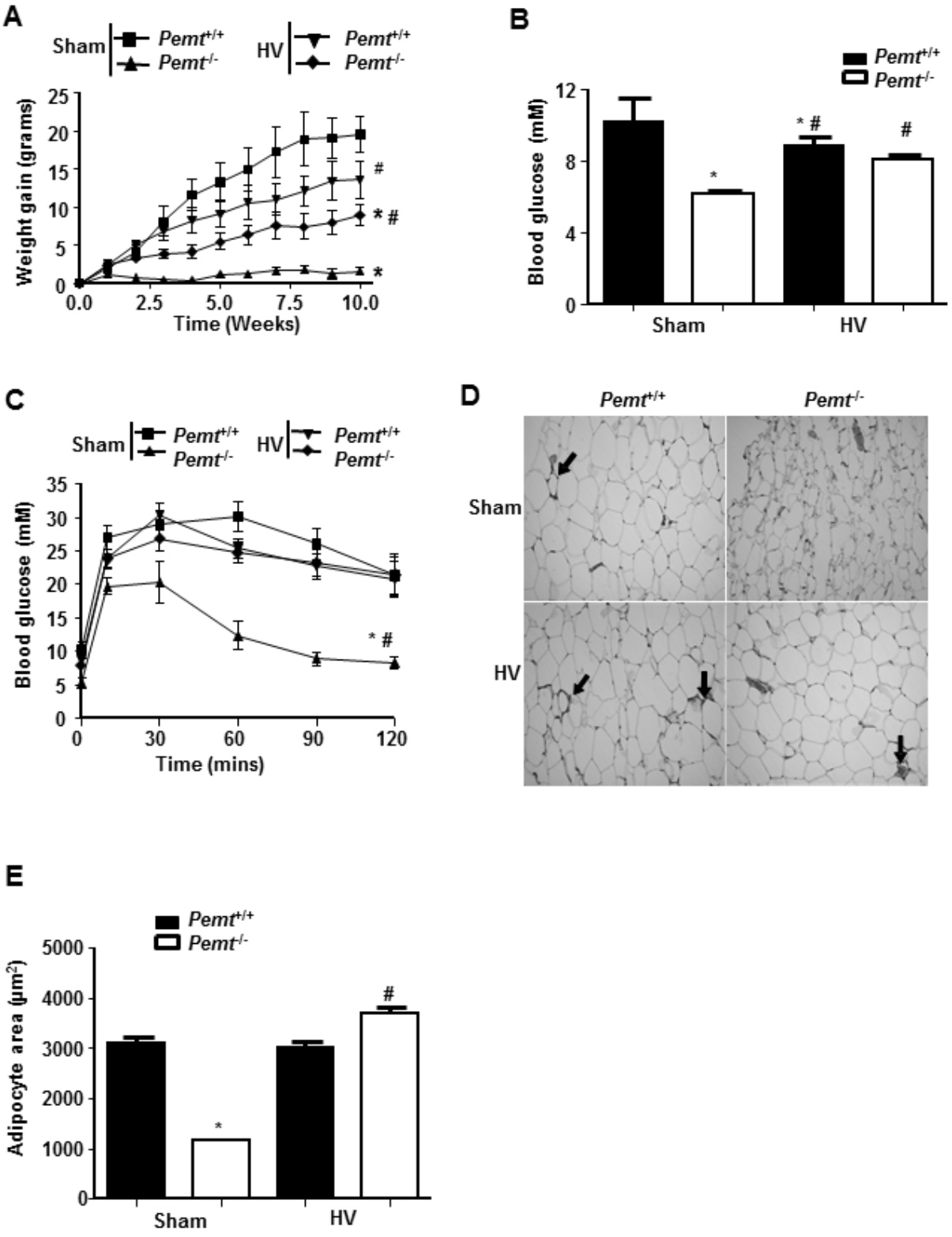
A
Sham
Pemt+/+
Pemt-/-
HV
Pemt+/+
Pemt-/-
Weight gain (grams)
Time (Weeks)
B
Pemt+/+
Pemt-/-
Blood glucose (mM)
Sham
HV
C
Sham
Pemt+/+
Pemt-/-
HV
Pemt+/+
Pemt-/-
Blood glucose (mM)
Time (mins)
D
Pemt+/+
Pemt-/-
Sham
HV
E
Pemt+/+
Pemt-/-
Adipocyte area (μm2)
Sham
HV

Figure 2.2 HV decreases energy utilization in *Pemt*$^{-/-}$ mice

8-week-old male *Pemt*$^{-/-}$ and *Pemt*$^{+/+}$ mice were subjected to hepatic vagotomy (HV) and sham operation. After surgery, mice were fed the HF diet for 10 weeks. (A) Oxygen consumption. (B) Respiratory exchange ratio (RER). (C) Heat production. Data were analyzed by a two-way ANOVA, followed by post hoc Bonferroni's test. *$P < 0.05$, versus *Pemt*$^{+/+}$ mice on the same surgery; #$p < 0.05$, sham-operated mice vs HV-operated mice of the same genotype.

Figure 2.2

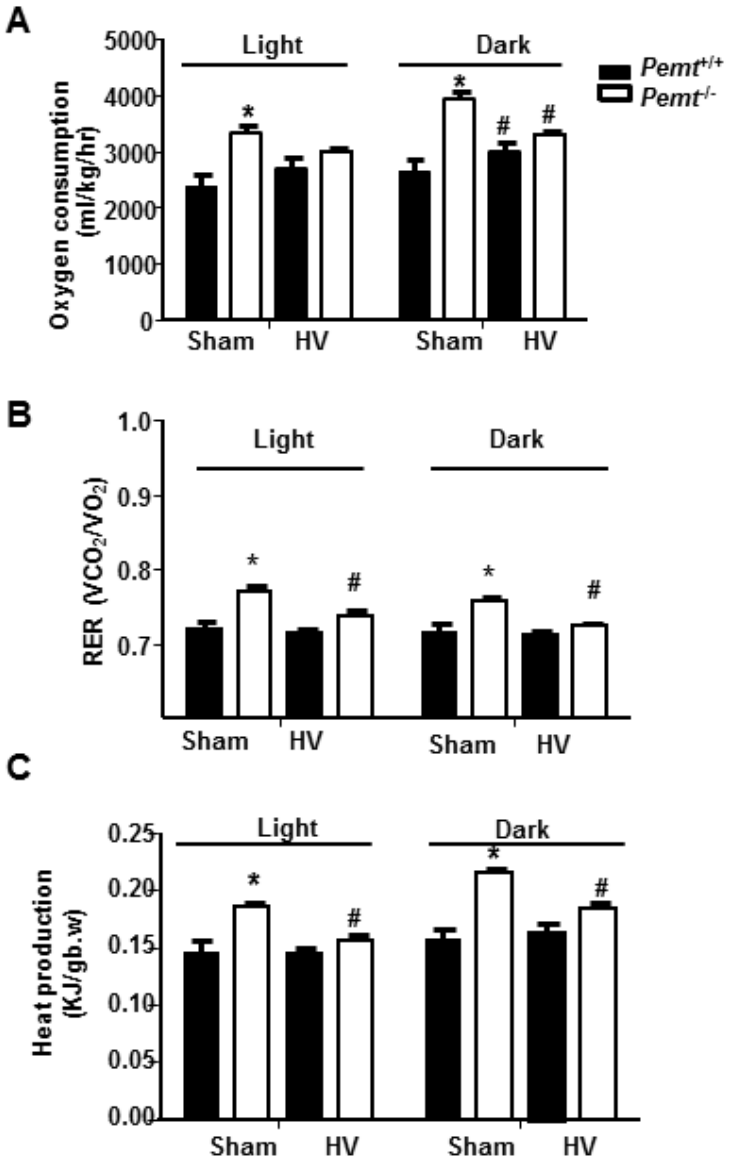
A
Light
Dark
Pemt+/+
Pemt-/-
Oxygen consumption (ml/kg/hr)
5000
4000
3000
2000
1000
0
Sham
HV
Sham
HV
B
Light
Dark
RER (VCO2/VO2)
1.0
0.9
0.8
0.7
Sham
HV
Sham
HV
C
Light
Dark
Heat production (KJ/gb.w)
0.25
0.20
0.15
0.10
0.05
0.00
Sham
HV
Sham
HV

Figure 2.3 HV protects *Pemt*$^{-/-}$ mice from HF-induced steatohepatitis

8-week-old male *Pemt*$^{-/-}$ and *Pemt*$^{+/+}$ mice were subjected to hepatic vagotomy (HV) and sham operation. After surgery, mice were fed the HF diet for 10 weeks. (A) Liver histology. (B) Plasma alanine aminotransferase (ALT) levels. (C) NAFLD activity score: steatosis, inflammation, and cell ballooning. (D) mRNA expression of inflammatory genes in the liver. Data were analyzed by a two-way ANOVA, followed by post hoc Bonferroni's test. *$P < 0.05$, versus *Pemt*$^{+/+}$ mice on the same surgery; #$p < 0.05$, sham-operated mice vs HV-operated mice of the same genotype.

Figure 2.3

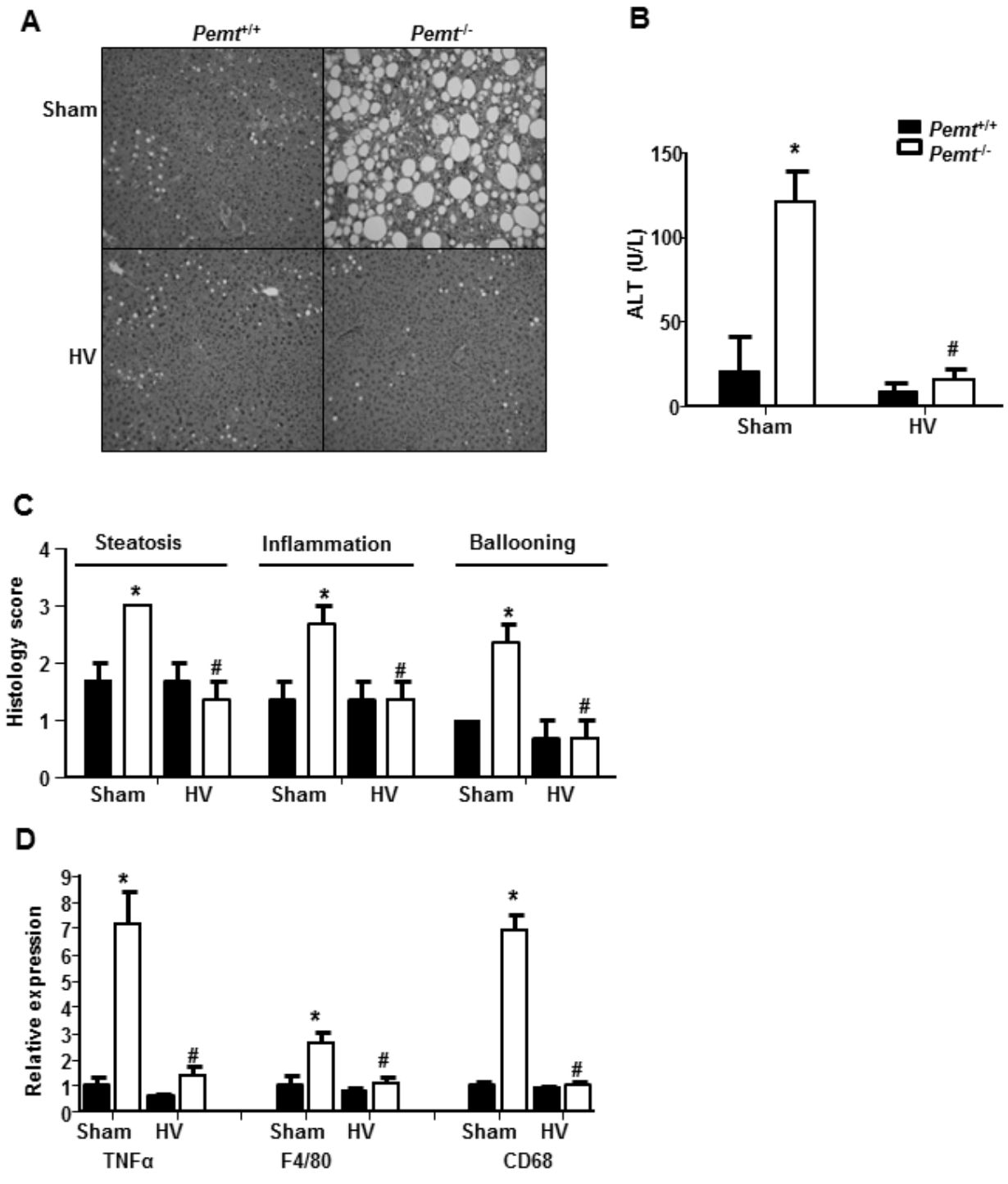
A
Pemt+/+
Pemt-/-
Sham
HV
B
Pemt+/+
Pemt-/-
ALT (U/L)
150
100
50
0
*
#
Sham
HV
C
Steatosis
Inflammation
Ballooning
Histology score
4
3
2
1
0
*
#
Sham
HV
D
Relative expression
9
8
7
6
5
4
3
2
1
0
TNFα
F4/80
CD68

Figure 2.4 HV alters the levels of hepatic cytokines

8-week-old male *Pemt*$^{+/+}$ and *Pemt*$^{-/-}$ mice were subjected to hepatic vagotomy (HV) and sham operation. After surgery, mice were fed the HF diet for 10 weeks. The in-tissue levels of chemokines in the liver: monocyte chemotactic protein (MCP)-1, RANTES; and cytokines in the liver: interleukin (IL)-10, IL-1α, IL-4, IL-6, tumor necrosis factor (TNF)α, transforming growth factor (TGF)-β and Leptin (n = 3). Data were analyzed by a two-way ANOVA, followed by post hoc Bonferroni's test. **P* < 0.05, versus *Pemt*$^{+/+}$ mice on the same surgery; #*p* < 0.05, sham-operated mice vs HV-operated mice of the same genotype.

Figure 2.4

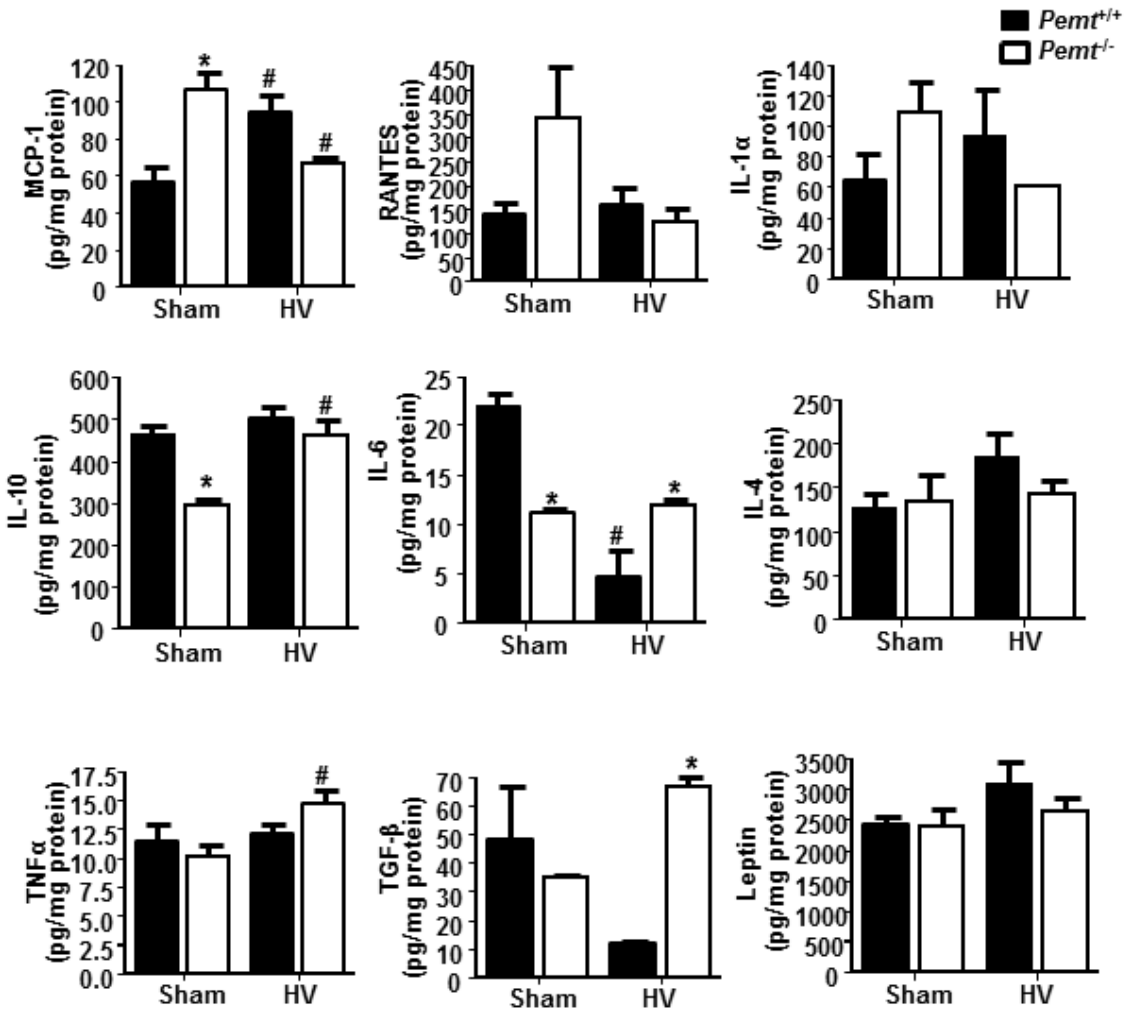
Pemt+/+
Pemt-/-
MCP-1 (pg/mg protein)
RANTES (pg/mg protein)
IL-1α (pg/mg protein)
IL-10 (pg/mg protein)
IL-6 (pg/mg protein)
IL-4 (pg/mg protein)
TNFα (pg/mg protein)
TGF-β (pg/mg protein)
Leptin (pg/mg protein)
Sham
HV

Figure 2.5 HV improves liver function of *Pemt*$^{-/-}$ mice

8-week-old male *Pemt*$^{-/-}$ and *Pemt*$^{+/+}$ mice were subjected to hepatic vagotomy (HV) and sham operation. After surgery, mice were fed the HF diet for 10 weeks. (A) Representative immunoblots of mitochondrial proteins: electron transport chain complex I, II, III, IV and V; uncoupling protein (UCP)2, porin (VDAC) and protein disulfide isomerase (PDI). (B) Densitometry for (A). (C) ER stress responsive C/EBP homologous protein (229). (D) Representative immunoblots of acetyl-CoA carboxylase (ACC), phospho-ACC (Ser79) and fatty acid synthase (FAS). (E) Densitometry for (D). (n = 3). Data were analyzed by a two-way ANOVA, followed by post hoc Bonferroni's test. **P* < 0.05, versus *Pemt*$^{+/+}$ mice on the same surgery; #*p* < 0.05, sham-operated mice vs HV-operated mice of the same genotype.

Figure 2.5

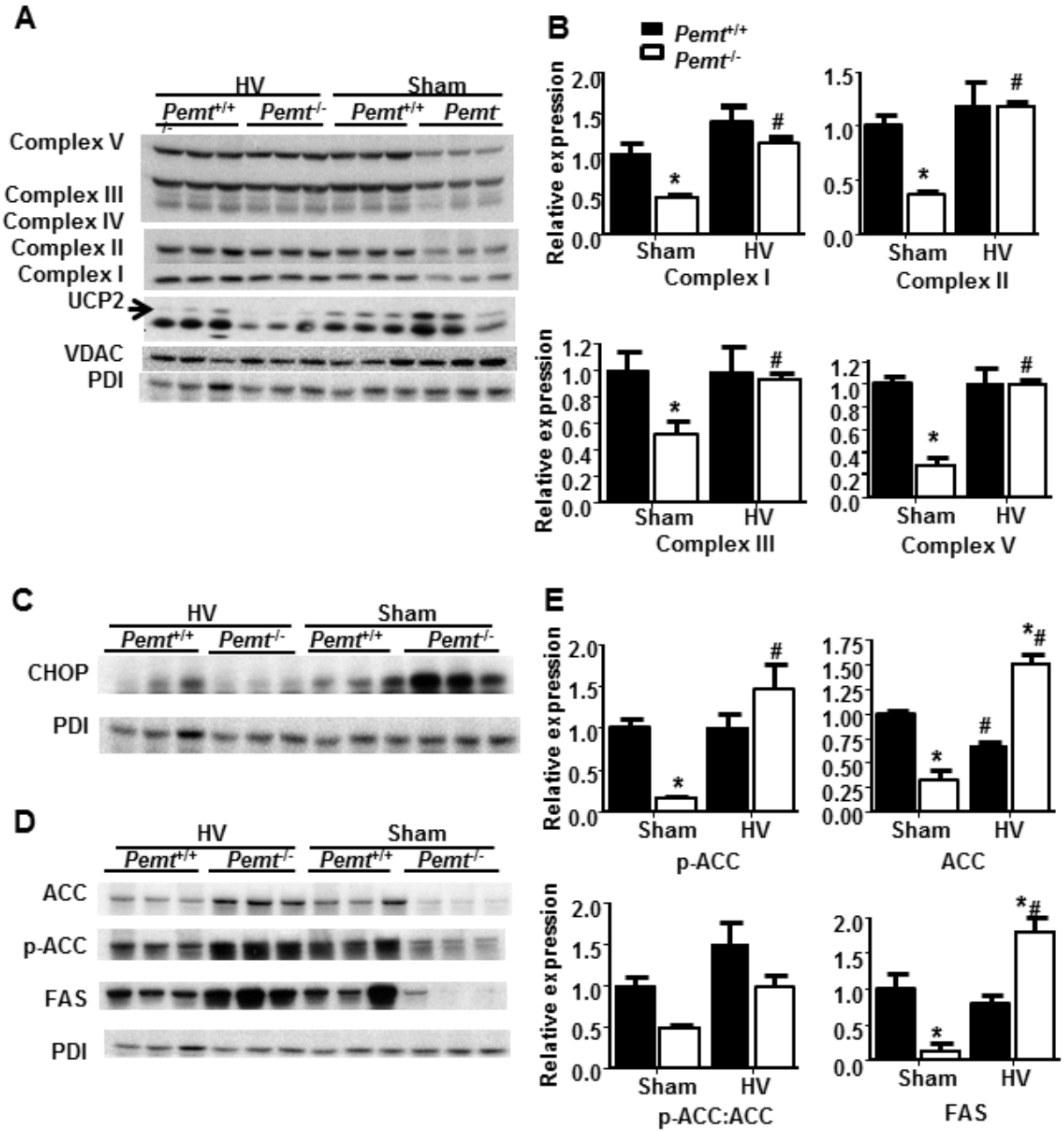
A
HV
Sham
Pemt+/+
Pemt-/-
Pemt+/+
Pemt-/-
Complex V
Complex III
Complex IV
Complex II
Complex I
UCP2
VDAC
PDI
B
Pemt+/+
Pemt-/-
Relative expression
Sham
HV
Complex I
Complex II
Complex III
Complex V
C
CHOP
PDI
D
ACC
p-ACC
FAS
PDI
E
p-ACC
ACC
p-ACC:ACC
FAS

Figure 2.6 HV normalizes hepatic glucose and lipid metabolism in *Pemt*$^{-/-}$ mice

8-week-old male *Pemt*$^{-/-}$ and *Pemt*$^{+/+}$ mice were subjected to hepatic vagotomy (HV) and sham operation. After surgery, mice were fed the HF diet for 10 weeks. The mRNA expression of genes in the liver: fatty acid uptake and metabolism related *malonyl-CoA decarboxylase (MCD)*, *Stearoyl-CoA desaturase (SCD)1*, *cluster of differentiation (CD)36*, *microsomal triglyceride transfer protein (MTTP)* and *uncoupling protein (UCP)2*; glucose metabolism related *phosphoenolpyruvate carboxykinase (PEPCK)* and *glucose-6-phosphatase (G6P)*; and transcriptional factors *peroxisome proliferator-activated receptor (PPAR)α*, *sterol response element-binding protein (SREBP)1c*, *PPARγ2*, and *PPARγ coactivator (PGC)1α* (n = 3). Data were analyzed by a two-way ANOVA, followed by post hoc Bonferroni's test. **P* < 0.05, versus *Pemt*$^{+/+}$ mice on the same surgery; #*p* < 0.05, sham-operated mice vs HV-operated mice of the same genotype.

Figure 2.6

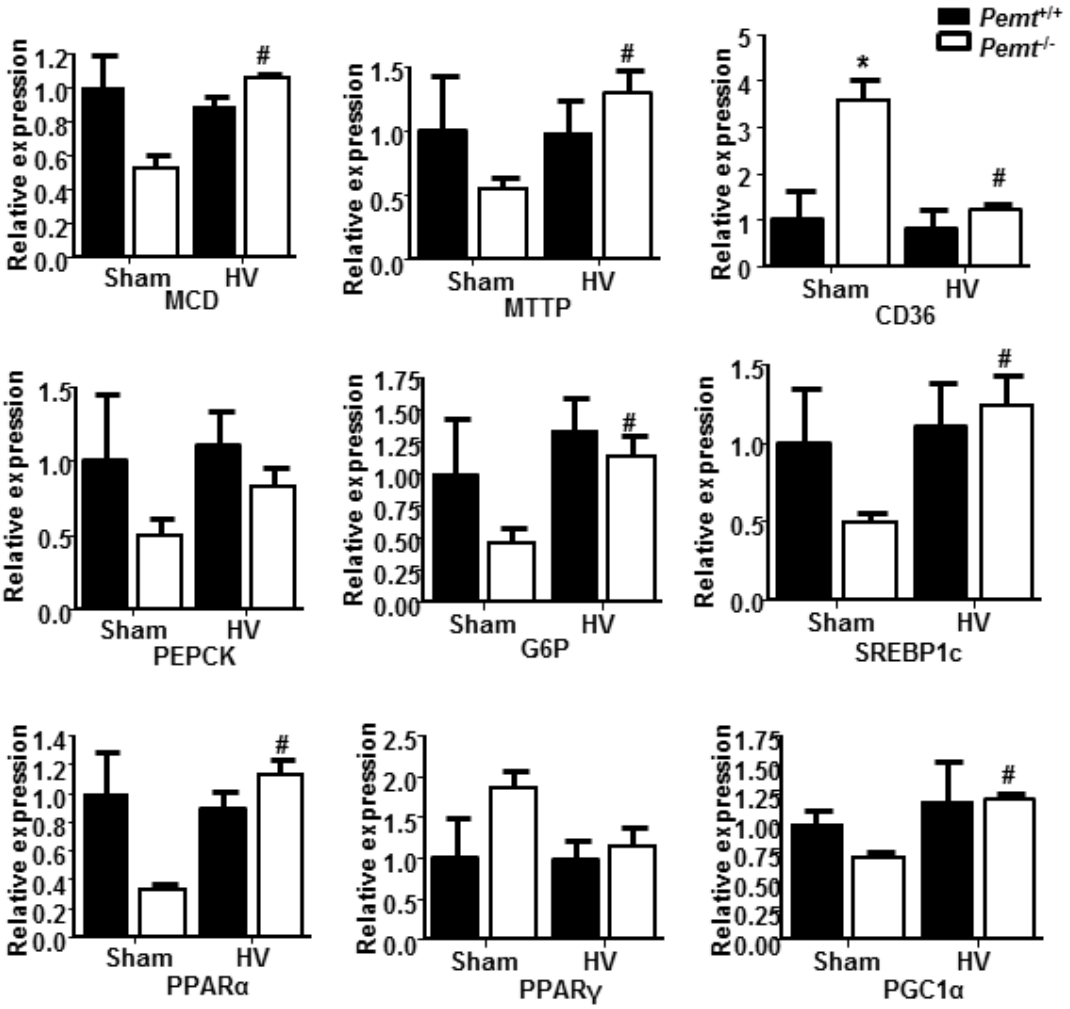
Pemt+/+
Pemt-/-
Relative expression
Sham
HV
MCD
MTTP
CD36
PEPCK
G6P
SREBP1c
PPARα
PPARγ
PGC1α
*
#

Figure 2.7 Capsaicin does not reverse the protection against DIO or the development of HF-induced NASH in *Pemt*$^{-/-}$ mice

Pemt$^{+/+}$ and *Pemt*$^{-/-}$ mice were subjected to capsaicin (Cap) or vehicle (Veh) treatment. After surgery, mice were fed the HF for 10 weeks. (A) Electron microscopy assessment of hepatic branch of vagus nerve: unmyelinated fibers (empty arrowheads), myelinated fibers (arrows) and disrupted unmyelinated fibers (solid arrowheads); magnification 10,000×. (B) Body weight gain. (C) Glucose tolerance test. (D) Liver sections stained with hematoxylin and eosin. (E) Hepatic triacylglycerol (25). (F) Plasma alanine aminotransferase (ALT). (G) Plasma TG. For panel B, data were analyzed by a one-way ANOVA analysis of variance. For panels E-G, data were analyzed by a two-way ANOVA, followed by post hoc Bonferroni's test. *$P < 0.05$, versus *Pemt*$^{+/+}$ mice on the same treatment.

Figure 2.7

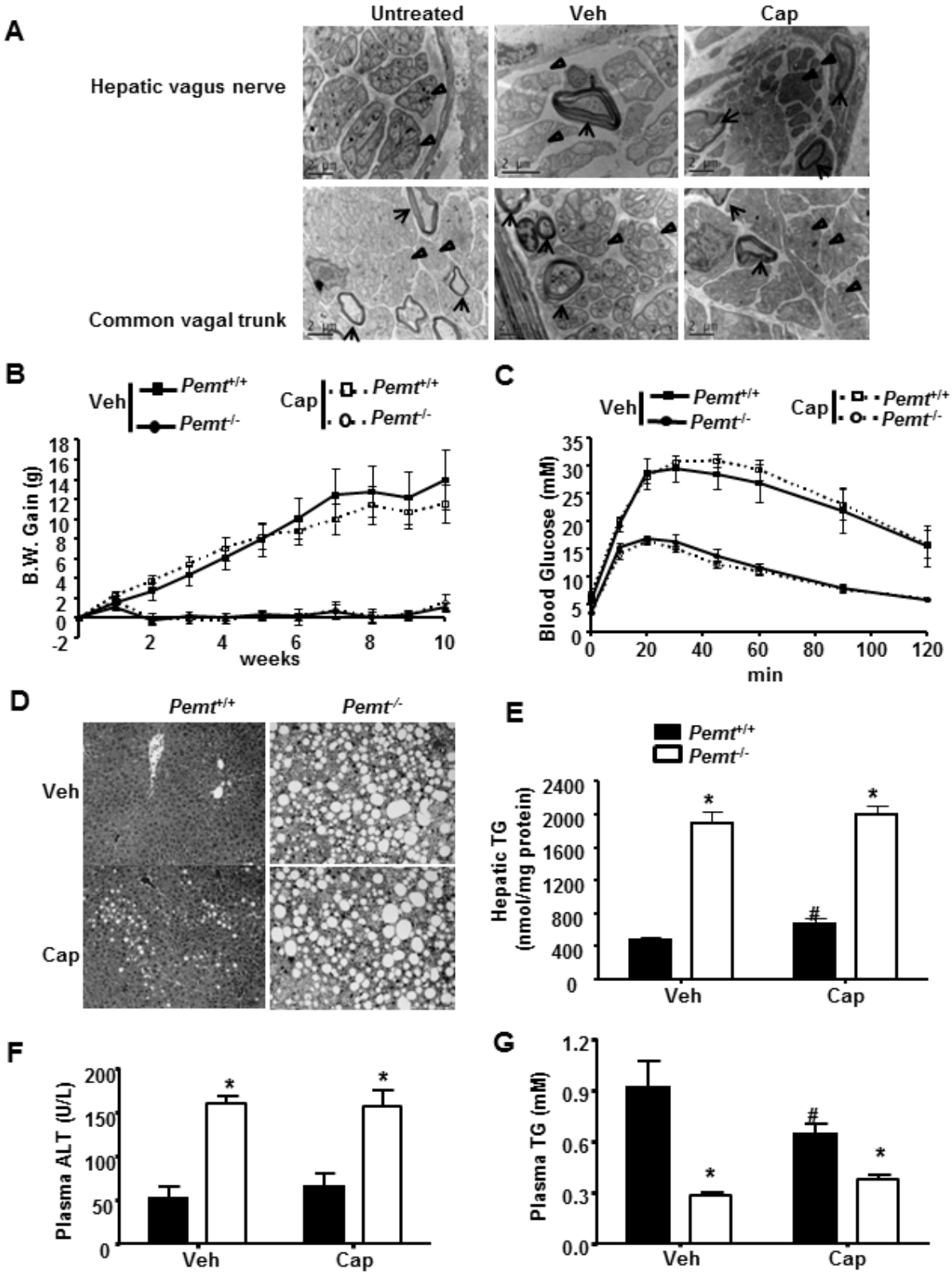
A
Untreated
Veh
Cap
Hepatic vagus nerve
Common vagal trunk
B
Veh
Pemt+/+
Pemt-/-
Cap
Pemt+/+
Pemt-/-
B.W. Gain (g)
weeks
C
Veh
Pemt+/+
Pemt-/-
Cap
Pemt+/+
Pemt-/-
Blood Glucose (mM)
min
D
Pemt+/+
Pemt-/-
Veh
Cap
E
Pemt+/+
Pemt-/-
Hepatic TG (nmol/mg protein)
Veh
Cap
F
Plasma ALT (U/L)
Veh
Cap
G
Plasma TG (mM)
Veh
Cap

2.5 References

1. Moore, J. B. (2010) *Proc Nutr Soc* **69**, 211-220

2. Matteoni, C. A., Younossi, Z. M., Gramlich, T., Boparai, N., Liu, Y. C., and McCullough, A. J. (1999) *Gastroenterology* **116**, 1413-1419

3. Anderson, N., and Borlak, J. (2008) *Pharmacol Rev* **60**, 311-357

4. Vetelainen, R., van Vliet, A., Gouma, D. J., and van Gulik, T. M. (2007) *Annals of Surgery* **245**, 20-30

5. Angulo, P. (2006) *Liver Transpl* **12**, 523-534

6. Puri, P., Baillie, R. A., Wiest, M. M., Mirshahi, F., Choudhury, J., Cheung, O., Sargeant, C., Contos, M. J., and Sanyal, A. J. (2007) *Hepatology* **46**, 1081-1090

7. Li, Z., Agellon, L. B., Allen, T. M., Umeda, M., Jewell, L., Mason, A., and Vance, D. E. (2006) *Cell Metab* **3**, 321-331

8. Ling, J., Chaba, T., Zhu, L. F., Jacobs, R. L., and Vance, D. E. (2012) *Hepatology* **55**, 1094-1102

9. Vance, D. E., Li, Z., and Jacobs, R. L. (2007) *J Biol Chem* **282**, 33237-33241

10. DeLong, C. J., Shen, Y. J., Thomas, M. J., and Cui, Z. (1999) *J Biol Chem* **274**, 29683-29688

11. Vance, D. E., and Vance, J. E. (2008) Phospholipid biosynthesis in eukaryotes. in *Biochemistry of Lipids, Lipoproteins and Membranes* (Vance, D. E., and Vance, J. E., ed.), 5th Ed., Elsevier, Amsterdam. pp 213–244

12. Karim, M., Jackson, P., and Jackowski, S. (2003) *Biochim Biophys Acta* **1633**, 1-12

13. Tang, W., Keesler, G. A., and Tabas, I. (1997) *J Biol Chem* **272**, 13146-13151

14. Niebergall, L. J., Jacobs, R. L., Chaba, T., and Vance, D. E. (2011) *Biochim Biophys Acta* **1811**, 1177-1185

15. Jacobs, R. L., Zhao, Y., Koonen, D. P., Sletten, T., Su, B., Lingrell, S., Cao, G., Peake, D. A., Kuo, M. S., Proctor, S. D., Kennedy, B. P., Dyck, J. R., and Vance, D. E. (2010) *J Biol Chem* **285**, 22403-22413

16. Katagiri, H., Yamada, T., and Oka, Y. (2007) *Circ Res* **101**, 27-39

17. Berthoud, H. R. (2004) *Anat Rec A Discov Mol Cell Evol Biol* **280**, 827-835

18. Berthoud, H. R. (2008) *Regulatory Peptides* **149**, 15-25

19. Uno, K., Katagiri, H., Yamada, T., Ishigaki, Y., Ogihara, T., Imai, J., Hasegawa, Y., Gao, J., Kaneko, K., Iwasaki, H., Ishihara, H., Sasano, H., Inukai, K., Mizuguchi, H., Asano, T., Shiota, M., Nakazato, M., and Oka, Y. (2006) *Science* **312**, 1656-1659

20. Bernal-Mizrachi, C., Xiaozhong, L., Yin, L., Knutsen, R. H., Howard, M. J., Arends, J. J., Desantis, P., Coleman, T., and Semenkovich, C. F. (2007) *Cell Metab* **5**, 91-102

21. Banni, S., Carta, G., Murru, E., Cordeddu, L., Giordano, E., Marrosu, F., Puligheddu, M., Floris, G., Asuni, G. P., Cappai, A. L., Deriu, S., and Follesa, P. (2012) *PLoS One* **7**, e44813

22. Warne, J. P., Foster, M. T., Horneman, H. F., Pecoraro, N. C., Ginsberg, A. B., Akana, S. F., and Dallman, M. F. (2007) *Endocrinology* **148**, 3288-3298

23. Kuksis, A., and Myher, J. J. (1989) *Adv Chromatogr* **28**, 267-332

24. Jacobs, R. L., Lingrell, S., Zhao, Y., Francis, G. A., and Vance, D. E. (2008) *J Biol Chem* **283**, 2147-2155

25. Brunt, E. M., Janney, C. G., Di Bisceglie, A. M., Neuschwander-Tetri, B. A., and Bacon, B. R. (1999) *Am J Gastroenterol* **94**, 2467-2474

26. Holzer, P. (1998) *Am J Physiol* **275**, G8-13

27. Wu, G., Zhang, L., Li, T., Lopaschuk, G., Vance, D. E., and Jacobs, R. L. (2012) *J Obes* **2012**, 319172

28. Lam, T. K., Pocai, A., Gutierrez-Juarez, R., Obici, S., Bryan, J., Aguilar-Bryan, L., Schwartz, G. J., and Rossetti, L. (2005) *Nat Med* **11**, 320-327

29. Pocai, A., Obici, S., Schwartz, G. J., and Rossetti, L. (2005) *Cell Metab* **1**, 53-61

30. Imai, J., Katagiri, H., Yamada, T., Ishigaki, Y., Suzuki, T., Kudo, H., Uno, K., Hasegawa, Y., Gao, J., Kaneko, K., Ishihara, H., Niijima, A., Nakazato, M., Asano, T., Minokoshi, Y., and Oka, Y. (2008) *Science* **322**, 1250-1254

31. Stearns, A. T., Balakrishnan, A., Radmanesh, A., Ashley, S. W., Rhoads, D. B., and Tavakkolizadeh, A. (2012) *Dig Dis Sci* **57**, 1281-1290

32. Tracey, K. J. (2005) *J Exp Med* **202**, 1017-1021

33. Luyer, M. D., Greve, J. W., Hadfoune, M., Jacobs, J. A., Dejong, C. H., and Buurman, W. A. (2005) *J Exp Med* **202**, 1023-1029

34. Borovikova, L. V., Ivanova, S., Zhang, M., Yang, H., Botchkina, G. I., Watkins, L. R., Wang, H., Abumrad, N., Eaton, J. W., and Tracey, K. J. (2000) *Nature* **405**, 458-462

35. Watkins, S. M., Zhu, X., and Zeisel, S. H. (2003) *The Journal of nutrition* **133**, 3386-3391

36. Izumida, Y., Yahagi, N., Takeuchi, Y., Nishi, M., Shikama, A., Takarada, A., Masuda, Y., Kubota, M., Matsuzaka, T., Nakagawa, Y., Iizuka, Y., Itaka, K., Kataoka, K.,

Shioda, S., Niijima, A., Yamada, T., Katagiri, H., Nagai, R., Yamada, N., Kadowaki, T., and Shimano, H. (2013) *Nat Commun* **4**, 2316

37. Uno, K., Yamada, T., Ishigaki, Y., Imai, J., Hasegawa, Y., Gao, J., Kaneko, K., Matsusue, K., Yamazaki, T., Oka, Y., and Katagiri, H. (2012) *Eur Heart J* **33**, 1279-1289

Chapter 3

Lack of Phosphatidylethanolamine N-methyltransferase Alters Phospholipid Composition Causing Stress in Hepatic Endoplasmic Reticulum

3.1 Introduction

The global incidence of non-alcoholic fatty liver disease (NAFLD) is rapidly rising as a complication of obesity and diabetes (1-3). Recent studies (4,5) have linked NAFLD with a reduced molar ratio of hepatic phosphatidylcholine (PC) to phosphatidylethanolamine (PE). A decrease in hepatic PC/PE ratio induces steatosis in mice and is also a feature of non-alcoholic steatohepatitis (NASH) patients (5). Moreover, in mice, the PC/PE ratio strongly predicts liver function and survival after partial hepatectomy (6).

In mice, ~70% of hepatic PC is synthesized via the CDP-choline pathway and 30% via the phosphatidylethanolamine *N*-methyltransferase (PEMT) pathway (7,8). Inhibition of either pathway results in steatosis (9), which is mainly due to decreased hepatic PC production and impaired very low density lipoprotein secretion (10). Mice lacking PEMT develop NASH when fed a HF (11) diet for 2 weeks (6,12).

The endoplasmic reticulum (ER) is responsible for the synthesis, folding, trafficking and maturation of proteins, for the synthesis of cholesterol, PC, PE, triacylglycerol (13) and for calcium homeostasis and drug metabolism (14,15). ER stress is associated with chronic syndromes such as obesity, diabetes, cardiovascular diseases and fatty liver (15-18). In response to ER stress, cells activate the unfolded protein response (19) to restore the homeostatic equilibrium caused by aberrant protein metabolism (20). The UPR is mediated by three transducers: protein kinase-like ER kinase (21), inositol-requiring enzyme-1 (IRE1) and activating transcription factor (ATF)6α (17,20), each of which triggers distinct and overlapping pathways to re-establish ER homeostasis. PERK inhibits protein translation and decreases protein production via phosphorylation of the

eukaryotic initiation factor 2α (eIF2α) (22). PERK activation also increases the pro-apoptotic proteins: C/EBP–homologous protein (19) and GADD34 (growth arrest and DNA damage-inducible protein 34) (23,24). IRE1 activation increases the spliced form of X-box binding protein-1 (XBP1s) mRNA, the product of which translocates to the nucleus and regulates the production of ER chaperones and proteins involved in ER-associated protein degradation (25). The cytosolic domain of IRE1 also activates the JNK pathway independent of XBP1s (26). The third canonical arm of the UPR involves ATF6α which, in response to ER stress, translocates to the Golgi and is cleaved to an active form which migrates to the nucleus and regulates expression of ER chaperones (27).

PEMT is active in the ER and ER-derived mitochondrial-associated membranes (28). Lack of PEMT leads to accumulation of hepatic PE (29). In the livers of *Pemt*$^{-/-}$ mice fed either a choline-deficient diet or a HF diet, PC is reduced and PE is increased resulting in a decreased PC/PE ratio (5,6). We hypothesized that an aberrant ER phospholipid composition in the livers of *Pemt*$^{-/-}$ mice leads to ER stress which sensitizes the liver to HF-induced NASH.

3.2 Materials and Methods

3.2.1 Animal handling, diets and treatments

All procedures were approved by the University of Alberta's Institutional Animal Care Committee in accordance with guidelines of the Canadian Council on Animal Care. Male C57BL/6 (backcrossed >7 generations) *Pemt*$^{+/+}$ and *Pemt*$^{-/-}$ mice (8-9 weeks

old)[11] were housed with free access to water and fed either standard chow diet (LabDiet, #5001) or a HF diet (Bio-Serv, #F3282) for 2 weeks. In separate experiments, *Pemt*$^{+/+}$ and *Pemt*$^{-/-}$ mice were administered 4-phenylbutyric acid (PBA, Scandinavian Formulas, dissolved in water) twice daily (total 1 g/kg body weight/day) or water by oral gavage during the HF feeding. All mice were fasted for 12 h before sacrifice. Tissues were collected and stored at -80°C until analysis or preserved in 10% phosphate-buffered formalin for histology.

3.2.2 Cell culture

McA-RH7777 cells stably expressing the pCI vector (pCI-McA) or human PEMT (PEMT-McA) (30) were maintained in Dulbecco's modified Eagle's medium (Invitrogen) containing 10% fetal bovine serum (Invitrogen) and geneticin G418 (0.2 mg/ml, Invitrogen). Cells were cultured at 37°C in 10 cm culture dishes in 5% CO_2, 90% relative humidity. PEMT activity in PEMT-McA cells was comparable to that in the livers from chow-fed *Pemt*$^{+/+}$ mice (30)**.** In some experiments, cells were incubated for 24 h ± 1 mM PBA (dissolved in distilled water).

3.2.3 Isolation of ER

The protocol for isolation of ER from mouse liver was adapted from Croze and Morre (31). The purity of ER isolated by this method has been extensively characterized (32). Age-matched male *Pemt*$^{+/+}$ and *Pemt*$^{-/-}$ mice were fed a chow or HF diet for two weeks, then fasted overnight and anesthetized by isoflurane. The livers (~1.0 g) were immediately dissected and transferred to 10 ml ice-cold homogenization buffer (0.5 M sucrose, 1% dextran, 37.5 mM Tris, 5 mM $MgCl_2$, 1 mM dithiothreitol and 0.1 mM phenylmethylsulfonyl fluoride, pH 7.4). The liver was chopped into small pieces and

homogenized with a polytron for 30 sec at 4,000 rpm. The homogenate was centrifuged at 5,000 g for 15 min and the ER fraction was isolated from the supernatant by ultracentrifugation on a sucrose gradient (from the top to the bottom: 8 ml 1.3 M sucrose, 8 ml 1.5 M sucrose, 6 ml 2 M sucrose). The ER fraction was collected and washed with ice-cold buffer (55 mM Tris, 5 mM $MgCl_2$, 1 mM dithiothreitol and 0.1 mM phenylmethylsulfonyl fluoride, pH 7.4). After centrifugation, the ER pellet was re-suspended in ice-cold buffer (0.25 M sucrose, 10 mM Tris, 1 mM dithiothreitol, and 0.1 mM phenylmethylsulfonyl fluoride, pH 7.4) containing a protease inhibitor cocktail (Sigma #P8340). The ER fraction was snap frozen in liquid nitrogen for further analysis.

3.2.4 Analytical procedures

Triacylglycerol (13) mass was measured by a commercially available kit (Roche Diagnostics) according to manufacturer's protocols. Hepatic lipids were extracted as described in section 2.2.3. Hepatic PC and PE were separated by thin-layer chromatography and quantified by a phosphorus assay (33) as described in section 2.2.3. Plasma alanine aminotransferase was measured using a kit (Biotron Diagnostics) according to manufacturer's protocols. Hepatic cytokines and chemokines were quantified at Eve Technologies Corp. (Calgary, Alberta) with the Bio-Plex™ 200 system (Bio-Rad Laboratories, Inc., Hercules, CA, USA), a Milliplex TGF-β 3-plex kit (Millipore, St. Charles, MO, USA) and a Milliplex Mouse Cytokine/Chemokine 32-plex kit (Millipore, St. Charles, MO, USA) according to manufacturers' protocols. The transforming growth factor (TGF)-β 3-plex kit quantified TGF-β1, TGF-β2 and TGF-β3. The 32-plex consisted of Eotaxin, G-CSF (granulocyte colony-stimulating factor), GM-CSF (granulocyte-macrophage colony-stimulating factor), interferon (IFN)γ, interleukin (IL)-

1α, IL-1β, IL-2, IL-3, IL-4, IL-5, IL-6, IL-7, IL-9, IL-10, IL-12 (p40), IL-12 (p70), IL-13, IL-15, IL-17, IP-10 (IFN-γ-inducible protein 10), KC (keratinocyte-derived cytokine), LIF (leukemia inhibitory factor), LIX (C-X-C motif chemokine 5), MCP (monocyte chemotactic protein)-1, M-CSF (macrophage colony-stimulating factor), MIG (CXCL9, chemokine C-X-C motif ligand 9), macrophage inflammatory protein (MIP)-1α, MIP-1β, MIP-2, RANTES (CCL5, chemokine C-C motif ligand 5), TNF (tumor necrosis factor)α, and VEGF (vascular endothelial growth factor).

3.2.5 Histology

A portion of liver was first fixed in 10% buffered formalin for at least 24 hours. Then, tissue was embedded in paraffin, sectioned, and subjected to hematoxylin and eosin (H&E) staining by the Histocore of Alberta Diabetes Institute (University of Alberta). Liver slices were scored for steatosis, hepatocellular ballooning, portal inflammation and lobular inflammation using a modified NAFLD scoring system (34). The histological analysis of liver slides was performed by pathologist Dr. Aducio Thiesen (University of Alberta).

3.2.6 Immunoblotting

Tissues homogenization and immunoblotting procedure were described in section 2.2.7. The membranes were probed with primary antibodies from Cell Signaling Technology (Danvers, MA) raised against phospho-PERK (p-PERK, thr980, 1:1,000 dilution, #3179), PERK (1:1,000 dilution, #3192), phospho-eIF2α (p-eIF2α, ser51, 1:1,000 dilution, #9721), eIF2α (1:1,000 dilution, #9722), IRE1α (1:1,000 dilution, #3294), XBP1s (1:1,000 dilution, #12782), CHOP (1:1,000 dilution, #2895), integrin β1 (1:1,000 dilution, #4706), α-Tubulin (1:1,000 dilution, #2144), phospho-JNK (p-JNK,

Thr183/Tyr185, 1:1,000 dilution, #4668), cleaved Caspase-3 (1:1,000 dilution, #9661), Caspase-3 (1:1,000 dilution, #9665), Cytochrome c (1:1,000 dilution, #4272), p62 (1:1,000 dilution, #5114), autophagy-related protein 7 (ATG7, 1:1,000 dilution, #2631), light chain 3 (LC3) (1:1,000 dilution, #2775) and BCL-2 (1:1,000 dilution, #2876, B-cell lymphoma 2); primary antibodies from Abcam against ATF6α (1:1,000 dilution, ab37149), phospho-IRE1α (p-IRE1α, Ser724, 1:1,000 dilution, ab48187), OXPHOS complexes (1:500 dilution, ab110413), uncoupling protein 2 (UCP2, 1:1,000 dilution, ab67241), actin (1:3,000 dilution, ab14128) and glyceraldehyde-3-phosphate dehydrogenase (GAPDH, 1:1,000 dilution, ab8245); primary antibodies against protein disulfide isomerase (PDI, 1:1,000 dilution, SPA-890), glucose-regulated protein 78 (BIP, 1:1,000 dilution, SPA-826) and calnexin (1:1,000 dilution, SPA-865) from Enzo Life Sciences, and primary antibody against Golgi-β1,4-galactosyltransferase from Santa Cruz Biotechnology (1:1,000 dilution, sc-22292-R). All primary antibodies were diluted with 5% (w/v) bovine serum albumin in T-TBS buffer (20 mM Tris-HCl, 150 mM NaCl, 0.1% Tween 20, pH 7.4). Secondary antibodies were goat anti-mouse and goat anti-rabbit IgG-horse radish peroxidase conjugate (Bio-Rad) and were diluted 1:5,000-1:10,000 with 1% (w/v) skim milk in T-TBS buffer. The immunoreactive bands were visualized by enhanced chemiluminescence system (Amersham Biosciences) according to the manufacturer's instructions and protein levels were quantified using ImageJ software.

3.2.7 Real-time quantitative PCR

Total RNA was isolated from snap-frozen liver using TRIzol reagent (Invitrogen). Total RNA was treated with DNase I (Invitrogen) then reverse-transcribed using an

oligo(dT)12–18 primer and Superscript II reverse transcriptase (Invitrogen). Primers (Table 3.1) were purchased from the Institute of Biomolecular Design, University of Alberta. mRNA levels were quantified by real-time quantitative PCR using a Rotor-Gene 3000 instrument (Montreal Biotech) and normalized to cyclophilin mRNA using a standard curve.

3.2.8 Statistical analysis

Data are mean values ± SEM. Comparisons between two groups were performed using Student's *t*-test. For all other comparisons, a two-way ANOVA, followed by post hoc Bonferroni's test of individual group differences was used. $P < 0.05$ was considered significant.

3.3 Results

3.3.1 ER stress in chow-fed *Pemt*$^{-/-}$ mice is associated with altered phospholipid levels in the ER

Chow-fed *Pemt*$^{-/-}$ mice developed steatosis and inflammation as shown by both H&E staining (Figure 3.1A) and histological NAFLD scoring (Figure 3.1B). In *Pemt*$^{+/+}$ mice, steatosis, inflammation and ballooning were scored as zero. To determine whether PEMT deficiency induced hepatic ER stress, we measured protein levels of BIP, CHOP, PDI and calnexin in the livers. BIP and CHOP were significantly higher in *Pemt*$^{-/-}$ mice than in *Pemt*$^{+/+}$ mice, whereas PDI and calnexin were comparable in the two genotypes (Figure 3.1C&D). We also examined proteins associated with the UPR to determine if the ER stress could be attributed to an activated UPR. However, p-PERK,

PERK and eIF2α were equivalent in both genotypes, while p-eIF2α, the downstream signal of p-PERK, was significantly lower in *Pemt*$^{-/-}$ mice (Figure 3.1C&D). In the IRE1 pathway, p-IRE1α was 69% lower in *Pemt*$^{-/-}$ mice than *Pemt*$^{+/+}$ mice, whereas IRE1α and the downstream protein, XBP1s, were equivalent (Figure 3.1C&D). Moreover, ATF6α was unaffected by PEMT deficiency (Figure 3.1C&D). Thus, chow-fed *Pemt*$^{-/-}$ mice exhibit hepatic ER stress without activation of the UPR.

An increased hepatic PC/PE ratio has been associated with ER stress in obese mice (35). To determine if ER stress in the livers of chow-fed *Pemt*$^{-/-}$ mice could have been caused by an altered ER phospholipid composition, we isolated ER from mouse livers. Purity of the ER fractions was indicated by enrichment of the ER proteins calnexin and PDI in the ER compared to the liver homogenate, and very low levels of markers of other cellular compartments including plasma membrane protein integrin β1, Golgi marker protein Golgi-β1,4-galactosyltransferase, mitochondrial protein UCP2 and cytosolic protein α-tubulin in the ER fraction (Figure 3.1E). The amount of PC in the ER from livers of *Pemt*$^{-/-}$ mice was lower, whereas PE was higher, than in *Pemt*$^{+/+}$ mice. Consequently, the PC/PE ratio in hepatic ER from *Pemt*$^{-/-}$ mice was significantly lower than in *Pemt*$^{+/+}$ mice (Figure 3.1F). Thus, ER stress in the livers of chow-fed *Pemt*$^{-/-}$ mice coincides with a lower PC/PE ratio in the ER.

3.3.2 *Pemt*$^{-/-}$ mice are more sensitive to HF-induced ER stress

To determine if pre-existing ER stress sensitized the liver to stress induced by HF, we compared levels of proteins involved in ER stress and the UPR pathway in the livers of *Pemt*$^{+/+}$ and *Pemt*$^{-/-}$ mice fed the HF diet for two weeks. CHOP and PDI were higher in *Pemt*$^{-/-}$ mice than in *Pemt*$^{+/+}$ mice, whereas BIP and calnexin were the same in the two

genotypes (Fig 2A&B). The UPR was more activated in the livers of *Pemt*$^{-/-}$ mice than *Pemt*$^{+/+}$ mice, and p-PERK, PERK and p-eIF2α were also higher in *Pemt*$^{-/-}$ mice whereas IRE1α was not altered. p-IRE1α was markedly lower in the livers of HF-fed mice of both genotypes than in chow-fed mice (data not shown). Despite no change in IRE1α, the amount of its downstream target XBP1s was 34% higher in *Pemt*$^{-/-}$ mice than in *Pemt*$^{+/+}$ mice (Figure 3.2A&B). Similarly, ATF6α was 50% higher in *Pemt*$^{-/-}$ mice than *Pemt*$^{+/+}$ mice (Figure 3.2A&B). The amount of PC and the PC/PE ratio, were also lower in hepatic ER from *Pemt*$^{-/-}$ mice than *Pemt*$^{+/+}$ mice (Figure 3.2C). Thus, upon HF feeding of the mice, PEMT deficiency increases ER stress in the liver and the induction of ER stress correlates with activation of the UPR.

3.3.3 PEMT deficiency increases ER stress in McA-RH7777 cells

McA-RH7777 cells lack PEMT enzymatic activity (28). To determine if PEMT deficiency increased ER stress in a cell model, levels of proteins associated with ER stress and the UPR were assessed in pCI-McA cells (McA-RH7777 cells expressing empty vector) and PEMT-McA cells (McA-RH7777 cells expressing human PEMT) (30). pCI-McA cells contained slightly more TG than did PEMT-McA cells (Figure 3.3A). Compared to pCI-McA cells, PEMT-McA cells contained the same amount of cellular PC, but 31% less PE, which increased the PC/PE ratio by 41% (Figure 3.3A). Consistent with data from the animal model, BIP, CHOP and PDI were higher in pCI-McA cells than in PEMT-McA cells, whereas, calnexin was the same (Figure 3.3B&C). In addition, p-PERK was significantly higher in pCI-McA cells than in PEMT-McA cells, whereas PERK, p-eIF2α, and eIF2α were unaltered by PEMT deficiency (Figure 3.3B&C). Although levels of p-IRE1α were comparable in pCI-McA and PEMT-McA

cells, IRE1α and its downstream signal XBP1s were significantly higher in pCI-McA cells (Figure 3.3B&C). ATF6α was not detectable in either pCI-McA or PEMT-McA cells (data not shown). These results indicate that PEMT deficiency in McA-RH7777 cells induces ER stress and activates the UPR.

3.3.4 PBA alleviates ER stress in McA-RH7777 cells

The chemical chaperone PBA protects primary hepatocytes from palmitate-mediated ER stress (36). We, therefore, determined if PBA alleviated ER stress in pCI-McA cells lacking PEMT. As expected, PBA largely prevented the elevation of p-PERK, IRE1α, XBP1s, BIP, CHOP and PDI in pCI-McA cells (Figure 3.3D&E) and other UPR proteins (PERK, p-eIF2α, eIF2α and p-IRE1α) and chaperone calnexin were unaltered by PBA (Figure 3.3D&E). Moreover, PBA did not significantly alter the amounts of all the above proteins in PEMT-McA cells. Thus, PBA alleviates ER stress in McA-RH7777 cells and attenuates activation of the UPR caused by PEMT deficiency.

3.3.5 PBA does not prevent HF-induced NASH in *Pemt*$^{-/-}$ mice

To determine if PBA attenuated NASH in HF-fed *Pemt*$^{-/-}$ mice, we administered PBA to HF-fed *Pemt*$^{+/+}$ and *Pemt*$^{-/-}$ mice at the same dosage and route of administration of PBA (oral gavage) as described (37). PBA did not alter body weight, brown or white adipose mass in either genotype (Figure 3.4A-C). PBA did not affect the mass of hepatic PC or PE in either genotype (Figure 3.4D). Nor did PBA prevent hepatomegaly or the increase in plasma ALT in *Pemt*$^{-/-}$ mice (Figure 3.5A, B). These observations are consistent with the pathological scoring of the liver sections in which HF-fed *Pemt*$^{-/-}$ mice exhibit profound lipid accumulation, and severe inflammation and ballooning, which were not improved by PBA (Figure 3.5C). However, PBA reduced hepatic TG

mass in *Pemt*$^{-/-}$ mice (Figure 3.5D). Thus, although PBA does not prevent NASH in HF-fed *Pemt*$^{-/-}$ mice, PBA alleviates hepatic TG accumulation.

We also determined if PBA attenuated macrophage infiltration and fibrogenesis in HF-fed *Pemt*$^{-/-}$ mice. mRNA encoding macrophage marker CD68 was higher in vehicle-treated *Pemt*$^{-/-}$ mice than in *Pemt*$^{+/+}$ mice (Figure 3.5E), and this increase was not prevented by PBA. Similarly, PBA had no significant effect on the mRNA level of *F4/80* in either genotype (Figure 3.5E). The livers of vehicle-treated *Pemt*$^{-/-}$ mice also exhibited fibrogenic features with higher levels of TGF-β1 and TGF-β2 compared to *Pemt*$^{+/+}$ mice, although TGF-β3 was lower in PEMT-deficient livers (Figure 3.5F). PBA did not reduce the amounts of any TGF-β family members in *Pemt*$^{-/-}$ or *Pemt*$^{+/+}$ mice (Figure 3.5F). Consequently, it appears that PBA does not diminish macrophage infiltration or fibrogenesis in HF-fed *Pemt*$^{-/-}$ mice.

3.3.6 PBA increases expression of genes involved in fatty acid oxidation

To unravel mechanisms underlying the decrease in hepatic TG in PBA-treated *Pemt*$^{-/-}$ mice (Figure 3.5D), we measured the amounts of TG and apoB in plasma, indicators of very low density lipoproteins. TG and apoB48 were markedly lower in plasma of vehicle-treated *Pemt*$^{-/-}$ mice compared to *Pemt*$^{+/+}$ mice (Figure 3.6A-C). However, PBA did not significantly increase the plasma content of TG, apoB100 or apoB48 in *Pemt*$^{+/+}$ or *Pemt*$^{-/-}$ mice (Figure 3.6A-C). These data suggest that in *Pemt*$^{-/-}$ mice the reduction of hepatic TG in response to PBA is not due to increased lipoprotein secretion.

We also analyzed the hepatic expression of mitochondrial electron transport chain proteins and genes related to fatty acid oxidation. In vehicle-treated *Pemt*$^{-/-}$ mice,

electron transport chain proteins, including complexes I, III, IV and V, but not complex II, were at least 50% lower than in *Pemt*$^{+/+}$ mice suggesting reduced capacity for mitochondrial energy production in *Pemt*$^{-/-}$ mice (Figure 3.7A). PBA increased complexes I and V in *Pemt*$^{-/-}$, but not *Pemt*$^{+/+}$ mice (Figure 3.7A). In vehicle-treated *Pemt*$^{-/-}$ mice, mRNAs encoding proteins involved in fatty acid oxidation [peroxisome proliferator-activated receptor (PPAR)α, CPT (carnitine palmitoyltransferase)1α, MCAD (medium-chain acyl-CoA dehydrogenase)] were lower than in *Pemt*$^{+/+}$ mice (Figure 3.7B). The mRNAs encoding CYP2E1 (cytochrome p450 2E1) and ACO (acyl-CoA oxidase 1), important in peroxisomal fatty acid oxidation, were also decreased by PEMT deficiency in vehicle-treated mice (Figure 3.7B). However, PBA doubled the mRNA level of CPT1α in *Pemt*$^{-/-}$ mice, suggesting an increased capacity for fatty acid oxidation without changing mRNAs encoding PPARα, MCAD, LCAD, CYP2E1 or ACO (Figure 3.7B). In *Pemt*$^{+/+}$ mice, PBA decreased mRNAs encoding PPARα, CPT1α and ACO with no effect on LCAD, MCAD or CYP2E1 (Figure 3.7B). In combination, these data suggest that PBA decreases hepatic TG at least partially through promoting fatty acid oxidation.

3.3.7 PBA minimally reduces ER stress in HF-fed *Pemt*$^{-/-}$ mice

Since PBA supressed ER stress in the livers of *ob/ob* mice (37), we determined if PBA alleviated HF-induced ER stress in the livers of *Pemt*$^{-/-}$ mice. As shown above, PEMT deficiency induced hepatic ER stress in HF-fed mice and also increased the amounts of CHOP, p-eIF2α, and ATF6α. However, PBA did not significantly reduce these proteins in *Pemt*$^{-/-}$ mice (Figure 3.8A&B). We conclude, therefore, that PBA minimally reduces hepatic ER stress in HF-fed *Pemt*$^{-/-}$ mice.

3.3.8 PBA reduces apoptosis but does not improve impaired autophagy in the livers of HF-fed *Pemt*$^{-/-}$ mice

Prolonged ER stress leads to apoptosis (14). Thus, we determined if apoptosis were more pronounced in the livers of HF-fed *Pemt*$^{-/-}$ mice than *Pemt*$^{+/+}$ mice. Indeed, the amounts of marker proteins of apoptosis (cytochrome c and cleaved-caspase 3) were higher in *Pemt*$^{-/-}$ mice than *Pemt*$^{+/+}$ mice, while uncleaved caspase 3 levels were equivalent (Figure 3.8C). In *Pemt*$^{-/-}$ mice, PBA reduced cytochrome c and cleaved-caspase 3 approximately to their levels in *Pemt*$^{+/+}$ mice (Figure 3.8C). However, PBA did not reduce the anti-apoptotic protein, BCL-2, or p-JNK, a stress/inflammation-induced transcription factor (Figure 3.8C). Thus, PBA reduces apoptosis in the livers of HF-fed *Pemt*$^{-/-}$ mice.

Impaired autophagy can contribute to hepatic lipid accumulation (38). We, therefore, compared levels of autophagy markers in the livers of *Pemt*$^{-/-}$ mice and *Pemt*$^{+/+}$ mice. When fed standard chow diet, *Pemt*$^{-/-}$ mice showed reduced level of ATG7, but comparable amounts of LC3 proteins and autophagy target protein p62 in comparison to *Pemt*$^{+/+}$ mice (Figure 3.9A). When challenged with the HF diet, the autophagosomal marker protein, LC3-II, in the livers of *Pemt*$^{-/-}$ mice was higher than in *Pemt*$^{+/+}$ mice. However, autophagic flow appeared to be impaired in *Pemt*$^{-/-}$ mice, since ATG7 was lower and, more importantly, p62 was higher than in *Pemt*$^{+/+}$ mice (Figure 3.9B). Moreover, PBA did not reduce the hepatic level of p62 in HF-fed mice of either genotype (Figure 3.9C). Thus, PBA appears to alleviate the HF-induced apoptosis in *Pemt*$^{-/-}$ mice but does not normalize the impaired autophagy.

3.3.9 Cytokine and chemokine levels in HF-fed *Pemt*$^{-/-}$ mice

Cytokines are critical mediators of hepatic inflammation and play a fundamental role in pathophysiology of acute and chronic fatty liver diseases (39). We, therefore, compared levels of cytokines and chemokines in HF-fed *Pemt*$^{+/+}$ and *Pemt*$^{-/-}$ mice with or without PBA treatment (Table 3.2). Compared to vehicle-treated *Pemt*$^{+/+}$ mice, vehicle-treated *Pemt*$^{-/-}$ mice had higher levels of chemotactic chemokines IP-10, MCP-1 and MIG, but lower levels of the anti-apoptotic cytokines IL-2, IL-9, IL-12 and IL-15. Vehicle-treated *Pemt*$^{-/-}$ compared to *Pemt*$^{+/+}$ mice also had reduced cytokines important for an immune response such as eotaxin, IFNγ, KC and MIP1α. VEGF, which is important for angiogenesis, was also decreased in vehicle-treated *Pemt*$^{-/-}$ mice. PBA reduced IL-7 and IL-12 (p40) in *Pemt*$^{+/+}$ mice. In *Pemt*$^{-/-}$ mice, PBA increased eotaxin, but decreased RANTES. Overall, levels of macrophage attractant chemokines in *Pemt*$^{-/-}$ mice were higher than in *Pemt*$^{+/+}$ mice, whereas levels of anti-apoptotic ILs were lower. Thus, PBA has only minor effects on levels of cytokines and chemokines in the livers of both genotypes.

3.4 Discussion

We report that PEMT deficiency leads to hepatic ER stress by altering phospholipid composition. We show that PEMT deficiency decreased PC and increased PE in the ER, coincident with ER stress. Similarly, expression of PEMT in McA-RH7777 cells, which lack PEMT activity, increased the PC/PE ratio and reversed activation of the UPR and ER stress. The pre-existing ER stress in the livers of chow-fed *Pemt*$^{-/-}$ mice promoted the development of HF-induced NASH. PBA alleviated ER stress caused by PEMT deficiency in McA-RH7777 cells and modestly reduced hepatic TG

accumulation in HF-fed *Pemt*$^{-/-}$ mice. Nevertheless, PBA only slightly attenuated ER stress and failed to suppress the development of NASH in HF-fed *Pemt*$^{-/-}$ mice.

3.4.1 Aberrant phospholipid composition of the ER induces ER stress

The composition of membrane lipids is a known regulator of ER stress. For example, palmitate and cholesterol induce ER stress in cells when these lipids are incorporated into the ER (40,41). In contrast, polyunsaturated fatty acids suppress ER stress (42). We made the surprising finding that even in chow-fed mice, lack of PEMT led to hepatic ER stress, despite only a small increase in TG content (Figure 3.1) (12) (33) (33) (33) (33) (11). Thus, TG accumulation is unlikely to be the primary trigger for this type of hepatic ER stress. In addition, the ER stress showed in the livers from chow-fed *Pemt*$^{-/-}$ mice is not accompanied with elevation of the UPR pathway (Figure 3.1D) (12) (33) (33) (33) (33), suggesting the ER stress caused by alteration of PC and PE in the ER is UPR-independent. Interestingly, the hepatic PC content and PC/ PE ratio were lower in hepatic ER from both chow-fed and HF-fed *Pemt*$^{-/-}$ mice than in *Pemt*$^{+/+}$ mice (Figure 3.1F and Figure 3.2C). A similar observation was made in McA-RH7777 cells without PEMT activity (Figure 3.3). Introduction of PEMT into McA-RH7777 cells reduced PE, increased the PC/PE ratio and suppressed ER stress (Figure 3.3). Furthermore, a higher PC/PE ratio in hepatic ER from *ob/ob* mice was reported to disrupt ER calcium homeostasis (35)**.** We conclude, therefore, that PEMT deficiency likely induces hepatic ER stress by altering the PC and PE composition of the ER.

Our study reveals some differences compared to a recent report on *ob/ob* mice (35), in which the PC/PE ratio in hepatic ER was higher than in lean mice, possibly because the CDP-choline and PEMT pathways were stimulated (35). We show that in

both chow-fed and HF-fed *Pemt*$^{-/-}$ mice the PC/PE ratio in the ER was lower than in *Pemt*$^{+/+}$ mice (6) (Figure 3.1F and Figure 3.2C). Even in chow-fed mice that exhibited only minor steatosis, PEMT deficiency caused hepatic ER stress (Figure 3.1). However, reduction of PEMT activity in *ob/ob* mice reduced the hepatic PC/PE ratio, alleviated ER stress, and reduced hepatic TG (35). The difference between these two studies might be explained by the distinct mechanisms for induction of ER stress in the different mouse models. As in *ob/ob* mice, hepatic fat accumulation in HF-fed *Pemt*$^{-/-}$ mice stimulated ER stress, but in chow-fed *Pemt*$^{-/-}$ mice, the amounts of hepatic TG, cholesterol and cholesteryl esters were very low compared to those in HF-fed *Pemt*$^{-/-}$ mice or *ob/ob* mice (12,43). Furthermore, absolute values for the PC/PE ratio were different in the two studies, perhaps due to different methodologies for ER isolation and lipid analysis (35). For example, in *ob/ob* mice the average PC/PE ratio was 1.97 compared to 1.30 for lean mice. In contrast, in our study, the PC/PE ratio was 2.59 ± 0.13 in chow-fed *Pemt*$^{+/+}$ mice and 1.58 ± 0.08 in chow-fed *Pemt*$^{-/-}$ mice. When challenged with the HF diet, the ratio in *Pemt*$^{+/+}$ mice was 2.14 ± 0.06 and in *Pemt*$^{-/-}$ mice was 1.30 ± 0.11. Thus, the PC/PE ratio appears to exhibit a “U-shaped” correlation with ER stress (Figure 3.10): an aberrant PC/PE ratio, either increased or decreased, would induce ER stress. Normalization of the PC/PE ratio in *ob/ob* mice improved hepatic ER function (35).

Recently, Hotamisligil’s group reported that a chronically enhanced physical association between ER and mitochondria in *ob/ob* mice caused mitochondrial dysfunction (44). However, contradictory results were reported elsewhere (45). In primary hepatocytes, the absence of PEMT changed mitochondrial morphology and

increased mitochondrial respiration and ATP production (30). It is possible that the morphological and functional changes in mitochondria in *Pemt*$^{-/-}$ mice are caused by ER stress. Nevertheless, we ascribe the induction of ER stress to decreased PC/PE ratio.

3.4.2 HF-fed *Pemt*$^{-/-}$ mice are useful for studying NASH

Our studies indicate that HF-fed *Pemt*$^{-/-}$ mice are a useful model for studying mechanisms underlying NASH. *Pemt*$^{-/-}$ mice experience liver failure when fed a choline-deficient diet for 3 days (5). When fed the HF diet for 2 weeks, they develop NASH (6). Due to choline insufficiency, *Pemt*$^{-/-}$ mice show little weight gain and are more insulin sensitive than *Pemt*$^{+/+}$ mice after 10 weeks of HF feeding (12). Interestingly, mice fed a methionine- and choline-deficient diet, a widely used NASH mouse model, are also insulin sensitive, but they show significant weight loss (46). Another factor that might contribute to the induction of NASH in HF-fed *Pemt*$^{-/-}$ mice is an impairment of autophagic flow (Figure 3.9). Furthermore, neuronal signals via the hepatic branch of the vagus nerve contribute to the development of NASH in HF-fed *Pemt*$^{-/-}$ mice (47). We have shown that hepatic vagotomy prevents HF-induced NASH in *Pemt*$^{-/-}$ mice (47). Thus, HF-fed *Pemt*$^{-/-}$ mice appears to be a very good mouse model for studying mechanisms underlying NASH.

3.4.3 PBA alleviates steatosis but not NASH in HF-fed *Pemt*$^{-/-}$ mice

PBA is a small chemical chaperone that stabilizes protein conformation and increases folding capacity of ER proteins (37,48,49). It is a FDA-approved drug used for treatment of urea cycle disorders and sickle cell disease (49). Induction of hepatic ER stress has been associated with obesity in genetic and dietary mouse models (18). Oral ingestion of PBA completely restores insulin signaling and glucose homeostasis in

ob/ob mice and improves hepatic lipid accumulation and hepatic ER stress (37). PBA also alleviates ischemia/reperfusion injury to the liver in mice by reducing ER stress and apoptosis (49). Moreover, pre-treatment of mice with PBA reduces oleate-mediated ER stress (50). On the basis of these studies, we delivered the same dosage of PBA via the same route (oral gavage) (37) to HF-fed *Pemt*$^{-/-}$ mice. PBA reduced hepatic lipid accumulation possibly via stimulating fatty acid oxidation, rather than by enhancing lipoprotein secretion (Figure 3.6 and Figure 3.7). The increased expression of fatty acid oxidation related genes such as *CPT1α* and the elevated protein levels of electron transport chain proteins (Figure 3.7) in PBA-treated *Pemt*$^{-/-}$ mice suggest an increased fatty acid oxidation. Whereas, the plasma TG and apoB proteins in *Pemt*$^{-/-}$ mice were not changed by PBA treatment (Figure 3.6 and Figure 3.7) suggests the reduced hepatic TG is unlikely caused by the alteration in the secretion of hepatic VLDL. However, in HF-fed *Pemt*$^{-/-}$ mice, PBA only slightly alleviated ER stress and inflammation and did not prevent fibrosis or NASH progression (Figure 3.5 and Figure 3.8). A similar result was obtained in methionine-choline-deficient mice, which also exhibit hepatic ER stress (51,52). In these mice, PBA alleviated ER stress but did not reverse NASH (53), although perhaps the small dosage of PBA (1/5 of that used in our study) diminished its efficacy. Taken together, these data show that PBA improves steatosis but does not effectively prevent NASH in HF-fed *Pemt*$^{-/-}$ mice.

In summary, PEMT deficiency disrupts the balance between PC and PE in hepatic ER, thereby leading to ER stress without activating the UPR. Pre-existing hepatic ER stress renders chow-fed *Pemt*$^{-/-}$ mice prone to the development of HF diet-induced NASH. In McA-RH7777 cells, PEMT deficiency activates the UPR and increases ER

stress, both of which are reversed by PEMT expression and alleviated by PBA. However, PBA has only a minor benefit in relieving HF-induced ER stress in *Pemt*$^{-/-}$ mice and fails to prevent HF-induced NASH.

Table 3.1 Primers used for real-time quantitative PCR

Abbreviations are: *Cd*, cluster of differentiation; *Ppar*, peroxisome proliferator activated receptor; *Cpt*, carnitine palmitoyltransferase; *Mcad*, medium-chain acyl-CoA dehydrogenase; *Lcad*, long-chain acyl-CoA dehydrogenase; *Cyp2E1,* cytochrome p450 2E1 and *Aco*, acyl-CoA oxidase 1.

gene	forward primer (5' -> 3')	reverse primer (5' -> 3')
Cyclophilin	TCC AAA GAC AGC AGA AAA CTT TCG	TCT TCT TGC TGG TCT TGC CAT TCC
Cd68	GCG GCT CCC TGT GTG TCT GAT	GGG CCT GTG GCT GGT CGT AG
F4/80	CCC TCG GGC TGT GAG ATT GTG	TGG CCA AGG CAA GAC ATA CCA G
Pparα	GAC CTG AAA GAT TCG GAA ACT	CGT CTT CTC GGC CAT ACA C
Cpt1α	TGA GTG GCG TCC TCT TTG G	CA GCG AGT AGC GCA TAG TCA TG
Mcad	TTA CCG AAG AGT TGG CGT ATG	ATC TTC TGG CCG TTG ATA ACA
Lcad	GCA AAA TAC TGG GCA TCT GAA	TCC GTG GAG TTG CAC ACA TT
Cyp2E1	GGT AAT GAG GCC CGC ATC CA	AGA GAA TAT CCG CAA TGA CA
Aco	CAG CAG GAG AAA TGG ATG CA	GGG CGT AGG TGC CAA TTA TCT

Table 3.2 Hepatic cytokines and chemokines in Veh- and PBA-treated mice

Pemt$^{-/-}$ and *Pemt*$^{+/+}$ mice were fed the HF diet for 2 weeks concurrently with treatment with vehicle (Veh) or PBA. Levels of cytokines and chemokines were measured in the livers of 4-6 mice in each group. Data are means (pg/mg protein) ± SEM. Data were analyzed by a two-way ANOVA, followed by post hoc Bonferroni's test. *$P < 0.05$ for *Pemt*$^{-/-}$ vs *Pemt*$^{+/+}$ mice with the same treatment; $^{\#}p < 0.05$ for Veh-treated vs PBA-treated mice of the same genotype. L, lower than detection limit.

Treatment	Veh		PBA	
Pemt genotype	*Pemt*$^{+/+}$	*Pemt*$^{-/-}$	*Pemt*$^{+/+}$	*Pemt*$^{-/-}$
Eotaxin	18.40 ± 0.69	9.69 ± 0.90*	17.70 ± 1.34	13.00 ± 0.83*$^{\#}$
G-CSF	L	L	L	L
GM-CSF	10.90 ± 2.31	L	9.84 ± 1.37	L
IFNγ	5.68 ± 0.57	1.87 ± 0.10*	5.00 ± 0.73	1.54 ± 0.30*
IL-1α	29.20 ± 0.95	26.31 ± 1.58	29.13 ± 1.24	16.10 ± 4.49*
IL-1β	8.12 ± 0.91	3.44 ± 1.82	4.58 ± 1.74	4.97 ± 0.70
IL-2	14.50 ± 0.65	7.16 ± 1.13*	12.50 ± 0.43	8.83 ± 0.42*
IL-3	L	L	L	L
IL-4	0.26 ± 0.02	0.51 ± 0.15	0.21 ± 0.01	0.26 ± 0.02
IL-5	0.15 ± 0.03	0.01 ± 0.01	0.05 ± 0.03$^{\#}$	0.04 ± 0.02
IL-6	1.87 ± 0.18	1.34 ± 0.34*	1.40 ± 0.08	1.48 ± 0.16
IL-7	9.45 ± 0.90	6.27 ± 1.17	6.29 ± 0.65$^{\#}$	5.76 ± 0.56
IL-9	35.90 ± 0.59	17.60 ± 2.90*	35.80 ± 4.37	18.10 ± 0.80*
IL-10	4.79 ± 1.46	2.67 ± 0.75	3.18 ± 0.43	1.43 ± 0.20*

Table 3.2 cont.

Treatment	Veh		PBA	
Pemt genotype	*Pemt*$^{+/+}$	*Pemt*$^{-/-}$	*Pemt*$^{+/+}$	*Pemt*$^{-/-}$
IL-12 (p40)	26.20 ± 1.17	8.35 ± 4.42*	20.00 ± 0.99$^{\#}$	3.22 ± 1.41$^{\#}$
IL-12 (p70)	6.49 ± 5.05	11.30 ± 5.68	1.23 ± 0.21	4.59 ± 3.21
IL-13	1.04 ± 0.30	L	0.92 ± 0.26	L
IL-15	25.50 ± 4.51	1.52 ± 0.39*	18.70 ± 5.40	2.44 ± 0.45*
IL-17	0.19 ± 0.05	L	L	L
IP-10	8.87 ± 0.32	19.80 ± 1.29*	8.63 ± 1.06	23.80 ± 2.33*
KC	57.50 ± 5.43	35.50 ± 6.06*	83.10 ± 17.25	42.20 ± 1.86
LIF	0.54 ± 0.13	0.43 ± 0.14	0.25 ± 0.07	0.48 ± 0.06
LIX	2.66 ± 1.09	2.76 ± 1.47	1.94 ± 1.58	3.01 ± 1.78
MCP-1	13.10 ± 2.24	39.60 ± 5.95*	8.98 ± 1.69	33.40 ± 2.20*
M-CSF	3.12 ± 0.84	0.97 ± 0.08	1.26 ± 0.23	0.97 ± 0.28
MIG	33.10 ± 4.44	87.50 ± 12.72*	41.60 ± 12.77	51.60 ± 4.92
MIP-1α	18.60 ± 1.08	9.15 ± 0.84*	16.90 ± 0.85	10.70 ± 0.42*
MIP-1β	L	L	L	L
MIP-2	15.20 ± 4.97	7.15 ± 1.34	9.82 ± 1.89	7.97 ± 2.53
RANTES	4.99 ± 0.3	5.21 ± 0.35	5.44 ± 1.81	4.00 ± 0.16$^{\#}$
TNFα	2.98 ± 0.84	0.55 ± 0.00	2.15 ± 0.22	1.01 ± 0.37*
VEGF	1.01 ± 0.08	0.68 ± 0.09*	0.83 ± 0.06	0.88 ± 0.05

Figure 3.1 Chow-fed *Pemt*$^{-/-}$ mice exhibit hepatic ER stress and steatosis

Pemt$^{-/-}$ and *Pemt*$^{+/+}$ mice were fed standard chow diet. (A) H&E staining of liver sections; bar size: 50 μm. (B) NAFLD scores of liver H&E staining. For (A) and (B), 3 mice of each genotype were used. (C) Representative immunoblots for proteins implicated in ER stress and the UPR: BIP (glucose-regulated protein 78), CHOP (C/EBP–homologous protein), PDI (protein disulfide isomerase), calnexin, PERK (protein kinase-like ER kinase), p-PERK, eIF2α (the eukaryotic initiation factor 2α), p-eIF2α, IRE1α (inositol-requiring enzyme-1), p-IRE1α, XBP1s (the spliced form of X-box binding protein-1), ATF6α (activating transcription factor 6α), and loading control glyceraldehyde 3-phosphate dehydrogenase (GAPDH) in the liver homogenates. (D) Densitometric analysis of immunoblots in (C). (E) Immunoblotting of subcellular markers in homogenates and ER fractions isolated from mouse livers. Plasma membrane protein Integrin β1; Golgi marker β1,4-galactosyltransferase; ER markers PDI and calnexin; cytosolic marker α-tubulin; mitochondrial marker UCP2 (uncoupling protein 2). The same amount of protein was loaded in each lane. (F) Mass of phosphatidylcholine (PC) and phosphatidylethanolamine (PE) and PC/PE ratio in hepatic ER. Data were analyzed by Student's *t*-test. For panels D and F, data were from 6-7 mice of each genotype; *p < 0.05, *Pemt*$^{+/+}$ *vs Pemt*$^{-/-}$.

Figure 3.1

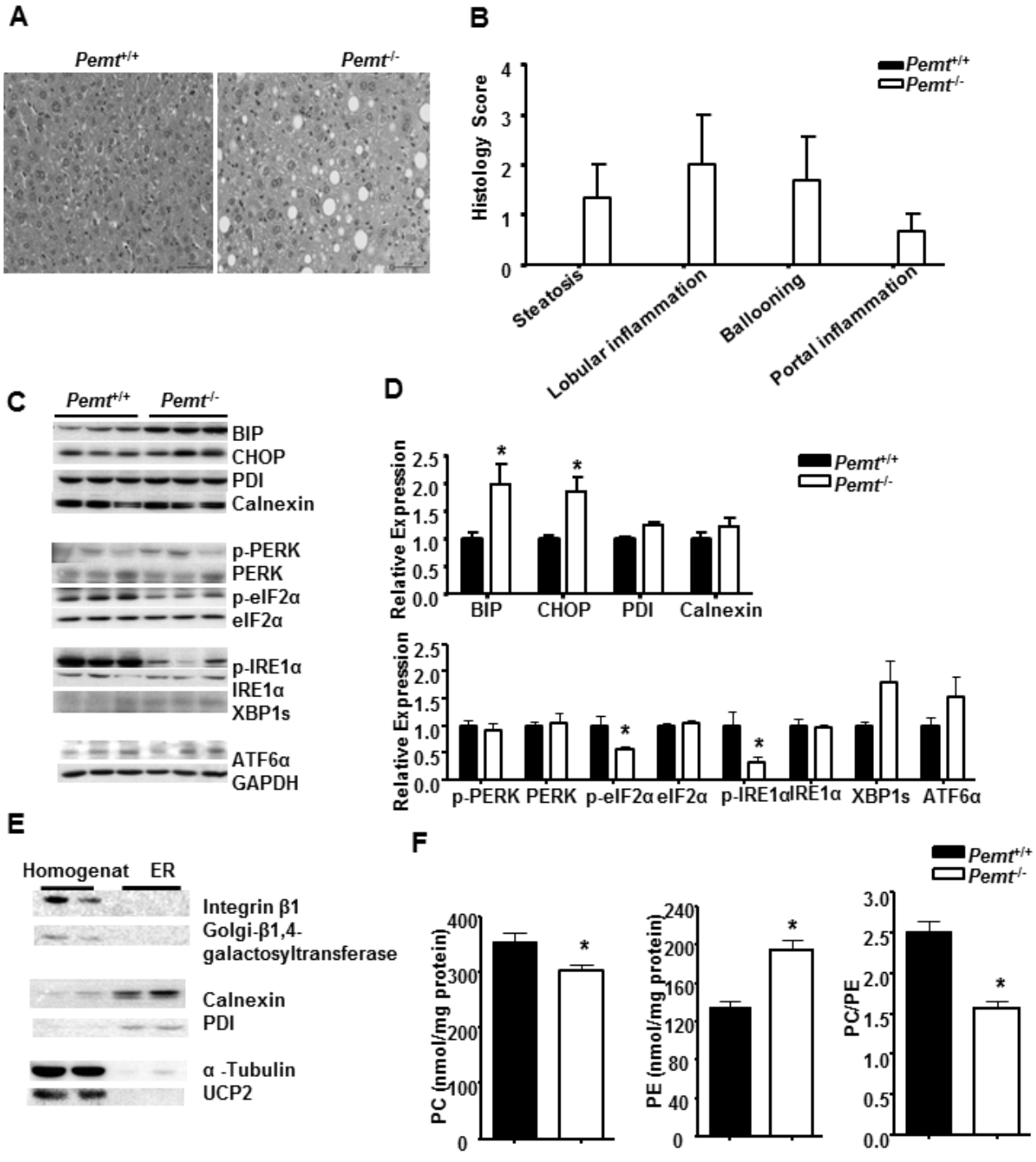
A
Pemt+/+
Pemt-/-
B
Pemt+/+
Pemt-/-
Histology Score
0
1
2
3
4
Steatosis
Lobular inflammation
Ballooning
Portal inflammation
C
Pemt+/+
Pemt-/-
BIP
CHOP
PDI
Calnexin
p-PERK
PERK
p-eIF2α
eIF2α
p-IRE1α
IRE1α
XBP1s
ATF6α
GAPDH
D
Pemt+/+
Pemt-/-
Relative Expression
0.0
0.5
1.0
1.5
2.0
2.5
BIP
CHOP
PDI
Calnexin
p-PERK
PERK
p-eIF2α
eIF2α
p-IRE1α
IRE1α
XBP1s
ATF6α
E
Homogenat
ER
Integrin β1
Golgi-β1,4-galactosyltransferase
Calnexin
PDI
α -Tubulin
UCP2
F
Pemt+/+
Pemt-/-
PC (nmol/mg protein)
0
100
200
300
400
PE (nmol/mg protein)
0
40
80
120
160
200
240
PC/PE
0.0
0.5
1.0
1.5
2.0
2.5
3.0

Figure 3.2 Increased ER stress in the livers of HF-fed *Pemt*$^{-/-}$ mice

Pemt$^{-/-}$ and *Pemt*$^{+/+}$ mice were fed the HF diet for 2 weeks. (A) Representative immunoblots of proteins implicated in ER stress and the UPR in the liver homogenates. (B) Densitometric analysis of immunoblots in (A). (C) Mass of phosphatidylcholine (PC) and phosphatidylethanolamine (PE) and PC/PE ratio in hepatic ER. Data were analyzed by a two-way ANOVA, followed by post hoc Bonferroni's test. All data were from 6-7 mice of each genotype; *$p < 0.05$, *Pemt*$^{+/+}$ *vs Pemt*$^{-/-}$.

Figure 3.2

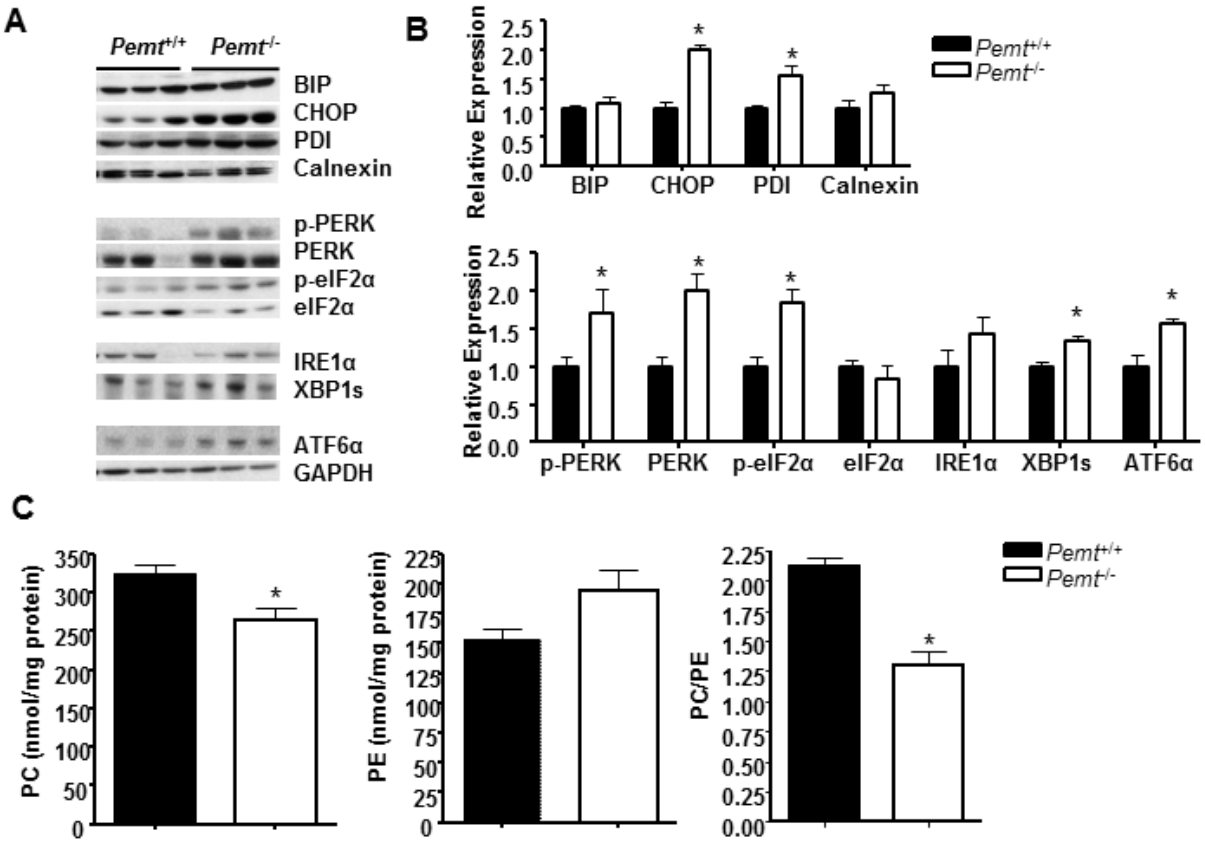
A
Pemt+/+
Pemt-/-
BIP
CHOP
PDI
Calnexin
p-PERK
PERK
p-eIF2α
eIF2α
IRE1α
XBP1s
ATF6α
GAPDH
B
Relative Expression
Pemt+/+
Pemt-/-
BIP
CHOP
PDI
Calnexin
p-PERK
PERK
p-eIF2α
eIF2α
IRE1α
XBP1s
ATF6α
C
PC (nmol/mg protein)
PE (nmol/mg protein)
PC/PE

Figure 3.3 ER stress in McA-RH7777 cells lacking PEMT is alleviated by 4-phenylbutyric acid (PBA)

(A) Mass of triacylglycerol (25), phosphatidylcholine (PC) and phosphatidylethanolamine (PE), and PC/PE ratio in pCI cells and McA cells expressing human PEMT (PEMT). (B and D) Representative immunoblots of proteins implicated in ER stress and the UPR in pCI and PEMT cells under basal conditions (B), and ± PBA (D). (C and E) Densitometric analysis of immunoblots in (B) and (D) respectively. Data were analyzed by a two-way ANOVA, followed by post hoc Bonferroni's test. $^{*}P < 0.05$, pCI *vs* PEMT; $^{\#}p < 0.05$, PBA-treated pCI-McA *vs* PBA-treated PEMT-McA. Data were collected from three independent experiments.

Figure 3.3

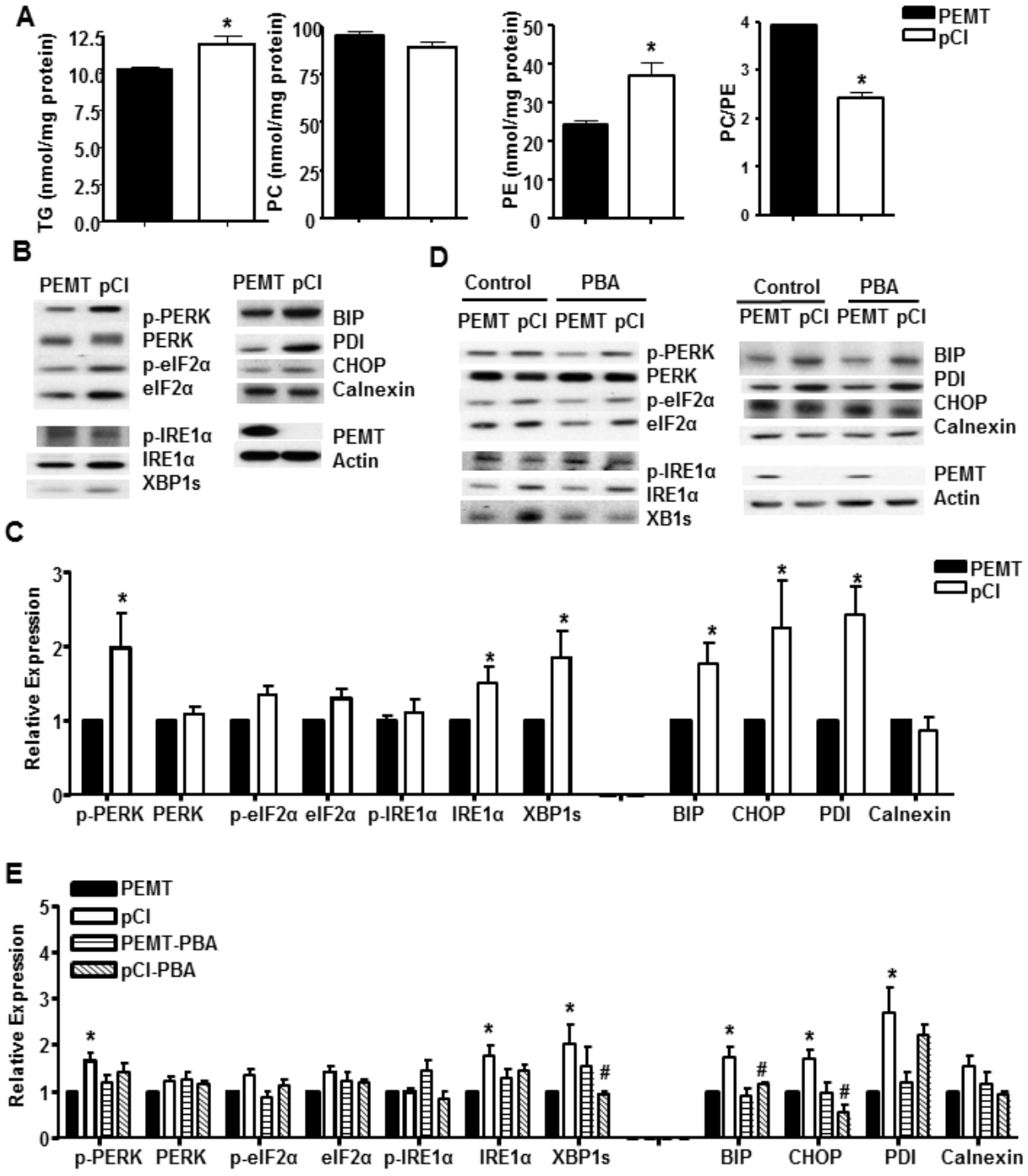
A
TG (nmol/mg protein)
PC (nmol/mg protein)
PE (nmol/mg protein)
PC/PE
PEMT
pCI
B
PEMT pCI
p-PERK
PERK
p-eIF2α
eIF2α
p-IRE1α
IRE1α
XBP1s
BIP
PDI
CHOP
Calnexin
PEMT
Actin
D
Control
PBA
C
Relative Expression
p-PERK PERK p-eIF2α eIF2α p-IRE1α IRE1α XBP1s BIP CHOP PDI Calnexin
E
PEMT
pCI
PEMT-PBA
pCI-PBA

Figure 3.4 PBA does not alter body mass, hepatic PC or PE in both *Pemt*$^{+/+}$ and *Pemt*$^{-/-}$ mice

Pemt$^{+/+}$ and *Pemt*$^{-/-}$ mice were fed the HF diet ± PBA for two weeks. (A) Body weight (B.W.) gain. (B) Weight of white adipose tissue as % B.W. (C) Weight of brown adipose tissue as % of B.W. (D) Mass of hepatic phosphatidylcholine (PC) and phosphatidylethanolamine (PE) and PC/PE ratio in the livers from HF-fed *Pemt*$^{+/+}$ or *Pemt*$^{-/-}$ mice. Data were analyzed by a two-way ANOVA, followed by post hoc Bonferroni's test. Data were from 4-7 mice of each genotype, $*p < 0.05$ for *Pemt*$^{+/+}$ *vs* *Pemt*$^{-/-}$ with the same treatment.

Figure 3.4

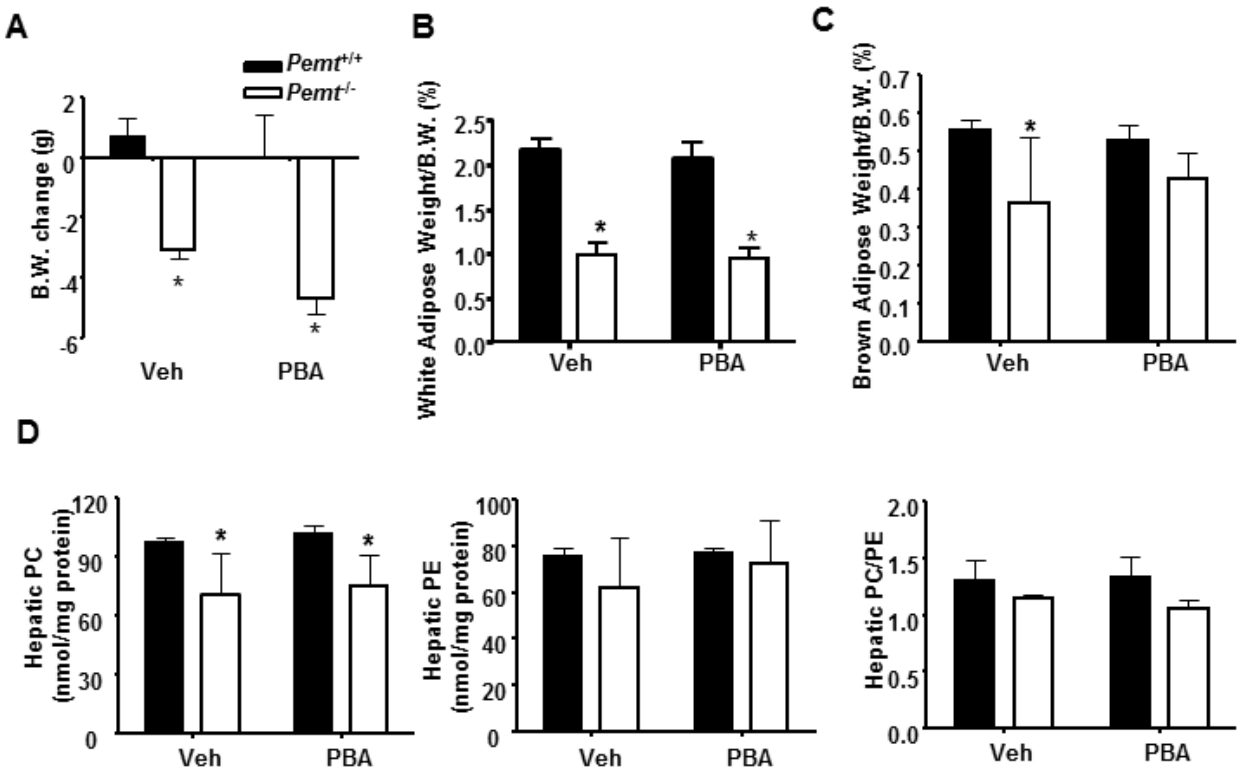
A
Pemt+/+
Pemt-/-
B.W. change (g)
2
0
-2
-4
-6
*
*
Veh
PBA
B
White Adipose Weight/B.W. (%)
2.5
2.0
1.5
1.0
0.5
0.0
*
*
Veh
PBA
C
Brown Adipose Weight/B.W. (%)
0.7
0.6
0.5
0.4
0.3
0.2
0.1
0.0
*
Veh
PBA
D
Hepatic PC (nmol/mg protein)
120
90
60
30
0
*
*
Veh
PBA
Hepatic PE (nmol/mg protein)
100
80
60
40
20
0
Veh
PBA
Hepatic PC/PE
2.0
1.5
1.0
0.5
0.0
Veh
PBA

Figure 3.5 PBA does not reverse NASH but improves steatosis in HF-fed *Pemt*$^{-/-}$ mice

Pemt$^{+/+}$ and *Pemt*$^{-/-}$ mice were fed the HF diet ± PBA for two weeks. (A) Percentage of liver weight to body weight (B.W.). (B) Plasma alanine aminotransferase (ALT). (C) H&E staining of liver sections (left) and NAFLD scores (right); size bar: 50 μm. (D) Hepatic triacylglycerol (25) mass. (E) Levels of mRNAs encoding cluster of differentiation (CD)68 and F4/80. (F) Levels of transforming growth factor (TGF)-β1, TGF-β2 and TGF-β3 in total liver homogenates. All data were from 6-7 mice of each genotype and treatment. Data were analyzed by a two-way ANOVA, followed by post hoc Bonferroni's test. *p < 0.05, *Pemt*$^{+/+}$ *vs Pemt*$^{-/-}$ (same treatment); #*p* < 0.05, PBA treatment *vs* Vehicle (Veh) for the same genotype.

Figure 3.5

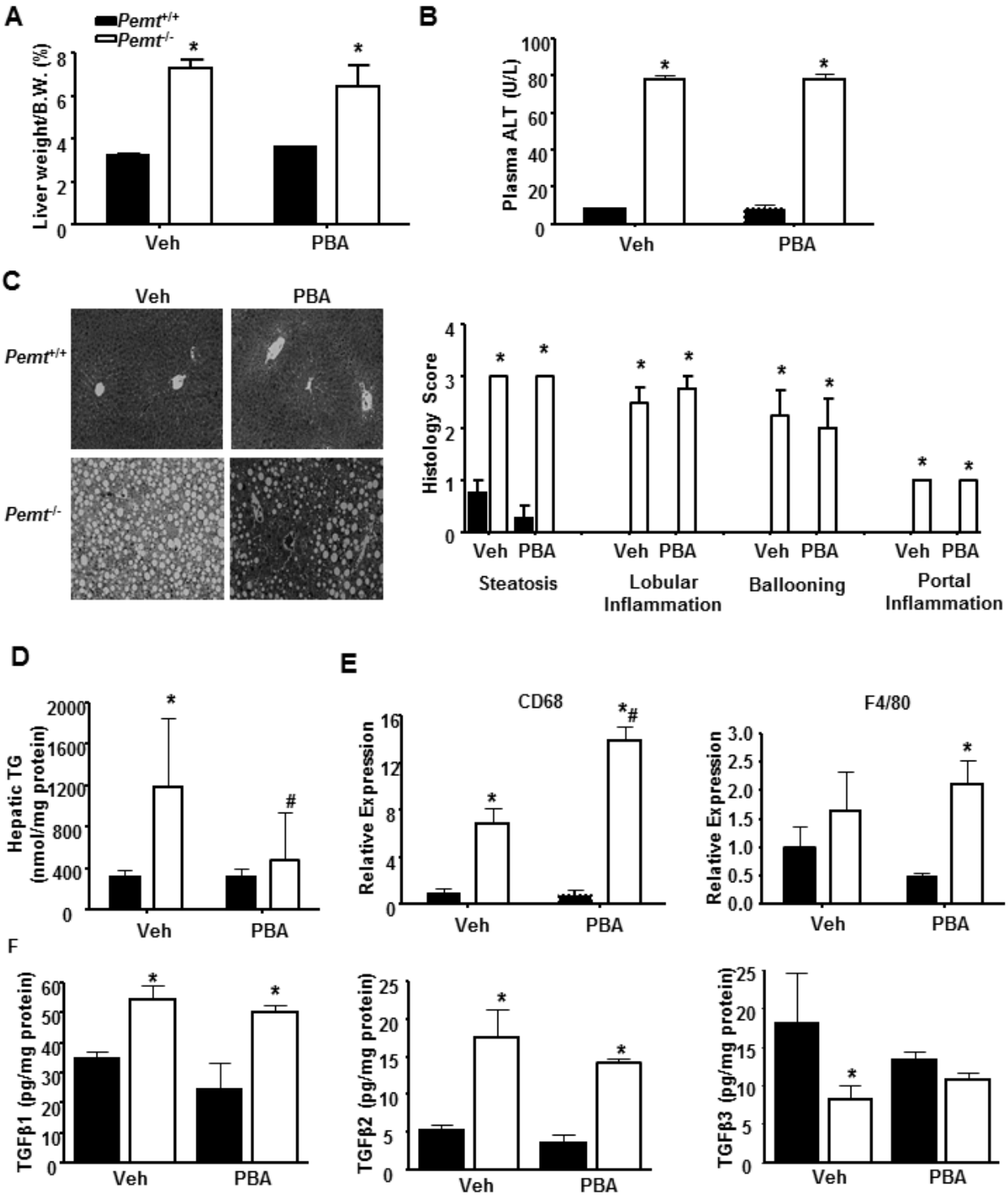
A
Pemt+/+
Pemt-/-
Liver weight/B.W. (%)
Veh
PBA
B
Plasma ALT (U/L)
C
Pemt+/+
Pemt-/-
Histology Score
Steatosis
Lobular Inflammation
Ballooning
Portal Inflammation
D
Hepatic TG (nmol/mg protein)
E
CD68
F4/80
Relative Expression
F
TGFβ1 (pg/mg protein)
TGFβ2 (pg/mg protein)
TGFβ3 (pg/mg protein)

Figure 3.6 PBA does not alter plasma levels of TG and apoB

Pemt$^{+/+}$ and *Pemt*$^{-/-}$ mice were fed the HF diet ± PBA for two weeks. (A) Plasma TG mass. (B) Representative immunoblots of plasma apoB100 and apoB48, and coomassie blue staining of membrane as loading control. (C) Densitometric analysis of immunoblots in panel B. All data were from 6-7 mice of each genotype and treatment. Data were analyzed by a two-way ANOVA, followed by post hoc Bonferroni's test. *p < 0.05, *Pemt*$^{+/+}$ *vs Pemt*$^{-/-}$ with the same treatment.

Figure 3.6

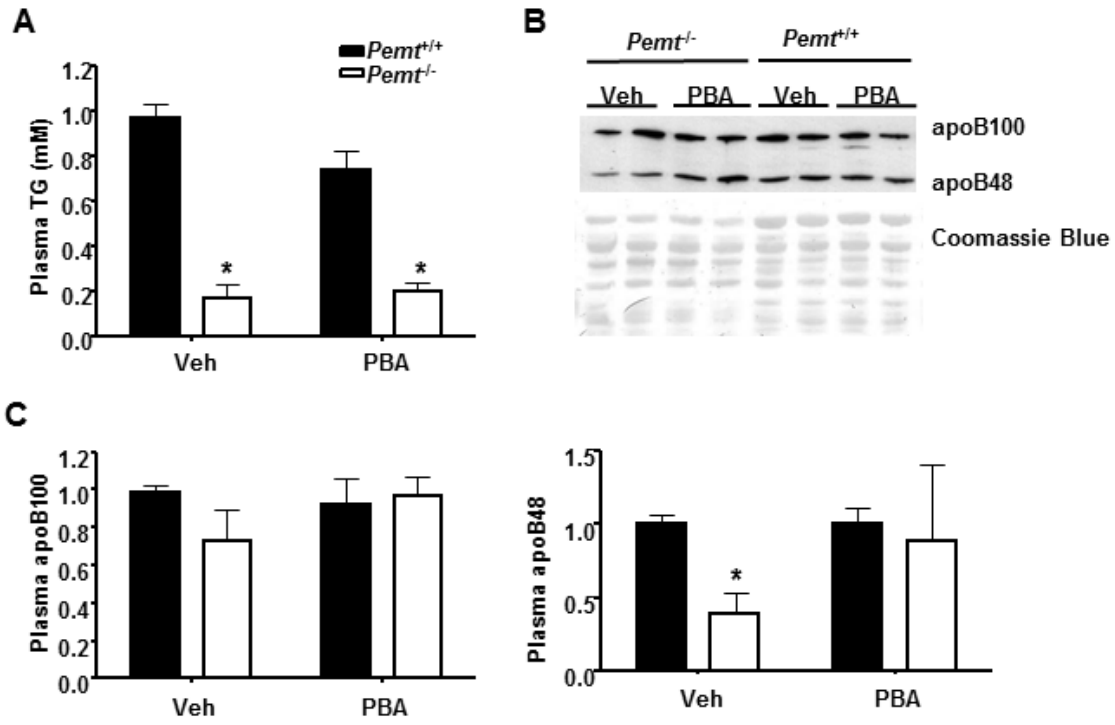
A
Pemt+/+
Pemt-/-
Plasma TG (mM)
1.2
1.0
0.8
0.6
0.4
0.2
0.0
*
*
Veh
PBA
B
Pemt-/-
Pemt+/+
Veh
PBA
Veh
PBA
apoB100
apoB48
Coomassie Blue
C
Plasma apoB100
1.2
1.0
0.8
0.6
0.4
0.2
0.0
Veh
PBA
Plasma apoB48
1.5
1.0
0.5
0.0
*
Veh
PBA

Figure 3.7 PBA increases expression of fatty acid oxidation-related genes

Pemt$^{+/+}$ and *Pemt*$^{-/-}$ mice were fed the HF diet ± PBA for two weeks. (A) Representative immunoblots and densitometric analysis for mitochondrial electron transport chain proteins in the liver homogenates. (B) Levels of mRNAs encoding peroxisome proliferator-activated receptor (PPAR)α, CPT1α (carnitine palmitoyltransferase 1α), LCAD (long-chain acyl-CoA dehydrogenase), MCAD (medium-chain acyl-CoA dehydrogenase), CYP2E1 (cytochrome p450 2E1) and ACO (acyl-CoA oxidase 1). All data were from 6-7 mice of each genotype and treatment. Data were analyzed by a two-way ANOVA, followed by post hoc Bonferroni's test. *$p < 0.05$, *Pemt*$^{+/+}$ *vs Pemt*$^{-/-}$ for the same treatment; #$p < 0.05$, PBA treatment *vs* Vehicle (Veh) for the same genotype.

Figure 3.7

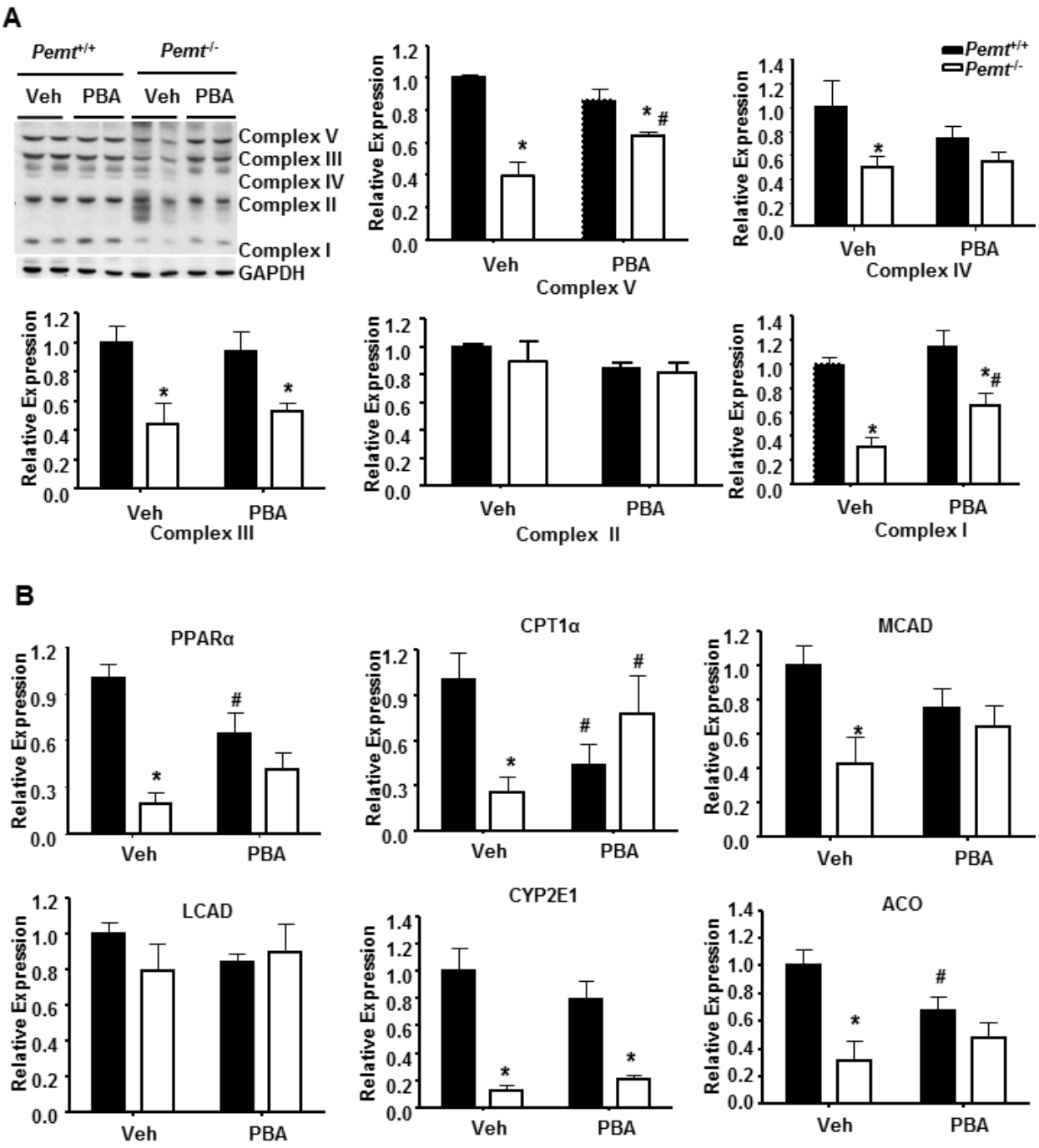
A
Pemt+/+
Pemt-/-
Veh
PBA
Veh
PBA
Complex V
Complex III
Complex IV
Complex II
Complex I
GAPDH
Relative Expression
Complex V
Complex IV
Complex III
Complex II
Complex I
B
PPARα
CPT1α
MCAD
LCAD
CYP2E1
ACO

Figure 3.8 PBA slightly improves ER stress and decreases apoptosis in HF-fed *Pemt*$^{-/-}$ mice

Pemt$^{+/+}$ and *Pemt*$^{-/-}$ mice were fed the HF diet and treated ± PBA for two weeks. (A) Representative immunoblots of proteins implicated in ER stress. (B) Densitometric analysis of immunoblots in panel A. (C) Representative immunoblots of cytochrome c, cleaved caspase-3, caspase-3, p-JNK, BCL-2 (B-cell lymphoma 2) and loading control GAPDH, and their densitometric analysis. All data were from 6-7 mice of each genotype and treatment. Data were analyzed by a two-way ANOVA, followed by post hoc Bonferroni's test. *$p < 0.05$, *Pemt*$^{+/+}$ *vs Pemt*$^{-/-}$ for the same treatment; #$p < 0.05$, PBA treatment *vs* Vehicle (Veh) within the same genotype.

Figure 3.8

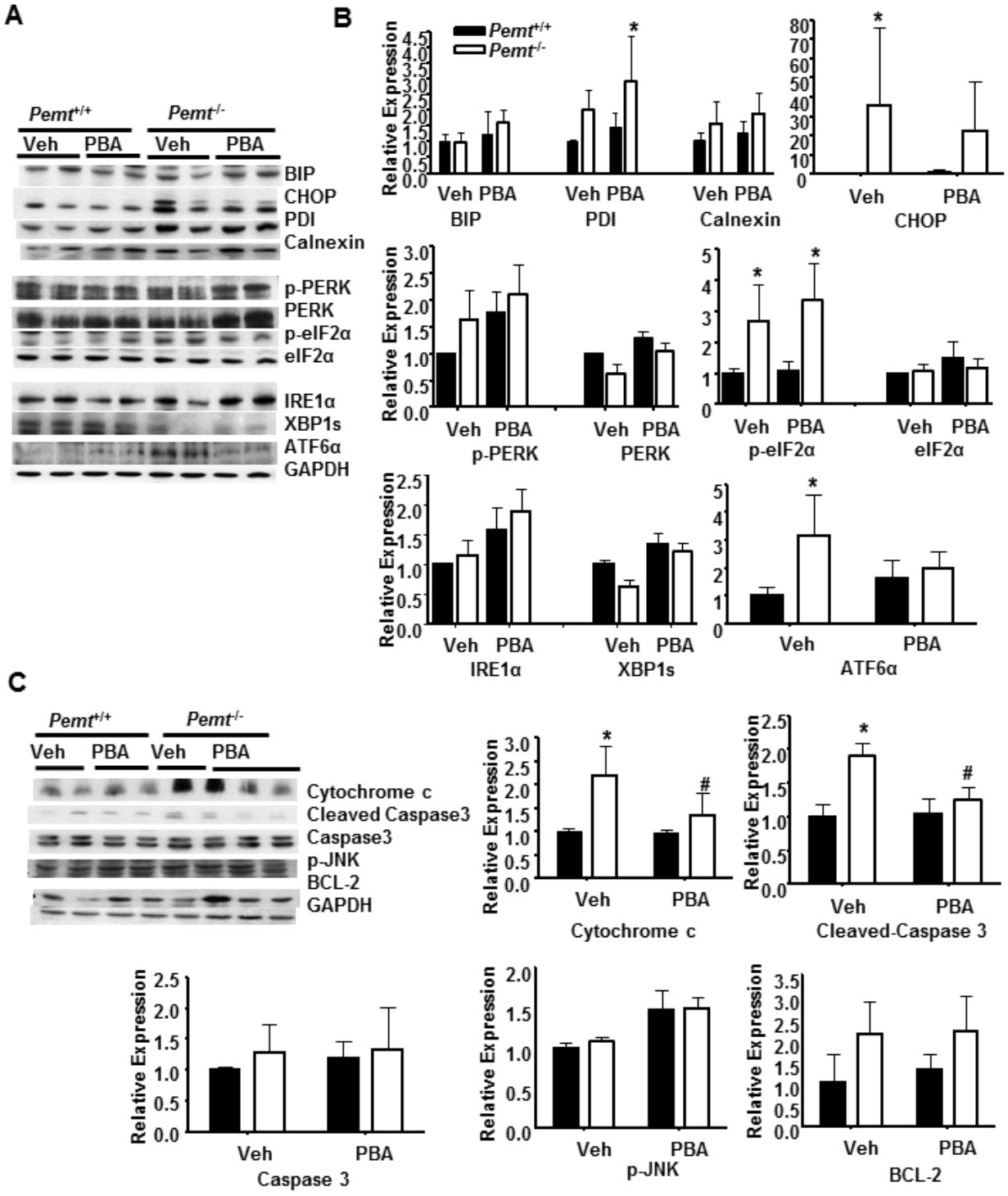
A
Pemt+/+
Pemt-/-
Veh
PBA
Veh
PBA
BIP
CHOP
PDI
Calnexin
p-PERK
PERK
p-eIF2α
eIF2α
IRE1α
XBP1s
ATF6α
GAPDH
B
Pemt+/+
Pemt-/-
Relative Expression
BIP
PDI
Calnexin
CHOP
p-PERK
PERK
p-eIF2α
eIF2α
IRE1α
XBP1s
ATF6α
C
Cytochrome c
Cleaved Caspase3
Caspase3
p-JNK
BCL-2
GAPDH
Cytochrome c
Cleaved-Caspase 3
Caspase 3
p-JNK
BCL-2

Figure 3.9 PBA does not improve the impaired autophagy in HF-fed *Pemt*$^{-/-}$ mice

(A) Representative immunoblots for LC3 (light chain 3), p62, ATG7 (autophagy-related protein 7), calnexin and PEMT in the livers of chow-fed mice, and densitometric analysis of the immunoblots. (B) Representative immunoblots for LC3, p62, ATG7, calnexin and PEMT in the livers of HF-fed mice and densitometric analysis of the immunoblots. (C) Representative immunoblots for p62 in the livers from *Pemt*$^{+/+}$ and *Pemt*$^{-/-}$ mice fed the HF diet and treated ± PBA for two weeks, and densitometric analysis of the immunoblots. Data were from 4-7 mice of each genotype. Data were analyzed by a two-way ANOVA, followed by post hoc Bonferroni's test; *$p < 0.05$ for *Pemt*$^{+/+}$ *vs Pemt*$^{-/-}$.

Figure 3.9

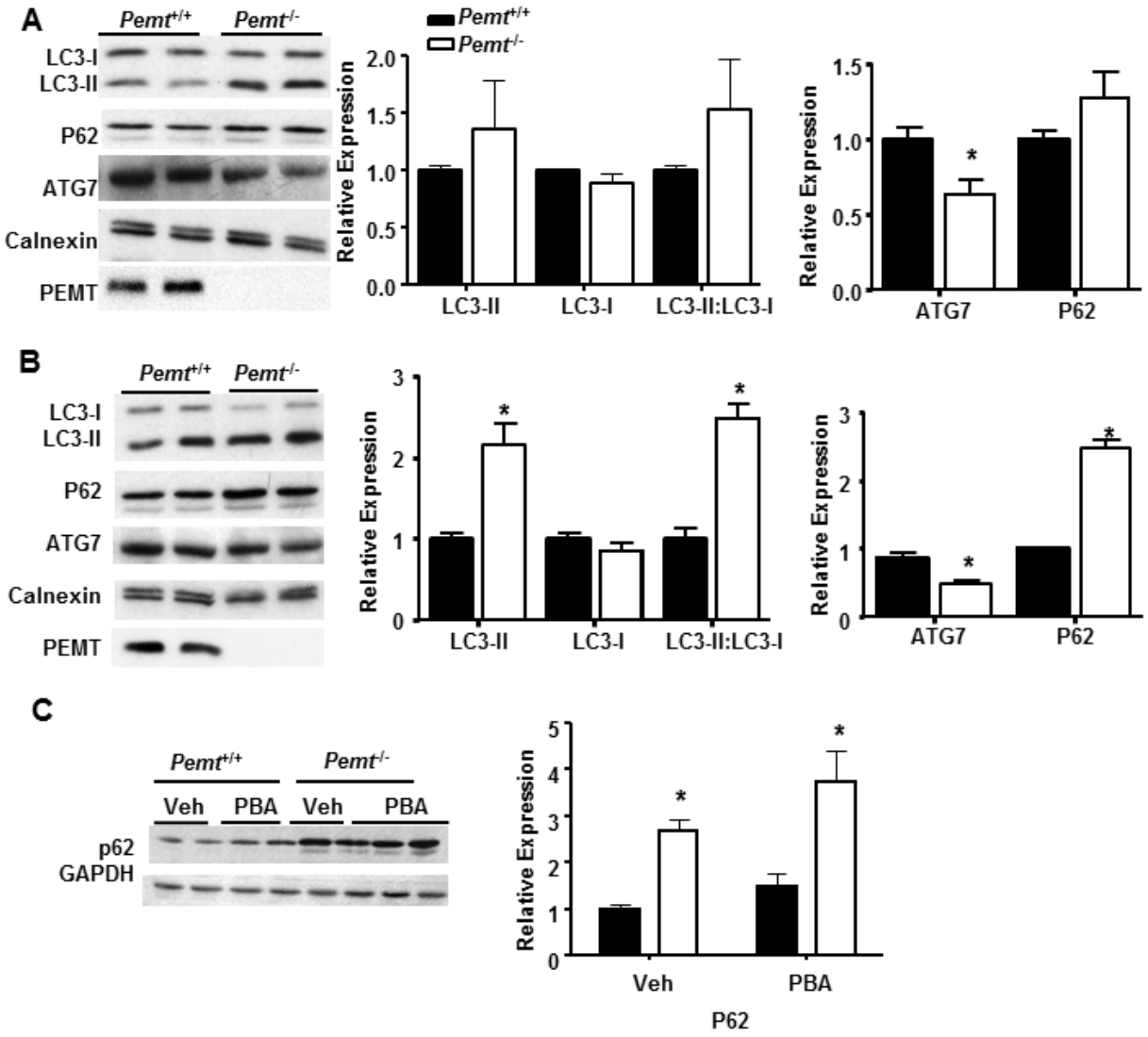
A
Pemt+/+
Pemt-/-
LC3-I
LC3-II
P62
ATG7
Calnexin
PEMT
Relative Expression
LC3-II
LC3-I
LC3-II:LC3-I
ATG7
P62
B
C
Veh
PBA
p62
GAPDH

Figure 3.10 PC/PE ratio in hepatic ER correlates with ER stress according to a hypothetical "U-shaped" curve

An aberrant PC/PE molar ratio, either higher or lower than optimum, leads to ER stress.

Figure 3.10

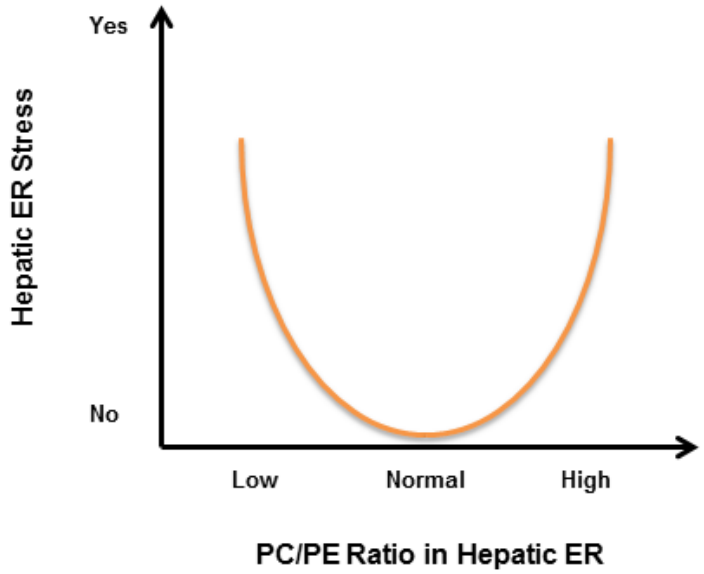
Yes
No
Hepatic ER Stress
Low
Normal
High
PC/PE Ratio in Hepatic ER

3.5 References

1. Moore, J. B. (2010) *Proc Nutr Soc* **69**, 211-220

2. Williams, C. D., Stengel, J., Asike, M. I., Torres, D. M., Shaw, J., Contreras, M., Landt, C. L., and Harrison, S. A. (2011) *Gastroenterology* **140**, 124-131

3. Ogden, C. L., Carroll, M. D., Curtin, L. R., McDowell, M. A., Tabak, C. J., and Flegal, K. M. (2006) *JAMA* **295**, 1549-1555

4. Puri, P., Baillie, R. A., Wiest, M. M., Mirshahi, F., Choudhury, J., Cheung, O., Sargeant, C., Contos, M. J., and Sanyal, A. J. (2007) *Hepatology* **46**, 1081-1090

5. Li, Z., Agellon, L. B., Allen, T. M., Umeda, M., Jewell, L., Mason, A., and Vance, D. E. (2006) *Cell Metab* **3**, 321-331

6. Ling, J., Chaba, T., Zhu, L. F., Jacobs, R. L., and Vance, D. E. (2012) *Hepatology* **55**, 1094-1102

7. Vance, D. E., Li, Z., and Jacobs, R. L. (2007) *J Biol Chem* **282**, 33237-33241

8. DeLong, C. J., Shen, Y. J., Thomas, M. J., and Cui, Z. (1999) *J Biol Chem* **274**, 29683-29688

9. Niebergall, L. J., Jacobs, R. L., Chaba, T., and Vance, D. E. (2011) *Biochim Biophys Acta* **1811**, 1177-1185

10. Noga, A. A., and Vance, D. E. (2003) *J Biol Chem* **278**, 21851-21859

11. Ali, A. T., Hochfeld, W. E., Myburgh, R., and Pepper, M. S. (2013) *Eur J Cell Biol* **92**, 229-236

12. Jacobs, R. L., Zhao, Y., Koonen, D. P., Sletten, T., Su, B., Lingrell, S., Cao, G., Peake, D. A., Kuo, M. S., Proctor, S. D., Kennedy, B. P., Dyck, J. R., and Vance, D. E. (2010) *J Biol Chem* **285**, 22403-22413

13. Tomlinson, E., Fu, L., John, L., Hultgren, B., Huang, X., Renz, M., Stephan, J. P., Tsai, S. P., Powell-Braxton, L., French, D., and Stewart, T. A. (2002) *Endocrinology* **143**, 1741-1747

14. Pagliassotti, M. J. (2012) *Annu Rev Nutr* **32**, 17-33

15. Hummasti, S., and Hotamisligil, G. S. (2010) *Circ Res* **107**, 579-591

16. Fu, S., Watkins, S. M., and Hotamisligil, G. S. (2012) *Cell Metab* **15**, 623-634

17. Hotamisligil, G. S. (2010) *Cell* **140**, 900-917

18. Ozcan, U., Cao, Q., Yilmaz, E., Lee, A. H., Iwakoshi, N. N., Ozdelen, E., Tuncman, G., Gorgun, C., Glimcher, L. H., and Hotamisligil, G. S. (2004) *Science* **306**, 457-461

19. O'Rourke, M. F., Staessen, J. A., Vlachopoulos, C., Duprez, D., and Plante, G. E. (2002) *Am J Hypertens* **15**, 426-444

20. Ron, D., and Walter, P. (2007) *Nat Rev Mol Cell Biol* **8**, 519-529

21. Hu, H. H., Perkins, T. G., Chia, J. M., and Gilsanz, V. (2013) *AJR Am J Roentgenol* **200**, 177-183

22. Harding, H. P., Zhang, Y., and Ron, D. (1999) *Nature* **397**, 271-274

23. Harding, H. P., Zhang, Y., Bertolotti, A., Zeng, H., and Ron, D. (2000) *Mol Cell* **5**, 897-904

24. Ma, Y., Brewer, J. W., Diehl, J. A., and Hendershot, L. M. (2002) *J Mol Biol* **318**, 1351-1365

25. Sidrauski, C., and Walter, P. (1997) *Cell* **90**, 1031-1039

26. Ogata, M., Hino, S., Saito, A., Morikawa, K., Kondo, S., Kanemoto, S., Murakami, T., Taniguchi, M., Tanii, I., Yoshinaga, K., Shiosaka, S., Hammarback, J. A., Urano, F., and Imaizumi, K. (2006) *Mol Cell Biol* **26**, 9220-9231

27. Chen, X., Shen, J., and Prywes, R. (2002) *J Biol Chem* **277**, 13045-13052

28. Cui, Z., Vance, J. E., Chen, M. H., Voelker, D. R., and Vance, D. E. (1993) *J Biol Chem* **268**, 16655-16663

29. Walkey, C. J., Donohue, L. R., Bronson, R., Agellon, L. B., and Vance, D. E. (1997) *Proc Natl Acad Sci U S A* **94**, 12880-12885

30. van der Veen, J. N., Lingrell, S., da Silva, R. P., Jacobs, R. L., and Vance, D. E. (2014) *Diabetes* **63**, 2620-2630

31. Croze, E. M., and Morre, D. J. (1984) *J Cell Physiol* **119**, 46-57

32. Vance, J. E., and Vance, D. E. (1988) *J Biol Chem* **263**, 5898-5909

33. Jacobs, R. L., Lingrell, S., Zhao, Y., Francis, G. A., and Vance, D. E. (2008) *J Biol Chem* **283**, 2147-2155

34. Brunt, E. M., Janney, C. G., Di Bisceglie, A. M., Neuschwander-Tetri, B. A., and Bacon, B. R. (1999) *Am J Gastroenterol* **94**, 2467-2474

35. Fu, S., Yang, L., Li, P., Hofmann, O., Dicker, L., Hide, W., Lin, X., Watkins, S. M., Ivanov, A. R., and Hotamisligil, G. S. (2011) *Nature* **473**, 528-531

36. Pfaffenbach, K. T., Gentile, C. L., Nivala, A. M., Wang, D., Wei, Y., and Pagliassotti, M. J. (2010) *Am J Physiol Endocrinol Metab* **298**, E1027-1035

37. Ozcan, U., Yilmaz, E., Ozcan, L., Furuhashi, M., Vaillancourt, E., Smith, R. O., Gorgun, C. Z., and Hotamisligil, G. S. (2006) *Science* **313**, 1137-1140

38. Singh, R., Kaushik, S., Wang, Y., Xiang, Y., Novak, I., Komatsu, M., Tanaka, K., Cuervo, A. M., and Czaja, M. J. (2009) *Nature* **458**, 1131-1135

39. Tilg, H., and Hotamisligil, G. S. (2006) *Gastroenterology* **131**, 934-945

40. Borradaile, N. M., Han, X., Harp, J. D., Gale, S. E., Ory, D. S., and Schaffer, J. E. (2006) *J Lipid Res* **47**, 2726-2737

41. Li, Y., Ge, M., Ciani, L., Kuriakose, G., Westover, E. J., Dura, M., Covey, D. F., Freed, J. H., Maxfield, F. R., Lytton, J., and Tabas, I. (2004) *J Biol Chem* **279**, 37030-37039

42. Kim, S. J., Zhang, Z., Saha, A., Sarkar, C., Zhao, Z., Xu, Y., and Mukherjee, A. B. (2010) *Neurosci Lett* **479**, 292-296

43. Wu, G., Zhang, L., Li, T., Lopaschuk, G., Vance, D. E., and Jacobs, R. L. (2012) *J Obes* **2012**, 319172

44. Arruda, A. P., Pers, B. M., Parlakgul, G., Guney, E., Inouye, K., and Hotamisligil, G. S. (2014) *Nat Med* **20**, 1427-1435

45. Tubbs, E., Theurey, P., Vial, G., Bendridi, N., Bravard, A., Chauvin, M. A., Ji-Cao, J., Zoulim, F., Bartosch, B., Ovize, M., Vidal, H., and Rieusset, J. (2014) *Diabetes* **63**, 3279-3294

46. Kanuri, G., and Bergheim, I. (2013) *Int J Mol Sci* **14**, 11963-11980

47. Gao, X., van der Veen, J. N., Zhu, L., Chaba, T., Ordonez, M., Lingrell, S., Koonen, D. P., Dyck, J. R., Gomez-Munoz, A., Vance, D. E., and Jacobs, R. L. (2015) *J Hepatol* **62**, 913-920

48. Cohen, F. E., and Kelly, J. W. (2003) *Nature* **426**, 905-909

49. Vilatoba, M., Eckstein, C., Bilbao, G., Smyth, C. A., Jenkins, S., Thompson, J. A., Eckhoff, D. E., and Contreras, J. L. (2005) *Surgery* **138**, 342-351

50. Ota, T., Gayet, C., and Ginsberg, H. N. (2008) *J Clin Invest* **118**, 316-332

51. Soon, R. K., Jr., Yan, J. S., Grenert, J. P., and Maher, J. J. (2010) *Gastroenterology* **139**, 1730-1739, 1739 e1731

52. Gonzalez-Rodriguez, A., Mayoral, R., Agra, N., Valdecantos, M. P., Pardo, V., Miquilena-Colina, M. E., Vargas-Castrillon, J., Lo Iacono, O., Corazzari, M., Fimia, G. M., Piacentini, M., Muntane, J., Bosca, L., Garcia-Monzon, C., Martin-Sanz, P., and Valverde, A. M. (2014) *Cell Death Dis* **5**, e1179

53. Henkel, A. S., Dewey, A. M., Anderson, K. A., Olivares, S., and Green, R. M. (2012) *Am J Physiol Gastrointest Liver Physiol* **303**, G54-59

Chapter 4

Decreased lipogenesis in white adipose tissue contributes to the resistance to high fat diet-induced obesity in phosphatidylethanolamine *N*-methyltransferase deficient mice

4.1 Introduction

Phosphatidylethanolamine *N*-methyltransferase (PEMT) is a small integral membrane protein (~22 kDa) that catalyzes the production of phosphatidylcholine (PC) via three sequential methylations of phosphatidylethanolamine (PE) using *S*-adenosylmethionine as a methyl donor (1-3). PEMT is enriched in the liver and contributes ~30% of hepatic PC biosynthesis, while the remaining 70% of hepatic PC is synthesized via the CDP-choline pathway (4,5). Hepatic PC is required to maintain membrane integrity (6) and normal very low density lipoprotein secretion (7-9). In mice, inhibition of either the CDP-choline pathway in the liver by liver-specific deletion of CTP:phosphocholine cytidylyltransferase (LCT) α, the rate limiting enzyme in the CDP-choline pathway, or the PEMT pathway results in steatosis (10). The reduction of hepatic PC and the decreased PC/PE ratio lead to steatosis (6,11). Despite contributing to a relatively small portion of hepatic PC synthesis, the importance of the PEMT pathway has been highlighted by feeding *Pemt*$^{-/-}$ mice a choline-deficient diet (6) or a HF diet (12). The choline-deficient diet limits the substrate availability for the CDP-choline pathway. On this diet, *Pemt*$^{-/-}$ mice develop severe liver failure and typically die in five days (6,13,14). When fed the HF diet for 10 weeks, *Pemt*$^{-/-}$ mice develop severe non-alcoholic steatohepatitis, but these mice are resistant to diet induced obesity (DIO) and insulin resistance (12). In contrast to *Pemt*$^{-/-}$ mice, *LCTα*$^{-/-}$ mice are not protected from DIO (12), although they also develop steatohepatitis (10-12). Thus, the resistance to DIO in *Pemt*$^{-/-}$ mice does not appear to rely on decreased very low density lipoprotein secretion, which is present in both *Pemt*$^{-/-}$ and *LCTα*$^{-/-}$ mice (7,8), and the potential mechanisms remain to be explored.

Other than in the liver, PEMT is also present in mature 3T3-L1 adipocytes and mouse white adipose tissue (WAT) (15,16). During 3T3-L1 differentiation, mRNA levels of *PEMT*, along with those of adipocyte differentiation markers such as peroxisome proliferator-activated receptor (PPAR)γ and fatty acid binding protein 4 (FABP4), are induced (15). PEMT protein expression and enzyme activity, both of which are absent in the 3T3-L1 fibroblast, are induced after 5 days of differentiation (16). PC is required for lipid droplet expansion (16-18), and the lack of PC may affect lipid droplet morphology by preventing lipid droplet coalescence (19,20). On the other hand, a relative increase in the amount of PE on the surface of lipid droplet may directly induce lipid droplet fusion (21). During 3T3-L1 differentiation, levels of both PC and PE are greatly increased (16). However, a reduced PC/PE ratio is concomitant with lipid droplet formation during cell differentiation (16). Attenuation of PEMT in 3T3-L1 adipocytes increases basal triacylglycerol (22) lipolysis (16). Thus, a role for PE in lipid droplet formation and stability has been proposed (16).

Although the presence of PEMT in WAT has been recently reported (16), it remains unclear whether WAT contributes to the resistance to DIO in *Pemt*$^{-/-}$ mice. To address this topic, we fed *Pemt*$^{-/-}$ and *Pemt*$^{+/+}$ mice the HF diet for 2 weeks, as both *Pemt*$^{+/+}$ and *Pemt*$^{-/-}$ mice showed a slight but significant weight gain after fed one week of HF diet (data not shown). We compared adipocyte differentiation, adipogenesis and lipolysis in gonadal WAT. We also examined endocrine function of WAT by comparing the tissue levels of cytokines and chemokines from mice fed the HF diet for 2 weeks and mice fed the HF diet for 10 weeks. Our data suggest that the capability for

differentiation and lipolysis in WAT is unaffected in *Pemt*$^{-/-}$ mice, while decreased lipogenesis contributes to the resistance to DIO in these mice.

4.2 Materials and methods

4.2.1 Animal handling and diets

All procedures were approved by the University of Alberta's Institutional Animal Care Committee in accordance with guidelines of the Canadian Council on Animal Care. Male C57Bl/6 *Pemt*$^{+/+}$ and *Pemt*$^{-/-}$ (backcrossed >7 generations) mice were housed with free access to water and standard chow diet (LabDiet, #5001). 8-9 weeks old *Pemt*$^{+/+}$ and *Pemt*$^{-/-}$ mice were fed the HF diet (Bio-Serv, #F3282) for 2 or 10 weeks. Tissues were collected in the morning (9:00-11:00 a.m.) from mice fasted for 12 h or without fasting. Blood was collected by cardiac puncture. Tissues were either used immediately for fatty acid incorporation and lipolysis studies, or stored at -80 °C until analysis.

4.2.2 Analytical procedures

Plasma triacylglycerol (22) levels and non-esterified fatty acids (NEFA) were determined using commercially available kits according to the manufacturer's protocols (Roche Diagnostics and Wako Chemicals GmbH, USA). Tissue levels of cytokines and chemokines were quantified using ELISA kits from eBioscience or Preprotech. Protein concentrations were determined by the Bradford assay (Bio-Rad) using bovine serum albumin as standard.

4.2.3 Mass spectrometric analysis of PC and PE

WAT homogenates (100 μg protein) from both *Pemt*$^{+/+}$ and *Pemt*$^{-/-}$ mice were used for lipid extraction (23). Internal phospholipid standards were added to the homogenates for quantification of the lipid species. The lipids were quantified using liquid chromatography–mass spectrometry (LC–MS) (24). The acyl residues of the lipid species were determined using fragmentation analysis (25). This analysis was performed by Dr. Martin Hermansson (University of Alberta).

4.2.4 PC synthesis

WAT explants were freshly dissected from fasted mice fed the HF diet for 2 weeks. The explants were then sliced into small pieces (~40 mg/piece, on ice) and incubated for 4 h in DMEM containing 1% fatty acid-free bovine serum albumin with 5 μCi/ml [^{3}H]-oleic acid and 200 μM oleic acid (Sigma). After 4 h of incubation, WAT was extensively washed with cold-PBS for three times, and then homogenized. Lipids were extracted from WAT homogenates. Phospholipids were separated by thin-layer chromatography in chloroform:methanol:acetic acid:water (25:15:4:2, v/v). Bands corresponding to PC were scraped and radioactivity was determined a scintillation counter (PerkinElmer).

4.2.5 Immunoblotting

Tissues were homogenized in buffer (25 mM Tris–HCl, 500 mM sucrose, 1 mM EDTA, 1 mM dithiothreitol, and 0.1 mM phenylmethylsulfonyl fluoride, pH 7.4) with addition of protease inhibitor cocktail (Sigma #P8340) and phosphatase inhibitor cocktail 3 (Sigma #P0044), followed by sonication for 10 sec. Twenty micrograms of protein were heated for 10 min at 95°–100°C in sample buffer (125 mM Tris-HCl, 25% glycerol, 2% SDS, 0.25% 2-mercaptoethanol, 0.025% bromophenol blue, pH 6.8) and electrophoresed on a SDS-polyacrylamide gel. Proteins were transferred to a

polyvinylidene fluoride membrane and the membrane was then probed with primary antibodies against FABP4 (1:1000 dilution, Cell signaling #2120), PPARγ (1:1000 dilution, Cell signaling #24443), CCAAT/enhancer-binding protein β (C/EBPβ, 1:500 dilution, Santa Cruz sc150), total acetyl-CoA carboxylase (ACC, 1:1000 dilution, Cell signaling #3662), phospho-ACC (Ser79, 1:1000 dilution, Cell signaling #3661), and fatty acid synthase (FAS, 1:1000 dilution, Cell signaling #3189), total hormone-sensitive lipase (HSL, 1:1000 dilution, Cell signaling #4107), phospho-HSL (Ser660, 1:1000 dilution, Cell signaling #4126), adipose triglyceride lipase (ATGL, 1:1000 dilution, Cell signaling #2138), triacylglycerol hydrolase (TGH, gift from Dr. Richard Lehner, University of Alberta, 1:1000 dilution) and glyceraldehyde 3-phosphate dehydrogenase (GAPDH, 1:12,000 dilution, Abcam #ab8245). The immunoreactive bands were visualized by enhanced chemiluminescence system (Amersham Biosciences) according to the manufacturer's instructions.

4.2.6 Real-time quantitative PCR

Total RNA was isolated from snap-frozen liver tissue using TRIzol reagent (Invitrogen). Total RNA was treated with DNase I (Invitrogen), then reverse-transcribed using oligo(dT)12–18 primers and Superscript II reverse transcriptase (Invitrogen). Real-time quantitative PCR was performed using a Rotor-Gene 3000 instrument (Montreal Biotech). Data analyses were performed using the Rotor-Gene 6.0.19 program (Montreal Biotech). mRNA levels were normalized to β-Actin mRNA using a standard curve. Primer sequences are listed in table 4.1.

4.2.7 Histology

A portion of the gonadal WAT was fixed in 10% buffered formalin and subjected to hematoxylin and eosin staining as described in section 2.2.4. The size of individual adipocytes was quantified using ImageJ software from the National Institutes of Health.

4.2.8 *De novo* lipogenesis

Pemt$^{+/+}$ and *Pemt*$^{-/-}$ mice were fed the HF diet for 2 weeks. Mice were fasted for 2 h and *de novo* TG synthesis was estimated by i.p. injection of these mice with 25 µCi [^{14}C]acetate (4.175 nmol) in 250 µM cold sodium acetate in saline (total volume of 200 µl). WAT was collected 2 h after injection. Lipids were extracted from WAT homogenates (1 mg of protein in 1 ml of PBS) with 4 ml of chloroform/methanol (2/1, v/v) as described in section 2.2.3. Neutral lipids were separated by thin-layer chromatography in hexane:diisopropylether:acetic acid (65:35:2, v/v) and visualized by iodine vapor. Bands corresponding to TG were scraped and radioactivity was determined by a scintillation counter.

4.2.9 Fatty acid oxidation

The rate of WAT fatty acid oxidation was determined as described before with minor modification (26). Freshly isolated gonadal WAT was gently homogenized in ice-cold buffer (25 mM Tris-HCl, 500 mM sucrose, 1 mM EDTA, pH 7.4) followed by sonication for 10 sec. After centrifugation at 500 ×*g* for 10 min at 4°C, supernatant was collected and protein concentration was determined as described earlier. The rate of ([1-^{14}C]palmitate oxidation was determined by measuring the amount of $^{14}CO_2$ released (complete oxidation) and the amount of ^{14}C labeled acid-soluble metabolites (incomplete oxidation) over 1 h of incubation. Briefly, 300-500 µg protein homogenate (in volume of 200 µl) was preincubated with the reaction mixture at 37°C for 5 min in a

25 ml glass vial. The glass vial was fitted with a center Eppendorf tube containing Whatman filter paper and was then capped with a rubber stopper. The final concentrations of assay mixture were 115 mM NaCl, 2.6 mM KCl, 10 mM Tris-HCl (pH=7.4), 1.2 mM KH_2PO4, 10 mM $NaHCO_3$, 0.2 mM EDTA, 0.3% (w/v) fatty acid-free BSA, 2 mM L-carnitine, 5 mM ATP, 0.5 mM malate, 0.1 mM coenzyme A. The reaction was initiated by injecting the substrate, BSA-conjugated 0.2 mM palmitate (with molar ratio 6:1 for palmitate:BSA) containing 0.5 μCi/ml [1-^{14}C]-palmitate through the rubber stopper. After 60 min of incubation at 37°C, 300 μl of 3 M percholoric acid was injected to stop the reaction, followed by an injection of 150 μl of 1 M NaOH to the filter paper to capture the released CO_2. The vials were left at room temperature for 2 h to capture the released CO_2. The radioactivity of CO_2 captured by the filter papers and the radioactivity in acid-soluble metabolites (the supernatants of the assay mixture) were then measured by a scintillation counter.

4.2.10 TG lipolysis

To measure the capability for TG lipolysis, gonadal WAT explants were freshly dissected from fasted mice fed the HF diet for 2 weeks. The explants were then sliced into small pieces (~20 mg/piece, on ice) and cultured for up to 3 h in DMEM containing 4% fatty acid-free bovine serum albumin with or without addition of 20 μM isoproterenol bitartrate (Sigma). After 1, 2 and 3 h of incubation, the culture medium was collected and the released NEFA and glycerol were determined using the HR Series NEFA-$HR_{(2)}$ kit (Wako diagnostics) and the Serum Triglyceride Determination Kit (Roche Diagnostics, USA), respectively.

4.2.11 Statistical analysis

Data are presented as mean values ± standard error of the mean (27). For all comparisons, an unpaired two-tailed Student's *t*-test was employed. $P < 0.05$ was considered significant. Unless otherwise indicated, six to eight animals were used per experimental group.

4.3 Results

4.3.1 WAT mass is reduced in Pemt$^{-/-}$ mice after 2 weeks of HF diet feeding

Pemt$^{-/-}$ mice are protected from DIO (12). After 2 weeks of HF diet, *Pemt*$^{-/-}$ mice showed less body weight gain (Figure 4.1A) and reduced WAT mass than *Pemt*$^{+/+}$ mice (Figure 4.1B). However, at this stage, *Pemt*$^{-/-}$ mice already developed hepatomegaly and fatty liver (Figure 4.1C&D) as reported before (11). Plasma TG and NEFA were also lower in *Pemt*$^{-/-}$ mice compared to *Pemt*$^{+/+}$ mice (Figure 4.1E&F), which was similar to our previous observations in mice fed the HF diet for 10 weeks (12).

When mice were fed chow diet, there was no difference in PC and PE mass or the ratio of PC/PE in WAT between genotypes (Figure 4.2A&B). We also quantified the PC and PE molecular species by tandem mass spectrometry. As we have seen before in the liver (12), the amounts of long chain, polyunsaturated PC species (16:0/18:2, 18:0/18:2, 18:0/18:3) in WAT were slightly but significantly decreased in *Pemt*$^{-/-}$ mice versus *Pemt*$^{+/+}$ mice (Figure 4.2C). In both genotypes, the two most abundant PC species were 16:0/18:2 and 18:0/18:2, and together they constituted ~50% of total PC species. There was no difference among other PC species. In addition, no difference was present in the amounts of PE species between *Pemt*$^{+/+}$ mice and *Pemt*$^{-/-}$ mice

(Figure 4.2D). To investigate the synthesis of PC, we labeled WAT explants from *Pemt*$^{+/+}$ and *Pemt*$^{-/-}$ mice fed the HF diet with [^{3}H]-oleic acid. *Pemt*$^{-/-}$ mice had less [^{3}H]-oleic acid incorporated into PC than *Pemt*$^{+/+}$ mice (Figure 4.2E). Together, *Pemt*$^{-/-}$ mice have similar amounts of PC and PE in WAT as *Pemt*$^{+/+}$ mice, although the incorporation of [^{3}H]-oleic acid into PC is reduced compared to *Pemt*$^{+/+}$ mice.

4.3.2 PEMT deficiency does not impair adipocyte differentiation

Histological analysis revealed that WAT from *Pemt*$^{-/-}$ mice fed the HF diet for 2 weeks had smaller adipocytes than that from *Pemt*$^{+/+}$ mice (Figure 4.3A&B), which is consistent with our previous report in mice fed the HF diet for 10 weeks (12). PEMT expression is upregulated in 3T3-L1 adipocytes during cell differentiation (15,16). To evaluate whether deletion of *PEMT* in mice results in impaired adipocyte differentiation in WAT, we examined the protein levels of the adipose differentiation markers FABP4, PPARγ and C/EBPβ. Protein levels of these markers were not different between *Pemt*$^{-/-}$ and *Pemt*$^{+/+}$ mice fed either chow (Figure 4.3C) or the HF diet for 2 weeks (Figure 4.3D). In addition, the levels of mRNA for *PPARγ* and its downstream genes cluster of differentiation (CD)36 and lipoprotein lipase in *Pemt*$^{-/-}$ mice were comparable to that in *Pemt*$^{+/+}$ mice (Figure 4.3E). Hence, PEMT deficiency in mice does not impair adipocyte differentiation in WAT.

4.3.3 PEMT deficiency and lipogenesis in WAT

To explore further the explanation for lower WAT mass in *Pemt*$^{-/-}$ mice after 2 weeks of HF diet, we first assayed protein expression of enzymes involved in *de novo* lipogenesis (DNL) by immunoblotting ACC and FAS, two key enzymes in *de novo* fatty acid synthesis. While the expression of FAS in *Pemt*$^{-/-}$ mice was not different from that

in *Pemt*$^{+/+}$ mice (Figure 4.4A&B), total-ACC was significantly lower in *Pemt*$^{-/-}$ mice compared to *Pemt*$^{+/+}$ mice (Figure 4.4A&B). The level of phospho-ACC (Ser79), an inactive form of ACC, was not altered by the genotype, and this led to a higher ratio of phospho-ACC to total ACC in *Pemt*$^{-/-}$ mice than *Pemt*$^{+/+}$ mice (Figure 4.4B), indicating a down-regulation of ACC enzyme activity. Levels of mRNAs encoding FAS, ACC and sterol regulatory element-binding protein (SREBP)-1c, a key transcriptional regulator for lipogenesis, in *Pemt*$^{-/-}$ mice were indistinguishable from those in *Pemt*$^{+/+}$ mice (Figure 4.4C). Except for a slight increase in the expression of ATP citrate lyase (ACLY) in *Pemt*$^{-/-}$ mice, expression of other lipogenenic genes, including acyl CoA:monoacylglycerol acyltransferase (MGAT)-1, glycerol-3-phosphate acyltransferase (GPAT)-1, acyl CoA:diacylglycerol acyltransferase (DGAT)-1, DGAT-2 and stearoyl-CoA desaturase (SCD)-1, was not different between genotypes (Figure 4.4C). Most importantly, we estimated *in vivo* lipogenesis by i.p. injecting mice with [^{14}C]acetate. *Pemt*$^{-/-}$ mice incorporated significantly less [^{14}C]acetate into TG than *Pemt*$^{+/+}$ mice in WAT (Figure 4.4D), while plasma [^{14}C]TG was too low to detect by scintillation counter. Thus, impaired DNL may contribute to the lack of WAT hypertrophy in HF-fed *Pemt*$^{-/-}$ mice.

4.3.4 PEMT deficiency does not affect TG mobilization from WAT

In humans, plasma NEFA contribute over 50% of hepatic TG accumulation compared with only ~15% contribution from the diet, and the remaining from DNL (28). Plasma NEFA are mainly derived from WAT. To examine whether lower WAT mass in HF-fed *Pemt*$^{-/-}$ mice is caused by enhanced lipolysis, the lipolytic capability of WAT was first examined *ex vivo*. Under basal conditions, the release of glycerol and NEFA from

WAT explants was comparable between *Pemt*$^{+/+}$ and *Pemt*$^{-/-}$ mice (Figure 4.5A). When incubated with isoproterenol, which stimulates lipolysis, the production of glycerol and fatty acids from WAT explants from *Pemt*$^{+/+}$ mice was doubled after 3 h of incubation (Figure 4.5B). Compared with *Pemt*$^{+/+}$ mice, *Pemt*$^{-/-}$ mice showed the same rate for the release of glycerol (Figure 4.5B). But after 3 h of culture, explants from *Pemt*$^{-/-}$ mice released 50% fewer fatty acids into the culture medium than from *Pemt*$^{+/+}$ mice (Figure 4.5B). The lower amounts of fatty acids released from WAT in *Pemt*$^{-/-}$ mice suggested a higher rate of fatty acid re-esterification. Overall, both basal and stimulated lipolytic capabilities of WAT explants are not affected by PEMT deficiency.

We also determined the expression of lipolytic enzymes by immunoblotting. In mice, ATGL and HSL are two major enzymes for TG hydrolysis in WAT, responsible for more than 95% TG hydrolase activity (29,30). After 2 weeks of HF diet, the expression of ATGL and phospho-HSL (Ser660, activates HSL enzyme activity) in *Pemt*$^{-/-}$ mice was indistinguishable from that in *Pemt*$^{+/+}$ mice (Figure 4.5C&D). The total-HSL protein in *Pemt*$^{-/-}$ mice was less than half of that in *Pemt*$^{+/+}$ mice, which led to a trend toward an increase in the ratio of phospho-HSL to total-HSL in *Pemt*$^{-/-}$ mice (Figure 4.5D), suggesting the presence of an activation of HSL enzyme activity in these mice. However, after feeding the HF diet for 10 weeks, the protein levels of phospho-HSL, total-HSL and ATGL were significantly lower in *Pemt*$^{-/-}$ mice than those in *Pemt*$^{+/+}$ mice (Figure 4.6). Moreover, the protein level of TGH, a TG hydrolase abundantly expressed in the liver as well as adipose tissue (31-33), was higher in *Pemt*$^{-/-}$ mice than that in *Pemt*$^{+/+}$ mice when mice were fed the HF diet for either 2 or 10 weeks (Figure 4.5D and Figure 4.6). The differences in the expression of phospho-HSL and ATGL in *Pemt*$^{-/-}$

mice after 10 weeks of HF diet could be explained by an increased lipolysis in *Pemt*$^{+/+}$ mice caused by WAT hypertrophy, which did not occur in *Pemt*$^{-/-}$ mice. Together, the lack of significant difference in the lipolytic enzyme expression in *Pemt*$^{-/-}$ mice versus *Pemt*$^{+/+}$ mice after 2 weeks of HF diet suggests that the reduced WAT mass in *Pemt*$^{-/-}$ mice is not due to increased lipolysis.

An increased energy catabolism in WAT is unlikely to account for the resistance to the DIO in *Pemt*$^{-/-}$ mice. We attempted to determine the rate of fatty acid oxidation *ex vivo* using WAT explants (26). As expected, the fatty acid oxidation rate in WAT explants was significantly lower than that in brown adipose tissue and liver (data not shown). Although complete fatty acid oxidation was too low to be quantified in WAT explants, we determined that incomplete fatty acid oxidation rate (~30 nmol/mg protein/min) in *Pemt*$^{-/-}$ mice was not distinct from that in *Pemt*$^{+/+}$ mice (Figure 4.5E).

4.3.5 PEMT deficiency does not affect endocrine function of WAT

Beyond being an energy storage tissue, WAT is also an important endocrine organ for secretion of cytokines and chemokines (34). After 2 weeks of HF diet, *Pemt*$^{-/-}$ mice had comparable levels of the tissue cytokines, including leptin, interleukin (IL)-1, IL-4, tumor necrosis factor (TNF)α and IL-10, and chemokine RANTES in WAT, compared with *Pemt*$^{+/+}$ mice (Figure 4.7A). However in the liver, *Pemt*$^{-/-}$ mice already showed higher levels of inflammatory cytokine TNFα, anti-inflammatory cytokine IL-10, and chemokine RANTES than *Pemt*$^{+/+}$ mice (Figure 4.7B). There was no significant difference in the levels of IL-1, IL-4 or leptin in the liver between *Pemt*$^{+/+}$ and *Pemt*$^{-/-}$ mice (Figure 4.7B).

In contrast to the mice fed the HF diet for 2 weeks, levels of cytokines and chemokines in WAT were strikingly different in mice fed the HF diet for 10 weeks. Compared to mice fed the HF diet for 2 weeks, the leptin level was greatly increased in *Pemt*$^{+/+}$ mice after being fed the HF diet for 10 weeks (Figure 4.7A and Figure 4.8). In contrast, the leptin level in *Pemt*$^{-/-}$ mice fed the HF diet for 10 weeks was not different from *Pemt*$^{-/-}$ mice fed the HF diet for 2 weeks (Figure 4.7A and Figure 4.8). *Pemt*$^{-/-}$ mice fed the HF diet for 10 weeks also displayed lower levels of inflammatory cytokine TNFα and chemokines, MCP-1 and RANTES, but significantly higher levels of anti-inflammatory cytokine IL-10 than *Pemt*$^{+/+}$ mice (Figure 4.8).

4.4 Discussion

PEMT is present in WAT and induced by the HF diet (16), although the enzyme activity is insignificant compared with that in the liver (<1%). When fed chow diet, PEMT deficiency in mice did not change the mass of PC and PE in WAT (Figure 4.2). Beyond being a storage tissue, WAT also plays an important role in regulating whole body energy metabolism by secreting adipokines such as adiponectin and leptin (34). After 10 weeks of HF diet, plasma levels of adiponection and leptin are 20 and 85% reduced, respectively, in *Pemt*$^{-/-}$ as compared to *Pemt*$^{+/+}$ mice (12). Thus, the question whether or not WAT contributes to the resistance to DIO in *Pemt*$^{-/-}$ mice remains. We fed *Pemt*$^{+/+}$ and *Pemt*$^{-/-}$ mice the HF diet for 2 weeks to investigate the contribution of WAT to the resistance to DIO in *Pemt*$^{-/-}$ mice. Both *Pemt*$^{+/+}$ and *Pemt*$^{-/-}$ mice showed a slight but significant weight gain after fed one week of HF diet (data not shown). While *Pemt*$^{+/+}$ mice continued gaining weight throughout the 10 weeks of HF diet feeding, *Pemt*$^{-/-}$ mice

failed to gain further weight over the rest of feeding period (data not shown). Thus, 2 weeks of HF diet feeding is the best choice to clarify the importance of PEMT in WAT to the resistance to DIO and development of HF-induced steatohepatitis. Here we provide strong evidence supporting that a reduced lipogenesis in WAT, rather than an impaired differentiation or an increased lipolysis, contributes at least partially to the lack of WAT hypertrophy in HF-fed *Pemt*$^{-/-}$ mice.

4.4.1 Decreased lipogenesis, rather than altered differentiation, accounts for the lack of WAT hypertrophy in HF-fed *Pemt*$^{-/-}$ mice

PEMT expression is greatly induced during 3T3-L1 cell differentiation (15,16). Thus, attenuation of PEMT could hinder adipocyte differentiation and lipogenesis, resulting in lack of adipose hypertrophy in HF-fed *Pemt*$^{-/-}$ mice. However, this is unlikely to be the case, since the protein levels of adipose differentiation markers, FABP4, PPARγ and C/EBPβ, were not different between *Pemt*$^{+/+}$ and *Pemt*$^{-/-}$ mice fed either chow diet or the HF diet (Figure 4.3).

PPARγ belongs to the nuclear hormone receptor family and is highly expressed in adipose tissues (35). Upon binding to its ligands such as fatty acids and its obligate receptor retinoid X receptor, PPARγ is one of the master regulators for gene expression in adipogenesis, lipid metabolism and glucose homeostasis, thereby regulating whole body energy metabolism and insulin sensitivity (35,36). Thiazolidinediones, drugs used for treatment of type 2 diabetes, mainly act via PPARγ (37). In our study, the transcriptional levels of PPARγ and downstream genes CD36 and lipoprotein lipase (35) were similar between the two genotypes of mice (Figure 4.3).

Furthermore, the lack of adipose hypertrophy in HF-fed *Pemt*$^{-/-}$ mice could be explained by aberrant adipogenesis. In comparison to *Pemt*$^{+/+}$ mice, a reduction in the expression of ACC in *Pemt*$^{-/-}$ mice suggests that an impaired DNL might take place in these mice. Indeed, the *in vivo* study clearly showed less incorporation from [^{14}C]acetate into TG in WAT of *Pemt*$^{-/-}$ mice than in *Pemt*$^{+/+}$ mice (Figure 4.4D).

4.4.2 Lipolysis in WAT is unaffected

In 3T3-L1 adipocytes, PEMT deficiency results in an increase in basal TG lipolysis (16). Defective lipolysis leads to adipose hypertrophy, while a stimulated lipolysis may result in adipose hypotrophy. We hypothesized that increased lipolysis in WAT from *Pemt*$^{-/-}$ compared to *Pemt*$^{+/+}$ mice releases fatty acids which would then be distributed to other metabolic tissues for energy metabolism in the muscle and/or brown adipose tissue or stored in the liver, resulting in HF-induced steatohepatitis in *Pemt*$^{-/-}$ mice. However, our data show that lipolysis was not increased in WAT of *Pemt*$^{-/-}$ mice. In the *ex vivo* assay, the release of glycerol and fatty acids from WAT explants was comparable between *Pemt*$^{+/+}$ and *Pemt*$^{-/-}$ mice under basal condition (Figure 4.5A), and isoproterenol stimulated lipolysis to a similar extent in *Pemt*$^{+/+}$ and *Pemt*$^{-/-}$ mice (Figure 4.5B).

ATGL and HSL are two major enzymes for TG hydrolysis in mouse WAT, accounting for over 95% TG hydrolase activity (29,30). Absence of ATGL impairs TG mobilization from WAT, greatly decreases plasma fatty acids and causes massive TG accumulation in the muscle, heart and WAT (38). Although HSL deficient mice are not obese or overweight, they have diacylglycerol accumulation in various tissues (39-41). Moreover, the HSL enzyme activity is regulated by a complicated protein

phosphorylation mechanism (30). In the current study, the expression of ATGL and phospho-HSL (Ser660) in *Pemt*$^{-/-}$ mice was indistinguishable from that in *Pemt*$^{+/+}$ mice when mice fed the HF diet for 2 weeks (Figure 4.5C&D). However, after 10 weeks of feeding, the expression of ATGL and phospho-HSL in *Pemt*$^{-/-}$ mice was dramatically lower than in *Pemt*$^{+/+}$ mice (Figure 4.6). This could be a compensatory mechanism to maintain WAT mass in *Pemt*$^{-/-}$ mice, or it could be due to the up-regulation of ATGL and phospho-HSL in *Pemt*$^{+/+}$ mice fed the HF diet for 10 weeks compared with *Pemt*$^{+/+}$ mice fed the HF diet for 2 weeks. Taken together, there is no indication for either an increased lipolysis or impaired lipolysis in WAT from *Pemt*$^{-/-}$ mice and the WAT hypotrophy in *Pemt*$^{-/-}$ mice is unlikely to be caused by a hyperactive lipolysis process.

4.4.3 WAT functions normally as an endocrine organ

Other than being a tissue for energy storage, WAT has also emerged to play an active role in energy metabolism and inflammation by producing adipokines (34). Adipose dysfunction, reflected by impaired mitochondrial function, adipose hypoxia or adipose inflammation, is linked to obesity and its related metabolic syndrome via its primary role in altering its pro-inflammatory adipokine secretion pattern (42). We compared the tissue levels of cytokines (IL-1, IL-4, IL-10 and TNFα) and chemokines (MCP-1 and RANTES) in mice fed the HF diet for 2 weeks or 10 weeks. In contrast to the difference in cytokines and chemokines between *Pemt*$^{+/+}$ and *Pemt*$^{-/-}$ mice after 10 weeks of HF diet feeding (Figure 4.8), the lack of difference in mice fed the HF diet for 2 weeks (Figure 4.7A) suggests that this difference could be caused by aberrant metabolism in both *Pemt*$^{+/+}$ and *Pemt*$^{-/-}$ mice after long-term feeding. Indeed, the HF diet causes around 20 g of body weight gain over 10 weeks of feeding in *Pemt*$^{+/+}$ mice (12),

while *Pemt*$^{-/-}$ mice does not gain weight but develop severe steatohepatitis (11,12). This increment of WAT in *Pemt*$^{+/+}$ mice stimulates the secretion of the satiety hormone leptin. Contrarily in *Pemt*$^{-/-}$ mice after 10 weeks of HF diet, the lack of WAT hypertrophy results in the low level of plasma leptin (12). This lower level of leptin in *Pemt*$^{-/-}$ mice fed the HF diet for 10 weeks leads to a higher food intake than in *Pemt*$^{+/+}$ mice (12). Consistent with our data, the food intake is not different between *Pemt*$^{+/+}$ and *Pemt*$^{-/-}$ mice after fed the HF diet for 10 days (12).

Moreover, alterations of the levels of cytokines and chemokines in the liver from *Pemt*$^{-/-}$ mice fed the HF diet for 2 weeks (Figure 4.7B) is unlikely caused by WAT, since there was no difference in the levels of cytokines and chemokines in WAT at this stage (Figure 4.7A). Additionally, after 10 weeks of the HF diet, *Pemt*$^{-/-}$ mice presented an anti-inflammatory pattern of cytokines and chemokines in WAT with dramatically lower pro-inflammatory cytokine TNFα and chemokine RANTES, but significantly higher anti-inflammatory cytokine IL-10 level than *Pemt*$^{+/+}$ mice (Figure 4.8).

Collectively, the lack of PEMT does not alter adipocyte differentiation, the capability for TG mobilization or the role of adipose as an endocrine organ. Impairment in DNL in WAT contributes at least partially to the protection against obesity in HF-fed *Pemt*$^{-/-}$ mice. However, that the difference of cytokines and chemokines and in the expression of lipolytic enzymes in WAT in *Pemt*$^{-/-}$ mice is seen at 10 weeks but not at 2 weeks suggests that the resistance to DIO phenotype is subsequent to the fatty liver phenotype.

Table 4.1 Primers for real-time quantitative PCR

Abbreviations are: *Acc*, acetyl-CoA carboxylase; *Fas,* fatty acid synthase; *Lpl*, lipoprotein lipase; *Cd*, cluster of differentiation; *Srebp*, sterol regulatory element binding protein; *Ppar*, peroxisome proliferator activated receptor; *Mgat*, acyl CoA:monoacylglycerol acyltransferase; *Gpat*, glycerol-3-phosphate acyltransferase; *Dgat,* acyl CoA:diacylglycerol acyltransferase; *Scd*, stearoyl-CoA desaturase; *Acly,* ATP citrate lyase.

gene	forward primer (5' -> 3')	reverse primer (5' -> 3')
β-Actin	AAG GCC AAC CGT GAA AAG AT	GTG GTA CGA CCA GAG GCA TAC
Acc	GGC GAC TTA CGT TCC TAG TTG	AGG TGT CGA TAA ATG CGG TCC
Fas	TTC CGT CAC TTC CAG TTA GAG	TTC AGT GAG GCG TAG TAG ACA
Lpl	CCT ACT TCA GCT GGC CTG ACT GGT	ACT GCT GAG TCC TTT CCC TTC TGC
Cd36	TGG CTA AAT GAG ACT GGG ACC	ACA TCA CCA CTC CAA TCC CAA G
Pparγ	TTG ACA TCA AGC CCT TTA CCA	GGT TCT ACT TTG ATC GCA CTT T
Srebp-1c	ATG GAT TGC ACA TTT GAA GAC	CTC TCA GGA GAG TTG GCA CC
Mgat-1	GCT ATT TCC TGG CTT TAC ATC G	AAC CCT TTG CGC TGG CGG AT
Gpat-1	CAA CAC CAT CCC CGA CAT C	TTT TTC CGC AGC ATT CTG ATA A
Dgat-1	GGA TCT GAG GTG CCA TCG T	CCA CCA GGA TGC CAT ACT TG
Dgat-2	GGC TAC GTT GGC TGG TAA CTT	TTC AGG GTG ACT GCG TTC TT
Scd-1	GTT GCC AGT TTC TTT CGT G	GGG AAG CCA AGT TTC TAC ACA
Acly	GCC CTG GAA GTG GAG AAG AT	CCG TCC ACA TTC AGG ATA AGA

Figure 4.1 *Pemt*$^{-/-}$ mice fed the HF diet for 2 weeks lack WAT hypertrophy but develop fatty liver

After 2 weeks of HF diet, *Pemt*$^{-/-}$ mice showed less body weight gain (A), less adiposity (B), larger liver (C), higher amounts of hepatic triacylglycerol (25) accumulation (D), but lower levels of plasma TG (E), compared with *Pemt*$^{+/+}$ mice under both fasting and non-fasting states. (F) NEFA (non-esterified fatty acids) in *Pemt*$^{+/+}$ and *Pemt*$^{-/-}$ mice under both fasting and non-fasting states. n=5-6, *p < 0.05 by Student's *t*-test, *Pemt*$^{+/+}$ *vs* *Pemt*$^{-/-}$; and #p < 0.05 by Student *t*-test, non-fasting *vs* fasting within the same genotype.

Figure 4.1

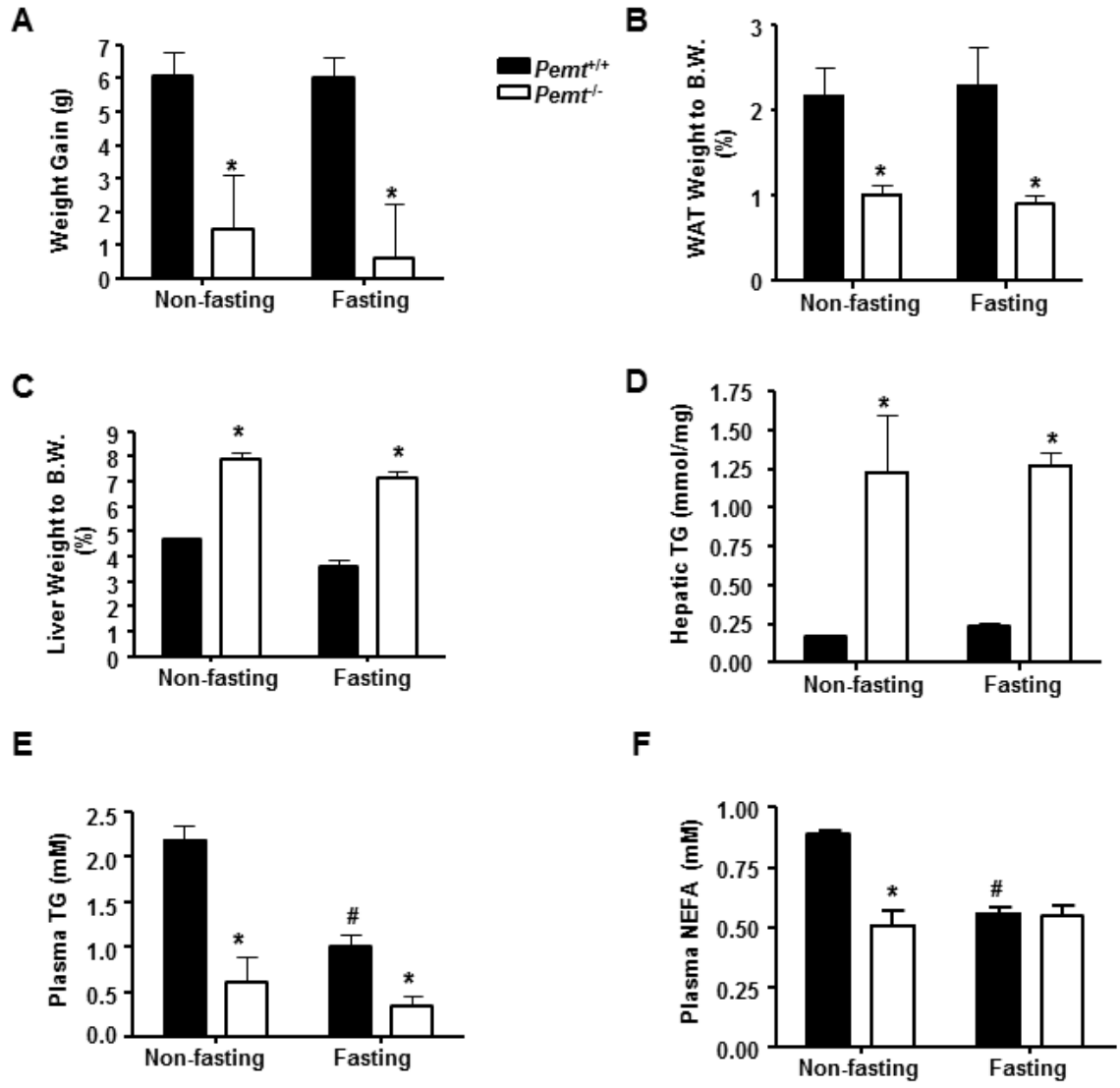
A
Weight Gain (g)
Pemt+/+
Pemt-/-
Non-fasting
Fasting
B
WAT Weight to B.W. (%)
C
Liver Weight to B.W. (%)
D
Hepatic TG (mmol/mg)
E
Plasma TG (mM)
F
Plasma NEFA (mM)

Figure 4.2 PC and PE in WAT in *Pemt*$^{+/+}$ and *Pemt*$^{-/-}$ mice

(394) WAT was collected from 14-16 weeks old male *Pemt*$^{+/+}$ and *Pemt*$^{-/-}$ mice fed chow diet. Phosphatidylcholine (PC) and phosphatidylethanolamine (PE) extracted from WAT were determined by liquid chromatography–mass spectrometry. (A) PC and PE values were expressed as nmol/mg protein. (B) PC/PE ratio. (C) PC species and (D) PE species. (E) The synthesis of PC was determined by incubating WAT explants from *Pemt*$^{+/+}$ and *Pemt*$^{-/-}$ mice fed the HF diet for 2 weeks with [^{3}H]-oleic acid for 4 h. n=5-6, *$p < 0.05$ by Student's *t*-test, *Pemt*$^{+/+}$ *vs Pemt*$^{-/-}$.

Figure 4.2

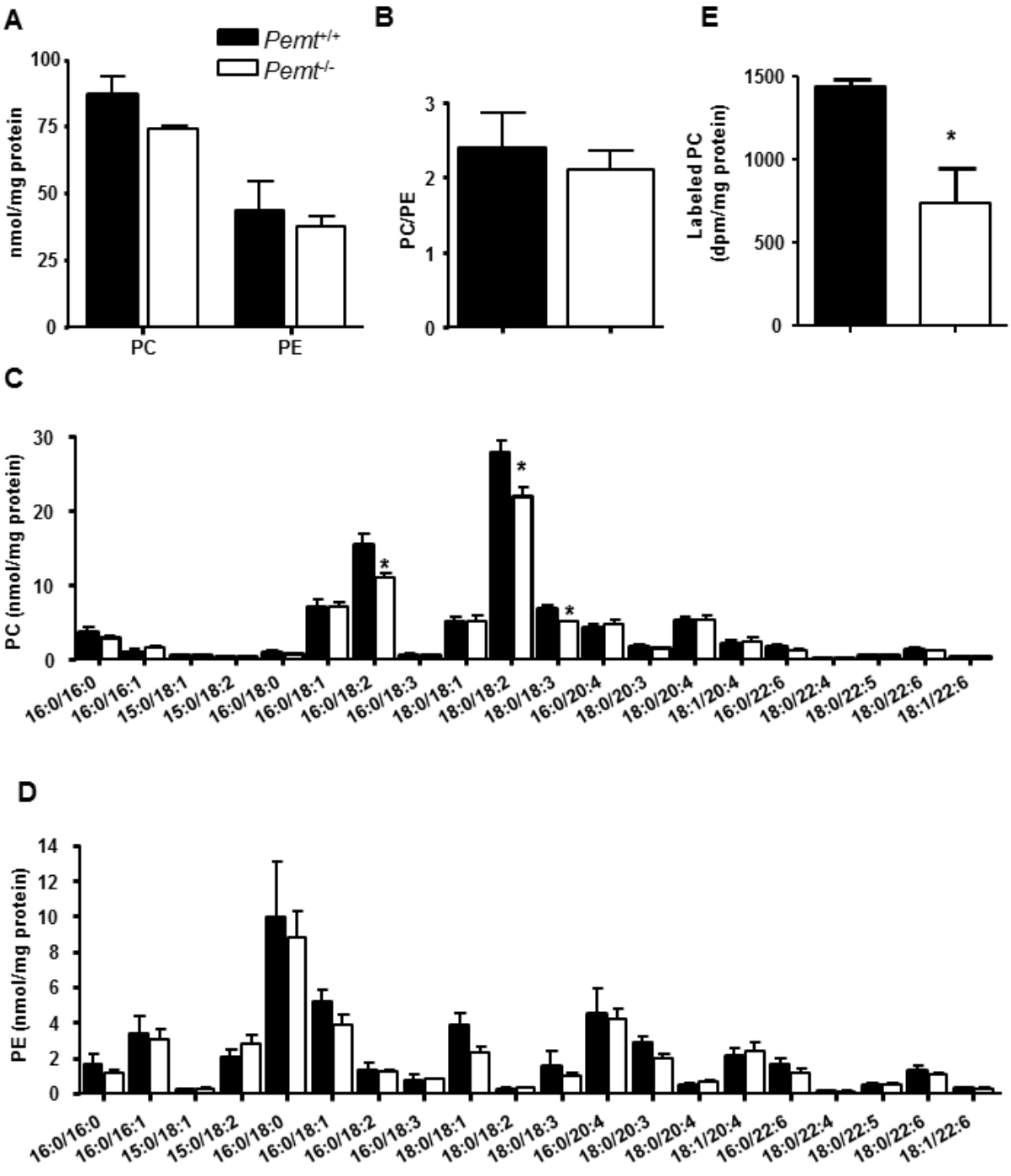
A
Pemt+/+
Pemt-/-
nmol/mg protein
100
75
50
25
0
PC
PE
B
PC/PE
3
2
1
0
E
Labeled PC
(dpm/mg protein)
1500
1000
500
0
*
C
PC (nmol/mg protein)
30
20
10
0
16:0/16:0
16:0/16:1
15:0/18:1
15:0/18:2
16:0/18:0
16:0/18:1
16:0/18:2
16:0/18:3
18:0/18:1
18:0/18:2
18:0/18:3
16:0/20:4
18:0/20:3
18:0/20:4
18:1/20:4
16:0/22:6
18:0/22:4
18:0/22:5
18:0/22:6
18:1/22:6
D
PE (nmol/mg protein)
14
12
10
8
6
4
2
0

Figure 4.3 Expression of differentiation markers in WAT

Pemt$^{+/+}$ and *Pemt*$^{-/-}$ mice were fed the HF diet for 2 weeks. (A) Hematoxylin and eosin staining of gonadal WAT. (B) Adipocyte area quantified by Image J. (C-D) Representative immunoblots for fatty acid binding protein 4 (FABP4), CCAAT/enhancer-binding protein β (C/EBPβ) and peroxisome proliferator-activated receptor (PPAR)γ in WAT from *Pemt*$^{+/+}$ and *Pemt*$^{-/-}$ mice fed chow (C) or the HF diet for 2 weeks (D). Glyceraldehyde 3-phosphate dehydrogenase (GAPDH) was loaded as a loading control. (E) The relative levels of mRNAs encoding PPARγ, cluster of differentiation (CD)36 and lipoprotein lipase (LPL) in WAT. mRNA levels were determined by RT-qPCR. Data were presented relative to mRNA of β-actin in the same samples. n=4-6, *$p < 0.05$ by Student's *t*-test*, Pemt*$^{+/+}$ *vs Pemt*$^{-/-}$*.*

Figure 4.3

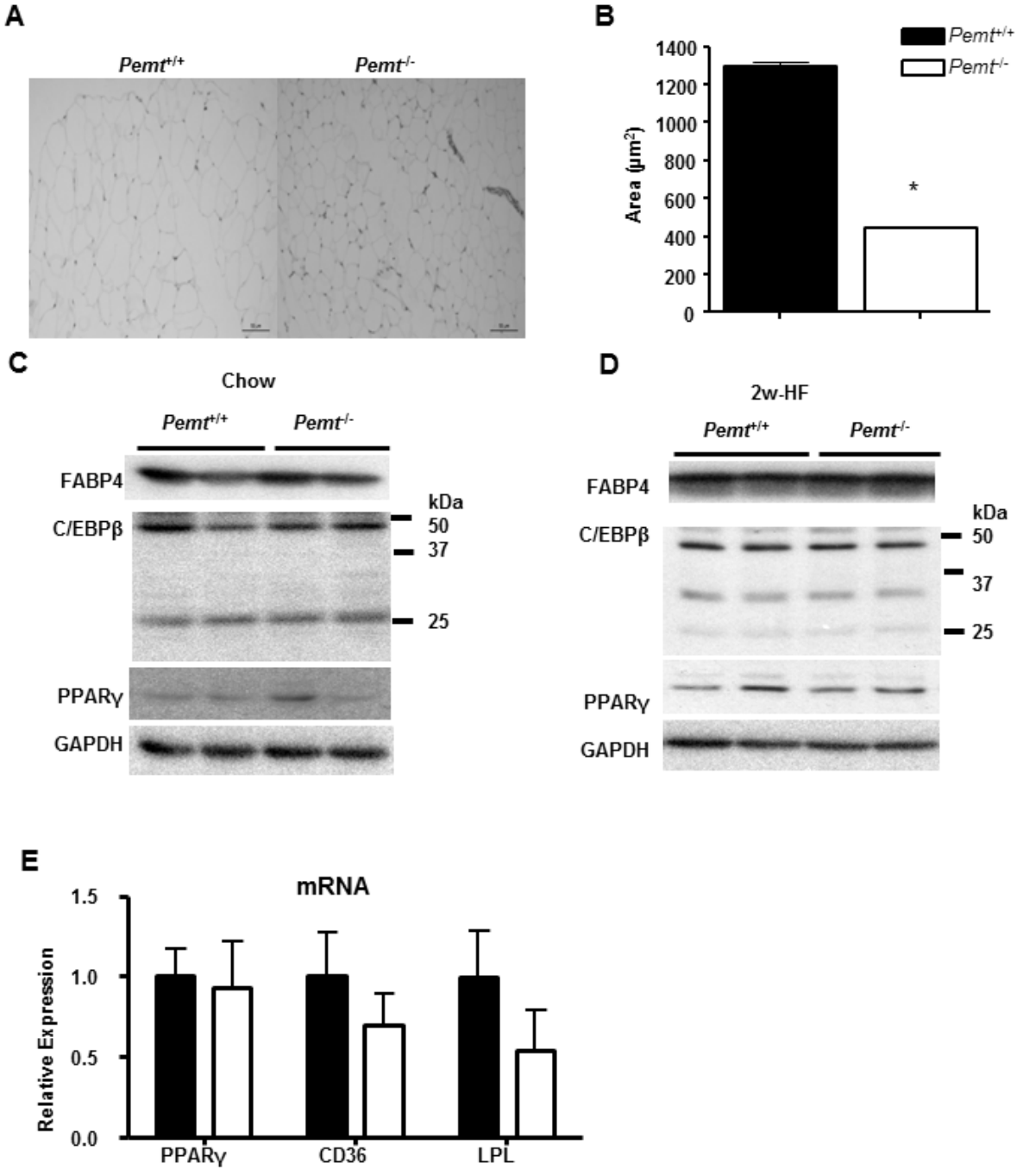
A
Pemt+/+
Pemt-/-
B
Pemt+/+
Pemt-/-
Area (μm2)
1400
1200
1000
800
600
400
200
0
*
C
Chow
Pemt+/+
Pemt-/-
FABP4
C/EBPβ
PPARγ
GAPDH
kDa
50
37
25
D
2w-HF
Pemt+/+
Pemt-/-
FABP4
C/EBPβ
PPARγ
GAPDH
kDa
50
37
25
E
mRNA
Relative Expression
1.5
1.0
0.5
0.0
PPARγ
CD36
LPL

Figure 4.4 Lipogenesis in WAT

(A and B) *De novo* lipogenesis related enzyme expression in non-fasting *Pemt*$^{+/+}$ and *Pemt*$^{-/-}$ mice fed the HF diet for 2 weeks: (A) Representative immunoblots for phospho-acetyl-CoA carboxylase (p-ACC), total acetyl-CoA carboxylase (ACC) and fatty acid synthase (FAS); glyceraldehyde 3-phosphate dehydrogenase (GAPDH) was loaded as a loading control. (B) The densitometry for panel A. (C) The relative levels of mRNAs encoding sterol regulatory element-binding protein (SREBP)-1c, ACC, FAS, acyl CoA:monoacylglycerol acyltransferase (MGAT)-1, glycerol-3-phosphate acyltransferase (GPAT)-1, acyl CoA:diacylglycerol acyltransferase (DGAT)-1, DGAT-2, stearoyl-CoA desaturase (SCD)-1 and ATP citrate lyase (ACLY) in WAT *Pemt*$^{+/+}$ and *Pemt*$^{-/-}$ mice fed the HF diet for 2 weeks. RNA was isolated from WAT of non-fasted mice (4-5 mice/group) and mRNA levels were determined by RT-qPCR. Data are presented relative to mRNA of *β-actin* in the same samples. (D) *De novo* lipogenesis was determined by i.p. injection of [^{14}C]acetate into *Pemt*$^{+/+}$ and *Pemt*$^{-/-}$ mice fed the HF diet for 2 weeks. Labeled TG was extracted from WAT, separated by thin-layer chromatography, and quantified by a scintillation counter. n=4-6, *$p < 0.05$ by Student's *t*-test*, Pemt*$^{+/+}$ *vs Pemt*$^{-/-}$*.*

Figure 4.4

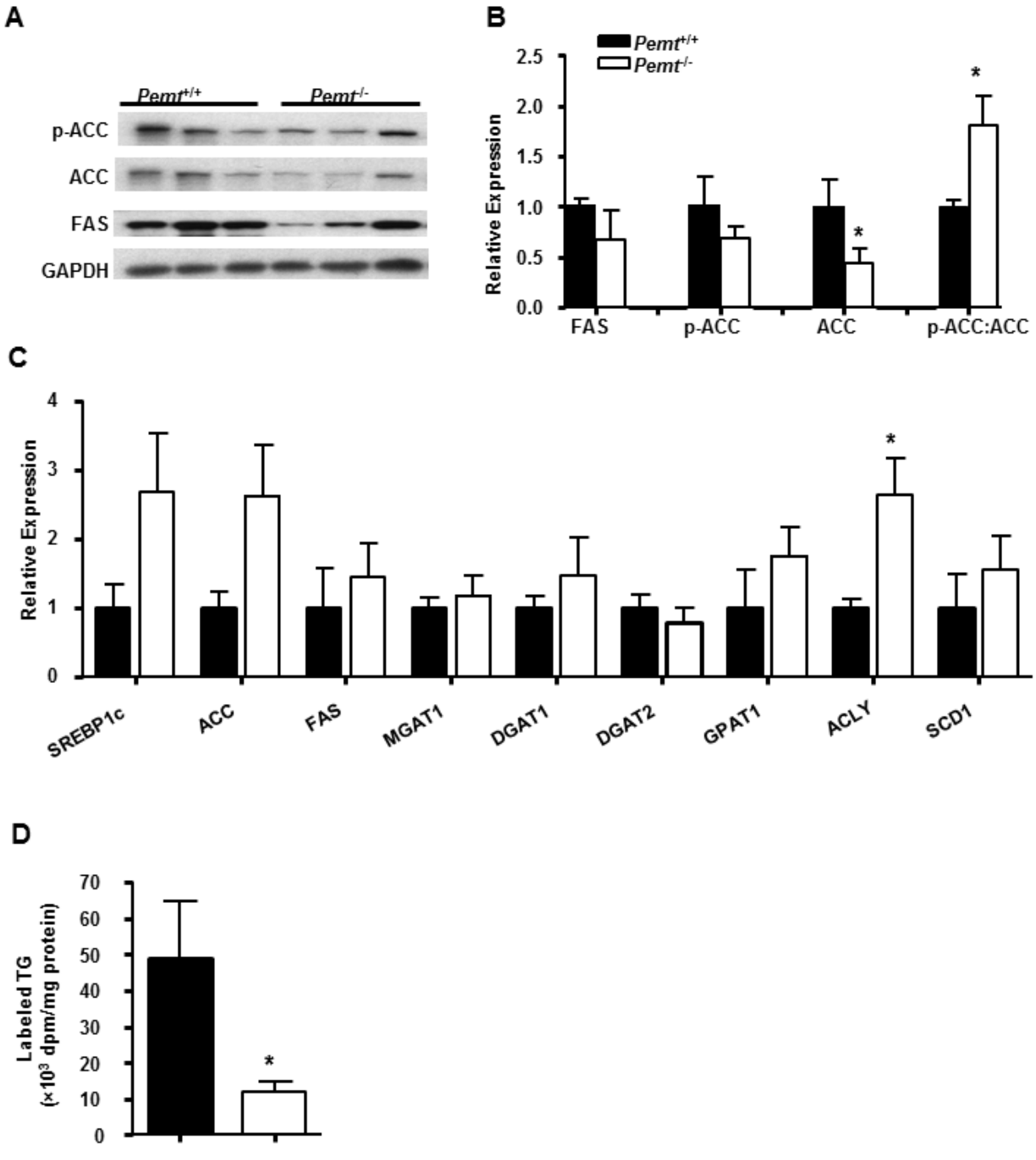
A
Pemt+/+
Pemt-/-
p-ACC
ACC
FAS
GAPDH
B
Pemt+/+
Pemt-/-
Relative Expression
2.5
2.0
1.5
1.0
0.5
0.0
*
*
FAS
p-ACC
ACC
p-ACC:ACC
C
Relative Expression
4
3
2
1
0
*
SREBP1c
ACC
FAS
MGAT1
DGAT1
DGAT2
GPAT1
ACLY
SCD1
D
Labeled TG
(×10³ dpm/mg protein)
70
60
50
40
30
20
10
0
*

Figure 4.5 Intact lipolytic capability in WAT

Pemt$^{+/+}$ and *Pemt*$^{-/-}$ mice were fed the HF diet for 2 weeks. The release of glycerol and NEFA (non-esterified fatty acids) under (A) basal state and under (B) stimulation by isoproterenol. (C) Representative immunoblots for lipolytic enzymes: phospho-HSL (p-HSL), total-HSL (HSL), adipose triglyceride lipase (ATGL) and triacylglycerol hydrolase (TGH). (D) The densitometry for the immunoblots in panel C. (E) The incomplete fatty acid oxidation rate of WAT homogenate was measured by incubation of WAT homogenate with [1-^{14}C]palmitate: acid-soluble metabolites (ASM). n=5-7, *p < 0.05 by Student's *t*-test*, Pemt*$^{+/+}$ *vs Pemt*$^{-/-}$*.*

Figure 4.5

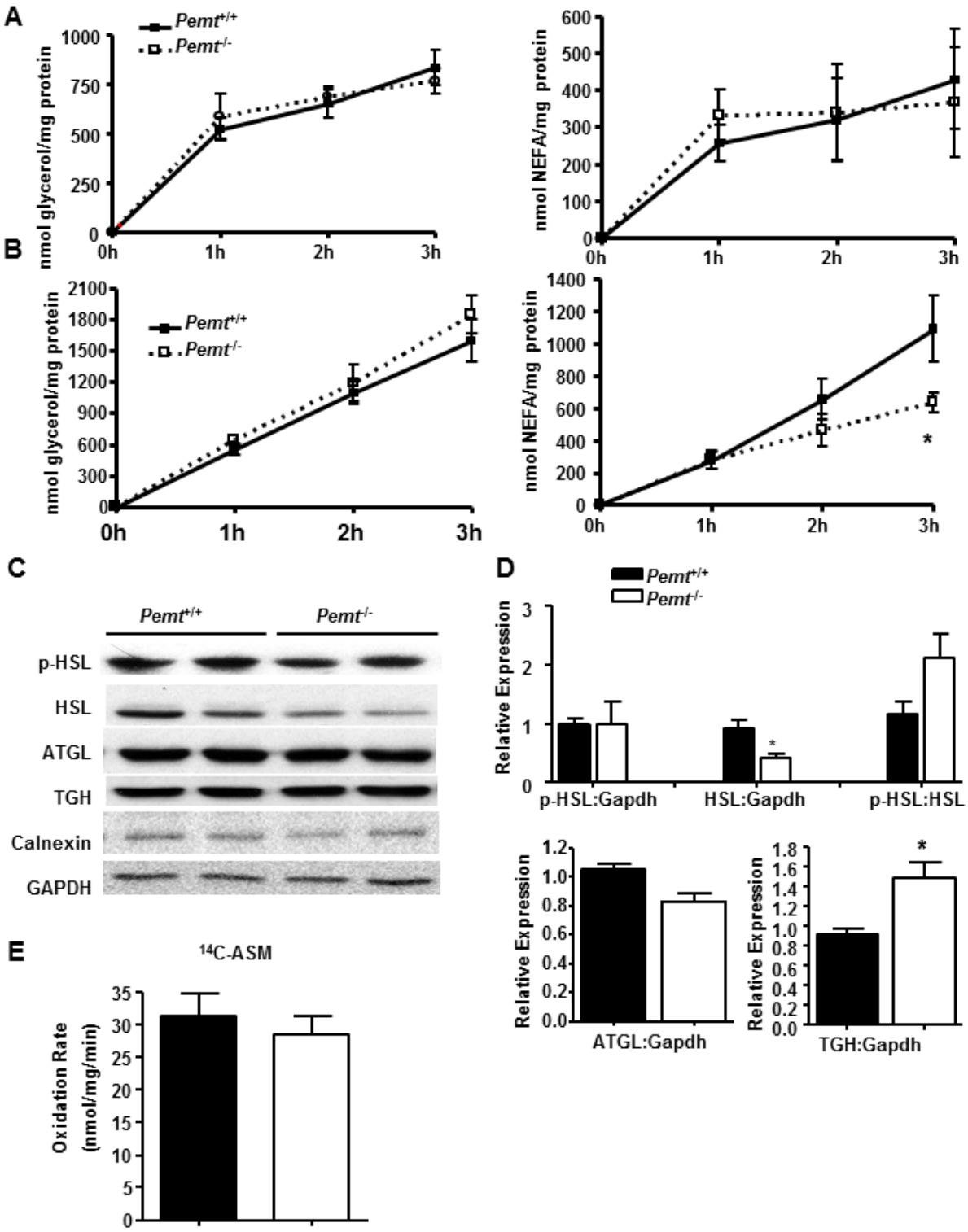
A
Pemt+/+
Pemt-/-
nmol glycerol/mg protein
nmol NEFA/mg protein
0h
1h
2h
3h
B
C
Pemt+/+
Pemt-/-
p-HSL
HSL
ATGL
TGH
Calnexin
GAPDH
D
Relative Expression
p-HSL:Gapdh
HSL:Gapdh
p-HSL:HSL
ATGL:Gapdh
TGH:Gapdh
E
14C-ASM
Oxidation Rate (nmol/mg/min)

Figure 4.6 Lipolytic enzyme expression in WAT from *Pemt*$^{+/+}$ and *Pemt*$^{-/-}$ mice fed the HF diet for 10 weeks

Pemt$^{+/+}$ and *Pemt*$^{-/-}$ mice were fed the HF diet for 10 weeks. Representative immunoblots (left) for lipolytic enzymes, phospho-hormone-sensitive lipase (p-HSL), total hormone-sensitive lipase (HSL), adipose triglyceride lipase (ATGL), triacylglycerol hydrolase (TGH), and loading control glyceraldehyde 3-phosphate dehydrogenase (GAPDH). The densitometry for the immunoblots (right). n=5-6, *$p < 0.05$ by Student's *t*-test*, Pemt*$^{+/+}$ *vs Pemt*$^{-/-}$*.*

Figure 4.6

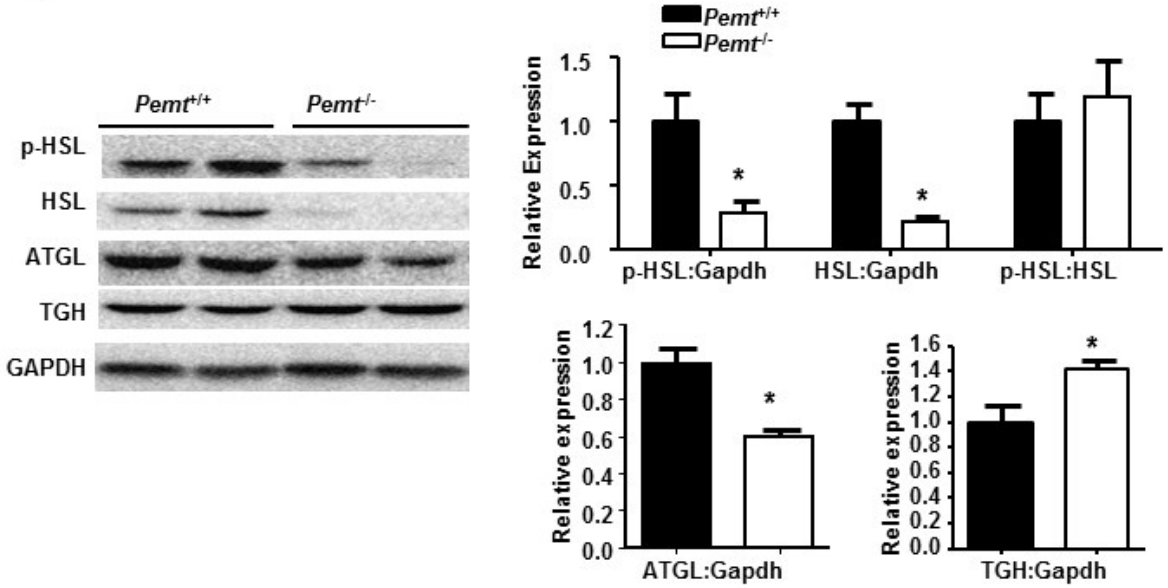
Pemt+/+
Pemt-/-
p-HSL
HSL
ATGL
TGH
GAPDH
Relative Expression
1.5
1.0
0.5
0.0
*
*
p-HSL:Gapdh
HSL:Gapdh
p-HSL:HSL
Relative expression
1.2
1.0
0.8
0.6
0.4
0.2
0.0
*
ATGL:Gapdh
Relative expression
1.6
1.4
1.2
1.0
0.8
0.6
0.4
0.2
0.0
*
TGH:Gapdh

Figure 4.7 Cytokines and chemokines in WAT and liver from *Pemt*$^{+/+}$ and *Pemt*$^{-/-}$ mice fed the HF diet for 2 weeks

Pemt$^{+/+}$ and *Pemt*$^{-/-}$ mice were fed the HF diet for 2 weeks. Levels of cytokines and chemokines in (A) WAT and (B) liver: RANTES, tumor necrosis factor (TNF)α, interleukin (IL)-10, IL-4, IL-1α and leptin. n=3, *$p < 0.05$ by Student's *t*-test*, Pemt*$^{+/+}$ *vs Pemt*$^{-/-}$*.*

Figure 4.7

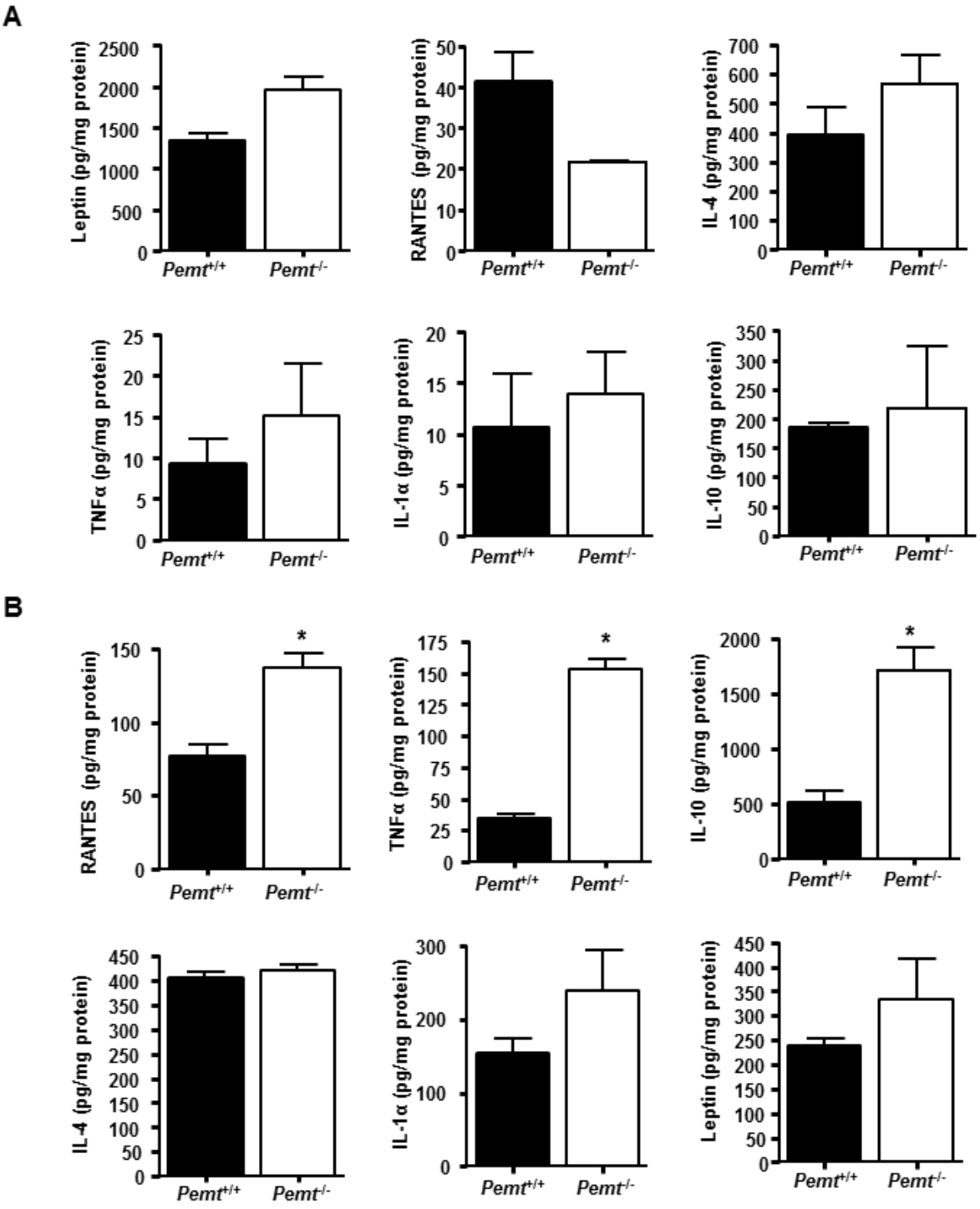
A
Leptin (pg/mg protein)
2500
2000
1500
1000
500
0
Pemt+/+
Pemt-/-
RANTES (pg/mg protein)
50
40
30
20
10
0
IL-4 (pg/mg protein)
700
600
500
400
300
200
100
TNFα (pg/mg protein)
25
20
15
10
5
IL-1α (pg/mg protein)
20
15
10
5
IL-10 (pg/mg protein)
350
300
250
200
150
B
*
RANTES (pg/mg protein)
150
100
50
TNFα (pg/mg protein)
175
150
125
100
75
IL-10 (pg/mg protein)
2000
1500
1000
500
IL-4 (pg/mg protein)
450
400
350
300
250
IL-1α (pg/mg protein)
300
200
100
Leptin (pg/mg protein)

Figure 4.8 Cytokines and chemokines in WAT from *Pemt*$^{+/+}$ and *Pemt*$^{-/-}$ mice fed the HF diet for 10 weeks

Cytokines and chemokines in WAT from *Pemt*$^{+/+}$ and *Pemt*$^{-/-}$ mice fed the HF diet for 10 weeks, including tumor necrosis factor (TNF)α, interleukin (IL)-10,IL-4, IL-1α and leptin. n=3, *$p < 0.05$ by Student's *t*-test*, Pemt*$^{+/+}$ *vs Pemt*$^{-/-}$*.*

Figure 4.8

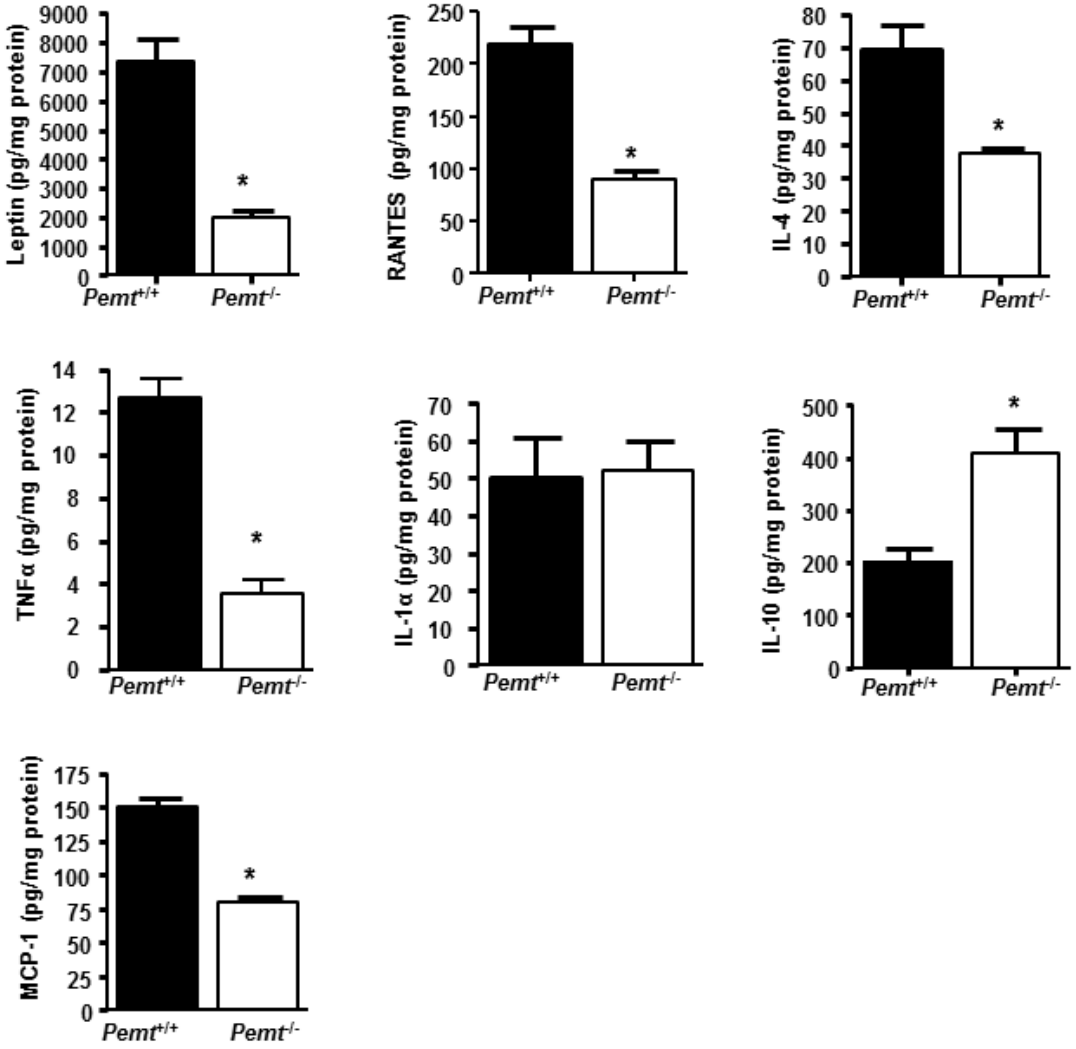
Leptin (pg/mg protein)
9000
8000
7000
6000
5000
4000
3000
2000
1000
0
*
Pemt+/+
Pemt-/-
RANTES (pg/mg protein)
250
200
150
100
50
0
*
Pemt+/+
Pemt-/-
IL-4 (pg/mg protein)
80
70
60
50
40
30
20
10
0
*
Pemt+/+
Pemt-/-
TNFα (pg/mg protein)
14
12
10
8
6
4
2
0
*
Pemt+/+
Pemt-/-
IL-1α (pg/mg protein)
70
60
50
40
30
20
10
0
Pemt+/+
Pemt-/-
IL-10 (pg/mg protein)
500
400
300
200
100
0
*
Pemt+/+
Pemt-/-
MCP-1 (pg/mg protein)
175
150
125
100
75
50
25
0
*
Pemt+/+
Pemt-/-

4.5 References

1. Cui, Z., Vance, J. E., Chen, M. H., Voelker, D. R., and Vance, D. E. (1993) *J Biol Chem* **268**, 16655-16663

2. Vance, D. E. (2014) *Biochim Biophys Acta* **1838**, 1477-1487

3. Bremer, J., and Greenberg, D. M. (1961) *Biochimica Et Biophysica Acta* **46**, 205-&

4. DeLong, C. J., Shen, Y. J., Thomas, M. J., and Cui, Z. (1999) *J Biol Chem* **274**, 29683-29688

5. Reo, N. V., Adinehzadeh, M., and Foy, B. D. (2002) *Biochim Biophys Acta* **1580**, 171-188

6. Li, Z., Agellon, L. B., Allen, T. M., Umeda, M., Jewell, L., Mason, A., and Vance, D. E. (2006) *Cell Metab* **3**, 321-331

7. Jacobs, R. L., Devlin, C., Tabas, I., and Vance, D. E. (2004) *J Biol Chem* **279**, 47402-47410

8. Noga, A. A., and Vance, D. E. (2003) *J Biol Chem* **278**, 21851-21859

9. Yao, Z. M., and Vance, D. E. (1988) *J Biol Chem* **263**, 2998-3004

10. Niebergall, L. J., Jacobs, R. L., Chaba, T., and Vance, D. E. (2011) *Biochim Biophys Acta* **1811**, 1177-1185

11. Ling, J., Chaba, T., Zhu, L. F., Jacobs, R. L., and Vance, D. E. (2012) *Hepatology* **55**, 1094-1102

12. Jacobs, R. L., Zhao, Y., Koonen, D. P., Sletten, T., Su, B., Lingrell, S., Cao, G., Peake, D. A., Kuo, M. S., Proctor, S. D., Kennedy, B. P., Dyck, J. R., and Vance, D. E. (2010) *J Biol Chem* **285**, 22403-22413

13. Li, Z., Agellon, L. B., and Vance, D. E. (2005) *J Biol Chem* **280**, 37798-37802

14. Zhu, X., Song, J., Mar, M. H., Edwards, L. J., and Zeisel, S. H. (2003) *Biochem J* **370**, 987-993

15. Cole, L. K., and Vance, D. E. (2010) *J Biol Chem* **285**, 11880-11891

16. Horl, G., Wagner, A., Cole, L. K., Malli, R., Reicher, H., Kotzbeck, P., Kofeler, H., Hofler, G., Frank, S., Bogner-Strauss, J. G., Sattler, W., Vance, D. E., and Steyrer, E. (2011) *J Biol Chem* **286**, 17338-17350

17. Kasturi, R., and Wakil, S. J. (1983) *J Biol Chem* **258**, 3559-3564

18. Bartz, R., Li, W. H., Venables, B., Zehmer, J. K., Roth, M. R., Welti, R., Anderson, R. G., Liu, P., and Chapman, K. D. (2007) *J Lipid Res* **48**, 837-847

19. Guo, Y., Walther, T. C., Rao, M., Stuurman, N., Goshima, G., Terayama, K., Wong, J. S., Vale, R. D., Walter, P., and Farese, R. V. (2008) *Nature* **453**, 657-661

20. Krahmer, N., Guo, Y., Wilfling, F., Hilger, M., Lingrell, S., Heger, K., Newman, H. W., Schmidt-Supprian, M., Vance, D. E., Mann, M., Farese, R. V., Jr., and Walther, T. C. (2011) *Cell Metab* **14**, 504-515

21. Hafez, I. M., and Cullis, P. R. (2001) *Adv Drug Deliv Rev* **47**, 139-148

22. Tomlinson, E., Fu, L., John, L., Hultgren, B., Huang, X., Renz, M., Stephan, J. P., Tsai, S. P., Powell-Braxton, L., French, D., and Stewart, T. A. (2002) *Endocrinology* **143**, 1741-1747

23. Folch, J., Lees, M., and Sloane Stanley, G. H. (1957) *J Biol Chem* **226**, 497-509

24. Hermansson, M., Uphoff, A., Kakela, R., and Somerharju, P. (2005) *Anal Chem* **77**, 2166-2175

25. Kainu, V., Hermansson, M., and Somerharju, P. (2008) *J Biol Chem* **283**, 3676-3687

26. Hirschey, M. D., Shimazu, T., Goetzman, E., Jing, E., Schwer, B., Lombard, D. B., Grueter, C. A., Harris, C., Biddinger, S., Ilkayeva, O. R., Stevens, R. D., Li, Y., Saha, A. K., Ruderman, N. B., Bain, J. R., Newgard, C. B., Farese, R. V., Jr., Alt, F. W., Kahn, C. R., and Verdin, E. (2010) *Nature* **464**, 121-125

27. Bernal-Mizrachi, C., Xiaozhong, L., Yin, L., Knutsen, R. H., Howard, M. J., Arends, J. J., Desantis, P., Coleman, T., and Semenkovich, C. F. (2007) *Cell Metab* **5**, 91-102

28. Donnelly, K. L., Smith, C. I., Schwarzenberg, S. J., Jessurun, J., Boldt, M. D., and Parks, E. J. (2005) *J Clin Invest* **115**, 1343-1351

29. Schweiger, M., Schreiber, R., Haemmerle, G., Lass, A., Fledelius, C., Jacobsen, P., Tornqvist, H., Zechner, R., and Zimmermann, R. (2006) *J Biol Chem* **281**, 40236-40241

30. Zechner, R., Kienesberger, P. C., Haemmerle, G., Zimmermann, R., and Lass, A. (2009) *J Lipid Res* **50**, 3-21

31. Dolinsky, V. W., Sipione, S., Lehner, R., and Vance, D. E. (2001) *Biochim Biophys Acta* **1532**, 162-172

32. Wei, E., Gao, W., and Lehner, R. (2007) *J Biol Chem* **282**, 8027-8035

33. Dolinsky, V. W., Gilham, D., Alam, M., Vance, D. E., and Lehner, R. (2004) *Cell Mol Life Sci* **61**, 1633-1651

34. Waki, H., and Tontonoz, P. (2007) *Annu Rev Pathol* **2**, 31-56

35. Ahmadian, M., Suh, J. M., Hah, N., Liddle, C., Atkins, A. R., Downes, M., and Evans, R. M. (2013) *Nat Med* **19**, 557-566

36. Tontonoz, P., and Spiegelman, B. M. (2008) *Annu Rev Biochem* **77**, 289-312

37. Hauner, H. (2002) *Diabetes Metab Res Rev* **18 Suppl 2**, S10-15

38. Haemmerle, G., Lass, A., Zimmermann, R., Gorkiewicz, G., Meyer, C., Rozman, J., Heldmaier, G., Maier, R., Theussl, C., Eder, S., Kratky, D., Wagner, E. F., Klingenspor, M., Hoefler, G., and Zechner, R. (2006) *Science* **312**, 734-737

39. Haemmerle, G., Zimmermann, R., Hayn, M., Theussl, C., Waeg, G., Wagner, E., Sattler, W., Magin, T. M., Wagner, E. F., and Zechner, R. (2002) *J Biol Chem* **277**, 4806-4815

40. Wang, S. P., Laurin, N., Himms-Hagen, J., Rudnicki, M. A., Levy, E., Robert, M. F., Pan, L., Oligny, L., and Mitchell, G. A. (2001) *Obes Res* **9**, 119-128

41. Osuga, J., Ishibashi, S., Oka, T., Yagyu, H., Tozawa, R., Fujimoto, A., Shionoiri, F., Yahagi, N., Kraemer, F. B., Tsutsumi, O., and Yamada, N. (2000) *Proc Natl Acad Sci U S A* **97**, 787-792

42. Bluher, M. (2013) *Best Pract Res Clin Endocrinol Metab* **27**, 163-177

Chapter 5

Insufficient glucose supply is linked to hypothermia upon cold exposure in mice lacking phosphatidylethanolamine *N*-methyltransferase

5.1 Introduction

Phosphatidylethanolamine *N*-methyltransferase (PEMT) catalyzes phosphatidylcholine (PC) biosynthesis via three sequential methylation steps of phosphatidylethanolamine (PE) (1). In the liver, PEMT contributes ~30% of hepatic PC production, whereas the remaining 70% of hepatic PC is synthesized via the CDP-choline pathway (2,3). Normal levels of hepatic PC are required to maintain membrane integrity (4) and normal very low density lipoprotein (VLDL) secretion (5-7). In mice, inhibition of either the CDP-choline pathway, by liver-specific deletion of CTP:phosphocholine cytidylyltransferase (LCT)α or elimination of the PEMT pathway reduces hepatic PC content and causes hepatic steatosis (8). The importance of the PEMT pathway has been highlighted in *Pemt*$^{-/-}$ mice fed either a choline-deficient diet (4) or a HF diet (9). When fed the HF diet for 10 weeks, *Pemt*$^{-/-}$ mice develop severe non-alcoholic steatohepatitis, but are protected against diet-induced obesity (DIO) and insulin resistance (9). HF-fed *Pemt*$^{-/-}$ mice also exhibit higher oxygen consumption and heat production than HF-fed *Pemt*$^{+/+}$ *mice* (9). *LCTα*$^{-/-}$ mice fed the HF diet develop steatohepatitis (8-10), but are not protected from DIO (9). Thus, we conclude that resistance of *Pemt*$^{-/-}$ mice to DIO does not appear to rely primarily on decreased hepatic PC or decreased VLDL secretion (5,6).

BAT is a highly oxidative and vascularized tissue, enriched with mitochondria and nerve fibers (11). An unique feature of BAT is the presence of uncoupling protein (UCP)1, which uncouples proton gradients (generated via oxidative phosphorylation) from ATP synthesis thereby generating heat (11). BAT-mediated thermogenesis is critical for maintaining body temperature for small mammals and is also involved in

regulation of energy metabolism (11-13). Moreover, BAT is also present in adult humans (14-16). Thus, selective activation of BAT-mediated thermogenesis opens a potential avenue for treatment of metabolic syndrome such as DIO and diabetes (17).

In this study, the contribution of BAT to the resistance of *Pemt*$^{-/-}$ mice to DIO is investigated. We hypothesized that more energy were utilized for BAT-mediated thermogenesis, which contributes to the resistance to DIO in HF-fed *Pemt*$^{-/-}$ mice. After consuming the HF diet for 2 weeks, *Pemt*$^{-/-}$ mice failed to maintain body temperature above 28˚C during a cold challenge. Choline supplementation completely reversed the hypothermia in HF-fed *Pemt*$^{-/-}$ mice. Our results suggest that in HF-fed *Pemt*$^{-/-}$ mice, reduction in substrate supply (plasma glucose), caused by compromised hepatic glucose production, rather than an impaired capability for thermogenesis in BAT, causes cold-induced hypothermia.

5.2 Materials and methods

5.2.1 Animal handling and diets

All procedures were approved by the University of Alberta's Institutional Animal Care Committee in accordance with guidelines of the Canadian Council on Animal Care. Male C57Bl/6 *Pemt*$^{+/+}$ and *Pemt*$^{-/-}$ mice were housed with free access to water and chow (LabDiet, #5001). *Pemt*$^{+/+}$ and *Pemt*$^{-/-}$ mice (8-9 weeks old) were fed the HF diet (Bio-Serv, #F3282) for 2 weeks. Tissues were collected from mice that had either been fasted for 12 h or not fasted. Blood was collected by cardiac puncture. Tissues were either used immediately for assessment of fatty acid oxidation, or stored at -80°C.

The procedure for the cold challenge was adapted from a previous study (18). Mice were fasted for 4 h then transferred to the cold room (4°C) with individual housing, no bedding, food or water for up to 4 h. Rectal body temperature was determined hourly using a mouse rectal probe (model 4600 Precision Thermometer). When the body temperature dropped below 28°C, the mice were removed from the cold room. Tissues were collected immediately after the cold exposure.

5.2.2 Analytical procedures

Plasma triacylglycerol (19) and TG extracted from tissue (liver and BAT) homogenates were quantified using a commercially available kit from Roche Diagnostics according to manufacturer's protocols. Plasma non-esterified fatty acids and glucose were quantified using commercially available kits from Wako Chemicals GmbH and BioAssay Systems (20), respectively, according to manufacturers' protocols. Plasma thyroid hormones, triiodothyronine (T3) and its prohormone thyroxine (T4), were quantified by commercially available ELISA kits (Leinco Technologies, Inc.) according to the manufacturer's protocols. Plasma epinephrine and norepinephrine were quantified with a commercially available 2-CAT (A-N) research ELISA kit (Labor Diagnostika Nord) according to manufacturer's protocols. PC and PE extracted from BAT homogenates were quantified as previously described (21) in section 2.2.3. Protein concentrations were determined by the Bradford assay (Bio-Rad).

5.2.3 Fatty acid oxidation

The rate of fatty acid oxidation was determined as described with minor modifications (22). Freshly isolated interscapular BAT was homogenized as described

in section 4.2.9. 1.5-2 mg protein homogenates (in volume of 250 μl) were used to determine the rate of ([1-^{14}C]palmitate oxidation as described in section 4.2.9.

5.2.4 Real-time quantitative PCR and qnalysis of mitochondrial DNA content

RNA isolation, cDNA synthesis and real-time quantitative PCR were performed as described previously (23). mRNA levels were normalized to *β-actin* mRNA. Mitochondrial DNA content was determined as described previously (23). Total genomic DNA from BAT was isolated by a DNEasy kit (Qiagen) according to manufacturer's protocols. The mitochondrial DNA content was calculated using real-time qPCR by measuring a mitochondrial gene *Nd1* versus a nuclear gene *Lpl.* Primer sequences were listed in Table 5.1.

5.2.5 Immunoblotting

Tissues homogenization and immunoblotting procedure were described in section 2.2.7. Proteins were transferred to a polyvinylidene fluoride membrane and the membrane was then probed with primary antibodies against FABP4 (1:1000 dilution, Cell signaling #2120), PPARγ (1:1000 dilution, Cell signaling #24443), CCAAT/enhancer-binding protein β (C/EBPβ, 1:500 dilution, Santa Cruz sc150), PGC1α (1:1000 dilution, Abcam #ab54481), phosphoenolpyruvate carboxykinase (PEPCK, 1:1000 dilution, Abcam #ab70358), UCP1 (1:1000 dilution, Abcam #ab10983), porin (VDAC, 1:1000 dilution, Abcam # ab14734), OXPHOS complexes (1:500 dilution, Abcam #ab110413), calnexin (1:1000 dilution, Enzo Life Sciences, SPA-865), total hormone-sensitive lipase (HSL, 1:1000 dilution, Cell signaling #4107), phospho-HSL (Ser660, 1:1000 dilution, Cell signaling #4126), adipose triacylglycerol lipase (ATGL, 1:1000 dilution, Cell signaling #2138), TG hydrolase (TGH, gift from Dr. Richard

Lehner), α-Tubulin (1:12,000 dilution, Abcam #ab4074) or glyceraldehyde 3-phosphate dehydrogenase (GAPDH, 1:12,000 dilution, Abcam # ab8245). The immunoreactive bands were visualized by enhanced chemiluminescence system (Amersham Biosciences) according to the manufacturer's instructions and protein levels were quantified using ImageJ software.

5.2.6 Systolic Blood Pressure

Systolic blood pressure was measured of conscious animals indirectly using a commercially available computerized tail cuff plethysmography system (Kent Scientific Corporation, Torrington, CT) (24).

5.2.7 Assessment of Cardiac Function

Transthoracic echocardiography was performed as described (25) on mildly anesthetized mice using a Vevo 770 High-Resolution Imaging System equipped with a 30-MHz transducer (RMV-707b; VisualSonics, Toronto, Canada). The mice were placed on a heated electrocardiograph platform to acquire physiological parameters. The transducer was placed at the suprasternal notch, so that the ascending aorta, aortic arch, origin of the brachiocephalic vessels, descending thoracic aorta and right pulmonary artery can be visualized. The leaflets of the aortic valve in the aortic root can often be seen as well. Pulse Doppler flows were acquired from the ascending and descending arteries, as well as m-modes for the transverse arch. The transducer was placed just below the sternum using minimal pressure and angled toward the apex of the heart in order to obtain images for analysis of cardiac and aortic structures and function. Aortic diameter was measured at the level of the Valsalva sinus from the m-mode image. For transmitral recordings a depth setting of 4-7 mm was used and 6-9

mm was used for trans-aortic recordings. The transthoracic echocardiography analysis of cardiac function was performed and analyzed by Ms Donna Beker in Cardiovascular Research Center, University of Alberta.

5.2.8 Histology

A portion of BAT was fixed in 10% buffered formalin and subjected to hematoxylin and eosin staining as described in section 2.2.4 by the Histocore of Alberta Diabetes Institute (University of Alberta).

5.2.9 Statistical Analysis

Data are means ± SEM. Comparisons between two groups were performed using Student's *t*-test. For all other comparisons, a two-way ANOVA, followed by post hoc Bonferroni's test of individual group differences was used. $P < 0.05$ was considered significant. Unless otherwise indicated, 5-7 animals were used per group.

5.3 Results

5.3.1 PEMT deficiency does not alter thermogenic features of BAT

PEMT is highly expressed in the liver and is present at very low levels in WAT (1). PEMT protein (Figure 5.1) and its enzymatic activity (data not shown) were undetectable in BAT. When fed standard chow diet, BAT from *Pemt*$^{-/-}$ mice contained the same amount of PC, but higher level of PE, compared to BAT from *Pemt*$^{+/+}$ mice under both fasting and non-fasting condition (Figure 5.2A). However, the PC/PE molar ratio in BAT (1.22 ± 0.00) was significantly lower than in the liver (10). Moreover, the PC/PE ratio in BAT of *Pemt*$^{-/-}$ mice under non-fasting conditions was lower than in

Pemt$^{+/+}$ mice **(**Figure 5.2A). Furthermore, the mass of TG in BAT was not different between *Pemt* genotypes (Figure 5.2A).

We next explored the thermogenic capacity of BAT. The protein levels of the adipocyte differentiation markers FABP4 and C/EBPβ were not different between *Pemt* genotypes (Figure 5.2B&C), suggesting that PEMT deficiency did not impair the differentiation of brown adipocytes. Nor was the protein level of PGC1α, a key regulator of oxidative metabolism and UCP1-meditated thermogenesis in BAT (26), different between the genotypes. Moreover, levels of electron transport chain proteins (complexes I to V) were the same in BAT from *Pemt*$^{-/-}$ and *Pemt*$^{+/+}$ mice (Fig. 2B&C). In contrast, the amount of UCP1 protein in *Pemt*$^{-/-}$ mice was higher than in *Pemt*$^{+/+}$ mice (Figure 5.2B&C). Together, chow-fed *Pemt*$^{-/-}$ mice show no defect in thermogenic features in BAT.

To assess the oxidative capacity of BAT, we measured the rate of fatty acid oxidation *ex vivo* using BAT homogenates. The rates of complete fatty acid oxidation (measured by amount of released $^{14}CO_2$) and incomplete fatty acid oxidation (measured by the amounts of ^{14}C-labeled acid-soluble metabolites) were equivalent in *Pemt*$^{-/-}$ and *Pemt*$^{+/+}$ mice (Figure 5.2D). To evaluate the capacity for thermogenesis, we transferred chow-fed *Pemt*$^{-/-}$ and *Pemt*$^{+/+}$ mice to 4°C. Mice of both genotypes maintained their body temperature above 33°C throughout the cold exposure (Figure 5.2E). Thus, chow-fed *Pemt*$^{-/-}$ mice show normal thermogenesis in BAT.

Pemt$^{-/-}$ mice are resistant to DIO because of higher energy expenditure as indicated by higher oxygen consumption and heat production than in *Pemt*$^{+/+}$ mice (9). To determine whether or not BAT-mediated thermogenesis contributed to the protection

against DIO, we evaluated the properties of BAT from *Pemt*$^{-/-}$ and *Pemt*$^{+/+}$ mice fed the HF diet for 2 weeks. The mass of BAT, the levels of PC and PE and the PC/PE ratio in BAT were not different between *Pemt*$^{-/-}$ and *Pemt*$^{+/+}$ mice (Figure 5.2A&C). However, BAT from *Pemt*$^{-/-}$ mice contained slightly less TG than did BAT from *Pemt*$^{+/+}$ mice under non-fasting condition (Figure 5.2A&D). Fasting greatly reduced TG storage in both genotypes (Figure 5.3A), indicating that the rate of fasting-induced lipolysis was intact in BAT from *Pemt*$^{-/-}$ mice. The levels of PPARγ and FABP4 proteins were the same in HF-fed *Pemt*$^{-/-}$ mice and HF-fed *Pemt*$^{+/+}$ mice, but the amount of C/EBPβ protein was reduced by PEMT deficiency (Figure 5.3B). Moreover, the amounts of PGC1α, UCP1, mitochondrial marker protein VDAC and electron transport chain proteins were similar in the two genotypes (Figure 5.3E). PEMT deficiency did not alter mitochondrial number (Figure 5.3F). Furthermore, the rates of complete and incomplete fatty acid oxidation in *Pemt*$^{-/-}$ mice were similar to those in *Pemt*$^{+/+}$ mice (Figure 5.3G). Overall, these data demonstrate that BAT of *Pemt*$^{-/-}$ mice fed the HF diet exhibits normal thermogenic features.

5.3.2 HF-fed *Pemt*$^{-/-}$ mice are hypothermic upon cold exposure

To determine whether or not PEMT deficiency affected thermogenesis, we transferred HF-fed *Pemt*$^{-/-}$ and *Pemt*$^{+/+}$ mice to 4°C. Unexpectedly, HF-fed *Pemt*$^{-/-}$ mice were unable to maintain their body temperature upon cold exposure, as the rectal body temperature rapidly (within 2-3 h) dropped below 28°C (Figure 5.4). In contrast, *Pemt*$^{+/+}$ mice were able to maintain their body temperature above 30°C throughout the 4 h cold exposure (Figure 5.4). Thus, it appears that HF-fed *Pemt*$^{-/-}$ mice are hypothermic upon cold exposure.

Cold activates the sympathetic nervous system, particularly via the release of norepinephrine which stimulates BAT-mediated thermogenesis to maintain core body temperature (11). Plasma levels of epinephrine and norepinephrine were not lower in *Pemt*$^{-/-}$ mice than in *Pemt*$^{+/+}$ mice (Figure 5.5A). Following cold exposure, the protein levels of phospho-HSL total-HSL and ATGL in BAT from *Pemt*$^{-/-}$ mice were indistinguishable from those in *Pemt*$^{+/+}$ mice (Figure 5.5B). In contrast, the amount of TGH protein was lower in BAT from *Pemt*$^{-/-}$ mice than *Pemt*$^{+/+}$ mice (Figure 5.5B). In addition, the amount of the mitochondrial protein VDAC and the mitochondrial number (Figure 5.5C&D) were not influenced by *Pemt* genotype. The level of PGC1α in BAT from *Pemt*$^{-/-}$ mice was slightly lower than that in *Pemt*$^{+/+}$ mice, whereas the amount of UCP1 protein was 2-fold higher in *Pemt*$^{-/-}$ mice. Moreover, the amounts of mitochondrial electron transport chain proteins were equivalent in BAT from *Pemt*$^{+/+}$ and *Pemt*$^{-/-}$ mice, except for a slightly higher amount of complex V in *Pemt*$^{-/-}$ mice (Figure 5.5C). Additionally, BAT from *Pemt*$^{-/-}$ mice contained higher levels of mRNAs involved in fatty acid oxidation including *CPT1α* (carnitine palmitoyltransferase 1α) and *LCAD* (long-chain acyl-CoA dehydrogenase) than did *Pemt*$^{+/+}$ mice (Figure 5.5E). The amounts of mRNAs encoding MCAD (medium-chain acyl-CoA dehydrogenase) and PDK4 (pyruvate dehydrogenase kinase isozyme 4) were not different between genotypes (Figure 5.5E). Consequently, cold exposure reduced the amount of TG in BAT from mice of both genotypes compared to BAT collected from non-fasted mice (Figure 5.3A and Figure 5.5F). After cold exposure, however, BAT from *Pemt*$^{-/-}$ mice contained 49% less TG than BAT from *Pemt*$^{+/+}$ mice (Figure 5.5F)**.** Thus, in *Pemt*$^{-/-}$ mice the HF-induced hypothermia is not caused by an impaired thermogenic capacity of BAT.

Cold exposure also stimulates peripheral lipolysis in white adipose tissue (WAT) to provide substrates for thermogenesis (11). Following cold exposure, WAT from *Pemt*$^{-/-}$ mice contained 1.7-fold more phospho-HSL and the same amount of total-HSL (Figure 5.6A) than did *Pemt*$^{+/+}$ mice. Thus, the ratio of phospho-HSL/HSL in WAT of *Pemt*$^{-/-}$ mice was higher than in *Pemt*$^{+/+}$ mice, indicating more activated HSL in *Pemt*$^{-/-}$ mice. In addition, the amounts of ATGL and TGH proteins in WAT from *Pemt*$^{-/-}$ mice were higher than in *Pemt*$^{+/+}$ mice (Figure 5.6A). These data suggest that capability for lipolysis in WAT was increased in *Pemt*$^{-/-}$ mice. Thus, the exacerbation of cold-induced hypothermia in *Pemt*$^{-/-}$ mice does not appear to be caused by inefficient lipolysis in WAT.

Cold exposure is known to stimulate cardiac output and blood flow to BAT (27,28). To determine if the cold-induced hypothermia in HF-fed *Pemt*$^{-/-}$ mice could be attributed to an insufficient circulation system, we first measured systolic blood pressure in *Pemt*$^{+/+}$and *Pemt*$^{-/-}$ mice with a computerized tail cuff plethysmography system (24). Systolic blood pressure in HF-fed *Pemt*$^{-/-}$ mice was 20% higher than in HF-fed *Pemt*$^{+/+}$ mice (Figure 5.7A), but heart weights were the same in mice of both genotypes (Figure 5.7B). To examine cardiac function, the mice were subjected to echocardiography. In *Pemt*$^{-/-}$ mice, the ejection fraction, fraction shortening and cardiac output were 17%, 21% and 25% lower than in *Pemt*$^{+/+}$ mice respectively (Figure 5.7C). However, heart rate was not altered by the *Pemt* genotype (Table 5.2). Consistently, *Pemt*$^{-/-}$ mice exhibited lower mitral early and late ventricular filling velocities, suggesting that *Pemt*$^{-/-}$ mice had diastolic dysfunction and longer left ventricle isovolumic contraction time than

Pemt$^{+/+}$ mice (Table 5.2). These data indicate that the HF-induced hypothermia in *Pemt*$^{-/-}$ mice is likely linked to hypertension, accompanied by reduced cardiac output.

5.3.3 Choline supplementation reverses cold-induced hypothermia in HF-fed *Pemt*$^{-/-}$ mice

Pemt$^{-/-}$ mice are resistant to DIO due to choline insufficiency (9) and HF-induced steatohepatitis in *Pemt*$^{-/-}$ mice is improved by dietary addition of choline (10). To determine whether the hypothermia in HF-fed *Pemt*$^{-/-}$ mice was also related to choline insufficiency, we increased the amount of choline by 2-fold in the HF diet that we fed for 2 weeks. Remarkably, choline supplementation completely prevented the hypothermia in HF-fed *Pemt*$^{-/-}$ mice (Figure 5.8A). All *Pemt*$^{+/+}$ mice that were fed either the HF or the choline-supplemented-HF (HFCS) diet maintained their body temperature upon cold exposure. Moreover, the HFCS diet increased body weight in *Pemt*$^{-/-}$ mice without significantly increasing the weight of BAT and WAT (Figure 5.8B-D). In *Pemt*$^{+/+}$ mice, HFCS did not alter body weight gain or the mass of BAT or WAT (Figure 5.8B-D). The weights of heart and kidney were not different among the four groups of mice (Figure 5.8E-F). The HFCS diet increased blood pressure in *Pemt*$^{+/+}$ mice but not in *Pemt*$^{-/-}$ mice (Figure 5.8G), implying that the change in blood pressure was not a critical factor for the hypothermia. Surprisingly, in HF-fed *Pemt*$^{-/-}$ mice the cold-induced weight loss was less than in *Pemt*$^{+/+}$ mice and was normalized by choline supplementation (Figure 5.8H). However, a 4 h fasting period prior to the cold exposure led to the same amounts of weight loss in the four groups of mice (Figure 5.8I). These data demonstrate that choline supplementation prevents cold-induced hypothermia in HF-fed *Pemt*$^{-/-}$ mice and the higher blood pressure in the HF-fed *Pemt*$^{-/-}$ mice does not contribute to this process.

5.3.4 Choline supplementation normalizes plasma glucose in HF-fed *Pemt*$^{-/-}$ mice

The attenuation of cold-induced weight loss was completely reversed by choline supplementation of the HF diet (Figure 5.8H). Since thyroid hormones are also involved in the regulation of thermogenesis in BAT (11), we measured plasma levels of these hormones in *Pemt*$^{+/+}$ and *Pemt*$^{-/-}$ mice fed the HF diet and the HFCS diet. In comparison to HF-fed *Pemt*$^{+/+}$ mice, the plasma level of T4 was 38% higher in HF-fed *Pemt*$^{-/-}$ mice and this increase was prevented by choline supplementation (Figure 5.9). However, the plasma level of T3, the more active form of the hormone, was 69% lower in *Pemt*$^{-/-}$ mice compared to *Pemt*$^{+/+}$ mice, and this difference was not eliminated by the HFCS diet (Figure 5.9). Thus, cold-induced hypothermia in HF-fed *Pemt*$^{-/-}$ mice is not likely due to insufficient thyroid hormone.

To gain further insight into the mechanism underlying the severe cold sensitivity of *Pemt*$^{-/-}$ mice, we investigated the status of energy supply in plasma after cold exposure. As shown in Figure 5.6B, the levels of fatty acids in plasma of HF-fed *Pemt*$^{-/-}$ mice were the same as in *Pemt*$^{+/+}$ mice, and were not changed by the HFCS diet (Figure 5.10A). Plasma of HF-fed *Pemt*$^{-/-}$ mice and *Pemt*$^{+/+}$ mice also contained the same amounts of TG (Figure 5.9A). The HFCS diet increased the amounts of plasma TG in *Pemt*$^{+/+}$, but not in *Pemt*$^{-/-}$ mice (Figure 5.10A). However, the levels of plasma glucose in HF-fed *Pemt*$^{-/-}$ mice were 49% lower than in *Pemt*$^{+/+}$ mice (Figure 5.10A). Although the HFCS diet did not alter plasma glucose levels in *Pemt*$^{+/+}$ mice, plasma glucose was increased by 180% in *Pemt*$^{-/-}$ mice (Figure 5.10A). Thus, these data suggest that impaired gluconeogenesis reflected by insufficient plasma glucose level, rather than TG, contributes to the cold-induced hypothermia in HF-fed *Pemt*$^{-/-}$ mice.

Liver is the major site of glucose production (29). HF-fed *Pemt*$^{-/-}$ mice, but not HF-fed *Pemt*$^{+/+}$ mice, developed hepatomegaly and contained 1.6-fold more hepatic TG than did the *Pemt*$^{+/+}$ mice (Figure 5.10B). Supplementation of the HF diet with choline greatly improved the hepatomegaly in *Pemt*$^{-/-}$ mice. In addition, the HFCS diet doubled the amounts of hepatic TG in *Pemt*$^{+/+}$ mice, but did not change hepatic TG in *Pemt*$^{-/-}$ mice (Figure 5.10B). To further determine if differences in plasma glucose in *Pemt*$^{+/+}$ and *Pemt*$^{-/-}$ mice were due to different regulation of hepatic gluconeogenesis in the liver, we measured the amounts of PEPCK and its transcriptional regulator PGC1α (Figure 5.10C). Compared to the livers of HF-fed *Pemt*$^{+/+}$ mice, the livers of HF-fed *Pemt*$^{-/-}$ mice contained 46% less PEPCK protein. Choline supplementation completely restored the amounts of this protein to that in HF-fed *Pemt*$^{+/+}$ mice. Similarly, the amounts of PGC1α in the livers of *Pemt*$^{-/-}$ mice were 68% lower than in HF-fed *Pemt*$^{+/+}$ mice and the HFCS diet restored the levels of this protein to that in HF-fed *Pemt*$^{+/+}$ mice. Moreover, the HFCS diet increased the low levels of TG in BAT from *Pemt*$^{-/-}$ mice to that in *Pemt*$^{+/+}$ mice (Figure 5.10D). Thus, it appears that impaired hepatic gluconeogenesis in HF-fed *Pemt*$^{-/-}$ mice and insufficient plasma glucose contribute to hypothermia upon cold exposure.

5.4 Discussion

We initiated our study to unravel the contribution of BAT to the resistance to DIO in *Pemt*$^{-/-}$ mice. PEMT activity is undetectable in BAT. HF-fed *Pemt*$^{-/-}$ mice show intact thermogenic features in BAT. Unexpectedly, HF-fed *Pemt*$^{-/-}$ mice are cold sensitive and this is prevented by supplementary choline. Further studies strongly suggest that the

hypothermia of *Pemt*$^{-/-}$ mice upon cold exposure is caused by reduced supply of substrate, particularly glucose, as a fuel for thermogenesis. The results strongly support a critical role for glucose as an energy substrate for thermogenesis in BAT.

5.4.1 HF-fed *Pemt*$^{-/-}$ mice develop hypothermia upon cold exposure, but does not show a dysfunctional BAT

Cold exposure activates the sympathetic nervous system and stimulates energy utilization for thermogenesis, particularly in BAT, to maintain core body temperature (11). Cold-induced sympathetic activity stimulates β-adrenergic receptors on brown adipocytes and promotes lipolysis for UCP1-mediated thermogenesis. Cold exposure also challenges the cardiovascular system because of the high demand for energy supply to BAT for heat production. Thus, maintenance of body temperature upon acute exposure to cold is a high energy-consuming process, as indicated by the depletion of glycogen in the liver (30,31). We found that HF-fed *Pemt*$^{-/-}$ mice were hypothermic upon cold exposure, while chow-fed *Pemt*$^{-/-}$ mice were not (Figs. 1D and 3). The hypothermia in HF-fed *Pemt*$^{-/-}$ mice is unlikely due to differences in the mass of adipose tissue since chow- and HF-fed *Pemt*$^{-/-}$ mice have a similar body weights (32).

As in chow-fed *Pemt*$^{-/-}$ mice, the amounts of PGC1α, UCP1 and mitochondrial electron transport chain proteins in BAT from HF-fed *Pemt*$^{-/-}$ mice were equivalent to those in HF-fed *Pemt*$^{+/+}$ mice (Figure 5.3E). The mitochondrial number and the capacity for fatty acid oxidation in BAT were not different between genotypes either (Figs. 2). Moreover, upon cold exposure, levels of mitochondrial electron transport chain proteins and mitochondrial number were the same in BAT from both genotypes (Figure 5.5C). Although the level of PGC1α was slightly lower in BAT from *Pemt*$^{-/-}$ mice than in *Pemt*$^{+/+}$

mice, the amount of UCP1 was higher (Figure 5.5C). In addition, levels of mRNAs encoding *CPT1α* and *LCAD* were higher in *Pemt*$^{-/-}$ mice than in *Pemt*$^{+/+}$ mice (Figure 5.5E). Although HF-fed *Pemt*$^{-/-}$ mice were cold-sensitive, they consumed more oxygen and generated more heat than the HF-fed *Pemt*$^{+/+}$ mice (9,33). Together, the hypothermia in HF-fed *Pemt*$^{-/-}$ mice is not caused by an impaired oxidative capacity in BAT.

Norepinephrine is considered to be the main effector of the sympathetic nervous system (11). Mice lacking dopamine β-hydroxylase, which is responsible for the synthesis of norepinephrine and epinephrine, are cold sensitive due to impaired activation of UCP1-mediated thermogenesis in BAT and peripheral vasoconstriction (34). Furthermore, mice lacking all three known β-adrenergic receptors exhibit reduced lipolysis in WAT, leading to adipose hypertrophy, and are intolerant to cold due to defective thermogenesis (35,36). We have shown that following cold exposure, plasma levels of norepinephrine and epinephrine were the same between genotypes (Figure 5.5A).

Cold exposure is known to stimulate lipolysis in both BAT and WAT to provide energy for thermogenesis. In BAT from *Pemt*$^{-/-}$ mice, the amounts of phospho-HSL and ATGL were the same as in *Pemt*$^{+/+}$ mice (Figure 5.5B), consistent with the observation that cold exposure reduced TG levels in BAT in both genotypes (Figure 5.5F vs Figure 5.3A). Cold exposure also raised plasma levels of fatty acids to the same levels in HF-fed *Pemt*$^{+/+}$ and *Pemt*$^{-/-}$ mice (Figure 5.6B), However, protein levels of phospho-HSL, ATGL and TGH proteins in WAT were higher in *Pemt*$^{-/-}$ mice than in *Pemt*$^{+/+}$ mice

(Figure 5.6A). Therefore, the hypothermia in HF-fed *Pemt*$^{-/-}$ mice is not due to impairment of cold-induced sympathetic activation of BAT or WAT.

BAT is highly vascularized (17) and cold exposure increases cardiac output and promotes blood flow to BAT (27). We found that systolic blood pressure was higher in HF-fed *Pemt*$^{-/-}$ mice than in HF-fed *Pemt*$^{+/+}$ mice (Figure 5.7A), consistent with the observation that hypertensive patients are often sensitive to cold (37); the HF-fed *Pemt*$^{-/-}$ mice also exhibited reduced cardiac output (Figure 5.7C), which might compensate for the high blood pressure. It is unlikely, however, that the increased blood pressure accounts for the hypothermia in HF-fed *Pemt*$^{-/-}$ mice because blood pressure was not decreased by choline supplementation and choline elevated blood pressure in *Pemt*$^{+/+}$ mice (Figure 5.8G).

5.4.2 Insufficient glucose supply is the primary cause of HF-induced hypothermia in *Pemt*$^{-/-}$ mice

BAT consumes not only fatty acids but also large amounts of glucose from blood (38,39). Cold exposure profoundly increases (by 95-fold) glucose uptake by BAT in rats (40). Chronic infusion of norepinephrine into rats via subcutaneously implanted mini-pumps also markedly increases (by ~50-fold) glucose uptake by BAT (41). Moreover, mice with transplanted BAT have lower body weight, improved glucose tolerance and increased insulin sensitivity, providing strong support for a fundamental role of BAT in global glucose homeostasis (42). Moreover, in humans, glucose uptake by BAT is reported to be temperature-sensitive (43,44), and cold exposure stimulates glucose uptake by BAT (45). Recent studies demonstrate that BAT in humans plays a

physiologically significant role in whole body glucose homeostasis, insulin sensitivity and energy expenditure (12,13).

Levels of plasma fatty acids and TG in HF-fed *Pemt*$^{-/-}$ mice were comparable to those in HF-fed *Pemt*$^{+/+}$ mice (Figure 5.10A), indicating an intact capability for mobilization of energy storage and fat supply for thermogenesis. Thus, the 49% lower level of plasma glucose in *Pemt*$^{-/-}$ mice compared to *Pemt*$^{+/+}$ mice (Figure 5.10A) might explain why these mice are hypothermic. Indeed, dietary choline supplementation completely reversed the hypothermia and the hypoglycemia in *Pemt*$^{-/-}$ mice (Figs. 7A and Figure 5.10A). In addition, the amounts of PEPCK and PGC1α in the livers of *Pemt*$^{-/-}$ mice were only 46% and 32%, respectively, of those in *Pemt*$^{+/+}$ mice (Figure 5.10C). These observations are consistent with the findings that PEMT deficiency impairs hepatic gluconeogenesis and reduces hepatic glycogen stores (10,46). The increased plasma glucose in HFCS-fed *Pemt*$^{-/-}$ mice is in agreement with the restored protein expression of PEPCK and an increase in PGC1α in the liver (Figure 5.10C). Indeed, HF-fed *Pemt*$^{-/-}$ mice show an attenuated hepatic gluconeogenesis and reduced hepatic glycogen; choline supplementation increases hepatic gluconeogenesis, plasma glucose and hepatic glycogen in HF-fed *Pemt*$^{-/-}$ mice (46). Thus, we conclude that compromised hepatic gluconeogenesis and diminished glycogen stores reduces plasma glucose in HF-fed *Pemt*$^{-/-}$ mice, leading to reduced supply of energy to BAT and consequently cold intolerance.

In summary, HF-fed *Pemt*$^{-/-}$ mice become hypothermic upon cold exposure. Our data show that the thermogenic capacity of BAT is intact in HF-fed *Pemt*$^{-/-}$ mice and also exclude hypertension as the main determinant of the hypothermia. Choline

supplementation prevents the hypothermia and restores the lower levels of plasma glucose. Thus, the impairment of hepatic gluconeogenesis in HF-fed *Pemt*$^{-/-}$ mice limits the supply of glucose to BAT and causes cold-induced hypothermia.

Table 5.1 Primers for real-time quantitative PCR

Abbreviations are: *Cpt1α*, carnitine palmitoyltransferase 1α; *Lcad*, long-chain acyl-CoA dehydrogenase; *Mcad*, medium-chain acyl-CoA dehydrogenase; *Pdk4*, pyruvate dehydrogenase kinase isozyme 4, *Nd1*, NADH dehydrogenase, subunit 1 (complex I); and *Lpl*, lipoprotein lipase.

gene	forward primer (5' -> 3')	reverse primer (5' -> 3')
β-Actin	AAG GCC AAC CGT GAA AAG AT	GTG GTA CGA CCA GAG GCA TAC
Cpt1α	TGA GTG GCG TCC TCT TTG G	CA GCG AGT AGC GCA TAG TCA TG
Mcad	TTA CCG AAG AGT TGG CGT ATG	ATC TTC TGG CCG TTG ATA ACA
Lcad	GCA AAA TAC TGG GCA TCT GAA	TCC GTG GAG TTG CAC ACA TT
Pdk4	CCA GGC CAA CCA ATC CAC A	AAC TAA AGA GGC GGT CAG TAA
Nd1	ACA CTT ATT ACA ACC CAA GAA CAC AT	TCA TAT TAT GGC TAT GGG TCA GG
Lpl	GAA AGG TGT GGG GAG ACA AG	TCT GTC AAA GGC ACT GAA CG

Table 5.2 PEMT deficiency results in reduced cardiac output

Cardiac function was determined by echocardiography. Data were expressed as means ± SEM. *P<0.05 vs wild type by Student *t*-test. Abbreviations are: HR, heart rate; s, systolic; d, diastolic; LVPW, left ventricle posterior wall thickness; LVID, left ventricle internal diameter; IVS, intraventricular septum thickness; LV, left ventricle; Vol, volume; Vel, velocity; IVRT, the left ventricle isovolumic relaxation time; IVCT, the left ventricle isovolumic contraction time; LA, left atrium inner diameter.

Parameters	***Pemt*$^{+/+}$** **n=6**	***Pemt*$^{-/-}$** **n=6**
HR (bpm)	522 ± 17.6	491 ± 2.7
LVPW:s (mm)	1.22 ± 0.05	1.07 ± 0.08
LVID:s (mm)	2.80 ± 0.09	2.95 ± 0.16
IVS:s (mm)	1.27 ± 0.04	1.10 ± 0.06*
LV Vol: s (μL)	29.18 ± 3.0	35.44 ± 4.4
LVPW:d (mm)	0.85 ± 0.02	0.80 ± 0.05
LVID:d (mm)	3.91 ± 0.12	3.79 ± 0.14
IVS:d (mm)	0.90 ± 0.03	0.85 ± 0.03
LV Vol:d (μL)	65.2 ± 4.9	65.0 ± 5.2
Stroke Vol.	36.1 ± 2.8	29.5 ± 1.9
Mitral E/A	1.28 ± 0.08	1.23 ± 0.03
Mitral E Vel (mm/sec)	904.6 ± 81.1	596.3 ± 40.7*
Mitral A Vel (mm/sec)	704.4 ± 40.5	488.8 ± 37.4*
IVRT (ms)	19.3 ± 0.6	21.0 ± 1.5
IVCT(ms)	11.54 ± 1.11	15.6 ± 0.79*
LA (mm)	1.91 ± 0.15	2.15 ± 0.09

Figure 5.1 PEMT protein is undetectable in BAT

Pemt$^{+/+}$ and *Pemt*$^{-/-}$ mice were fed the HF diet for 2 weeks. Immunoblots of PEMT and loading control calnexin in the liver, BAT, and WAT homogenates. The same amount of protein was loaded in each lane.

Figure 5.1

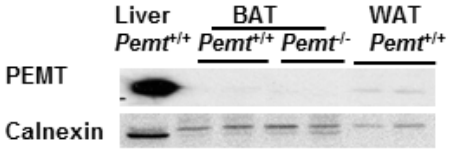

Figure 5.2 Chow-fed *Pemt*$^{-/-}$ mice do not develop hyperthermia upon cold exposure

Pemt$^{+/+}$ and *Pemt*$^{-/-}$ mice (10-11 weeks old) were fed standard chow diet. (A) The mass of phosphatidylcholine (PC), phosphatidylethanolamine (PE) and triacylglycerol (25), and the PC/PE ratio in BAT from mice with or without overnight fasting. (B) Representative immunoblots of fatty acid binding protein 4 (FABP4), CCAAT/enhancer-binding protein β (C/EBPβ), PPARγ coactivator 1α (PGC1α), uncoupling protein (UCP)1, electron transport chain complexes I-V and loading control glyceraldehyde 3-phosphate dehydrogenase (GAPDH). (C) Densitometric analysis for panel B. (D) Rates of complete ($^{14}CO_2$) and incomplete [^{14}C-acid-soluble metabolites (ASM)] fatty acid oxidation in BAT homogenates were measured by incubation with [1-^{14}C]palmitate. (E) Rectal temperature (temp.) during cold challenge. Mice were fasted for 4 h then placed at 4°C without bedding, food or water. All data were from 4-7 mice of each group; *p < 0.05 by two-way ANOVA for *Pemt*$^{+/+}$ *vs Pemt*$^{-/-}$.

Figure 5.2

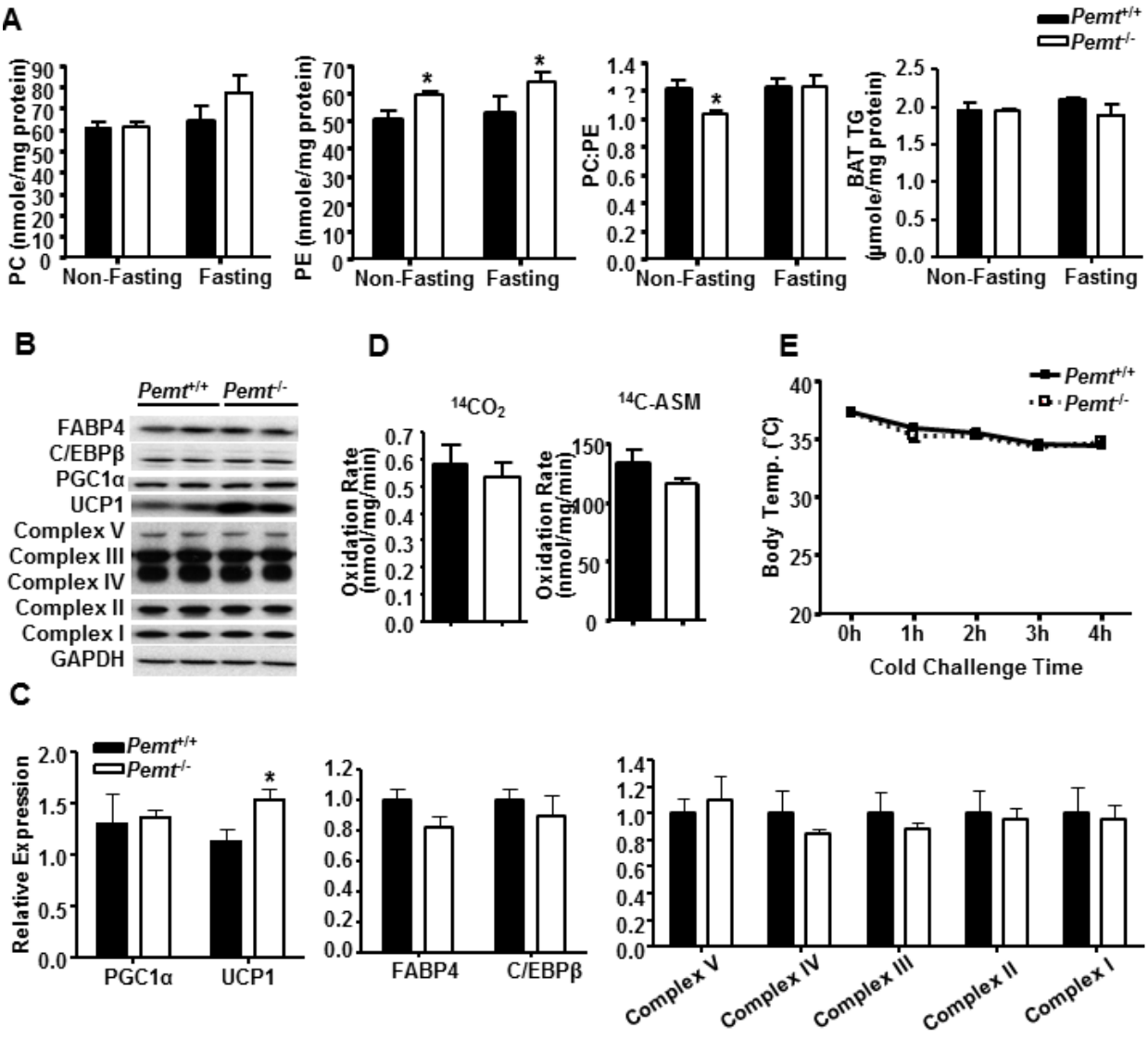
A
Pemt+/+
Pemt-/-
PC (nmole/mg protein)
PE (nmole/mg protein)
PC:PE
BAT TG (μmole/mg protein)
Non-Fasting
Fasting
B
Pemt+/+
Pemt-/-
FABP4
C/EBPβ
PGC1α
UCP1
Complex V
Complex III
Complex IV
Complex II
Complex I
GAPDH
D
14CO2
14C-ASM
Oxidation Rate (nmol/mg/min)
E
Body Temp. (°C)
0h
1h
2h
3h
4h
Cold Challenge Time
C
Relative Expression
PGC1α
UCP1
FABP4
C/EBPβ
Complex V
Complex IV
Complex III
Complex II
Complex I

Figure 5.3 Oxidative capacity in BAT from HF-fed *Pemt*$^{-/-}$ mice and *Pemt*$^{+/+}$ mice

Pemt$^{+/+}$ and *Pemt*$^{-/-}$ mice (8-9 weeks old) were fed the HF diet for 2 weeks. (A) The mass of phosphatidylcholine (PC), phosphatidylethanolamine (PE) and triacylglycerol (25) and the PC/PE ratio in BAT from mice with or without overnight fasting. (B-G) Data were from mice after overnight fasting. (B) Representative immunoblots of C/EBPβ, FABP4, PPARγ and their densitometric analysis relative to the loading control calnexin. (C) Weight of BAT as % body weight (B.W.). (D) Hematoxylin and eosin staining of BAT; size bar = 50 μm. (E) Representative immunoblots of PGC1α, UCP1, VDAC and electron transport chain complexes I-V and their densitometric analysis relative to the loading control calnexin. (F) Mitochondrial copy number was assessed as the ratio of mitochondrial DNA (Mito ND1) to nuclear DNA (nLPL). (G) The rates of complete ($^{14}CO_2$) and incomplete (^{14}C-ASM) fatty acid oxidation were measured in BAT homogenates. All data were from 4-7 mice of each group; $^{*}p < 0.05$ by two-way ANOVA for *Pemt*$^{+/+}$ *vs* *Pemt*$^{-/-}$; $^{\#}p < 0.05$ by two-way ANOVA, for the same genotype under fasting and non-fasting conditions.

Figure 5.3

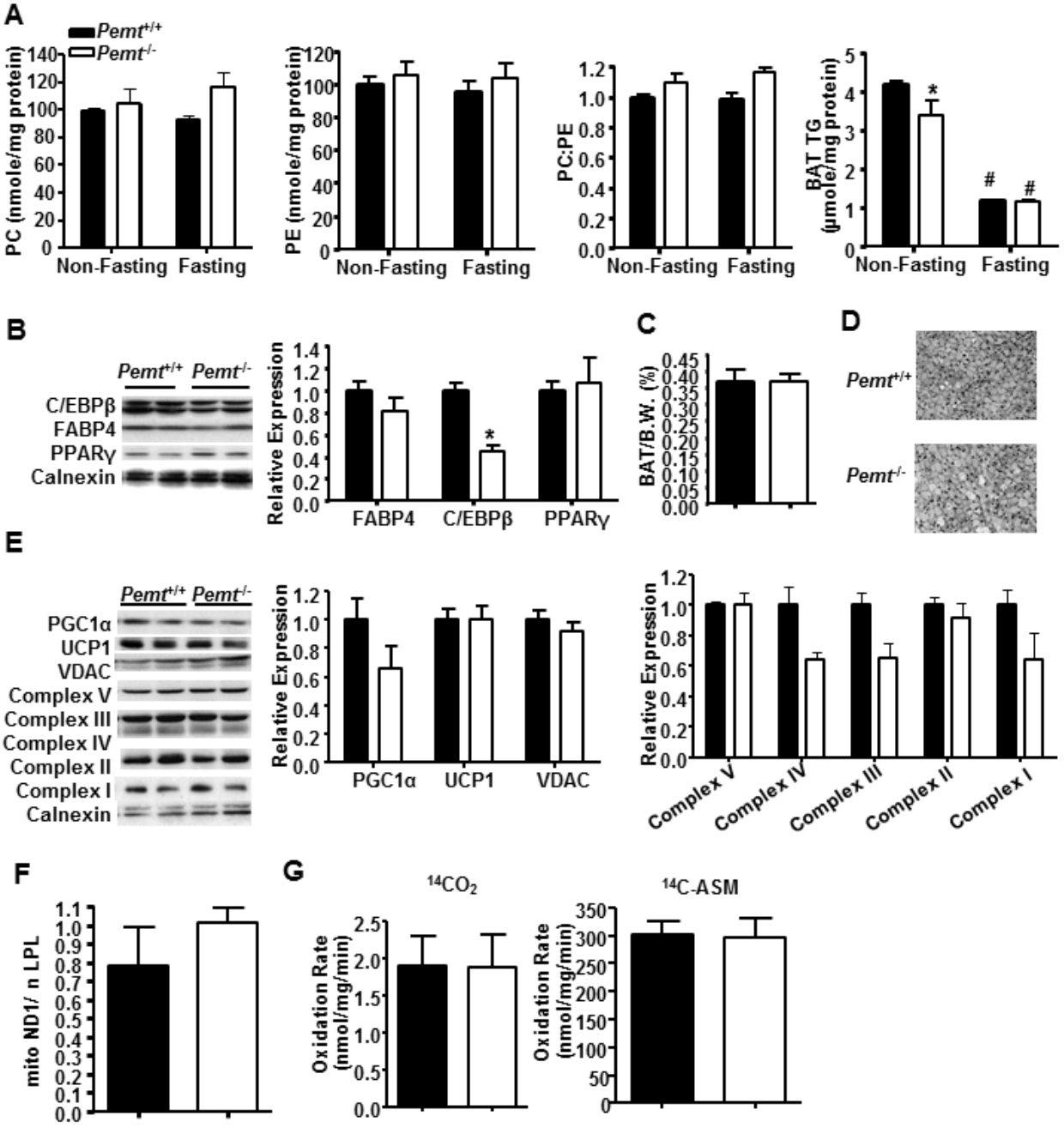
A
Pemt+/+
Pemt-/-
PC (nmole/mg protein)
PE (nmole/mg protein)
PC:PE
BAT TG (µmole/mg protein)
Non-Fasting
Fasting
B
C/EBPβ
FABP4
PPARγ
Calnexin
Relative Expression
C
BAT/B.W. (%)
D
E
PGC1α
UCP1
VDAC
Complex V
Complex III
Complex IV
Complex II
Complex I
F
mito ND1/ n LPL
G
14CO2
14C-ASM
Oxidation Rate (nmol/mg/min)

Figure 5.4 HF-fed *Pemt*$^{-/-}$ mice are hypothermic upon cold exposure

Pemt$^{+/+}$ and *Pemt*$^{-/-}$ mice (8-9 weeks old) were fed the HF diet for 2 weeks, followed by 4 h fasting and cold exposure. Rectal temperature was monitored during cold exposure hourly. Data were from 5-6 mice of each genotype; *$p < 0.05$ by Student *t*-test for *Pemt*$^{+/+}$ *vs Pemt*$^{-/-}$.

Figure 5.4

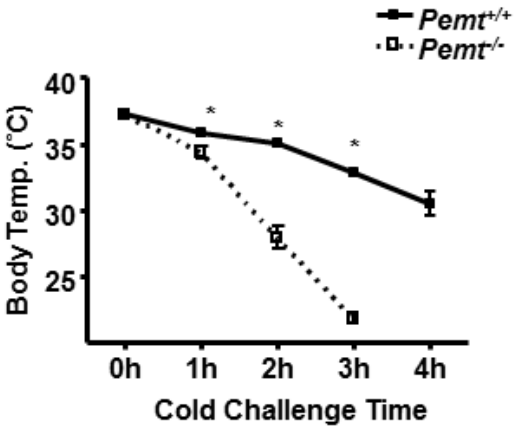
Pemt+/+
Pemt-/-
Body Temp. (°C)
40
35
30
25
*
*
*
0h
1h
2h
3h
4h
Cold Challenge Time

Figure 5.5 Oxidative capacity of BAT is not impaired in HF-fed *Pemt*$^{-/-}$ mice upon cold challenge

Pemt$^{+/+}$ and *Pemt*$^{-/-}$ mice (8-9 weeks old) were fed the HF diet for 2 weeks, followed by 4 h fasting and cold exposure. (A) Plasma levels of epinephrine (E) and norepinephrine (NE). (B) Representative immunoblots of lipolytic enzymes in BAT: phospho-hormone-sensitive lipase (p-HSL), total-HSL (HSL), ATGL (adipose triacylglycerol lipase), TGH (TG hydrolase). Amounts of the proteins were quantified by densitometric analysis relative to the loading control calnexin. (C) Representative immunoblots of PGC1α, UCP1, mitochondrial marker VDAC and the electron transport chain complexes I-V in BAT and their densitometric analysis relative to the loading control calnexin. (D) Mitochondrial copy number in BAT was assessed as the ratio of mitochondrial DNA (Mito ND1) to nuclear DNA (nLPL). (E) Levels of mRNAs encoding CPT1α (carnitine palmitoyltransferase 1α), LCAD (long-chain acyl-CoA dehydrogenase), MCAD (medium-chain acyl-CoA dehydrogenase) and PDK4 (pyruvate dehydrogenase kinase isozyme 4) in BAT. (F) Mass of TG in BAT. All data were from 4-7 mice of each group; *$p < 0.05$ by Student *t*-test for *Pemt*$^{+/+}$ *vs Pemt*$^{-/-}$.

Figure 5.5

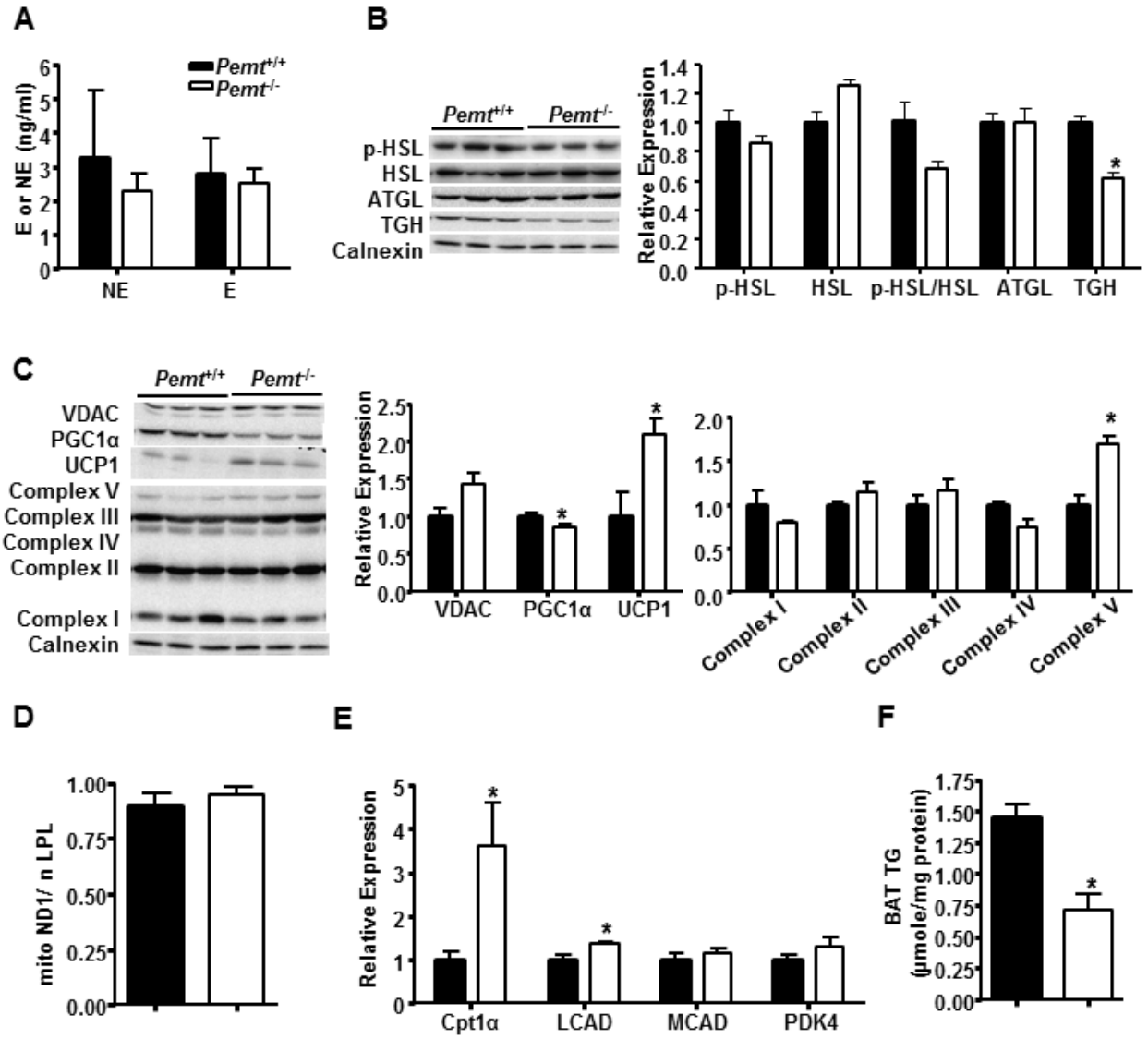
A
B
C
D
E
F
Pemt+/+
Pemt-/-
E or NE (ng/ml)
NE
E
p-HSL
HSL
ATGL
TGH
Calnexin
Relative Expression
p-HSL
HSL
p-HSL/HSL
ATGL
TGH
VDAC
PGC1α
UCP1
Complex V
Complex III
Complex IV
Complex II
Complex I
Calnexin
Complex I
Complex II
Complex III
Complex IV
Complex V
mito ND1/ n LPL
Cpt1α
LCAD
MCAD
PDK4
BAT TG
(μmole/mg protein)

Figure 5.6 Capacity for cold-stimulated TG lipolysis in WAT

Pemt$^{+/+}$ and *Pemt*$^{-/-}$ mice (8-9 weeks old) were fed the HF diet for 2 weeks followed by a 4 h fast and cold exposure. (A) Representative immunoblots of lipolytic enzymes: phospho-hormone-sensitive lipase (p-HSL), total-HSL (HSL), ATGL (adipose triacylglycerol lipase), TGH (TG hydrolase) and their densitometric analysis relative to the loading control glyceraldehyde 3-phosphate dehydrogenase (GAPDH). (B) Levels of plasma non-esterified fatty acids (NEFA). All data were from 5-7 mice of each group; *$p < 0.05$ by Student *t*-test for *Pemt*$^{+/+}$ *vs Pemt*$^{-/-}$.

Figure 5.6

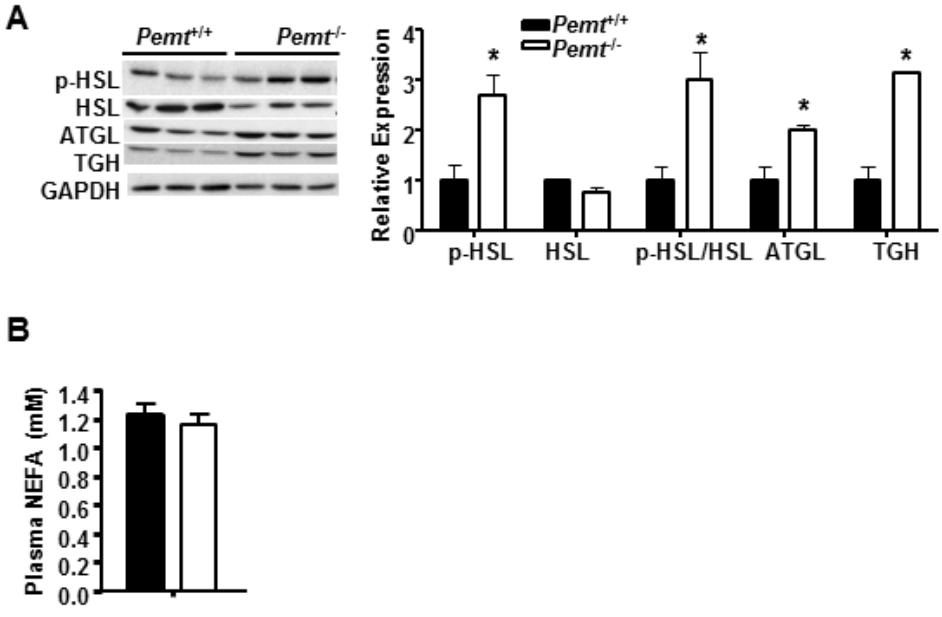
A
Pemt+/+
Pemt-/-
p-HSL
HSL
ATGL
TGH
GAPDH
Relative Expression
0
1
2
3
4
*
p-HSL
HSL
p-HSL/HSL
ATGL
TGH
B
Plasma NEFA (mM)
0.0
0.2
0.4
0.6
0.8
1.0
1.2
1.4

Figure 5.7 Blood pressure and cardiac output in HF-fed *Pemt*$^{+/+}$ and *Pemt*$^{-/-}$ mice

The mice were fed the HF diet for 2 weeks. (A) Systolic blood pressure was measured by a computerized tail cuff plethysmography system. (B) Heart mass was presented as % of body weight (B.W.) and as % of tibia length (cm). (C) *In vivo* cardiac function was determined by echocardiography: left ventricle ejection faction, fraction shortening and cardiac output. All data were from 5-6 mice of each genotype; *$p < 0.05$ by Student *t*-test for *Pemt*$^{+/+}$ *vs Pemt*$^{-/-}$.

Figure 5.7

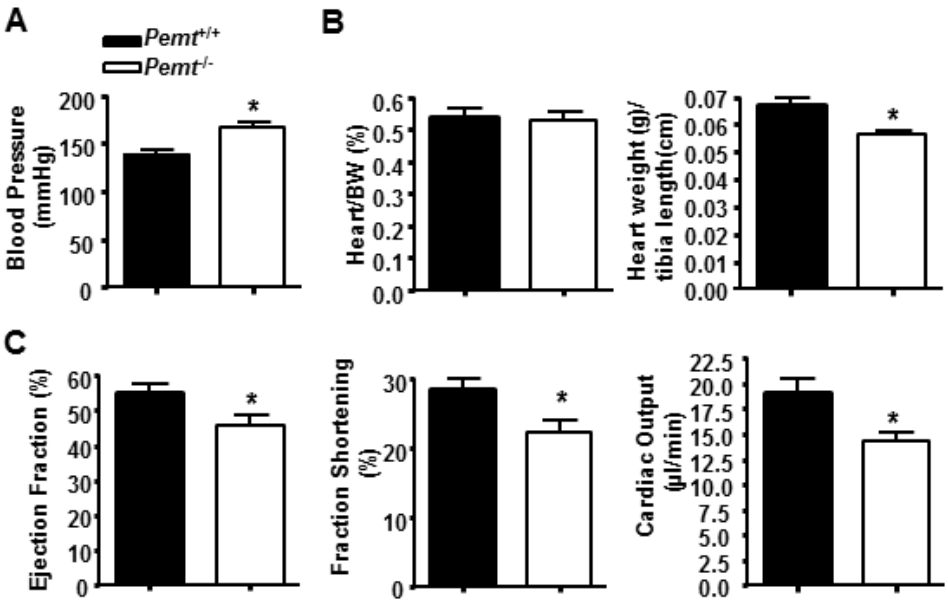
A
Pemt+/+
Pemt-/-
Blood Pressure (mmHg)
200
150
100
50
0
*
B
Heart/BW (%)
0.6
0.5
0.4
0.3
0.2
0.1
0.0
Heart weight (g)/ tibia length(cm)
0.07
0.06
0.05
0.04
0.03
0.02
0.01
0.00
*
C
Ejection Fraction (%)
60
50
40
30
20
10
0
*
Fraction Shortening (%)
30
20
10
0
*
Cardiac Output (µl/min)
22.5
20.0
17.5
15.0
12.5
10.0
7.5
5.0
2.5
0.0
*

Figure 5.8 Choline supplementation prevents hypothermia in HF-fed *Pemt*$^{-/-}$ mice

Pemt$^{+/+}$ and *Pemt*$^{-/-}$ mice were fed the HF or choline-supplemented HF (HFCS) diet for 2 weeks followed by a 4 h fast and cold exposure. (A) Rectal temperature during cold challenge. (B) Body weight (B.W.) gain during the 2 weeks of HF feeding. (C) BAT weight as % of B.W. (D) WAT weight as % of B.W. (E) Heart weight as % of B.W. (F) Kidney weight as % of B.W. (G) Systolic blood pressure in mice fed the HF or HFCS diet for 2 weeks without fasting or cold exposure. (H) Cold-induced weight loss in g (left panel) and as % of B.W. (right panel). (I) Fasting-induced weight loss in g (left panel) and as % of B.W. (right panel). All data were from 4-7 mice of each group; $^{*}p < 0.05$ by two-way ANOVA for *Pemt*$^{+/+}$ *vs* *Pemt*$^{-/-}$; $^{\#}p < 0.05$ by two-way ANOVA for HF diet *vs* HFCS diet with the same genotype.

Figure 5.8

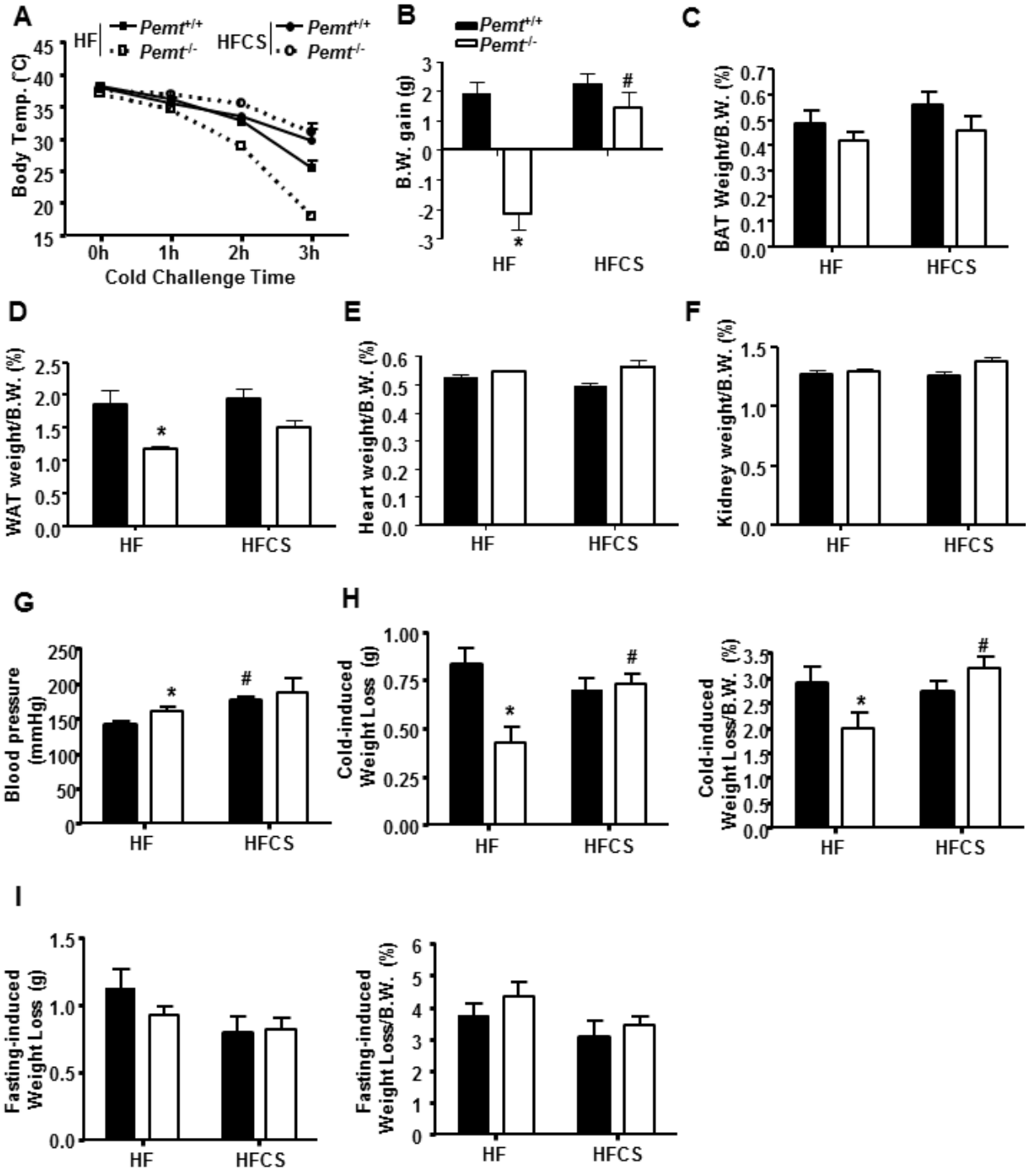
A
HF
Pemt+/+
Pemt-/-
HFCS
Pemt+/+
Pemt-/-
Body Temp. (°C)
Cold Challenge Time
0h
1h
2h
3h
B
Pemt+/+
Pemt-/-
B.W. gain (g)
HF
HFCS
C
BAT Weight/B.W. (%)
HF
HFCS
D
WAT weight/B.W. (%)
HF
HFCS
E
Heart weight/B.W. (%)
HF
HFCS
F
Kidney weight/B.W. (%)
HF
HFCS
G
Blood pressure (mmHg)
HF
HFCS
H
Cold-induced Weight Loss (g)
HF
HFCS
Cold-induced Weight Loss/B.W. (%)
HF
HFCS
I
Fasting-induced Weight Loss (g)
HF
HFCS
Fasting-induced Weight Loss/B.W. (%)
HF
HFCS

Figure 5.9 Plasma thyroid hormones in *Pemt*$^{+/+}$ and *Pemt*$^{-/-}$ mice fed the HF or HFCS diets for 2 weeks, followed by cold exposure

Plasma thyroid hormones: thyroxine T4 (left panel) and triiodothyronine T3 (right panel). All data were from 4-7 mice of each group; *p < 0.05 by two-way ANOVA, *Pemt*$^{+/+}$ *vs* *Pemt*$^{-/-}$; #p < 0.05 by two-way ANOVA, the same genotype under HF-feeding *vs* HFCS feeding.

Figure 5.9

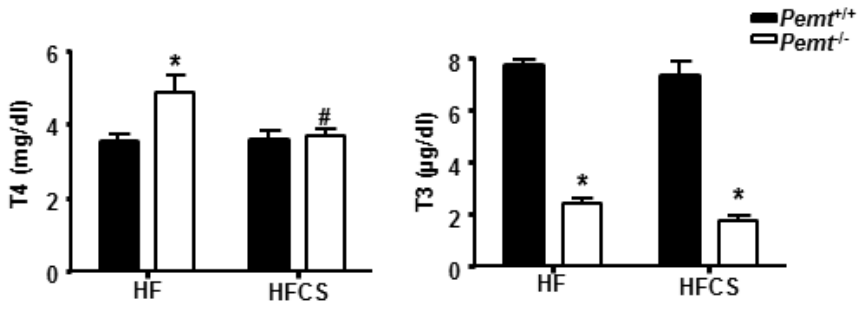

Figure 5.10 Choline normalizes reduced plasma glucose in HF-fed *Pemt*$^{-/-}$ mice

Pemt$^{+/+}$ and *Pemt*$^{-/-}$ mice were fed the HF diet or choline-supplemented HF diet (HFCS) for 2 weeks, followed by a 4 h fast and cold exposure. (A) Plasma levels of fatty acids (NEFA), triacylglycerol (25) and glucose. (B) Left panel: liver weight as % of body weight (B.W.); right panel: mass of hepatic TG. (C) Representative immunoblots of phosphoenolpyruvate carboxykinase (PEPCK), PGC1α, protein disulfide isomerase (PDI) and glyceraldehyde 3-phosphate dehydrogenase (GAPDH); amounts of proteins were quantified by densitometric analysis and normalized to amount of GAPDH. (D) Mass of TG in BAT. Data were from 4-7 mice of each group; $^{*}p < 0.05$ by two-way ANOVA for *Pemt*$^{+/+}$ *vs* *Pemt*$^{-/-}$; $^{\#}p < 0.05$ by two-way ANOVA for HF diet *vs* HFCS diet for the same genotype.

Figure 5.10

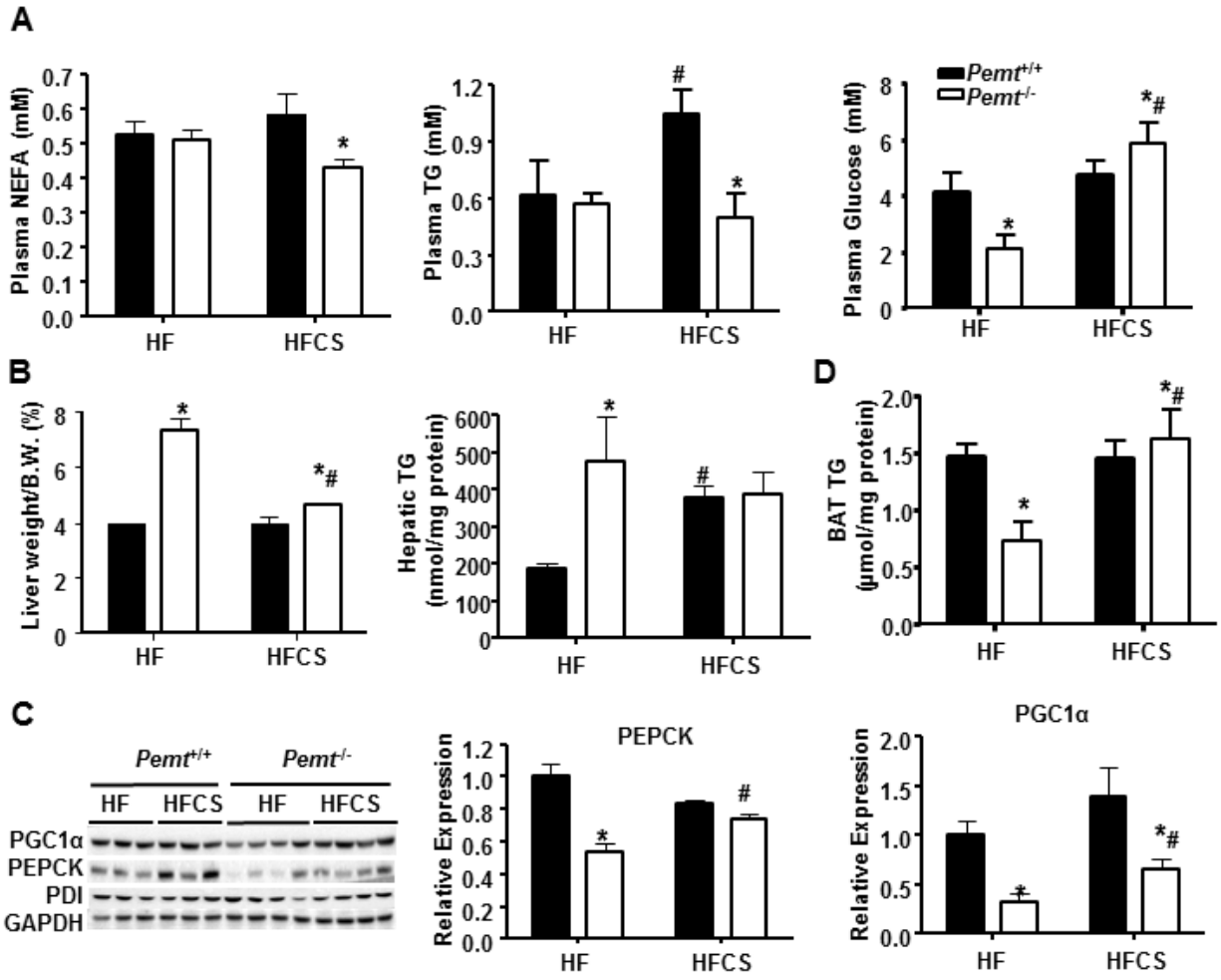
A
Plasma NEFA (mM)
Plasma TG (mM)
Plasma Glucose (mM)
Pemt+/+
Pemt-/-
HF
HFCS
B
Liver weight/B.W. (%)
Hepatic TG (nmol/mg protein)
D
BAT TG (μmol/mg protein)
C
Pemt+/+
Pemt-/-
HF
HFCS
PGC1α
PEPCK
PDI
GAPDH
Relative Expression
PEPCK
PGC1α

5.5 References

1. Vance, D. E. (2014) *Biochim Biophys Acta* **1838**, 1477-1487

2. DeLong, C. J., Shen, Y. J., Thomas, M. J., and Cui, Z. (1999) *J Biol Chem* **274**, 29683-29688

3. Reo, N. V., Adinehzadeh, M., and Foy, B. D. (2002) *Biochim Biophys Acta* **1580**, 171-188

4. Li, Z., Agellon, L. B., Allen, T. M., Umeda, M., Jewell, L., Mason, A., and Vance, D. E. (2006) *Cell Metab* **3**, 321-331

5. Jacobs, R. L., Devlin, C., Tabas, I., and Vance, D. E. (2004) *J Biol Chem* **279**, 47402-47410

6. Noga, A. A., and Vance, D. E. (2003) *J Biol Chem* **278**, 21851-21859

7. Yao, Z. M., and Vance, D. E. (1988) *J Biol Chem* **263**, 2998-3004

8. Niebergall, L. J., Jacobs, R. L., Chaba, T., and Vance, D. E. (2011) *Biochim Biophys Acta* **1811**, 1177-1185

9. Jacobs, R. L., Zhao, Y., Koonen, D. P., Sletten, T., Su, B., Lingrell, S., Cao, G., Peake, D. A., Kuo, M. S., Proctor, S. D., Kennedy, B. P., Dyck, J. R., and Vance, D. E. (2010) *J Biol Chem* **285**, 22403-22413

10. Ling, J., Chaba, T., Zhu, L. F., Jacobs, R. L., and Vance, D. E. (2012) *Hepatology* **55**, 1094-1102

11. Cannon, B., and Nedergaard, J. (2004) *Physiol Rev* **84**, 277-359

12. Chondronikola, M., Volpi, E., Borsheim, E., Porter, C., Annamalai, P., Enerback, S., Lidell, M. E., Saraf, M. K., Labbe, S. M., Hurren, N. M., Yfanti, C., Chao, T.,

Andersen, C. R., Cesani, F., Hawkins, H., and Sidossis, L. S. (2014) *Diabetes* **63**, 4089-4099

13. Matsushita, M., Yoneshiro, T., Aita, S., Kameya, T., Sugie, H., and Saito, M. (2014) *Int J Obes (Lond)* **38**, 812-817

14. Virtanen, K. A., Lidell, M. E., Orava, J., Heglind, M., Westergren, R., Niemi, T., Taittonen, M., Laine, J., Savisto, N. J., Enerback, S., and Nuutila, P. (2009) *N Engl J Med* **360**, 1518-1525

15. Cypess, A. M., Lehman, S., Williams, G., Tal, I., Rodman, D., Goldfine, A. B., Kuo, F. C., Palmer, E. L., Tseng, Y. H., Doria, A., Kolodny, G. M., and Kahn, C. R. (2009) *N Engl J Med* **360**, 1509-1517

16. Zingaretti, M. C., Crosta, F., Vitali, A., Guerrieri, M., Frontini, A., Cannon, B., Nedergaard, J., and Cinti, S. (2009) *FASEB J* **23**, 3113-3120

17. Peirce, V., Carobbio, S., and Vidal-Puig, A. (2014) *Nature* **510**, 76-83

18. Vergnes, L., Chin, R., Young, S. G., and Reue, K. (2011) *J Biol Chem* **286**, 380-390

19. Tomlinson, E., Fu, L., John, L., Hultgren, B., Huang, X., Renz, M., Stephan, J. P., Tsai, S. P., Powell-Braxton, L., French, D., and Stewart, T. A. (2002) *Endocrinology* **143**, 1741-1747

20. Wang, H., Yu, M., Ochani, M., Amella, C. A., Tanovic, M., Susarla, S., Li, J. H., Yang, H., Ulloa, L., Al-Abed, Y., Czura, C. J., and Tracey, K. J. (2003) *Nature* **421**, 384-388

21. Jacobs, R. L., Lingrell, S., Zhao, Y., Francis, G. A., and Vance, D. E. (2008) *J Biol Chem* **283**, 2147-2155

22. Hirschey, M. D., Shimazu, T., Goetzman, E., Jing, E., Schwer, B., Lombard, D. B., Grueter, C. A., Harris, C., Biddinger, S., Ilkayeva, O. R., Stevens, R. D., Li, Y., Saha, A. K., Ruderman, N. B., Bain, J. R., Newgard, C. B., Farese, R. V., Jr., Alt, F. W., Kahn, C. R., and Verdin, E. (2010) *Nature* **464**, 121-125

23. van der Veen, J. N., Lingrell, S., da Silva, R. P., Jacobs, R. L., and Vance, D. E. (2014) *Diabetes* **63**, 2620-2630

24. Odenbach, J., Wang, X., Cooper, S., Chow, F. L., Oka, T., Lopaschuk, G., Kassiri, Z., and Fernandez-Patron, C. (2011) *Hypertension* **57**, 123-130

25. Cole, L. K., Dolinsky, V. W., Dyck, J. R., and Vance, D. E. (2011) *Circ Res* **108**, 686-694

26. Liang, H., and Ward, W. F. (2006) *Adv Physiol Educ* **30**, 145-151

27. Jansky, L., and Hart, J. S. (1968) *Can J Physiol Pharmacol* **46**, 653-659

28. Alexander, G., Bell, A. W., and Hales, J. R. (1973) *J Physiol* **234**, 65-77

29. Wahren, J., and Ekberg, K. (2007) *Annu Rev Nutr* **27**, 329-345

30. Barnett, S. A., Coleman, E. M., and Manly, B. M. (1960) *Q J Exp Physiol Cogn Med Sci* **45**, 40-49

31. Meneghini, A., Ferreira, C., Abreu, L. C., Valenti, V. E., Ferreira, M., C, F. F., and Murad, N. (2009) *Clinics (Sao Paulo)* **64**, 921-926

32. Gao, X., van der Veen, J. N., Hermansson, M., Ordonez, M., Gomez-Munoz, A., Vance, D. E., and Jacobs, R. L. (2014) *Biochim Biophys Acta* **1851**, 152-162

33. Gao, X., van der Veen, J. N., Zhu, L., Chaba, T., Ordonez, M., Lingrell, S., Koonen, D. P., Dyck, J. R., Gomez-Munoz, A., Vance, D. E., and Jacobs, R. L. (2015) *J Hepatol* **62**, 913-920

34. Thomas, S. A., and Palmiter, R. D. (1997) *Nature* **387**, 94-97

35. Bachman, E. S., Dhillon, H., Zhang, C. Y., Cinti, S., Bianco, A. C., Kobilka, B. K., and Lowell, B. B. (2002) *Science* **297**, 843-845

36. Jimenez, M., Leger, B., Canola, K., Lehr, L., Arboit, P., Seydoux, J., Russell, A. P., Giacobino, J. P., Muzzin, P., and Preitner, F. (2002) *FEBS Lett* **530**, 37-40

37. Figueroa, J. J., Basford, J. R., and Low, P. A. (2010) *Cleve Clin J Med* **77**, 298-306

38. Townsend, K. L., and Tseng, Y. H. (2014) *Trends Endocrinol Metab* **25**, 168-177

39. Peirce, V., and Vidal-Puig, A. (2013) *Lancet Diabetes Endocrinol* **1**, 353-360

40. Shibata, H., Perusse, F., Vallerand, A., and Bukowiecki, L. J. (1989) *Am J Physiol* **257**, R96-101

41. Liu, X., Perusse, F., and Bukowiecki, L. J. (1994) *Am J Physiol* **266**, R914-920

42. Stanford, K. I., Middelbeek, R. J., Townsend, K. L., An, D., Nygaard, E. B., Hitchcox, K. M., Markan, K. R., Nakano, K., Hirshman, M. F., Tseng, Y. H., and Goodyear, L. J. (2013) *J Clin Invest* **123**, 215-223

43. Ouellet, V., Routhier-Labadie, A., Bellemare, W., Lakhal-Chaieb, L., Turcotte, E., Carpentier, A. C., and Richard, D. (2011) *J Clin Endocrinol Metab* **96**, 192-199

44. Persichetti, A., Sciuto, R., Rea, S., Basciani, S., Lubrano, C., Mariani, S., Ulisse, S., Nofroni, I., Maini, C. L., and Gnessi, L. (2013) *PLoS One* **8**, e63391

45. Orava, J., Nuutila, P., Lidell, M. E., Oikonen, V., Noponen, T., Viljanen, T., Scheinin, M., Taittonen, M., Niemi, T., Enerback, S., and Virtanen, K. A. (2011) *Cell Metab* **14**, 272-279

46. Wu, G., Zhang, L., Li, T., Zuniga, A., Lopaschuk, G. D., Li, L., Jacobs, R. L., and Vance, D. E. (2013) *J Biol Chem* **288**, 837-847

Chapter 6

Conclusion and Future Directions

6.1 Conclusion

PEMT is only quantitatively significant for PC production in the liver, contributing to ~30% of hepatic PC production, with the remaining ~70% deriving from the CDP-choline pathway (1,2). Inhibition of either the PEMT pathway or the CDP-choline pathway results in steatosis (3), which is largely due to reduced hepatic PC production and impaired VLDL secretion from the liver (4). Unexpectedly, *Pemt*$^{-/-}$ mice are protected from HF-induced obesity, whereas *LCTα*$^{-/-}$ mice are not (5). Upon HF feeding, both *Pemt*$^{-/-}$ and *LCTα*$^{-/-}$ mice develop NASH (5). The experiments outlined in this thesis provide insights into the underlying mechanisms (summarized in Figure 6.1) by which HF-fed *Pemt*$^{-/-}$ mice are protected from DIO but develop NASH.

The vagus nerve is implicated in regulating energy metabolism via relaying signals through afferent and efferent nerve fibers (6). In chapter 2, complete hepatic vagotomy (HV), disrupting both the afferent and efferent vagus nerve, prevents the development of HF-induced NASH in *Pemt*$^{-/-}$ mice, but also promotes diet-induced weight gain and insulin resistance. These effects are associated with elevated hepatic PC, improved hepatic energy metabolism, and reduced global energy metabolism. It appears that in *Pemt*$^{-/-}$ mice HF-induced NASH and obesity are closely related to each other. In addition, HV decreases the elevated heat production throughout light and dark cycles in HF-fed *Pemt*$^{-/-}$ mice, indicating the alteration of global metabolism could be at least partially attributed to thermogenesis. Regardless, these experiments clearly show that neuronal signals relayed through the hepatic vagus nerve are involved in the protection against DIO and the development of NASH in HF-fed *Pemt*$^{-/-}$ mice. The majority (80%) of vagus nerve fibers are afferent fibers (7). Afferent vagus nerves originating from the

liver have been shown to be of great importance in energy metabolism (8-11). However, deafferentation of the hepatic vagus nerve by capsaicin has no significant effect on either the protection against DIO or the HF-induced NASH in *Pemt*$^{-/-}$ mice. Together, these studies highlight the physiological importance of neuronal signals via the hepatic branch of the vagus nerve, in particular the efferent nerves, in the protection against DIO and the development of NASH in HF-fed *Pemt*$^{-/-}$ mice.

Acetylcholine is the major neurotransmitter released from the vagal efferent endings (12). Acetylcholine acts through acetylcholine receptors in the central and peripheral tissues. In the brain, muscarinic acetylcholine receptors mediated cholinergic signals are implicated in the development of DIO (13,14). In the peripheral tissues, α7 nicotinic acetylcholine receptor (nAChR) plays a principle role in the cholinergic inflammatory reflex (15,16). Interestingly, the protection against DIO in HF-fed *Pemt*$^{-/-}$ mice is prevented by dietary addition of choline (5). The development of NASH in HF-fed *Pemt*$^{-/-}$ mice is also alleviated by dietary choline supplementation (17). Furthermore, ongoing studies in our lab suggest that HF-fed *Pemt*$^{-/-}$ mice are choline deficient (i.e. exhibiting reduced levels of choline metabolites in plasma, including choline, phosphocholine and glycerophosphocholine (unpublished data). PEMT is the only known endogenous pathway for choline production. Thus, our studies on the hepatic vagus nerve also underscore the importance of PEMT-mediated endogenous choline production in the transmission of neuronal signals via the vagus nerve, in response to excess calories.

The ER is involved in various cellular functions such as the synthesis of proteins and lipids, calcium homeostasis and drug metabolism (18,19). In response to ER stress

caused by protein overload, the UPR is activated to restore cellular homeostasis (20). ER stress is associated with symptoms of metabolic syndrome, including obesity and fatty liver disease (19,21-23). In mouse livers, PEMT is located in the ER and MAM (mitochondrial-associated membranes) (24). Lack of PEMT leads to accumulation of hepatic PE (25). In Chapter 3, PEMT deficiency results in lower PC and higher PE in the ER fractions isolated from chow-fed mouse livers, resulting in a reduced PC/PE ratio. The livers from chow-fed *Pemt*$^{-/-}$ mice, where there is negligible amount of TG accumulation, exhibit ER stress, but no activation of the UPR. Similarly, McA-RH7777 cells, lacking PEMT activity, also show increased cellular PE and a decreased PC/PE ratio, in comparison to McA-RH7777 cells expressing human PEMT. Although the cellular TG levels are comparable, McA-RH7777 cells demonstrate ER stress and an activated UPR. Thus, PEMT deficiency appears to lead to ER stress by altering the phospholipid composition and PC/PE ratio in the ER. Taking the previous finding in *ob/ob* mice, where an increased PC/PE ratio in hepatic ER is associated with ER stress, into consideration, it is proposed that an altered PC/PE ratio, either higher or lower than the normal value will lead to ER stress (Figure 3.10). Furthermore, the HF diet causes more intensive ER stress and more active UPR in the livers from *Pemt*$^{-/-}$ mice than from *Pemt*$^{+/+}$ mice. Thus, the predisposition to ER stress in *Pemt*$^{-/-}$ mice likely sensitizes the livers to HF-induced NASH. Based on these findings, PBA, a FDA-approved chemical ER chaperone, has been applied to alleviate ER stress in McA-RH7777 cells and HF-fed *Pemt*$^{-/-}$ mice. PBA improves ER stress and inactivates the UPR in McA-RH7777 cells. However, PBA does not reduce hepatic ER stress or the progression of NASH in HF-fed *Pemt*$^{-/-}$ mice. Moreover, PBA treatment did reduce hepatic lipid accumulation

and apoptotic signalling in HF-fed *Pemt*$^{-/-}$ mice. Together, for the first time, alteration of phospholipid compositions in the ER, in particular a reduction in the PC/PE ratio was identified to be a cause for ER stress. Predisposition to the ER stress in the liver caused by PEMT deficiency sensitizes the liver to HF-induced NASH.

WAT functions as an energy storage tissue and an active endocrine organ. PEMT has been reported to be present in WAT, as well as in 3T3-L1 adipocytes (26,27). PEMT is concomitantly and strongly induced during 3T3-L1 adipocyte differentiation and attenuation of PEMT in 3T3-L1 adipocytes increases basal TG lipolysis (27). Following these findings, (gonadal) WAT in *Pemt*$^{-/-}$ mice were closely examined in *Pemt*$^{+/+}$ and *Pemt*$^{-/-}$ mice fed the HF diet for 2 weeks, after which *Pemt*$^{-/-}$ mice already show WAT hypotrophy and fatty liver versus *Pemt*$^{+/+}$ mice (Chapter 4). The PC and PE mass in WAT is not different between genotypes, although polyunsaturated PC species (16:0/18:2, 18:0/18:2, 18:0/18:3) are slightly decreased in *Pemt*$^{-/-}$ versus *Pemt*$^{+/+}$ mice. In addition, WAT explants from *Pemt*$^{-/-}$ mice show reduced incorporation of PC from oleic acid and a reduction in lipogenesis. PEMT deficiency has no effect on adipocyte differentiation and lipolytic capability in WAT. Moreover, the endocrine function of WAT appears to be intact in *Pemt*$^{-/-}$ mice, since the levels of cytokines and chemokines in WAT are the same *Pemt*$^{+/+}$ mice. Together, a reduced lipogenesis in WAT contributes to the resistance to DIO in *Pemt*$^{-/-}$ mice.

Contrary to WAT, BAT is a highly oxidative and innervated tissue (28). BAT-mediated thermogenesis through UCP1 is critical in regulating the whole body energy metabolism (28-30). PEMT mRNA has been detected in BAT from five-day-old *Pemt*$^{+/+}$ mice (27). But the contribution of BAT-mediated thermogenesis to the protection against

DIO in *Pemt*$^{-/-}$ mice is unknown. Thus, the capability of thermogenesis under cold stimulation in *Pemt*$^{-/-}$ mice fed either standard chow diet or the HF diet was explored in Chapter 5. PEMT protein and enzyme activity are undetectable in BAT from adult mice. *Pemt*$^{-/-}$ mice fed standard chow diet show intact thermogenic features and are able to maintain their body temperature upon cold exposure. However, when placed on the HF diet for 2 weeks, *Pemt*$^{-/-}$ mice are cold sensitive, although the capacity for thermogenesis and lipolysis in BAT remain intact. The cold-stimulated energy mobilization from WAT is also normal in *Pemt*$^{-/-}$ mice as in *Pemt*$^{+/+}$ mice. Interestingly, HF-fed *Pemt*$^{-/-}$ mice are hypertensive, accompanied with reduced cardiac output. However, dietary addition of choline prevents the HF-induced hypothermia in *Pemt*$^{-/-}$ mice upon cold exposure, but not the higher blood pressure. On the other hand, dietary addition of choline increases plasma glucose, potentially via improving the impaired hepatic gluconeogenesis in HF-fed *Pemt*$^{-/-}$ mice. The alteration of plasma glucose appears to be associated with levels of stored TG in BAT. Together, we have shown a functional link between PEMT and thermogenesis, although it remains to be determined whether the heat production in BAT from HF-fed *Pemt*$^{-/-}$ mice under physiological condition is indeed increased. Moreover, our findings highlight the importance of glucose as a substrate for thermogenesis during cold exposure in mice.

In summary, PEMT is functionally significant in the liver, and also present in WAT, but not in BAT. The vagal signals, particularly transmitted through the hepatic vagal efferent nerve, are directly involved in the protection against DIO and HF-induced NASH in *Pemt*$^{-/-}$ mice. PEMT deficiency in the liver causes ER stress via altering the phospholipid composition in the ER, which predisposed the liver to the HF-induced

NASH progression. PEMT deficiency results in reduced lipogenesis in WAT, which contributes to the lack of WAT hypertrophy in HF-fed *Pemt*$^{-/-}$ mice. While it remains to be determined whether BAT-mediated thermogenesis is increased under physiological conditions, PEMT is important for maintaining body temperature during cold exposure, through regulating the supply of plasma glucose.

Beyond revealing the mechanisms for the protection against DIO and the development of HF-induced NASH in *Pemt*$^{-/-}$ mice, this thesis also suggests potential treatment strategies for obesity and NASH in humans. Hepatic vagotomy, a surgical procedure for treating peptic ulcers (31,32), could be applied to patients with obesity (33) and NASH. Targeting ER stress could also be beneficial to alleviate ER stress-associated metabolic conditions (34). Although PBA does not fully prevent the NASH progression in HF-fed *Pemt*$^{-/-}$ mice, it does improve lipid accumulation and apoptosis in their livers. Herein, other chemical chaperones or alternative strategies targeting ER stress might be beneficial for treatment of NASH.

The studies outlined in this thesis further support that HF-fed *Pemt*$^{-/-}$ mice could be a useful mouse model for studying NASH. To understand the development of NASH, from onset to progression, and to further pursue potential treatments, NASH models with adequate resemblance to human NASH are in demand. However, there are limitations for all current mouse models (35,36). As in humans, mice fed the HF or western-type diet display weight gain and insulin resistance, but they do not develop severe NASH as other mouse models such as mice fed methionine and choline deficient (MCD) diet (36). In addition, the development of NASH in such mouse models requires long periods of feeding (37,38). Mice with genetic defects such as lack of leptin

(*ob/ob* mice) have also been extensively studied. The drawbacks of this genetic mouse model rely on the controversial association between leptin and NAFLD in humans (36,39), and on the requirement for a "second hit" such as HF for the progression from steatosis to NASH (36,40). The MCD model is by far the most widely used NASH mouse model. Mice rapidly develop steatosis within one week of the MCD diet, mainly due to the increased uptake of fatty acids and reduced secretion of VLDL (35). Unlike obesity associated NASH in humans, these mice are insulin sensitive and exhibit dramatic weight loss (35% over four weeks of feeding) (41,42). Due to these limitations, consideration should be taken into extrapolating studies in these mouse models to causes for progression of NASH in humans.

HF-fed *Pemt*$^{-/-}$ mice are a useful model for NASH as supported by the current studies, as well as previous reports. *Pemt*$^{-/-}$ mice show liver failure within three days when fed a choline deficient diet (43). When fed the HF diet, *Pemt*$^{-/-}$ mice develop NASH within two weeks (17). HF-fed *Pemt*$^{-/-}$ mice are insulin sensitive as in the MCD model, but they exhibit no weight loss (5,17). Thus, HF-fed *Pemt*$^{-/-}$ mice are better than the MCD model in the sense of no body weight loss. The thesis further unravels the underlying mechanisms for NASH development in HF-fed *Pemt*$^{-/-}$ mice: both neuronal signals via the vagus nerve and predisposition to ER stress in the liver are involved; and an impaired autophagy might also contribute to HF-induced NASH in *Pemt*$^{-/-}$ mice.

6.2 Future directions

While studies here have greatly enhanced our understanding of PEMT and its functional significance in obesity, fatty liver and thermogenesis, a few aspects might be

worthwhile for future investigation. Following the lead in Chapter 2, it is likely that acetylcholine is the signal transmitted through the vagus nerve that is implicated in the protection against DIO and NASH progression in HF-fed *Pemt*$^{-/-}$ mice. To support this hypothesis, the resistance to DIO in HF-fed *Pemt*$^{-/-}$ mice is reversed by dietary choline supplementation (5) and NASH development in these mice is also alleviated by choline (17). In addition to acting as a substrate for PC production via the CDP-choline pathway, choline is also the precursor for acetylcholine. The vagal efferent effect is regulated mainly by the release of acetylcholine in the central and the peripheral tissues (12). Future investigations would shed light on the role of acetylcholine and further on how it functions: in the peripheral via the nAChR, or in the central via muscarinic acetylcholine receptor, or both. A second interesting finding is the impaired autophagy in the livers from HF-fed *Pemt*$^{-/-}$ mice in Chapter 3. Autophagy, a newly defined cell "self-eating" process, has been shown to be implicated in various pathological conditions, as well as in fatty liver (44,45). Although the accumulation of cellular PE in the livers from *Pemt*$^{-/-}$ mice increases lipidation of LC3, which is required for the extension and formation of autophagosomes, the autophagic flow is impaired, reflected by accumulation of autophagy target protein p62. It would be interesting to determine whether HF-induced NASH in *Pemt*$^{-/-}$ mice is attributed to this impaired autophagy. One last unresolved puzzle is located in Chapter 5, where HF-fed *Pemt*$^{-/-}$ mice are hypertensive and show a reduced cardiac output. It is largely unknown regarding the mechanisms by which these mice are hypertensive and the correlation between hypertension and the resistance to DIO and/or NASH in HF-fed *Pemt*$^{-/-}$ mice.

Figure 6.1 Summary of mechanisms for the resistance to DIO and the development in HF-fed *Pemt*$^{-/-}$ mice

PEMT is functionally significant in the liver, and also present in WAT, but not in BAT. Studies in Chapter 2 suggest that the vagal signals, particularly transmitted through the hepatic vagal efferent nerve, are implicated in the protection against DIO and the development of NASH in HF-fed *Pemt*$^{-/-}$ mice. Studies in Chapter 3 demonstrate that PEMT deficiency in the liver alters the phospholipid composition in the ER, causes ER stress, and this predisposition to ER stress sensitizes the liver to the HF-induced NASH progression. In Chapter 4, PEMT deficiency is shown to result in reduced lipogenesis in WAT, which contributes to the protection against DIO in HF-fed *Pemt*$^{-/-}$ mice. Although it remains to be determined whether BAT-mediated thermogenesis is increased under physiological conditions, studies in Chapter 5 show that PEMT is important for maintaining body temperature during cold exposure, through regulating the supply of plasma glucose derived from the liver.

Figure 6.1

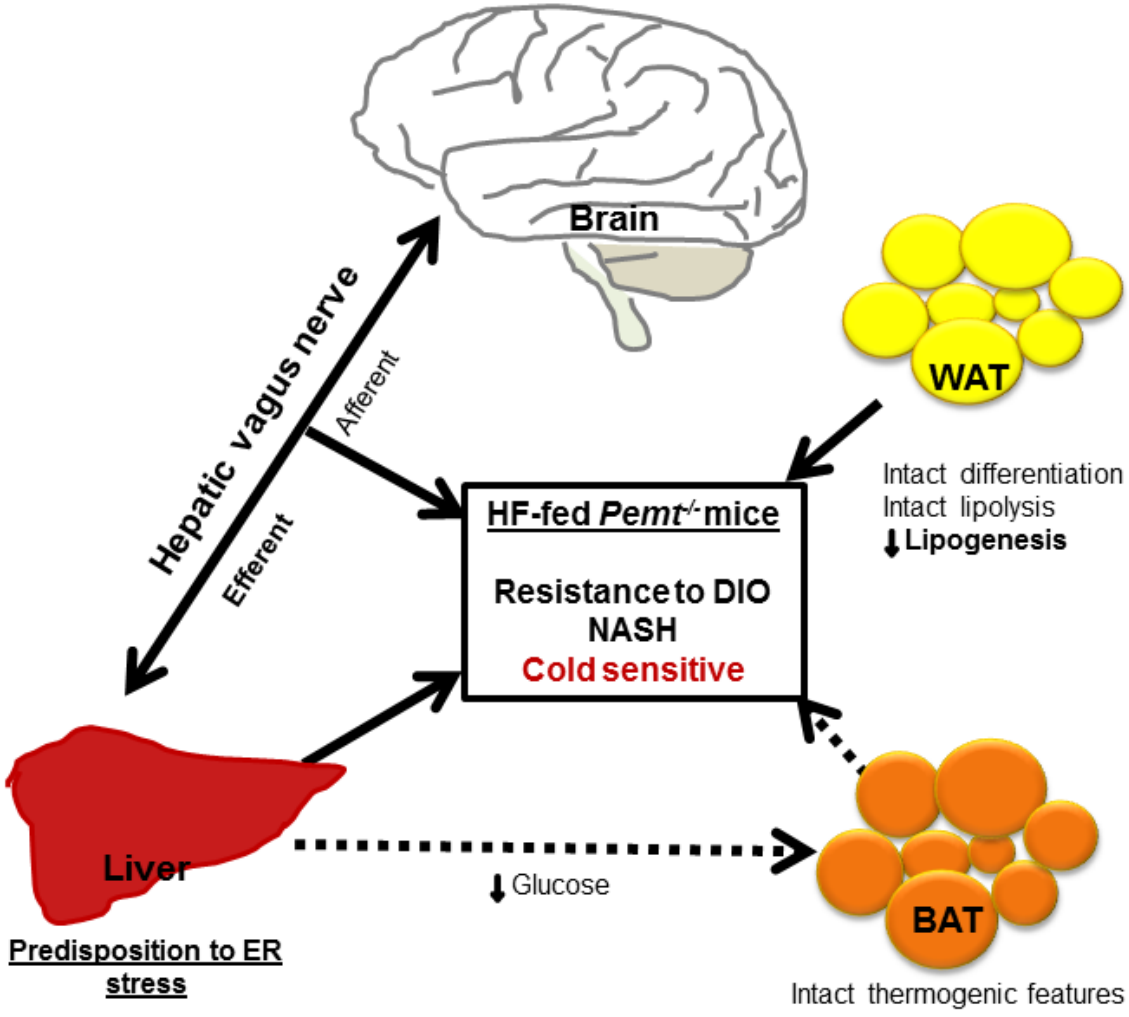
Brain
Hepatic vagus nerve
Afferent
Efferent
WAT
Intact differentiation
Intact lipolysis
⬇Lipogenesis
HF-fed Pemt-/- mice
Resistance to DIO
NASH
Cold sensitive
Liver
Predisposition to ER stress
⬇Glucose
BAT
Intact thermogenic features

6.3 References

1. Reo, N. V., Adinehzadeh, M., and Foy, B. D. (2002) *Biochim Biophys Acta* **1580**, 171-188
2. DeLong, C. J., Shen, Y. J., Thomas, M. J., and Cui, Z. (1999) *J Biol Chem* **274**, 29683-29688
3. Niebergall, L. J., Jacobs, R. L., Chaba, T., and Vance, D. E. (2011) *Biochim Biophys Acta* **1811**, 1177-1185
4. Noga, A. A., and Vance, D. E. (2003) *J Biol Chem* **278**, 21851-21859
5. Jacobs, R. L., Zhao, Y., Koonen, D. P., Sletten, T., Su, B., Lingrell, S., Cao, G., Peake, D. A., Kuo, M. S., Proctor, S. D., Kennedy, B. P., Dyck, J. R., and Vance, D. E. (2010) *J Biol Chem* **285**, 22403-22413
6. Katagiri, H., Yamada, T., and Oka, Y. (2007) *Circ Res* **101**, 27-39
7. Berthoud, H. R., and Neuhuber, W. L. (2000) *Auton Neurosci* **85**, 1-17
8. Uno, K., Katagiri, H., Yamada, T., Ishigaki, Y., Ogihara, T., Imai, J., Hasegawa, Y., Gao, J., Kaneko, K., Iwasaki, H., Ishihara, H., Sasano, H., Inukai, K., Mizuguchi, H., Asano, T., Shiota, M., Nakazato, M., and Oka, Y. (2006) *Science* **312**, 1656-1659
9. Imai, J., Katagiri, H., Yamada, T., Ishigaki, Y., Suzuki, T., Kudo, H., Uno, K., Hasegawa, Y., Gao, J., Kaneko, K., Ishihara, H., Niijima, A., Nakazato, M., Asano, T., Minokoshi, Y., and Oka, Y. (2008) *Science* **322**, 1250-1254
10. Bernal-Mizrachi, C., Xiaozhong, L., Yin, L., Knutsen, R. H., Howard, M. J., Arends, J. J., Desantis, P., Coleman, T., and Semenkovich, C. F. (2007) *Cell Metab* **5**, 91-102

11. Izumida, Y., Yahagi, N., Takeuchi, Y., Nishi, M., Shikama, A., Takarada, A., Masuda, Y., Kubota, M., Matsuzaka, T., Nakagawa, Y., Iizuka, Y., Itaka, K., Kataoka, K., Shioda, S., Niijima, A., Yamada, T., Katagiri, H., Nagai, R., Yamada, N., Kadowaki, T., and Shimano, H. (2013) *Nat Commun* **4**, 2316

12. Pavlov, V. A., Parrish, W. R., Rosas-Ballina, M., Ochani, M., Puerta, M., Ochani, K., Chavan, S., Al-Abed, Y., and Tracey, K. J. (2009) *Brain Behav Immun* **23**, 41-45

13. Gautam, D., Gavrilova, O., Jeon, J., Pack, S., Jou, W., Cui, Y., Li, J. H., and Wess, J. (2006) *Cell Metab* **4**, 363-375

14. Maresca, A., and Supuran, C. T. (2008) *Expert Opinion on Therapeutic Targets* **12**, 1167-1175

15. Wang, H., Yu, M., Ochani, M., Amella, C. A., Tanovic, M., Susarla, S., Li, J. H., Yang, H., Ulloa, L., Al-Abed, Y., Czura, C. J., and Tracey, K. J. (2003) *Nature* **421**, 384-388

16. Borovikova, L. V., Ivanova, S., Zhang, M., Yang, H., Botchkina, G. I., Watkins, L. R., Wang, H., Abumrad, N., Eaton, J. W., and Tracey, K. J. (2000) *Nature* **405**, 458-462

17. Ling, J., Chaba, T., Zhu, L. F., Jacobs, R. L., and Vance, D. E. (2012) *Hepatology* **55**, 1094-1102

18. Pagliassotti, M. J. (2012) *Annu Rev Nutr* **32**, 17-33

19. Hummasti, S., and Hotamisligil, G. S. (2010) *Circ Res* **107**, 579-591

20. Ron, D., and Walter, P. (2007) *Nat Rev Mol Cell Biol* **8**, 519-529

21. Fu, S., Watkins, S. M., and Hotamisligil, G. S. (2012) *Cell Metab* **15**, 623-634

22. Hotamisligil, G. S. (2010) *Cell* **140**, 900-917

23. Ozcan, U., Cao, Q., Yilmaz, E., Lee, A. H., Iwakoshi, N. N., Ozdelen, E., Tuncman, G., Gorgun, C., Glimcher, L. H., and Hotamisligil, G. S. (2004) *Science* **306**, 457-461

24. Cui, Z., Vance, J. E., Chen, M. H., Voelker, D. R., and Vance, D. E. (1993) *J Biol Chem* **268**, 16655-16663

25. Walkey, C. J., Donohue, L. R., Bronson, R., Agellon, L. B., and Vance, D. E. (1997) *Proc Natl Acad Sci U S A* **94**, 12880-12885

26. Cole, L. K., and Vance, D. E. (2010) *J Biol Chem* **285**, 11880-11891

27. Horl, G., Wagner, A., Cole, L. K., Malli, R., Reicher, H., Kotzbeck, P., Kofeler, H., Hofler, G., Frank, S., Bogner-Strauss, J. G., Sattler, W., Vance, D. E., and Steyrer, E. (2011) *J Biol Chem* **286**, 17338-17350

28. Cannon, B., and Nedergaard, J. (2004) *Physiol Rev* **84**, 277-359

29. Chondronikola, M., Volpi, E., Borsheim, E., Porter, C., Annamalai, P., Enerback, S., Lidell, M. E., Saraf, M. K., Labbe, S. M., Hurren, N. M., Yfanti, C., Chao, T., Andersen, C. R., Cesani, F., Hawkins, H., and Sidossis, L. S. (2014) *Diabetes* **63**, 4089-4099

30. Matsushita, M., Yoneshiro, T., Aita, S., Kameya, T., Sugie, H., and Saito, M. (2014) *Int J Obes (Lond)* **38**, 812-817

31. Sachdeva, A. K., Zaren, H. A., and Sigel, B. (1991) *Med Clin North Am* **75**, 999-1012

32. Chang, T. M., Chan, D. C., Liu, Y. C., Tsou, S. S., and Chen, T. H. (2001) *Am J Surg* **181**, 372-376

33. Boss, T., Peters, J., Patti, M., Lustig, R., and Kral, J. (2007) Laparoscopic truncal vagotomy for weight-loss: initial experience in 15 patients from a prospective, multi-center study [Abstract]. in *Scientific Session of the Society of American Gastrointestinal and Endoscopic Surgeons*, Las Vegas, Nevada, USA

34. Cao, S. S., and Kaufman, R. J. (2013) *Expert Opin Ther Targets* **17**, 437-448

35. Anstee, Q. M., and Goldin, R. D. (2006) *Int J Exp Pathol* **87**, 1-16

36. Kanuri, G., and Bergheim, I. (2013) *Int J Mol Sci* **14**, 11963-11980

37. Varela-Rey, M., Embade, N., Ariz, U., Lu, S. C., Mato, J. M., and Martinez-Chantar, M. L. (2009) *Int J Biochem Cell Biol* **41**, 969-976

38. Omagari, K., Kato, S., Tsuneyama, K., Inohara, C., Kuroda, Y., Tsukuda, H., Fukazawa, E., Shiraishi, K., and Mune, M. (2008) *Dig Dis Sci* **53**, 3206-3212

39. Chalasani, N., Crabb, D. W., Cummings, O. W., Kwo, P. Y., Asghar, A., Pandya, P. K., and Considine, R. V. (2003) *Am J Gastroenterol* **98**, 2771-2776

40. Faggioni, R., Fantuzzi, G., Gabay, C., Moser, A., Dinarello, C. A., Feingold, K. R., and Grunfeld, C. (1999) *Am J Physiol* **276**, R136-142

41. Rinella, M. E., and Green, R. M. (2004) *J Hepatol* **40**, 47-51

42. Rinella, M. E., Elias, M. S., Smolak, R. R., Fu, T., Borensztajn, J., and Green, R. M. (2008) *J Lipid Res* **49**, 1068-1076

43. Li, Z., Agellon, L. B., Allen, T. M., Umeda, M., Jewell, L., Mason, A., and Vance, D. E. (2006) *Cell Metab* **3**, 321-331

44. Mizushima, N., Levine, B., Cuervo, A. M., and Klionsky, D. J. (2008) *Nature* **451**, 1069-1075

45. Singh, R., Kaushik, S., Wang, Y., Xiang, Y., Novak, I., Komatsu, M., Tanaka, K., Cuervo, A. M., and Czaja, M. J. (2009) *Nature* **458**, 1131-1135

References

Ahmadian, M., Suh, J.M., Hah, N., Liddle, C., Atkins, A.R., Downes, M., and Evans, R.M. (2013). PPARgamma signaling and metabolism: the good, the bad and the future. Nat Med *19*, 557-566.

Akesson, B. (1978). Autoregulation of phospholipid N-methylation by the membrane phosphatidylethanolamine content. FEBS Lett *92*, 177-180.

Alemany, S., Varela, I., Harper, J.F., and Mato, J.M. (1982). Calmodulin regulation of phospholipid and fatty acid methylation by rat liver microsomes. J Biol Chem *257*, 9249-9251.

Alemany, S., Varela, I., and Mato, J.M. (1981). Stimulation by vasopressin and angiotensin of phospholipid methyltransferase in isolated rat hepatocytes. FEBS Lett *135*, 111-114.

Alexander, G., Bell, A.W., and Hales, J.R. (1973). Effects of cold exposure on tissue blood flow in the new-born lamb. J Physiol *234*, 65-77.

Ali, A.T., Hochfeld, W.E., Myburgh, R., and Pepper, M.S. (2013). Adipocyte and adipogenesis. Eur J Cell Biol *92*, 229-236.

Almind, K., Manieri, M., Sivitz, W.I., Cinti, S., and Kahn, C.R. (2007). Ectopic brown adipose tissue in muscle provides a mechanism for differences in risk of metabolic syndrome in mice. Proc Natl Acad Sci U S A *104*, 2366-2371.

Alvaro, D., Cantafora, A., Attili, A.F., Ginanni Corradini, S., De Luca, C., Minervini, G., Di Biase, A., and Angelico, M. (1986). Relationships between bile salts hydrophilicity

and phospholipid composition in bile of various animal species. Comp Biochem Physiol B *83*, 551-554.

Angulo, P. (2006). Nonalcoholic fatty liver disease and liver transplantation. Liver Transpl *12*, 523-534.

Anstee, Q.M., and Goldin, R.D. (2006). Mouse models in non-alcoholic fatty liver disease and steatohepatitis research. Int J Exp Pathol *87*, 1-16.

Anunciado-Koza, R.P., Zhang, J., Ukropec, J., Bajpeyi, S., Koza, R.A., Rogers, R.C., Cefalu, W.T., Mynatt, R.L., and Kozak, L.P. (2011). Inactivation of the mitochondrial carrier SLC25A25 (ATP-Mg2+/Pi transporter) reduces physical endurance and metabolic efficiency in mice. J Biol Chem *286*, 11659-11671.

Arruda, A.P., Pers, B.M., Parlakgul, G., Guney, E., Inouye, K., and Hotamisligil, G.S. (2014). Chronic enrichment of hepatic endoplasmic reticulum-mitochondria contact leads to mitochondrial dysfunction in obesity. Nat Med *20*, 1427-1435.

Bachman, E.S., Dhillon, H., Zhang, C.Y., Cinti, S., Bianco, A.C., Kobilka, B.K., and Lowell, B.B. (2002). betaAR signaling required for diet-induced thermogenesis and obesity resistance. Science *297*, 843-845.

Bahceci, M., Gokalp, D., Bahceci, S., Tuzcu, A., Atmaca, S., and Arikan, S. (2007). The correlation between adiposity and adiponectin, tumor necrosis factor alpha, interleukin-6 and high sensitivity C-reactive protein levels. Is adipocyte size associated with inflammation in adults? J Endocrinol Invest *30*, 210-214.

Bailey, D., and O'Hare, P. (2007). Transmembrane bZIP transcription factors in ER stress signaling and the unfolded protein response. Antioxid Redox Signal *9*, 2305-2321.

Baker, T.K., Carfagna, M.A., Gao, H., Dow, E.R., Li, Q., Searfoss, G.H., and Ryan, T.P. (2001). Temporal gene expression analysis of monolayer cultured rat hepatocytes. Chem Res Toxicol *14*, 1218-1231.

Bal, N.C., Maurya, S.K., Sopariwala, D.H., Sahoo, S.K., Gupta, S.C., Shaikh, S.A., Pant, M., Rowland, L.A., Bombardier, E., Goonasekera, S.A.*, et al.* (2012). Sarcolipin is a newly identified regulator of muscle-based thermogenesis in mammals. Nat Med *18*, 1575-1579.

Banchio, C., Lingrell, S., and Vance, D.E. (2007). Sp-1 binds promoter elements that are regulated by retinoblastoma and regulate CTP:phosphocholine cytidylyltransferase-alpha transcription. J Biol Chem *282*, 14827-14835.

Banchio, C., Schang, L.M., and Vance, D.E. (2003). Activation of CTP:phosphocholine cytidylyltransferase alpha expression during the S phase of the cell cycle is mediated by the transcription factor Sp1. J Biol Chem *278*, 32457-32464.

Banchio, C., Schang, L.M., and Vance, D.E. (2004). Phosphorylation of Sp1 by cyclin-dependent kinase 2 modulates the role of Sp1 in CTP:phosphocholine cytidylyltransferase alpha regulation during the S phase of the cell cycle. J Biol Chem *279*, 40220-40226.

Banni, S., Carta, G., Murru, E., Cordeddu, L., Giordano, E., Marrosu, F., Puligheddu, M., Floris, G., Asuni, G.P., Cappai, A.L.*, et al.* (2012). Vagus nerve stimulation reduces body weight and fat mass in rats. PLoS One *7*, e44813.

Barnett, S.A., Coleman, E.M., and Manly, B.M. (1960). Mortality, growth and liver glycogen in young mice exposed to cold. Q J Exp Physiol Cogn Med Sci *45*, 40-49.

Bartelt, A., Bruns, O.T., Reimer, R., Hohenberg, H., Ittrich, H., Peldschus, K., Kaul, M.G., Tromsdorf, U.I., Weller, H., Waurisch, C.*, et al.* (2011). Brown adipose tissue activity controls triglyceride clearance. Nat Med *17*, 200-205.

Bartness, T.J., and Song, C.K. (2007). Thematic review series: adipocyte biology. Sympathetic and sensory innervation of white adipose tissue. J Lipid Res *48*, 1655-1672.

Bartness, T.J., Vaughan, C.H., and Song, C.K. (2010). Sympathetic and sensory innervation of brown adipose tissue. Int J Obes (Lond) *34 Suppl 1*, S36-42.

Bartz, R., Li, W.H., Venables, B., Zehmer, J.K., Roth, M.R., Welti, R., Anderson, R.G., Liu, P., and Chapman, K.D. (2007). Lipidomics reveals that adiposomes store ether lipids and mediate phospholipid traffic. J Lipid Res *48*, 837-847.

Batterham, R.L., Heffron, H., Kapoor, S., Chivers, J.E., Chandarana, K., Herzog, H., Le Roux, C.W., Thomas, E.L., Bell, J.D., and Withers, D.J. (2006). Critical role for peptide YY in protein-mediated satiation and body-weight regulation. Cell Metab *4*, 223-233.

Bautista, D.M., Siemens, J., Glazer, J.M., Tsuruda, P.R., Basbaum, A.I., Stucky, C.L., Jordt, S.E., and Julius, D. (2007). The menthol receptor TRPM8 is the principal detector of environmental cold. Nature *448*, 204-208.

Ben Mosbah, I., Alfany-Fernandez, I., Martel, C., Zaouali, M.A., Bintanel-Morcillo, M., Rimola, A., Rodes, J., Brenner, C., Rosello-Catafau, J., and Peralta, C. (2010). Endoplasmic reticulum stress inhibition protects steatotic and non-steatotic livers in partial hepatectomy under ischemia-reperfusion. Cell Death Dis *1*, e52.

Bernal-Mizrachi, C., Xiaozhong, L., Yin, L., Knutsen, R.H., Howard, M.J., Arends, J.J., Desantis, P., Coleman, T., and Semenkovich, C.F. (2007). An afferent vagal nerve pathway links hepatic PPARalpha activation to glucocorticoid-induced insulin resistance and hypertension. Cell Metab *5*, 91-102.

Bernstein, L.E., Berry, J., Kim, S., Canavan, B., and Grinspoon, S.K. (2006). Effects of etanercept in patients with the metabolic syndrome. Arch Intern Med *166*, 902-908.

Berry, R., and Rodeheffer, M.S. (2013). Characterization of the adipocyte cellular lineage in vivo. Nat Cell Biol *15*, 302-308.

Berthoud, H.R. (2004). Anatomy and function of sensory hepatic nerves. Anat Rec A Discov Mol Cell Evol Biol *280*, 827-835.

Berthoud, H.R. (2008). The vagus nerve, food intake and obesity. Regulatory Peptides *149*, 15-25.

Berthoud, H.R., and Jeanrenaud, B. (1979). Acute hyperinsulinemia and its reversal by vagotomy after lesions of the ventromedial hypothalamus in anesthetized rats. Endocrinology *105*, 146-151.

Berthoud, H.R., and Neuhuber, W.L. (2000). Functional and chemical anatomy of the afferent vagal system. Auton Neurosci *85*, 1-17.

Berthoud, H.R., Patterson, L.M., and Zheng, H. (2001). Vagal-enteric interface: vagal activation-induced expression of c-Fos and p-CREB in neurons of the upper gastrointestinal tract and pancreas. Anat Rec *262*, 29-40.

Bleijerveld, O.B., Brouwers, J.F., Vaandrager, A.B., Helms, J.B., and Houweling, M. (2007). The CDP-ethanolamine pathway and phosphatidylserine decarboxylation generate different phosphatidylethanolamine molecular species. J Biol Chem *282*, 28362-28372.

Bluher, M. (2013). Adipose tissue dysfunction contributes to obesity related metabolic diseases. Best Pract Res Clin Endocrinol Metab *27*, 163-177.

Blusztajn, J.K., Zeisel, S.H., and Wurtman, R.J. (1985). Developmental changes in the activity of phosphatidylethanolamine N-methyltransferases in rat brain. Biochem J *232*, 505-511.

Bodenlos, J.S., Kose, S., Borckardt, J.J., Nahas, Z., Shaw, D., O'Neil, P.M., and George, M.S. (2007). Vagus nerve stimulation acutely alters food craving in adults with depression. Appetite *48*, 145-153.

Boess, F., Kamber, M., Romer, S., Gasser, R., Muller, D., Albertini, S., and Suter, L. (2003). Gene expression in two hepatic cell lines, cultured primary hepatocytes, and liver slices compared to the in vivo liver gene expression in rats: possible implications for toxicogenomics use of in vitro systems. Toxicol Sci *73*, 386-402.

Bordicchia, M., Liu, D., Amri, E.Z., Ailhaud, G., Dessi-Fulgheri, P., Zhang, C., Takahashi, N., Sarzani, R., and Collins, S. (2012). Cardiac natriuretic peptides act via

p38 MAPK to induce the brown fat thermogenic program in mouse and human adipocytes. J Clin Invest *122*, 1022-1036.

Borovikova, L.V., Ivanova, S., Zhang, M., Yang, H., Botchkina, G.I., Watkins, L.R., Wang, H., Abumrad, N., Eaton, J.W., and Tracey, K.J. (2000). Vagus nerve stimulation attenuates the systemic inflammatory response to endotoxin. Nature *405*, 458-462.

Borradaile, N.M., Han, X., Harp, J.D., Gale, S.E., Ory, D.S., and Schaffer, J.E. (2006). Disruption of endoplasmic reticulum structure and integrity in lipotoxic cell death. J Lipid Res *47*, 2726-2737.

Boss, T., Peters, J., Patti, M., Lustig, R., and Kral, J. (2007). Laparoscopic truncal vagotomy for weight-loss: initial experience in 15 patients from a prospective, multi-center study [Abstract]. In Scientific Session of the Society of American Gastrointestinal and Endoscopic Surgeons (Las Vegas, Nevada, USA), pp. S299-493.

Bostrom, P., Wu, J., Jedrychowski, M.P., Korde, A., Ye, L., Lo, J.C., Rasbach, K.A., Bostrom, E.A., Choi, J.H., Long, J.Z.*, et al.* (2012). A PGC1-alpha-dependent myokine that drives brown-fat-like development of white fat and thermogenesis. Nature *481*, 463-468.

Bravo, R., Gutierrez, T., Paredes, F., Gatica, D., Rodriguez, A.E., Pedrozo, Z., Chiong, M., Parra, V., Quest, A.F., Rothermel, B.A.*, et al.* (2012). Endoplasmic reticulum: ER stress regulates mitochondrial bioenergetics. Int J Biochem Cell Biol *44*, 16-20.

Bremer, J., Figard, P.H., and Greenberg, D.M. (1960). The Biosynthesis of Choline and Its Relation to Phospholipid Metabolism. Biochimica Et Biophysica Acta *43*, 477-488.

Bremer, J., and Greenberg, D.M. (1960). Biosynthesis of choline in vitro. Biochim Biophys Acta *37*, 173-175.

Bremer, J., and Greenberg, D.M. (1961). Methyl Transfering Enzyme System of Microsomes in Biosynthesis of Lecithin (Phosphatidylcholine). Biochimica Et Biophysica Acta *46*, 205-&.

Bronner-Fraser, M. (1994). Neural crest cell formation and migration in the developing embryo. FASEB J *8*, 699-706.

Brown, M.S., Ye, J., Rawson, R.B., and Goldstein, J.L. (2000). Regulated intramembrane proteolysis: a control mechanism conserved from bacteria to humans. Cell *100*, 391-398.

Brunt, E.M., Janney, C.G., Di Bisceglie, A.M., Neuschwander-Tetri, B.A., and Bacon, B.R. (1999). Nonalcoholic steatohepatitis: a proposal for grading and staging the histological lesions. Am J Gastroenterol *94*, 2467-2474.

Cancello, R., Zulian, A., Maestrini, S., Mencarelli, M., Della Barba, A., Invitti, C., Liuzzi, A., and Di Blasio, A.M. (2012). The nicotinic acetylcholine receptor alpha7 in subcutaneous mature adipocytes: downregulation in human obesity and modulation by diet-induced weight loss. Int J Obes (Lond) *36*, 1552-1557.

Cannon, B., and Nedergaard, J. (2004). Brown adipose tissue: function and physiological significance. Physiol Rev *84*, 277-359.

Cannon, B., and Nedergaard, J. (2010). Metabolic consequences of the presence or absence of the thermogenic capacity of brown adipose tissue in mice (and probably in humans). Int J Obes (Lond) *34 Suppl 1*, S7-16.

Cao, H., Gerhold, K., Mayers, J.R., Wiest, M.M., Watkins, S.M., and Hotamisligil, G.S. (2008). Identification of a lipokine, a lipid hormone linking adipose tissue to systemic metabolism. Cell *134*, 933-944.

Cao, S.S., and Kaufman, R.J. (2013). Targeting endoplasmic reticulum stress in metabolic disease. Expert Opin Ther Targets *17*, 437-448.

Carnethon, M.R., Jacobs, D.R., Jr., Sidney, S., and Liu, K. (2003). Influence of autonomic nervous system dysfunction on the development of type 2 diabetes: the CARDIA study. Diabetes Care *26*, 3035-3041.

Castano, J.G., Alemany, S., Nieto, A., and Mato, J.M. (1980). Activation of phospholipid methyltransferase by glucagon in rat hepatocytes. J Biol Chem *255*, 9041-9043.

Chalasani, N., Crabb, D.W., Cummings, O.W., Kwo, P.Y., Asghar, A., Pandya, P.K., and Considine, R.V. (2003). Does leptin play a role in the pathogenesis of human nonalcoholic steatohepatitis? Am J Gastroenterol *98*, 2771-2776.

Chang, T.M., Chan, D.C., Liu, Y.C., Tsou, S.S., and Chen, T.H. (2001). Long-term results of duodenectomy with highly selective vagotomy in the treatment of complicated duodenal ulcers. Am J Surg *181*, 372-376.

Chang, T.Y., Chang, C.C., Ohgami, N., and Yamauchi, Y. (2006). Cholesterol sensing, trafficking, and esterification. Annu Rev Cell Dev Biol *22*, 129-157.

Chen, X., Shen, J., and Prywes, R. (2002). The luminal domain of ATF6 senses endoplasmic reticulum (ER) stress and causes translocation of ATF6 from the ER to the Golgi. J Biol Chem *277*, 13045-13052.

Cheung, G.W., Kokorovic, A., Lam, C.K., Chari, M., and Lam, T.K. (2009). Intestinal cholecystokinin controls glucose production through a neuronal network. Cell Metab *10*, 99-109.

Chiang, P.K., and Cantoni, G.L. (1979). Perturbation of biochemical transmethylations by 3-deazaadenosine in vivo. Biochem Pharmacol *28*, 1897-1902.

Chiva, V.A., Cao, D.M., and Mato, J.M. (1983). Stimulation by epidermal growth factor of phospholipid methyltransferase in isolated rat hepatocytes. FEBS Lett *160*, 101-104.

Chondronikola, M., Volpi, E., Borsheim, E., Porter, C., Annamalai, P., Enerback, S., Lidell, M.E., Saraf, M.K., Labbe, S.M., Hurren, N.M.*, et al.* (2014). Brown adipose tissue improves whole-body glucose homeostasis and insulin sensitivity in humans. Diabetes *63*, 4089-4099.

Chong, M.F., Fielding, B.A., and Frayn, K.N. (2007). Metabolic interaction of dietary sugars and plasma lipids with a focus on mechanisms and de novo lipogenesis. Proc Nutr Soc *66*, 52-59.

Cinti, S. (2005). The adipose organ. Prostaglandins Leukot Essent Fatty Acids *73*, 9-15.

Cinti, S. (2011). Between brown and white: novel aspects of adipocyte differentiation. Ann Med *43*, 104-115.

Cinti, S. (2012). The adipose organ at a glance. Dis Model Mech *5*, 588-594.

ClinicalTrials.gov (2012). US National Library of Medicine.

Cohen, F.E., and Kelly, J.W. (2003). Therapeutic approaches to protein-misfolding diseases. Nature *426*, 905-909.

Cohen, J.C., Horton, J.D., and Hobbs, H.H. (2011). Human fatty liver disease: old questions and new insights. Science *332*, 1519-1523.

Cole, L.K., Dolinsky, V.W., Dyck, J.R., and Vance, D.E. (2011). Impaired phosphatidylcholine biosynthesis reduces atherosclerosis and prevents lipotoxic cardiac dysfunction in ApoE-/- Mice. Circ Res *108*, 686-694.

Cole, L.K., Jacobs, R.L., and Vance, D.E. (2010). Tamoxifen induces triacylglycerol accumulation in the mouse liver by activation of fatty acid synthesis. Hepatology *52*, 1258-1265.

Cole, L.K., and Vance, D.E. (2010). A role for Sp1 in transcriptional regulation of phosphatidylethanolamine N-methyltransferase in liver and 3T3-L1 adipocytes. J Biol Chem *285*, 11880-11891.

Cook, K.S., Min, H.Y., Johnson, D., Chaplinsky, R.J., Flier, J.S., Hunt, C.R., and Spiegelman, B.M. (1987). Adipsin: a circulating serine protease homolog secreted by adipose tissue and sciatic nerve. Science *237*, 402-405.

Cribier, S., Morrot, G., Neumann, J.M., and Devaux, P.F. (1990). Lateral diffusion of erythrocyte phospholipids in model membranes comparison between inner and outer leaflet components. Eur Biophys J *18*, 33-41.

Croze, E.M., and Morre, D.J. (1984). Isolation of plasma membrane, golgi apparatus, and endoplasmic reticulum fractions from single homogenates of mouse liver. J Cell Physiol *119*, 46-57.

Cui, Z., Houweling, M., and Vance, D.E. (1994). Suppression of rat hepatoma cell growth by expression of phosphatidylethanolamine N-methyltransferase-2. J Biol Chem *269*, 24531-24533.

Cui, Z., Shen, Y.J., and Vance, D.E. (1997). Inverse correlation between expression of phosphatidylethanolamine N-methyltransferase-2 and growth rate of perinatal rat livers. Biochim Biophys Acta *1346*, 10-16.

Cui, Z., and Vance, D.E. (1996). Expression of phosphatidylethanolamine N-methyltransferase-2 is markedly enhanced in long term choline-deficient rats. J Biol Chem *271*, 2839-2843.

Cui, Z., Vance, J.E., Chen, M.H., Voelker, D.R., and Vance, D.E. (1993). Cloning and expression of a novel phosphatidylethanolamine N-methyltransferase. A specific biochemical and cytological marker for a unique membrane fraction in rat liver. J Biol Chem *268*, 16655-16663.

Cullinan, S.B., and Diehl, J.A. (2006). Coordination of ER and oxidative stress signaling: the PERK/Nrf2 signaling pathway. Int J Biochem Cell Biol *38*, 317-332.

Cullis, P.R., Fenske, D.B., and Hope, M.J. (1996). Physical properties and functional roles of lipids in membranes. In Biochemsitry of Lipids, Lipoproteins and Membranes, J.E.V. D.E.a.V, ed. (Amsterdam, Elsevier Sciences B.V), pp. 1-33.

Cummings, D.E., Purnell, J.Q., Frayo, R.S., Schmidova, K., Wisse, B.E., and Weigle, D.S. (2001). A preprandial rise in plasma ghrelin levels suggests a role in meal initiation in humans. Diabetes *50*, 1714-1719.

Cypess, A.M., Lehman, S., Williams, G., Tal, I., Rodman, D., Goldfine, A.B., Kuo, F.C., Palmer, E.L., Tseng, Y.H., Doria, A.*, et al.* (2009). Identification and importance of brown adipose tissue in adult humans. N Engl J Med *360*, 1509-1517.

Czech, M.P., Tencerova, M., Pedersen, D.J., and Aouadi, M. (2013). Insulin signalling mechanisms for triacylglycerol storage. Diabetologia *56*, 949-964.

da Costa, K.A., Kozyreva, O.G., Song, J., Galanko, J.A., Fischer, L.M., and Zeisel, S.H. (2006). Common genetic polymorphisms affect the human requirement for the nutrient choline. FASEB J *20*, 1336-1344.

Date, Y., Murakami, N., Toshinai, K., Matsukura, S., Niijima, A., Matsuo, H., Kangawa, K., and Nakazato, M. (2002). The role of the gastric afferent vagal nerve in ghrelin-induced feeding and growth hormone secretion in rats. Gastroenterology *123*, 1120-1128.

de Jesus, L.A., Carvalho, S.D., Ribeiro, M.O., Schneider, M., Kim, S.W., Harney, J.W., Larsen, P.R., and Bianco, A.C. (2001). The type 2 iodothyronine deiodinase is essential for adaptive thermogenesis in brown adipose tissue. J Clin Invest *108*, 1379-1385.

de Vree, J.M., Jacquemin, E., Sturm, E., Cresteil, D., Bosma, P.J., Aten, J., Deleuze, J.F., Desrochers, M., Burdelski, M., Bernard, O.*, et al.* (1998). Mutations in the MDR3 gene cause progressive familial intrahepatic cholestasis. Proc Natl Acad Sci U S A *95*, 282-287.

Deleault, N.R., Piro, J.R., Walsh, D.J., Wang, F., Ma, J., Geoghegan, J.C., and Supattapone, S. (2012). Isolation of phosphatidylethanolamine as a solitary cofactor for

prion formation in the absence of nucleic acids. Proc Natl Acad Sci U S A *109*, 8546-8551.

DeLong, C.J., Shen, Y.J., Thomas, M.J., and Cui, Z. (1999). Molecular distinction of phosphatidylcholine synthesis between the CDP-choline pathway and phosphatidylethanolamine methylation pathway. J Biol Chem *274*, 29683-29688.

Delzenne, N.M., Neyrinck, A.M., Backhed, F., and Cani, P.D. (2011). Targeting gut microbiota in obesity: effects of prebiotics and probiotics. Nat Rev Endocrinol *7*, 639-646.

Devlin, M.J. (2014). The "Skinny" on brown fat, obesity, and bone. Am J Phys Anthropol.

Dobrosotskaya, I.Y., Seegmiller, A.C., Brown, M.S., Goldstein, J.L., and Rawson, R.B. (2002). Regulation of SREBP processing and membrane lipid production by phospholipids in Drosophila. Science *296*, 879-883.

Dolinsky, V.W., Gilham, D., Alam, M., Vance, D.E., and Lehner, R. (2004). Triacylglycerol hydrolase: role in intracellular lipid metabolism. Cell Mol Life Sci *61*, 1633-1651.

Dolinsky, V.W., Sipione, S., Lehner, R., and Vance, D.E. (2001). The cloning and expression of a murine triacylglycerol hydrolase cDNA and the structure of its corresponding gene. Biochim Biophys Acta *1532*, 162-172.

Donath, M.Y., and Shoelson, S.E. (2011). Type 2 diabetes as an inflammatory disease. Nat Rev Immunol *11*, 98-107.

Dong, H., Wang, J., Li, C., Hirose, A., Nozaki, Y., Takahashi, M., Ono, M., Akisawa, N., Iwasaki, S., Saibara, T., *et al.* (2007). The phosphatidylethanolamine N-methyltransferase gene V175M single nucleotide polymorphism confers the susceptibility to NASH in Japanese population. J Hepatol *46*, 915-920.

Donnelly, K.L., Smith, C.I., Schwarzenberg, S.J., Jessurun, J., Boldt, M.D., and Parks, E.J. (2005). Sources of fatty acids stored in liver and secreted via lipoproteins in patients with nonalcoholic fatty liver disease. J Clin Invest *115*, 1343-1351.

Dowhan, W., and Bogdanov, M. (2012). Molecular genetic and biochemical approaches for defining lipid-dependent membrane protein folding. Biochim Biophys Acta *1818*, 1097-1107.

Du Vigneaud, V., Cohn, M., Chandler, J.P., Schenck, J.R., and Simmonds, S. (1974). Nutrition classics from The Journal of Biological Chemistry 140:625-641, 1941. The utilization of the methyl group of methionine in the biological synthesis of choline and creatine. Nutr Rev *32*, 144-146.

Dutsch, M., Eichhorn, U., Worl, J., Wank, M., Berthoud, H.R., and Neuhuber, W.L. (1998). Vagal and spinal afferent innervation of the rat esophagus: a combined retrograde tracing and immunocytochemical study with special emphasis on calcium-binding proteins. J Comp Neurol *398*, 289-307.

Eberle, D., Hegarty, B., Bossard, P., Ferre, P., and Foufelle, F. (2004). SREBP transcription factors: master regulators of lipid homeostasis. Biochimie *86*, 839-848.

Emoto, K., and Umeda, M. (2000). An essential role for a membrane lipid in cytokinesis. Regulation of contractile ring disassembly by redistribution of phosphatidylethanolamine. J Cell Biol *149*, 1215-1224.

Enerback, S., Jacobsson, A., Simpson, E.M., Guerra, C., Yamashita, H., Harper, M.E., and Kozak, L.P. (1997). Mice lacking mitochondrial uncoupling protein are cold-sensitive but not obese. Nature *387*, 90-94.

Faggioni, R., Fantuzzi, G., Gabay, C., Moser, A., Dinarello, C.A., Feingold, K.R., and Grunfeld, C. (1999). Leptin deficiency enhances sensitivity to endotoxin-induced lethality. Am J Physiol *276*, R136-142.

Farmer, S.R. (2006). Transcriptional control of adipocyte formation. Cell Metab *4*, 263-273.

Fast, D.G., and Vance, D.E. (1995). Nascent VLDL phospholipid composition is altered when phosphatidylcholine biosynthesis is inhibited: evidence for a novel mechanism that regulates VLDL secretion. Biochim Biophys Acta *1258*, 159-168.

Fatima, W., Shahid, A., Imran, M., Manzoor, J., Hasnain, S., Rana, S., and Mahmood, S. (2011). Leptin deficiency and leptin gene mutations in obese children from Pakistan. Int J Pediatr Obes *6*, 419-427.

Fedorenko, A., Lishko, P.V., and Kirichok, Y. (2012). Mechanism of fatty-acid-dependent UCP1 uncoupling in brown fat mitochondria. Cell *151*, 400-413.

Feldmann, H.M., Golozoubova, V., Cannon, B., and Nedergaard, J. (2009). UCP1 ablation induces obesity and abolishes diet-induced thermogenesis in mice exempt from thermal stress by living at thermoneutrality. Cell Metab *9*, 203-209.

Figueroa, J.J., Basford, J.R., and Low, P.A. (2010). Preventing and treating orthostatic hypotension: As easy as A, B, C. Cleve Clin J Med *77*, 298-306.

Fischer, L.M., da Costa, K.A., Kwock, L., Galanko, J., and Zeisel, S.H. (2010). Dietary choline requirements of women: effects of estrogen and genetic variation. Am J Clin Nutr *92*, 1113-1119.

Fischer, L.M., daCosta, K.A., Kwock, L., Stewart, P.W., Lu, T.S., Stabler, S.P., Allen, R.H., and Zeisel, S.H. (2007). Sex and menopausal status influence human dietary requirements for the nutrient choline. Am J Clin Nutr *85*, 1275-1285.

Fisher, F.M., Kleiner, S., Douris, N., Fox, E.C., Mepani, R.J., Verdeguer, F., Wu, J., Kharitonenkov, A., Flier, J.S., Maratos-Flier, E.*, et al.* (2012). FGF21 regulates PGC-1alpha and browning of white adipose tissues in adaptive thermogenesis. Genes Dev *26*, 271-281.

Folch, J., Lees, M., and Sloane Stanley, G.H. (1957). A simple method for the isolation and purification of total lipides from animal tissues. J Biol Chem *226*, 497-509.

Fu, L., John, L.M., Adams, S.H., Yu, X.X., Tomlinson, E., Renz, M., Williams, P.M., Soriano, R., Corpuz, R., Moffat, B.*, et al.* (2004). Fibroblast growth factor 19 increases metabolic rate and reverses dietary and leptin-deficient diabetes. Endocrinology *145*, 2594-2603.

Fu, S., Watkins, S.M., and Hotamisligil, G.S. (2012). The role of endoplasmic reticulum in hepatic lipid homeostasis and stress signaling. Cell Metab *15*, 623-634.

Fu, S., Yang, L., Li, P., Hofmann, O., Dicker, L., Hide, W., Lin, X., Watkins, S.M., Ivanov, A.R., and Hotamisligil, G.S. (2011). Aberrant lipid metabolism disrupts calcium

homeostasis causing liver endoplasmic reticulum stress in obesity. Nature *473*, 528-531.

Fullerton, M.D., Hakimuddin, F., and Bakovic, M. (2007). Developmental and metabolic effects of disruption of the mouse CTP:phosphoethanolamine cytidylyltransferase gene (Pcyt2). Mol Cell Biol *27*, 3327-3336.

Galic, S., Oakhill, J.S., and Steinberg, G.R. (2010). Adipose tissue as an endocrine organ. Mol Cell Endocrinol *316*, 129-139.

Gao, X., van der Veen, J.N., Hermansson, M., Ordonez, M., Gomez-Munoz, A., Vance, D.E., and Jacobs, R.L. (2014). Decreased lipogenesis in white adipose tissue contributes to the resistance to high fat diet-induced obesity in phosphatidylethanolamine N-methyltransferase deficient mice. Biochim Biophys Acta *1851*, 152-162.

Gao, X., van der Veen, J.N., Zhu, L., Chaba, T., Ordonez, M., Lingrell, S., Koonen, D.P., Dyck, J.R., Gomez-Munoz, A., Vance, D.E.*, et al.* (2015). Vagus nerve contributes to the development of steatohepatitis and obesity in Phosphatidylethanolamine N-Methyltransferase deficient mice. J Hepatol *62*, 913-920.

Gasparetti, A.L., de Souza, C.T., Pereira-da-Silva, M., Oliveira, R.L., Saad, M.J., Carneiro, E.M., and Velloso, L.A. (2003). Cold exposure induces tissue-specific modulation of the insulin-signalling pathway in Rattus norvegicus. J Physiol *552*, 149-162.

Gautam, D., Gavrilova, O., Jeon, J., Pack, S., Jou, W., Cui, Y., Li, J.H., and Wess, J. (2006a). Beneficial metabolic effects of M3 muscarinic acetylcholine receptor deficiency. Cell Metab *4*, 363-375.

Gautam, D., Han, S.J., Hamdan, F.F., Jeon, J., Li, B., Li, J.H., Cui, Y., Mears, D., Lu, H., Deng, C.*, et al.* (2006b). A critical role for beta cell M3 muscarinic acetylcholine receptors in regulating insulin release and blood glucose homeostasis in vivo. Cell Metab *3*, 449-461.

Gesta, S., Tseng, Y.H., and Kahn, C.R. (2007). Developmental origin of fat: tracking obesity to its source. Cell *131*, 242-256.

Giordano, A., Frontini, A., and Cinti, S. (2008). Adipose organ nerves revealed by immunohistochemistry. Methods Mol Biol *456*, 83-95.

Giordano, A., Song, C.K., Bowers, R.R., Ehlen, J.C., Frontini, A., Cinti, S., and Bartness, T.J. (2006). White adipose tissue lacks significant vagal innervation and immunohistochemical evidence of parasympathetic innervation. Am J Physiol Regul Integr Comp Physiol *291*, R1243-1255.

Giorgi, C., De Stefani, D., Bononi, A., Rizzuto, R., and Pinton, P. (2009). Structural and functional link between the mitochondrial network and the endoplasmic reticulum. Int J Biochem Cell Biol *41*, 1817-1827.

Gobley, M. (1847). Examen comparatif du jaune d'oeufe et de al matiere cerebrale. J Pharm Chim *11*, 409.

Goerke, J. (1998). Pulmonary surfactant: functions and molecular composition. Biochim Biophys Acta *1408*, 79-89.

Golozoubova, V., Gullberg, H., Matthias, A., Cannon, B., Vennstrom, B., and Nedergaard, J. (2004). Depressed thermogenesis but competent brown adipose tissue recruitment in mice devoid of all hormone-binding thyroid hormone receptors. Mol Endocrinol *18*, 384-401.

Gonzalez-Rodriguez, A., Mayoral, R., Agra, N., Valdecantos, M.P., Pardo, V., Miquilena-Colina, M.E., Vargas-Castrillon, J., Lo Iacono, O., Corazzari, M., Fimia, G.M., *et al.* (2014). Impaired autophagic flux is associated with increased endoplasmic reticulum stress during the development of NAFLD. Cell Death Dis *5*, e1179.

Gregor, M.F., and Hotamisligil, G.S. (2011). Inflammatory mechanisms in obesity. Annu Rev Immunol *29*, 415-445.

Guerra, C., Koza, R.A., Yamashita, H., Walsh, K., and Kozak, L.P. (1998). Emergence of brown adipocytes in white fat in mice is under genetic control. Effects on body weight and adiposity. J Clin Invest *102*, 412-420.

Guillouzo, A., Corlu, A., Aninat, C., Glaise, D., Morel, F., and Guguen-Guillouzo, C. (2007). The human hepatoma HepaRG cells: a highly differentiated model for studies of liver metabolism and toxicity of xenobiotics. Chem Biol Interact *168*, 66-73.

Guo, Y., Walther, T.C., Rao, M., Stuurman, N., Goshima, G., Terayama, K., Wong, J.S., Vale, R.D., Walter, P., and Farese, R.V. (2008). Functional genomic screen reveals genes involved in lipid-droplet formation and utilization. Nature *453*, 657-661.

Haemmerle, G., Lass, A., Zimmermann, R., Gorkiewicz, G., Meyer, C., Rozman, J., Heldmaier, G., Maier, R., Theussl, C., Eder, S., *et al.* (2006). Defective lipolysis and

altered energy metabolism in mice lacking adipose triglyceride lipase. Science *312*, 734-737.

Haemmerle, G., Zimmermann, R., Hayn, M., Theussl, C., Waeg, G., Wagner, E., Sattler, W., Magin, T.M., Wagner, E.F., and Zechner, R. (2002). Hormone-sensitive lipase deficiency in mice causes diglyceride accumulation in adipose tissue, muscle, and testis. J Biol Chem *277*, 4806-4815.

Hafez, I.M., and Cullis, P.R. (2001). Roles of lipid polymorphism in intracellular delivery. Adv Drug Deliv Rev *47*, 139-148.

Hansen, H.S., Lauritzen, L., Strand, A.M., Moesgaard, B., and Frandsen, A. (1995). Glutamate stimulates the formation of N-acylphosphatidylethanolamine and N-acylethanolamine in cortical neurons in culture. Biochim Biophys Acta *1258*, 303-308.

Harding, H.P., Zhang, Y., Bertolotti, A., Zeng, H., and Ron, D. (2000). Perk is essential for translational regulation and cell survival during the unfolded protein response. Mol Cell *5*, 897-904.

Harding, H.P., Zhang, Y., and Ron, D. (1999). Protein translation and folding are coupled by an endoplasmic-reticulum-resident kinase. Nature *397*, 271-274.

Harms, M., and Seale, P. (2013). Brown and beige fat: development, function and therapeutic potential. Nat Med *19*, 1252-1263.

Hauner, H. (2002). The mode of action of thiazolidinediones. Diabetes Metab Res Rev *18 Suppl 2*, S10-15.

Henkel, A.S., Dewey, A.M., Anderson, K.A., Olivares, S., and Green, R.M. (2012). Reducing endoplasmic reticulum stress does not improve steatohepatitis in mice fed a

methionine- and choline-deficient diet. Am J Physiol Gastrointest Liver Physiol *303*, G54-59.

Hermansson, M., Uphoff, A., Kakela, R., and Somerharju, P. (2005). Automated quantitative analysis of complex lipidomes by liquid chromatography/mass spectrometry. Anal Chem *77*, 2166-2175.

Hetz, C., Bernasconi, P., Fisher, J., Lee, A.H., Bassik, M.C., Antonsson, B., Brandt, G.S., Iwakoshi, N.N., Schinzel, A., Glimcher, L.H.*, et al.* (2006). Proapoptotic BAX and BAK modulate the unfolded protein response by a direct interaction with IRE1alpha. Science *312*, 572-576.

Hetz, C., Chevet, E., and Harding, H.P. (2013). Targeting the unfolded protein response in disease. Nat Rev Drug Discov *12*, 703-719.

Himms-Hagen, J., Melnyk, A., Zingaretti, M.C., Ceresi, E., Barbatelli, G., and Cinti, S. (2000). Multilocular fat cells in WAT of CL-316243-treated rats derive directly from white adipocytes. Am J Physiol Cell Physiol *279*, C670-681.

Hirschey, M.D., Shimazu, T., Goetzman, E., Jing, E., Schwer, B., Lombard, D.B., Grueter, C.A., Harris, C., Biddinger, S., Ilkayeva, O.R.*, et al.* (2010). SIRT3 regulates mitochondrial fatty-acid oxidation by reversible enzyme deacetylation. Nature *464*, 121-125.

Hoffman, D.R., Marion, D.W., Cornatzer, W.E., and Duerre, J.A. (1980). S-Adenosylmethionine and S-adenosylhomocystein metabolism in isolated rat liver. Effects of L-methionine, L-homocystein, and adenosine. J Biol Chem *255*, 10822-10827.

Holzer, P. (1998). Neural injury, repair, and adaptation in the GI tract. II. The elusive action of capsaicin on the vagus nerve. Am J Physiol *275*, G8-13.

Horl, G., Wagner, A., Cole, L.K., Malli, R., Reicher, H., Kotzbeck, P., Kofeler, H., Hofler, G., Frank, S., Bogner-Strauss, J.G.*, et al.* (2011). Sequential synthesis and methylation of phosphatidylethanolamine promote lipid droplet biosynthesis and stability in tissue culture and in vivo. J Biol Chem *286*, 17338-17350.

Hotamisligil, G.S. (2010). Endoplasmic reticulum stress and the inflammatory basis of metabolic disease. Cell *140*, 900-917.

Houweling, M., Cui, Z., Tessitore, L., and Vance, D.E. (1997). Induction of hepatocyte proliferation after partial hepatectomy is accompanied by a markedly reduced expression of phosphatidylethanolamine N-methyltransferase-2. Biochim Biophys Acta *1346*, 1-9.

Houweling, M., Tijburg, L.B., Jamil, H., Vance, D.E., Nyathi, C.B., Vaartjes, W.J., and van Golde, L.M. (1991). Phosphatidylcholine metabolism in rat liver after partial hepatectomy. Evidence for increased activity and amount of CTP:phosphocholine cytidylyltransferase. Biochem J *278 (Pt 2)*, 347-351.

Hu, H.H., Perkins, T.G., Chia, J.M., and Gilsanz, V. (2013). Characterization of human brown adipose tissue by chemical-shift water-fat MRI. AJR Am J Roentgenol *200*, 177-183.

Hummasti, S., and Hotamisligil, G.S. (2010). Endoplasmic reticulum stress and inflammation in obesity and diabetes. Circ Res *107*, 579-591.

Hundal, R.S., Petersen, K.F., Mayerson, A.B., Randhawa, P.S., Inzucchi, S., Shoelson, S.E., and Shulman, G.I. (2002). Mechanism by which high-dose aspirin improves glucose metabolism in type 2 diabetes. J Clin Invest *109*, 1321-1326.

Imai, J., Katagiri, H., Yamada, T., Ishigaki, Y., Suzuki, T., Kudo, H., Uno, K., Hasegawa, Y., Gao, J., Kaneko, K.*, et al.* (2008). Regulation of pancreatic beta cell mass by neuronal signals from the liver. Science *322*, 1250-1254.

Inokuma, K., Ogura-Okamatsu, Y., Toda, C., Kimura, K., Yamashita, H., and Saito, M. (2005). Uncoupling protein 1 is necessary for norepinephrine-induced glucose utilization in brown adipose tissue. Diabetes *54*, 1385-1391.

Izumida, Y., Yahagi, N., Takeuchi, Y., Nishi, M., Shikama, A., Takarada, A., Masuda, Y., Kubota, M., Matsuzaka, T., Nakagawa, Y.*, et al.* (2013). Glycogen shortage during fasting triggers liver-brain-adipose neurocircuitry to facilitate fat utilization. Nat Commun *4*, 2316.

Jacobs, R.L., Devlin, C., Tabas, I., and Vance, D.E. (2004). Targeted deletion of hepatic CTP:phosphocholine cytidylyltransferase alpha in mice decreases plasma high density and very low density lipoproteins. J Biol Chem *279*, 47402-47410.

Jacobs, R.L., Lingrell, S., Zhao, Y., Francis, G.A., and Vance, D.E. (2008). Hepatic CTP:phosphocholine cytidylyltransferase-alpha is a critical predictor of plasma high density lipoprotein and very low density lipoprotein. J Biol Chem *283*, 2147-2155.

Jacobs, R.L., Stead, L.M., Devlin, C., Tabas, I., Brosnan, M.E., Brosnan, J.T., and Vance, D.E. (2005). Physiological regulation of phospholipid methylation alters plasma homocysteine in mice. J Biol Chem *280*, 28299-28305.

Jacobs, R.L., Zhao, Y., Koonen, D.P., Sletten, T., Su, B., Lingrell, S., Cao, G., Peake, D.A., Kuo, M.S., Proctor, S.D.*, et al.* (2010). Impaired de novo choline synthesis explains why phosphatidylethanolamine N-methyltransferase-deficient mice are protected from diet-induced obesity. J Biol Chem *285*, 22403-22413.

Jacquemin, E., De Vree, J.M., Cresteil, D., Sokal, E.M., Sturm, E., Dumont, M., Scheffer, G.L., Paul, M., Burdelski, M., Bosma, P.J.*, et al.* (2001). The wide spectrum of multidrug resistance 3 deficiency: from neonatal cholestasis to cirrhosis of adulthood. Gastroenterology *120*, 1448-1458.

Jansky, L., and Hart, J.S. (1968). Cardiac output and organ blood flow in warm- and cold-acclimated rats exposed to cold. Can J Physiol Pharmacol *46*, 653-659.

Jenkins, G.M., and Frohman, M.A. (2005). Phospholipase D: a lipid centric review. Cell Mol Life Sci *62*, 2305-2316.

Jimenez, M., Leger, B., Canola, K., Lehr, L., Arboit, P., Seydoux, J., Russell, A.P., Giacobino, J.P., Muzzin, P., and Preitner, F. (2002). Beta(1)/beta(2)/beta(3)-adrenoceptor knockout mice are obese and cold-sensitive but have normal lipolytic responses to fasting. FEBS Lett *530*, 37-40.

Jin, X.H., Okamoto, Y., Morishita, J., Tsuboi, K., Tonai, T., and Ueda, N. (2007). Discovery and characterization of a Ca2+-independent phosphatidylethanolamine N-acyltransferase generating the anandamide precursor and its congeners. J Biol Chem *282*, 3614-3623.

Jonas, A., Phillips, M.A., (2008). Lipoprotein structure. In Biochemistry of Lipids, Lipoproteins and Membranes, D.E. Vance, and Vance, J.E., ed. (New York, Elsevier), pp. 485-506.

Kainu, V., Hermansson, M., and Somerharju, P. (2008). Electrospray ionization mass spectrometry and exogenous heavy isotope-labeled lipid species provide detailed information on aminophospholipid acyl chain remodeling. J Biol Chem *283*, 3676-3687.

Kajimura, S., and Saito, M. (2014). A new era in brown adipose tissue biology: molecular control of brown fat development and energy homeostasis. Annu Rev Physiol *76*, 225-249.

Kajimura, S., Seale, P., Kubota, K., Lunsford, E., Frangioni, J.V., Gygi, S.P., and Spiegelman, B.M. (2009). Initiation of myoblast to brown fat switch by a PRDM16-C/EBP-beta transcriptional complex. Nature *460*, 1154-1158.

Kajimura, S., Seale, P., and Spiegelman, B.M. (2010). Transcriptional control of brown fat development. Cell Metab *11*, 257-262.

Kammoun, H.L., Chabanon, H., Hainault, I., Luquet, S., Magnan, C., Koike, T., Ferre, P., and Foufelle, F. (2009). GRP78 expression inhibits insulin and ER stress-induced SREBP-1c activation and reduces hepatic steatosis in mice. J Clin Invest *119*, 1201-1215.

Kanda, H., Tateya, S., Tamori, Y., Kotani, K., Hiasa, K., Kitazawa, R., Kitazawa, S., Miyachi, H., Maeda, S., Egashira, K.*, et al.* (2006). MCP-1 contributes to macrophage infiltration into adipose tissue, insulin resistance, and hepatic steatosis in obesity. J Clin Invest *116*, 1494-1505.

Kanno, K., Wu, M.K., Scapa, E.F., Roderick, S.L., and Cohen, D.E. (2007). Structure and function of phosphatidylcholine transfer protein (PC-TP)/StarD2. Biochim Biophys Acta *1771*, 654-662.

Kanuri, G., and Bergheim, I. (2013). In Vitro and in Vivo Models of Non-Alcoholic Fatty Liver Disease (NAFLD). Int J Mol Sci *14*, 11963-11980.

Karim, M., Jackson, P., and Jackowski, S. (2003). Gene structure, expression and identification of a new CTP:phosphocholine cytidylyltransferase beta isoform. Biochim Biophys Acta *1633*, 1-12.

Kars, M., Yang, L., Gregor, M.F., Mohammed, B.S., Pietka, T.A., Finck, B.N., Patterson, B.W., Horton, J.D., Mittendorfer, B., Hotamisligil, G.S.*, et al.* (2010). Tauroursodeoxycholic Acid may improve liver and muscle but not adipose tissue insulin sensitivity in obese men and women. Diabetes *59*, 1899-1905.

Kasturi, R., and Wakil, S.J. (1983). Increased synthesis and accumulation of phospholipids during differentiation of 3T3-L1 cells into adipocytes. J Biol Chem *258*, 3559-3564.

Katagiri, H., Yamada, T., and Oka, Y. (2007). Adiposity and cardiovascular disorders: disturbance of the regulatory system consisting of humoral and neuronal signals. Circ Res *101*, 27-39.

Kathirvel, E., Morgan, K., Nandgiri, G., Sandoval, B.C., Caudill, M.A., Bottiglieri, T., French, S.W., and Morgan, T.R. (2010). Betaine improves nonalcoholic fatty liver and associated hepatic insulin resistance: a potential mechanism for hepatoprotection by betaine. Am J Physiol Gastrointest Liver Physiol *299*, G1068-1077.

Katz, J.E., Dlakic, M., and Clarke, S. (2003). Automated identification of putative methyltransferases from genomic open reading frames. Mol Cell Proteomics *2*, 525-540.

Kennedy, E.P., and Weiss, S.B. (1956). The function of cytidine coenzymes in the biosynthesis of phospholipides. J Biol Chem *222*, 193-214.

Kershaw, E.E., and Flier, J.S. (2004). Adipose tissue as an endocrine organ. J Clin Endocrinol Metab *89*, 2548-2556.

Kharbanda, K.K., Mailliard, M.E., Baldwin, C.R., Beckenhauer, H.C., Sorrell, M.F., and Tuma, D.J. (2007). Betaine attenuates alcoholic steatosis by restoring phosphatidylcholine generation via the phosphatidylethanolamine methyltransferase pathway. J Hepatol *46*, 314-321.

Kim, S.J., Zhang, Z., Saha, A., Sarkar, C., Zhao, Z., Xu, Y., and Mukherjee, A.B. (2010). Omega-3 and omega-6 fatty acids suppress ER- and oxidative stress in cultured neurons and neuronal progenitor cells from mice lacking PPT1. Neurosci Lett *479*, 292-296.

Koda, S., Date, Y., Murakami, N., Shimbara, T., Hanada, T., Toshinai, K., Niijima, A., Furuya, M., Inomata, N., Osuye, K.*, et al.* (2005). The role of the vagal nerve in peripheral PYY3-36-induced feeding reduction in rats. Endocrinology *146*, 2369-2375.

Kontani, Y., Wang, Y., Kimura, K., Inokuma, K.I., Saito, M., Suzuki-Miura, T., Wang, Z., Sato, Y., Mori, N., and Yamashita, H. (2005). UCP1 deficiency increases susceptibility to diet-induced obesity with age. Aging Cell *4*, 147-155.

Koren, M.S., and Holmes, M.D. (2006). Vagus nerve stimulation does not lead to significant changes in body weight in patients with epilepsy. Epilepsy Behav *8*, 246-249.

Kozak, L.P. (2010). Brown fat and the myth of diet-induced thermogenesis. Cell Metab *11*, 263-267.

Krahmer, N., Guo, Y., Wilfling, F., Hilger, M., Lingrell, S., Heger, K., Newman, H.W., Schmidt-Supprian, M., Vance, D.E., Mann, M.*, et al.* (2011). Phosphatidylcholine synthesis for lipid droplet expansion is mediated by localized activation of CTP:phosphocholine cytidylyltransferase. Cell Metab *14*, 504-515.

Kreier, F., Fliers, E., Voshol, P.J., Van Eden, C.G., Havekes, L.M., Kalsbeek, A., Van Heijningen, C.L., Sluiter, A.A., Mettenleiter, T.C., Romijn, J.A.*, et al.* (2002). Selective parasympathetic innervation of subcutaneous and intra-abdominal fat--functional implications. J Clin Invest *110*, 1243-1250.

Kuipers, F., Oude Elferink, R.P., Verkade, H.J., and Groen, A.K. (1997). Mechanisms and (patho)physiological significance of biliary cholesterol secretion. Subcell Biochem *28*, 295-318.

Kuksis, A., and Myher, J.J. (1989). Gas chromatographic analysis of plasma lipids. Adv Chromatogr *28*, 267-332.

Kumar, V.V. (1991). Complementary molecular shapes and additivity of the packing parameter of lipids. Proc Natl Acad Sci U S A *88*, 444-448.

Lafontan, M., and Berlan, M. (1993). Fat cell adrenergic receptors and the control of white and brown fat cell function. J Lipid Res *34*, 1057-1091.

Lahesmaa, M., Orava, J., Schalin-Jantti, C., Soinio, M., Hannukainen, J.C., Noponen, T., Kirjavainen, A., Iida, H., Kudomi, N., Enerback, S.*, et al.* (2014). Hyperthyroidism increases brown fat metabolism in humans. J Clin Endocrinol Metab *99*, E28-35.

Lam, T.K., Gutierrez-Juarez, R., Pocai, A., Bhanot, S., Tso, P., Schwartz, G.J., and Rossetti, L. (2007). Brain glucose metabolism controls the hepatic secretion of triglyceride-rich lipoproteins. Nat Med *13*, 171-180.

Lam, T.K., Pocai, A., Gutierrez-Juarez, R., Obici, S., Bryan, J., Aguilar-Bryan, L., Schwartz, G.J., and Rossetti, L. (2005). Hypothalamic sensing of circulating fatty acids is required for glucose homeostasis. Nat Med *11*, 320-327.

Lanthier, N., and Leclercq, I.A. (2014). Adipose tissues as endocrine target organs. Best Pract Res Clin Gastroenterol *28*, 545-558.

le Roux, C.W., Neary, N.M., Halsey, T.J., Small, C.J., Martinez-Isla, A.M., Ghatei, M.A., Theodorou, N.A., and Bloom, S.R. (2005). Ghrelin does not stimulate food intake in patients with surgical procedures involving vagotomy. J Clin Endocrinol Metab *90*, 4521-4524.

Lee, A.H., Scapa, E.F., Cohen, D.E., and Glimcher, L.H. (2008). Regulation of hepatic lipogenesis by the transcription factor XBP1. Science *320*, 1492-1496.

Lee, J.H., Giannikopoulos, P., Duncan, S.A., Wang, J., Johansen, C.T., Brown, J.D., Plutzky, J., Hegele, R.A., Glimcher, L.H., and Lee, A.H. (2011). The transcription factor cyclic AMP-responsive element-binding protein H regulates triglyceride metabolism. Nat Med *17*, 812-815.

Lee, Y.H., Petkova, A.P., Mottillo, E.P., and Granneman, J.G. (2012). In vivo identification of bipotential adipocyte progenitors recruited by beta3-adrenoceptor activation and high-fat feeding. Cell Metab *15*, 480-491.

Li, Y., Ge, M., Ciani, L., Kuriakose, G., Westover, E.J., Dura, M., Covey, D.F., Freed, J.H., Maxfield, F.R., Lytton, J.*, et al.* (2004). Enrichment of endoplasmic reticulum with cholesterol inhibits sarcoplasmic-endoplasmic reticulum calcium ATPase-2b activity in parallel with increased order of membrane lipids: implications for depletion of endoplasmic reticulum calcium stores and apoptosis in cholesterol-loaded macrophages. J Biol Chem *279*, 37030-37039.

Li, Z., Agellon, L.B., Allen, T.M., Umeda, M., Jewell, L., Mason, A., and Vance, D.E. (2006). The ratio of phosphatidylcholine to phosphatidylethanolamine influences membrane integrity and steatohepatitis. Cell Metab *3*, 321-331.

Li, Z., Agellon, L.B., and Vance, D.E. (2005). Phosphatidylcholine homeostasis and liver failure. J Biol Chem *280*, 37798-37802.

Liang, H., and Ward, W.F. (2006). PGC-1alpha: a key regulator of energy metabolism. Adv Physiol Educ *30*, 145-151.

Lidell, M.E., Betz, M.J., Dahlqvist Leinhard, O., Heglind, M., Elander, L., Slawik, M., Mussack, T., Nilsson, D., Romu, T., Nuutila, P.*, et al.* (2013). Evidence for two types of brown adipose tissue in humans. Nat Med *19*, 631-634.

Ling, J., Chaba, T., Zhu, L.F., Jacobs, R.L., and Vance, D.E. (2012). Hepatic ratio of phosphatidylcholine to phosphatidylethanolamine predicts survival after partial hepatectomy in mice. Hepatology *55*, 1094-1102.

Liu, X., Perusse, F., and Bukowiecki, L.J. (1994). Chronic norepinephrine infusion stimulates glucose uptake in white and brown adipose tissues. Am J Physiol *266*, R914-920.

Liu, X., Rossmeisl, M., McClaine, J., Riachi, M., Harper, M.E., and Kozak, L.P. (2003). Paradoxical resistance to diet-induced obesity in UCP1-deficient mice. J Clin Invest *111*, 399-407.

Lonnqvist, F., Nordfors, L., Jansson, M., Thorne, A., Schalling, M., and Arner, P. (1997). Leptin secretion from adipose tissue in women. Relationship to plasma levels and gene expression. J Clin Invest *99*, 2398-2404.

Lopez, M., Alvarez, C.V., Nogueiras, R., and Dieguez, C. (2013). Energy balance regulation by thyroid hormones at central level. Trends Mol Med *19*, 418-427.

Lowell, B.B., V, S.S., Hamann, A., Lawitts, J.A., Himms-Hagen, J., Boyer, B.B., Kozak, L.P., and Flier, J.S. (1993). Development of obesity in transgenic mice after genetic ablation of brown adipose tissue. Nature *366*, 740-742.

Lumeng, C.N., Bodzin, J.L., and Saltiel, A.R. (2007). Obesity induces a phenotypic switch in adipose tissue macrophage polarization. J Clin Invest *117*, 175-184.

Luyer, M.D., Greve, J.W., Hadfoune, M., Jacobs, J.A., Dejong, C.H., and Buurman, W.A. (2005). Nutritional stimulation of cholecystokinin receptors inhibits inflammation via the vagus nerve. J Exp Med *202*, 1023-1029.

M., G. (1847). Examen comparatif du jaune d'oeufe et de al matiere cerebrale. J Pharm Chim *11*, 409.

Ma, Y., Brewer, J.W., Diehl, J.A., and Hendershot, L.M. (2002). Two distinct stress signaling pathways converge upon the CHOP promoter during the mammalian unfolded protein response. J Mol Biol *318*, 1351-1365.

Madsen, L., Pedersen, L.M., Lillefosse, H.H., Fjaere, E., Bronstad, I., Hao, Q., Petersen, R.K., Hallenborg, P., Ma, T., De Matteis, R.*, et al.* (2010). UCP1 induction during recruitment of brown adipocytes in white adipose tissue is dependent on cyclooxygenase activity. PLoS One *5*, e11391.

Maresca, A., and Supuran, C.T. (2008). Muscarinic acetylcholine receptors as therapeutic targets for obesity. Expert Opinion on Therapeutic Targets *12*, 1167-1175.

Margetic, S., Gazzola, C., Pegg, G.G., and Hill, R.A. (2002). Leptin: a review of its peripheral actions and interactions. Int J Obes Relat Metab Disord *26*, 1407-1433.

Margoni, A., Fotis, L., and Papavassiliou, A.G. (2012). The transforming growth factor-beta/bone morphogenetic protein signalling pathway in adipogenesis. Int J Biochem Cell Biol *44*, 475-479.

Marin-Cao, D., Alvarez Chiva, V., and Mato, J.M. (1983). Beta-adrenergic control of phosphatidylcholine synthesis by transmethylation in hepatocytes from juvenile, adult and adrenalectomized rats. Biochem J *216*, 675-680.

Marrero, M.B., Lucas, R., Salet, C., Hauser, T.A., Mazurov, A., Lippiello, P.M., and Bencherif, M. (2010). An alpha7 nicotinic acetylcholine receptor-selective agonist reduces weight gain and metabolic changes in a mouse model of diabetes. J Pharmacol Exp Ther *332*, 173-180.

Marrif, H., Schifman, A., Stepanyan, Z., Gillis, M.A., Calderone, A., Weiss, R.E., Samarut, J., and Silva, J.E. (2005). Temperature homeostasis in transgenic mice lacking thyroid hormone receptor-alpha gene products. Endocrinology *146*, 2872-2884.

Matsushita, M., Yoneshiro, T., Aita, S., Kameya, T., Sugie, H., and Saito, M. (2014). Impact of brown adipose tissue on body fatness and glucose metabolism in healthy humans. Int J Obes (Lond) *38*, 812-817.

Matteoni, C.A., Younossi, Z.M., Gramlich, T., Boparai, N., Liu, Y.C., and McCullough, A.J. (1999). Nonalcoholic fatty liver disease: a spectrum of clinical and pathological severity. Gastroenterology *116*, 1413-1419.

Meneghini, A., Ferreira, C., Abreu, L.C., Valenti, V.E., Ferreira, M., C, F.F., and Murad, N. (2009). Memantine prevents cardiomyocytes nuclear size reduction in the left ventricle of rats exposed to cold stress. Clinics (Sao Paulo) *64*, 921-926.

Merida, I., and Mato, J.M. (1987). Inhibition by insulin of glucagon-dependent phospholipid methyltransferase phosphorylation in rat hepatocytes. Biochim Biophys Acta *928*, 92-97.

Michalik, L., Auwerx, J., Berger, J.P., Chatterjee, V.K., Glass, C.K., Gonzalez, F.J., Grimaldi, P.A., Kadowaki, T., Lazar, M.A., O'Rahilly, S.*, et al.* (2006). International Union of Pharmacology. LXI. Peroxisome proliferator-activated receptors. Pharmacol Rev *58*, 726-741.

Michalopoulos, G.K. (2007). Liver regeneration. J Cell Physiol *213*, 286-300.

Minahk, C., Kim, K.W., Nelson, R., Trigatti, B., Lehner, R., and Vance, D.E. (2008). Conversion of low density lipoprotein-associated phosphatidylcholine to triacylglycerol by primary hepatocytes. J Biol Chem *283*, 6449-6458.

Mizushima, N., Levine, B., Cuervo, A.M., and Klionsky, D.J. (2008). Autophagy fights disease through cellular self-digestion. Nature *451*, 1069-1075.

Mizushima, N., and Yoshimori, T. (2007). How to interpret LC3 immunoblotting. Autophagy *3*, 542-545.

Moore, J.B. (2010). Non-alcoholic fatty liver disease: the hepatic consequence of obesity and the metabolic syndrome. Proc Nutr Soc *69*, 211-220.

Moore, K.J., Sheedy, F.J., and Fisher, E.A. (2013). Macrophages in atherosclerosis: a dynamic balance. Nat Rev Immunol *13*, 709-721.

Mudd, S.H., Brosnan, J.T., Brosnan, M.E., Jacobs, R.L., Stabler, S.P., Allen, R.H., Vance, D.E., and Wagner, C. (2007). Methyl balance and transmethylation fluxes in humans. Am J Clin Nutr *85*, 19-25.

Mudd, S.H., and Poole, J.R. (1975). Labile methyl balances for normal humans on various dietary regimens. Metabolism *24*, 721-735.

Murano, I., Barbatelli, G., Giordano, A., and Cinti, S. (2009). Noradrenergic parenchymal nerve fiber branching after cold acclimatisation correlates with brown adipocyte density in mouse adipose organ. J Anat *214*, 171-178.

Musso, G., Gambino, R., and Cassader, M. (2011). Interactions between gut microbiota and host metabolism predisposing to obesity and diabetes. Annu Rev Med *62*, 361-380.

Nakagawa, A., Satake, H., Nakabayashi, H., Nishizawa, M., Furuya, K., Nakano, S., Kigoshi, T., Nakayama, K., and Uchida, K. (2004). Receptor gene expression of glucagon-like peptide-1, but not glucose-dependent insulinotropic polypeptide, in rat nodose ganglion cells. Auton Neurosci *110*, 36-43.

Nakamura, T., Furuhashi, M., Li, P., Cao, H., Tuncman, G., Sonenberg, N., Gorgun, C.Z., and Hotamisligil, G.S. (2010). Double-stranded RNA-dependent protein kinase links pathogen sensing with stress and metabolic homeostasis. Cell *140*, 338-348.

Nakatani, Y., Kaneto, H., Kawamori, D., Yoshiuchi, K., Hatazaki, M., Matsuoka, T.A., Ozawa, K., Ogawa, S., Hori, M., Yamasaki, Y.*, et al.* (2005). Involvement of endoplasmic reticulum stress in insulin resistance and diabetes. J Biol Chem *280*, 847-851.

Nedergaard, J., Bengtsson, T., and Cannon, B. (2007). Unexpected evidence for active brown adipose tissue in adult humans. Am J Physiol Endocrinol Metab *293*, E444-452.

Neuhuber, W.L. (1989). Vagal afferent fibers almost exclusively innervate islets in the rat pancreas as demonstrated by anterograde tracing. J Auton Nerv Syst *29*, 13-18.

Nguyen, K.D., Qiu, Y., Cui, X., Goh, Y.P., Mwangi, J., David, T., Mukundan, L., Brombacher, F., Locksley, R.M., and Chawla, A. (2011). Alternatively activated macrophages produce catecholamines to sustain adaptive thermogenesis. Nature *480*, 104-108.

Niebergall, L.J., Jacobs, R.L., Chaba, T., and Vance, D.E. (2011). Phosphatidylcholine protects against steatosis in mice but not non-alcoholic steatohepatitis. Biochim Biophys Acta *1811*, 1177-1185.

Nikonova, L., Koza, R.A., Mendoza, T., Chao, P.M., Curley, J.P., and Kozak, L.P. (2008). Mesoderm-specific transcript is associated with fat mass expansion in response to a positive energy balance. FASEB J *22*, 3925-3937.

Noga, A.A., Stead, L.M., Zhao, Y., Brosnan, M.E., Brosnan, J.T., and Vance, D.E. (2003). Plasma homocysteine is regulated by phospholipid methylation. J Biol Chem *278*, 5952-5955.

Noga, A.A., and Vance, D.E. (2003). A gender-specific role for phosphatidylethanolamine N-methyltransferase-derived phosphatidylcholine in the regulation of plasma high density and very low density lipoproteins in mice. J Biol Chem *278*, 21851-21859.

Noga, A.A., Zhao, Y., and Vance, D.E. (2002). An unexpected requirement for phosphatidylethanolamine N-methyltransferase in the secretion of very low density lipoproteins. J Biol Chem *277*, 42358-42365.

Nye, C., Kim, J., Kalhan, S.C., and Hanson, R.W. (2008). Reassessing triglyceride synthesis in adipose tissue. Trends Endocrinol Metab *19*, 356-361.

O'Rourke, M.F., Staessen, J.A., Vlachopoulos, C., Duprez, D., and Plante, G.E. (2002). Clinical applications of arterial stiffness; definitions and reference values. Am J Hypertens *15*, 426-444.

Odegaard, J.I., and Chawla, A. (2012). Connecting type 1 and type 2 diabetes through innate immunity. Cold Spring Harb Perspect Med *2*, a007724.

Odenbach, J., Wang, X., Cooper, S., Chow, F.L., Oka, T., Lopaschuk, G., Kassiri, Z., and Fernandez-Patron, C. (2011). MMP-2 mediates angiotensin II-induced hypertension under the transcriptional control of MMP-7 and TACE. Hypertension *57*, 123-130.

Ogata, M., Hino, S., Saito, A., Morikawa, K., Kondo, S., Kanemoto, S., Murakami, T., Taniguchi, M., Tanii, I., Yoshinaga, K.*, et al.* (2006). Autophagy is activated for cell survival after endoplasmic reticulum stress. Mol Cell Biol *26*, 9220-9231.

Ogbonnaya, S., and Kaliaperumal, C. (2013). Vagal nerve stimulator: Evolving trends. J Nat Sci Biol Med *4*, 8-13.

Ogden, C.L., Carroll, M.D., Curtin, L.R., McDowell, M.A., Tabak, C.J., and Flegal, K.M. (2006). Prevalence of overweight and obesity in the United States, 1999-2004. JAMA *295*, 1549-1555.

Okazaki, H., Igarashi, M., Nishi, M., Tajima, M., Sekiya, M., Okazaki, S., Yahagi, N., Ohashi, K., Tsukamoto, K., Amemiya-Kudo, M.*, et al.* (2006). Identification of a novel member of the carboxylesterase family that hydrolyzes triacylglycerol: a potential role in adipocyte lipolysis. Diabetes *55*, 2091-2097.

Omagari, K., Kato, S., Tsuneyama, K., Inohara, C., Kuroda, Y., Tsukuda, H., Fukazawa, E., Shiraishi, K., and Mune, M. (2008). Effects of a long-term high-fat diet and switching from a high-fat to low-fat, standard diet on hepatic fat accumulation in Sprague-Dawley rats. Dig Dis Sci *53*, 3206-3212.

Op den Kamp, J.A. (1979). Lipid asymmetry in membranes. Annu Rev Biochem *48*, 47-71.

Orava, J., Nuutila, P., Lidell, M.E., Oikonen, V., Noponen, T., Viljanen, T., Scheinin, M., Taittonen, M., Niemi, T., Enerback, S.*, et al.* (2011). Different metabolic responses of human brown adipose tissue to activation by cold and insulin. Cell Metab *14*, 272-279.

Osuga, J., Ishibashi, S., Oka, T., Yagyu, H., Tozawa, R., Fujimoto, A., Shionoiri, F., Yahagi, N., Kraemer, F.B., Tsutsumi, O.*, et al.* (2000). Targeted disruption of hormone-sensitive lipase results in male sterility and adipocyte hypertrophy, but not in obesity. Proc Natl Acad Sci U S A *97*, 787-792.

Ota, T., Gayet, C., and Ginsberg, H.N. (2008). Inhibition of apolipoprotein B100 secretion by lipid-induced hepatic endoplasmic reticulum stress in rodents. J Clin Invest *118*, 316-332.

Ouellet, V., Labbe, S.M., Blondin, D.P., Phoenix, S., Guerin, B., Haman, F., Turcotte, E.E., Richard, D., and Carpentier, A.C. (2012). Brown adipose tissue oxidative metabolism contributes to energy expenditure during acute cold exposure in humans. J Clin Invest *122*, 545-552.

Ouellet, V., Routhier-Labadie, A., Bellemare, W., Lakhal-Chaieb, L., Turcotte, E., Carpentier, A.C., and Richard, D. (2011). Outdoor temperature, age, sex, body mass index, and diabetic status determine the prevalence, mass, and glucose-uptake activity of 18F-FDG-detected BAT in humans. J Clin Endocrinol Metab *96*, 192-199.

Oyadomari, S., Harding, H.P., Zhang, Y., Oyadomari, M., and Ron, D. (2008). Dephosphorylation of translation initiation factor 2alpha enhances glucose tolerance and attenuates hepatosteatosis in mice. Cell Metab *7*, 520-532.

Ozcan, L., Ergin, A.S., Lu, A., Chung, J., Sarkar, S., Nie, D., Myers, M.G., Jr., and Ozcan, U. (2009). Endoplasmic reticulum stress plays a central role in development of leptin resistance. Cell Metab *9*, 35-51.

Ozcan, U., Cao, Q., Yilmaz, E., Lee, A.H., Iwakoshi, N.N., Ozdelen, E., Tuncman, G., Gorgun, C., Glimcher, L.H., and Hotamisligil, G.S. (2004). Endoplasmic reticulum stress links obesity, insulin action, and type 2 diabetes. Science *306*, 457-461.

Ozcan, U., Yilmaz, E., Ozcan, L., Furuhashi, M., Vaillancourt, E., Smith, R.O., Gorgun, C.Z., and Hotamisligil, G.S. (2006). Chemical chaperones reduce ER stress and restore glucose homeostasis in a mouse model of type 2 diabetes. Science *313*, 1137-1140.

Pagliassotti, M.J. (2012). Endoplasmic reticulum stress in nonalcoholic fatty liver disease. Annu Rev Nutr *32*, 17-33.

Pardo, J.V., Sheikh, S.A., Kuskowski, M.A., Surerus-Johnson, C., Hagen, M.C., Lee, J.T., Rittberg, B.R., and Adson, D.E. (2007). Weight loss during chronic, cervical vagus nerve stimulation in depressed patients with obesity: an observation. Int J Obes (Lond) *31*, 1756-1759.

Park, S.W., Zhou, Y., Lee, J., Lu, A., Sun, C., Chung, J., Ueki, K., and Ozcan, U. (2010). The regulatory subunits of PI3K, p85alpha and p85beta, interact with XBP-1 and increase its nuclear translocation. Nat Med *16*, 429-437.

Pavlov, V.A., Ochani, M., Gallowitsch-Puerta, M., Ochani, K., Huston, J.M., Czura, C.J., Al-Abed, Y., and Tracey, K.J. (2006). Central muscarinic cholinergic regulation of the systemic inflammatory response during endotoxemia. Proc Natl Acad Sci U S A *103*, 5219-5223.

Pavlov, V.A., Parrish, W.R., Rosas-Ballina, M., Ochani, M., Puerta, M., Ochani, K., Chavan, S., Al-Abed, Y., and Tracey, K.J. (2009). Brain acetylcholinesterase activity controls systemic cytokine levels through the cholinergic anti-inflammatory pathway. Brain Behav Immun *23*, 41-45.

Pavlov, V.A., and Tracey, K.J. (2012). The vagus nerve and the inflammatory reflex--linking immunity and metabolism. Nat Rev Endocrinol *8*, 743-754.

Pecheur, E.I., Martin, I., Maier, O., Bakowsky, U., Ruysschaert, J.M., and Hoekstra, D. (2002). Phospholipid species act as modulators in p97/p47-mediated fusion of Golgi membranes. Biochemistry *41*, 9813-9823.

Peirce, V., Carobbio, S., and Vidal-Puig, A. (2014). The different shades of fat. Nature *510*, 76-83.

Peirce, V., and Vidal-Puig, A. (2013). Regulation of glucose homoeostasis by brown adipose tissue. Lancet Diabetes Endocrinol *1*, 353-360.

Pelech, S.L., Power, E., and Vance, D.E. (1983). Activities of the phosphatidylcholine biosynthetic enzymes in rat liver during development. Can J Biochem Cell Biol *61*, 1147-1152.

Pelech, S.L., Pritchard, P.H., Sommerman, E.F., Percival-Smith, A., and Vance, D.E. (1984). Glucagon inhibits phosphatidylcholine biosynthesis via the CDP-choline and transmethylation pathways in cultured rat hepatocytes. Can J Biochem Cell Biol *62*, 196-202.

Perez-Gil, J. (2008). Properly interpreting lipid-protein specificities in pulmonary surfactant. Biophys J *94*, 1542-1543; discussion 1544.

Persichetti, A., Sciuto, R., Rea, S., Basciani, S., Lubrano, C., Mariani, S., Ulisse, S., Nofroni, I., Maini, C.L., and Gnessi, L. (2013). Prevalence, mass, and glucose-uptake activity of (1)(8)F-FDG-detected brown adipose tissue in humans living in a temperate zone of Italy. PLoS One *8*, e63391.

Peters, J.H., Ritter, R.C., and Simasko, S.M. (2006). Leptin and CCK selectively activate vagal afferent neurons innervating the stomach and duodenum. Am J Physiol Regul Integr Comp Physiol *290*, R1544-1549.

Petrovic, N., Shabalina, I.G., Timmons, J.A., Cannon, B., and Nedergaard, J. (2008). Thermogenically competent nonadrenergic recruitment in brown preadipocytes by a PPARgamma agonist. Am J Physiol Endocrinol Metab *295*, E287-296.

Petrovic, N., Walden, T.B., Shabalina, I.G., Timmons, J.A., Cannon, B., and Nedergaard, J. (2010). Chronic peroxisome proliferator-activated receptor gamma (PPARgamma) activation of epididymally derived white adipocyte cultures reveals a population of thermogenically competent, UCP1-containing adipocytes molecularly distinct from classic brown adipocytes. J Biol Chem *285*, 7153-7164.

Pfaffenbach, K.T., Gentile, C.L., Nivala, A.M., Wang, D., Wei, Y., and Pagliassotti, M.J. (2010). Linking endoplasmic reticulum stress to cell death in hepatocytes: roles of C/EBP homologous protein and chemical chaperones in palmitate-mediated cell death. Am J Physiol Endocrinol Metab *298*, E1027-1035.

Pfeifer, A., and Hoffmann, L.S. (2015). Brown, beige, and white: the new color code of fat and its pharmacological implications. Annu Rev Pharmacol Toxicol *55*, 207-227.

Phillips, R., Ursell, T., Wiggins, P., and Sens, P. (2009). Emerging roles for lipids in shaping membrane-protein function. Nature *459*, 379-385.

Pilgeram, L.O., and Greenberg, D.M. (1954). Susceptibility to experimental atherosclerosis and the methylation of ethanolamine 1,2-C14 to phosphatidyl choline. Science *120*, 760-761.

Pitombo, C., Araujo, E.P., De Souza, C.T., Pareja, J.C., Geloneze, B., and Velloso, L.A. (2006). Amelioration of diet-induced diabetes mellitus by removal of visceral fat. J Endocrinol *191*, 699-706.

Pocai, A., Lam, T.K., Gutierrez-Juarez, R., Obici, S., Schwartz, G.J., Bryan, J., Aguilar-Bryan, L., and Rossetti, L. (2005a). Hypothalamic K(ATP) channels control hepatic glucose production. Nature *434*, 1026-1031.

Pocai, A., Obici, S., Schwartz, G.J., and Rossetti, L. (2005b). A brain-liver circuit regulates glucose homeostasis. Cell Metab *1*, 53-61.

Post, J.A., Bijvelt, J.J., and Verkleij, A.J. (1995). Phosphatidylethanolamine and sarcolemmal damage during ischemia or metabolic inhibition of heart myocytes. Am J Physiol *268*, H773-780.

Prechtl, J.C., and Powley, T.L. (1985). Organization and distribution of the rat subdiaphragmatic vagus and associated paraganglia. J Comp Neurol *235*, 182-195.

Prechtl, J.C., and Powley, T.L. (1990). The fiber composition of the abdominal vagus of the rat. Anat Embryol (Berl) *181*, 101-115.

Pritchard, P.H., Chiang, P.K., Cantoni, G.L., and Vance, D.E. (1982). Inhibition of phosphatidylethanolamine N-methylation by 3-deazaadenosine stimulates the synthesis of phosphatidylcholine via the CDP-choline pathway. J Biol Chem *257*, 6362-6367.

Puri, P., Baillie, R.A., Wiest, M.M., Mirshahi, F., Choudhury, J., Cheung, O., Sargeant, C., Contos, M.J., and Sanyal, A.J. (2007). A lipidomic analysis of nonalcoholic fatty liver disease. Hepatology *46*, 1081-1090.

Puri, P., Mirshahi, F., Cheung, O., Natarajan, R., Maher, J.W., Kellum, J.M., and Sanyal, A.J. (2008). Activation and dysregulation of the unfolded protein response in nonalcoholic fatty liver disease. Gastroenterology *134*, 568-576.

Qian, S.W., Tang, Y., Li, X., Liu, Y., Zhang, Y.Y., Huang, H.Y., Xue, R.D., Yu, H.Y., Guo, L., Gao, H.D*., et al.* (2013). BMP4-mediated brown fat-like changes in white adipose tissue alter glucose and energy homeostasis. Proc Natl Acad Sci U S A *110*, E798-807.

Qiang, L., Wang, L., Kon, N., Zhao, W., Lee, S., Zhang, Y., Rosenbaum, M., Zhao, Y., Gu, W., Farmer, S.R*., et al.* (2012). Brown remodeling of white adipose tissue by SirT1-dependent deacetylation of Ppargamma. Cell *150*, 620-632.

Rajakumari, S., Wu, J., Ishibashi, J., Lim, H.W., Giang, A.H., Won, K.J., Reed, R.R., and Seale, P. (2013). EBF2 determines and maintains brown adipocyte identity. Cell Metab *17*, 562-574.

Refsum, H., Ueland, P.M., Nygard, O., and Vollset, S.E. (1998). Homocysteine and cardiovascular disease. Annu Rev Med *49*, 31-62.

Reo, N.V., Adinehzadeh, M., and Foy, B.D. (2002). Kinetic analyses of liver phosphatidylcholine and phosphatidylethanolamine biosynthesis using (13)C NMR spectroscopy. Biochim Biophys Acta *1580*, 171-188.

Resseguie, M., Song, J., Niculescu, M.D., da Costa, K.A., Randall, T.A., and Zeisel, S.H. (2007). Phosphatidylethanolamine N-methyltransferase (PEMT) gene expression is induced by estrogen in human and mouse primary hepatocytes. FASEB J *21*, 2622-2632.

Resseguie, M.E., da Costa, K.A., Galanko, J.A., Patel, M., Davis, I.J., and Zeisel, S.H. (2011). Aberrant estrogen regulation of PEMT results in choline deficiency-associated liver dysfunction. J Biol Chem *286*, 1649-1658.

Richter, W.O., Geiss, H.C., Aleksic, S., and Schwandt, P. (1996). Cardiac autonomic nerve function and insulin sensitivity in obese subjects. Int J Obes Relat Metab Disord *20*, 966-969.

Ridgway, N.D., and Vance, D.E. (1987). Purification of phosphatidylethanolamine N-methyltransferase from rat liver. J Biol Chem *262*, 17231-17239.

Ridgway, N.D., and Vance, D.E. (1988a). Kinetic mechanism of phosphatidylethanolamine N-methyltransferase. J Biol Chem *263*, 16864-16871.

Ridgway, N.D., and Vance, D.E. (1988b). Specificity of rat hepatic phosphatidylethanolamine N-methyltransferase for molecular species of diacyl phosphatidylethanolamine. J Biol Chem *263*, 16856-16863.

Ridgway, N.D., and Vance, D.E. (1989). In vitro phosphorylation of phosphatidylethanolamine N-methyltransferase by cAMP-dependent protein kinase:

lack of in vivo phosphorylation in response to N6-2'-O-dibutryladenosine 3',5'-cyclic monophosphate. Biochim Biophys Acta *1004*, 261-270.

Ridgway, N.D., Yao, Z., and Vance, D.E. (1989). Phosphatidylethanolamine levels and regulation of phosphatidylethanolamine N-methyltransferase. J Biol Chem *264*, 1203-1207.

Riekhof, W.R., Wu, J., Jones, J.L., and Voelker, D.R. (2007). Identification and characterization of the major lysophosphatidylethanolamine acyltransferase in Saccharomyces cerevisiae. J Biol Chem *282*, 28344-28352.

Rinella, M.E., Elias, M.S., Smolak, R.R., Fu, T., Borensztajn, J., and Green, R.M. (2008). Mechanisms of hepatic steatosis in mice fed a lipogenic methionine choline-deficient diet. J Lipid Res *49*, 1068-1076.

Rinella, M.E., and Green, R.M. (2004). The methionine-choline deficient dietary model of steatohepatitis does not exhibit insulin resistance. J Hepatol *40*, 47-51.

Robinson, K. (2001). Homocysteine and coronary artery disease. In Homocysteine in Health and Disease, D.W.J. R. Carmel, ed. (Cambridge, Cambridge University Pres), pp. 371–383.

Rock, C.O. (2008). Fatty acid and phospholipid metabolism in prokaryotes. In Biochemistry of Lipids, Lipoproteins and Membranes, D.E.V.a.J.E. Vance, ed. (Amsterdam), pp. 59-96.

Rodeheffer, M.S., Birsoy, K., and Friedman, J.M. (2008). Identification of white adipocyte progenitor cells in vivo. Cell *135*, 240-249.

Romeo, S., Cohen, J.C., and Hobbs, H.H. (2006). No association between polymorphism in PEMT (V175M) and hepatic triglyceride content in the Dallas Heart Study. In FASEB J, pp. 2180; author reply 2181-2182.

Ron, D., and Walter, P. (2007). Signal integration in the endoplasmic reticulum unfolded protein response. Nat Rev Mol Cell Biol *8*, 519-529.

Rosenwald, M., Perdikari, A., Rulicke, T., and Wolfrum, C. (2013). Bi-directional interconversion of brite and white adipocytes. Nat Cell Biol *15*, 659-667.

Rothwell, N.J., and Stock, M.J. (1979). A role for brown adipose tissue in diet-induced thermogenesis. Nature *281*, 31-35.

Ruiz de Azua, I., Gautam, D., Guettier, J.M., and Wess, J. (2011). Novel insights into the function of beta-cell M3 muscarinic acetylcholine receptors: therapeutic implications. Trends Endocrinol Metab *22*, 74-80.

Sachdeva, A.K., Zaren, H.A., and Sigel, B. (1991). Surgical treatment of peptic ulcer disease. Med Clin North Am *75*, 999-1012.

Saito, M., Okamatsu-Ogura, Y., Matsushita, M., Watanabe, K., Yoneshiro, T., Nio-Kobayashi, J., Iwanaga, T., Miyagawa, M., Kameya, T., Nakada, K.*, et al.* (2009). High incidence of metabolically active brown adipose tissue in healthy adult humans: effects of cold exposure and adiposity. Diabetes *58*, 1526-1531.

Saleem, S., Kim, Y.T., Maruyama, T., Narumiya, S., and Dore, S. (2009). Reduced acute brain injury in PGE2 EP3 receptor-deficient mice after cerebral ischemia. J Neuroimmunol *208*, 87-93.

Samborski, R.W., Ridgway, N.D., and Vance, D.E. (1990). Evidence that only newly made phosphatidylethanolamine is methylated to phosphatidylcholine and that phosphatidylethanolamine is not significantly deacylated-reacylated in rat hepatocytes. J Biol Chem *265*, 18322-18329.

Sanchez-Gurmaches, J., Hung, C.M., Sparks, C.A., Tang, Y., Li, H., and Guertin, D.A. (2012). PTEN loss in the Myf5 lineage redistributes body fat and reveals subsets of white adipocytes that arise from Myf5 precursors. Cell Metab *16*, 348-362.

Scherer, P.E. (2006). Adipose tissue: from lipid storage compartment to endocrine organ. Diabetes *55*, 1537-1545.

Scherer, P.E., Williams, S., Fogliano, M., Baldini, G., and Lodish, H.F. (1995). A novel serum protein similar to C1q, produced exclusively in adipocytes. J Biol Chem *270*, 26746-26749.

Schroder, M. (2008). Endoplasmic reticulum stress responses. Cell Mol Life Sci *65*, 862-894.

Schulz, T.J., Huang, T.L., Tran, T.T., Zhang, H., Townsend, K.L., Shadrach, J.L., Cerletti, M., McDougall, L.E., Giorgadze, N., Tchkonia, T.*, et al.* (2011). Identification of inducible brown adipocyte progenitors residing in skeletal muscle and white fat. Proc Natl Acad Sci U S A *108*, 143-148.

Schulz, T.J., and Tseng, Y.H. (2013). Brown adipose tissue: development, metabolism and beyond. Biochem J *453*, 167-178.

Schweiger, M., Schreiber, R., Haemmerle, G., Lass, A., Fledelius, C., Jacobsen, P., Tornqvist, H., Zechner, R., and Zimmermann, R. (2006). Adipose triglyceride lipase and

hormone-sensitive lipase are the major enzymes in adipose tissue triacylglycerol catabolism. J Biol Chem *281*, 40236-40241.

Seale, P., Bjork, B., Yang, W., Kajimura, S., Chin, S., Kuang, S., Scime, A., Devarakonda, S., Conroe, H.M., Erdjument-Bromage, H.*, et al.* (2008). PRDM16 controls a brown fat/skeletal muscle switch. Nature *454*, 961-967.

Seale, P., Conroe, H.M., Estall, J., Kajimura, S., Frontini, A., Ishibashi, J., Cohen, P., Cinti, S., and Spiegelman, B.M. (2011). Prdm16 determines the thermogenic program of subcutaneous white adipose tissue in mice. J Clin Invest *121*, 96-105.

Sellayah, D., Bharaj, P., and Sikder, D. (2011). Orexin is required for brown adipose tissue development, differentiation, and function. Cell Metab *14*, 478-490.

Sesca, E., Perletti, G.P., Binasco, V., Chiara, M., and Tessitore, L. (1996). Phosphatidylethanolamine N-methyltransferase 2 and CTP-phosphocholine cytidylyltransferase expressions are related with protein kinase C isozymes in developmental liver growth. Biochem Biophys Res Commun *229*, 158-162.

Shan, T., Liang, X., Bi, P., Zhang, P., Liu, W., and Kuang, S. (2013). Distinct populations of adipogenic and myogenic Myf5-lineage progenitors in white adipose tissues. J Lipid Res *54*, 2214-2224.

Sharp, L.Z., Shinoda, K., Ohno, H., Scheel, D.W., Tomoda, E., Ruiz, L., Hu, H., Wang, L., Pavlova, Z., Gilsanz, V.*, et al.* (2012). Human BAT possesses molecular signatures that resemble beige/brite cells. PLoS One *7*, e49452.

Shi, Y., Vattem, K.M., Sood, R., An, J., Liang, J., Stramm, L., and Wek, R.C. (1998). Identification and characterization of pancreatic eukaryotic initiation factor 2 alpha-subunit kinase, PEK, involved in translational control. Mol Cell Biol *18*, 7499-7509.

Shiao, Y.J., Balcerzak, B., and Vance, J.E. (1998). A mitochondrial membrane protein is required for translocation of phosphatidylserine from mitochondria-associated membranes to mitochondria. Biochem J *331 (Pt 1)*, 217-223.

Shibata, H., Perusse, F., Vallerand, A., and Bukowiecki, L.J. (1989). Cold exposure reverses inhibitory effects of fasting on peripheral glucose uptake in rats. Am J Physiol *257*, R96-101.

Shields, D.J., Agellon, L.B., and Vance, D.E. (2001). Structure, expression profile and alternative processing of the human phosphatidylethanolamine N-methyltransferase (PEMT) gene. Biochim Biophys Acta *1532*, 105-114.

Shields, D.J., Altarejos, J.Y., Wang, X., Agellon, L.B., and Vance, D.E. (2003a). Molecular dissection of the S-adenosylmethionine-binding site of phosphatidylethanolamine N-methyltransferase. J Biol Chem *278*, 35826-35836.

Shields, D.J., Lehner, R., Agellon, L.B., and Vance, D.E. (2003b). Membrane topography of human phosphatidylethanolamine N-methyltransferase. J Biol Chem *278*, 2956-2962.

Shields, D.J., Lingrell, S., Agellon, L.B., Brosnan, J.T., and Vance, D.E. (2005). Localization-independent regulation of homocysteine secretion by phosphatidylethanolamine N-methyltransferase. J Biol Chem *280*, 27339-27344.

Shimizu, T., Ohto, T., and Kita, Y. (2006). Cytosolic phospholipase A2: biochemical properties and physiological roles. IUBMB Life *58*, 328-333.

Shindou, H., and Shimizu, T. (2009). Acyl-CoA:lysophospholipid acyltransferases. J Biol Chem *284*, 1-5.

Sidrauski, C., and Walter, P. (1997). The transmembrane kinase Ire1p is a site-specific endonuclease that initiates mRNA splicing in the unfolded protein response. Cell *90*, 1031-1039.

Signorell, A., Gluenz, E., Rettig, J., Schneider, A., Shaw, M.K., Gull, K., and Butikofer, P. (2009). Perturbation of phosphatidylethanolamine synthesis affects mitochondrial morphology and cell-cycle progression in procyclic-form Trypanosoma brucei. Mol Microbiol *72*, 1068-1079.

Signorell, A., Rauch, M., Jelk, J., Ferguson, M.A., and Butikofer, P. (2008). Phosphatidylethanolamine in Trypanosoma brucei is organized in two separate pools and is synthesized exclusively by the Kennedy pathway. J Biol Chem *283*, 23636-23644.

Singh, R., Kaushik, S., Wang, Y., Xiang, Y., Novak, I., Komatsu, M., Tanaka, K., Cuervo, A.M., and Czaja, M.J. (2009). Autophagy regulates lipid metabolism. Nature *458*, 1131-1135.

Skipski, V.P., Barclay, M., Barclay, R.K., Fetzer, V.A., Good, J.J., and Archibald, F.M. (1967). Lipid composition of human serum lipoproteins. Biochem J *104*, 340-352.

Skurk, T., Alberti-Huber, C., Herder, C., and Hauner, H. (2007). Relationship between adipocyte size and adipokine expression and secretion. J Clin Endocrinol Metab *92*, 1023-1033.

Smit, J.J., Schinkel, A.H., Oude Elferink, R.P., Groen, A.K., Wagenaar, E., van Deemter, L., Mol, C.A., Ottenhoff, R., van der Lugt, N.M., van Roon, M.A.*, et al.* (1993). Homozygous disruption of the murine mdr2 P-glycoprotein gene leads to a complete absence of phospholipid from bile and to liver disease. Cell *75*, 451-462.

Song, J., da Costa, K.A., Fischer, L.M., Kohlmeier, M., Kwock, L., Wang, S., and Zeisel, S.H. (2005). Polymorphism of the PEMT gene and susceptibility to nonalcoholic fatty liver disease (NAFLD). FASEB J *19*, 1266-1271.

Soon, R.K., Jr., Yan, J.S., Grenert, J.P., and Maher, J.J. (2010). Stress signaling in the methionine-choline-deficient model of murine fatty liver disease. Gastroenterology *139*, 1730-1739, 1739 e1731.

Spalding, K.L., Arner, E., Westermark, P.O., Bernard, S., Buchholz, B.A., Bergmann, O., Blomqvist, L., Hoffstedt, J., Naslund, E., Britton, T.*, et al.* (2008). Dynamics of fat cell turnover in humans. Nature *453*, 783-787.

Stanford, K.I., Middelbeek, R.J., Townsend, K.L., An, D., Nygaard, E.B., Hitchcox, K.M., Markan, K.R., Nakano, K., Hirshman, M.F., Tseng, Y.H.*, et al.* (2013). Brown adipose tissue regulates glucose homeostasis and insulin sensitivity. J Clin Invest *123*, 215-223.

Stead, L.M., Brosnan, J.T., Brosnan, M.E., Vance, D.E., and Jacobs, R.L. (2006). Is it time to reevaluate methyl balance in humans? Am J Clin Nutr *83*, 5-10.

Stearns, A.T., Balakrishnan, A., Radmanesh, A., Ashley, S.W., Rhoads, D.B., and Tavakkolizadeh, A. (2012). Relative contributions of afferent vagal fibers to resistance to diet-induced obesity. Dig Dis Sci *57*, 1281-1290.

Steenbergen, R., Nanowski, T.S., Beigneux, A., Kulinski, A., Young, S.G., and Vance, J.E. (2005). Disruption of the phosphatidylserine decarboxylase gene in mice causes embryonic lethality and mitochondrial defects. J Biol Chem *280*, 40032-40040.

Sugita, M. (2006). Taste perception and coding in the periphery. Cell Mol Life Sci *63*, 2000-2015.

Sun, K., Kusminski, C.M., and Scherer, P.E. (2011). Adipose tissue remodeling and obesity. J Clin Invest *121*, 2094-2101.

Sundler, R., and Akesson, B. (1975a). Biosynthesis of phosphatidylethanolamines and phosphatidylcholines from ethanolamine and choline in rat liver. Biochem J *146*, 309-315.

Sundler, R., and Akesson, B. (1975b). Regulation of phospholipid biosynthesis in isolated rat hepatocytes. Effect of different substrates. J Biol Chem *250*, 3359-3367.

Tabas, I., and Ron, D. (2011). Integrating the mechanisms of apoptosis induced by endoplasmic reticulum stress. Nat Cell Biol *13*, 184-190.

Tang, W., Keesler, G.A., and Tabas, I. (1997). The structure of the gene for murine CTP:phosphocholine cytidylyltransferase, Ctpct. Relationship of exon structure to functional domains and identification of transcriptional start sites and potential upstream regulatory elements. J Biol Chem *272*, 13146-13151.

Tang, W., Zeve, D., Suh, J.M., Bosnakovski, D., Kyba, M., Hammer, R.E., Tallquist, M.D., and Graff, J.M. (2008). White fat progenitor cells reside in the adipose vasculature. Science *322*, 583-586.

Taub, R. (2004). Liver regeneration: from myth to mechanism. Nat Rev Mol Cell Biol *5*, 836-847.

Testerink, N., van der Sanden, M.H., Houweling, M., Helms, J.B., and Vaandrager, A.B. (2009). Depletion of phosphatidylcholine affects endoplasmic reticulum morphology and protein traffic at the Golgi complex. J Lipid Res *50*, 2182-2192.

Thomas, S.A., and Palmiter, R.D. (1997). Thermoregulatory and metabolic phenotypes of mice lacking noradrenaline and adrenaline. Nature *387*, 94-97.

Tian, Y., Jackson, P., Gunter, C., Wang, J., Rock, C.O., and Jackowski, S. (2006). Placental thrombosis and spontaneous fetal death in mice deficient in ethanolamine kinase 2. J Biol Chem *281*, 28438-28449.

Tilg, H., and Hotamisligil, G.S. (2006). Nonalcoholic fatty liver disease: Cytokine-adipokine interplay and regulation of insulin resistance. Gastroenterology *131*, 934-945.

Timmons, J.A., Wennmalm, K., Larsson, O., Walden, T.B., Lassmann, T., Petrovic, N., Hamilton, D.L., Gimeno, R.E., Wahlestedt, C., Baar, K.*, et al.* (2007). Myogenic gene expression signature establishes that brown and white adipocytes originate from distinct cell lineages. Proc Natl Acad Sci U S A *104*, 4401-4406.

Tomlinson, E., Fu, L., John, L., Hultgren, B., Huang, X., Renz, M., Stephan, J.P., Tsai, S.P., Powell-Braxton, L., French, D.*, et al.* (2002). Transgenic mice expressing human

fibroblast growth factor-19 display increased metabolic rate and decreased adiposity. Endocrinology *143*, 1741-1747.

Tontonoz, P., and Spiegelman, B.M. (2008). Fat and beyond: the diverse biology of PPARgamma. Annu Rev Biochem *77*, 289-312.

Toschi, A., Lee, E., Xu, L., Garcia, A., Gadir, N., and Foster, D.A. (2009). Regulation of mTORC1 and mTORC2 complex assembly by phosphatidic acid: competition with rapamycin. Mol Cell Biol *29*, 1411-1420.

Townsend, K.L., Suzuki, R., Huang, T.L., Jing, E., Schulz, T.J., Lee, K., Taniguchi, C.M., Espinoza, D.O., McDougall, L.E., Zhang, H.*, et al.* (2012). Bone morphogenetic protein 7 (BMP7) reverses obesity and regulates appetite through a central mTOR pathway. FASEB J *26*, 2187-2196.

Townsend, K.L., and Tseng, Y.H. (2014). Brown fat fuel utilization and thermogenesis. Trends Endocrinol Metab *25*, 168-177.

Tracey, K.J. (2002). The inflammatory reflex. Nature *420*, 853-859.

Tracey, K.J. (2005). Fat meets the cholinergic antiinflammatory pathway. J Exp Med *202*, 1017-1021.

Tracey, K.J. (2009). Reflex control of immunity. Nat Rev Immunol *9*, 418-428.

Tran, K.V., Gealekman, O., Frontini, A., Zingaretti, M.C., Morroni, M., Giordano, A., Smorlesi, A., Perugini, J., De Matteis, R., Sbarbati, A.*, et al.* (2012). The vascular endothelium of the adipose tissue gives rise to both white and brown fat cells. Cell Metab *15*, 222-229.

Tubbs, E., Theurey, P., Vial, G., Bendridi, N., Bravard, A., Chauvin, M.A., Ji-Cao, J., Zoulim, F., Bartosch, B., Ovize, M.*, et al.* (2014). Mitochondria-associated endoplasmic reticulum membrane (MAM) integrity is required for insulin signaling and is implicated in hepatic insulin resistance. Diabetes *63*, 3279-3294.

Uno, K., Katagiri, H., Yamada, T., Ishigaki, Y., Ogihara, T., Imai, J., Hasegawa, Y., Gao, J., Kaneko, K., Iwasaki, H.*, et al.* (2006). Neuronal pathway from the liver modulates energy expenditure and systemic insulin sensitivity. Science *312*, 1656-1659.

Uno, K., Yamada, T., Ishigaki, Y., Imai, J., Hasegawa, Y., Gao, J., Kaneko, K., Matsusue, K., Yamazaki, T., Oka, Y.*, et al.* (2012). Hepatic peroxisome proliferator-activated receptor-gamma-fat-specific protein 27 pathway contributes to obesity-related hypertension via afferent vagal signals. Eur Heart J *33*, 1279-1289.

Upton, J.P., Wang, L., Han, D., Wang, E.S., Huskey, N.E., Lim, L., Truitt, M., McManus, M.T., Ruggero, D., Goga, A.*, et al.* (2012). IRE1alpha cleaves select microRNAs during ER stress to derepress translation of proapoptotic Caspase-2. Science *338*, 818-822.

Vallerand, A.L., Perusse, F., and Bukowiecki, L.J. (1990). Stimulatory effects of cold exposure and cold acclimation on glucose uptake in rat peripheral tissues. Am J Physiol *259*, R1043-1049.

van der Veen, J.N., Lingrell, S., da Silva, R.P., Jacobs, R.L., and Vance, D.E. (2014). The concentration of phosphatidylethanolamine in mitochondria can modulate ATP production and glucose metabolism in mice. Diabetes *63*, 2620-2630.

van der Veen, J.N., Lingrell, S., and Vance, D.E. (2012). The membrane lipid phosphatidylcholine is an unexpected source of triacylglycerol in the liver. J Biol Chem *287*, 23418-23426.

van Helvoort, A., Smith, A.J., Sprong, H., Fritzsche, I., Schinkel, A.H., Borst, P., and van Meer, G. (1996). MDR1 P-glycoprotein is a lipid translocase of broad specificity, while MDR3 P-glycoprotein specifically translocates phosphatidylcholine. Cell *87*, 507-517.

van Marken Lichtenbelt, W.D., Vanhommerig, J.W., Smulders, N.M., Drossaerts, J.M., Kemerink, G.J., Bouvy, N.D., Schrauwen, P., and Teule, G.J. (2009). Cold-activated brown adipose tissue in healthy men. N Engl J Med *360*, 1500-1508.

van Meer, G., Voelker, D.R., and Feigenson, G.W. (2008). Membrane lipids: where they are and how they behave. Nat Rev Mol Cell Biol *9*, 112-124.

Vance, D.E. (2013). Physiological roles of phosphatidylethanolamine N-methyltransferase. Biochim Biophys Acta *1831*, 626-632.

Vance, D.E. (2014). Phospholipid methylation in mammals: from biochemistry to physiological function. Biochim Biophys Acta *1838*, 1477-1487.

Vance, D.E., and Vance, J. E. (2008). Phospholipid biosynthesis in eukaryotes. In Biochemistry of Lipids, Lipoproteins and Membranes, D.E. Vance, and Vance, J. E.,, ed. (Amsterdam, Elsevier), pp. 213–244.

Vance, D.E., Li, Z., and Jacobs, R.L. (2007). Hepatic phosphatidylethanolamine N-methyltransferase, unexpected roles in animal biochemistry and physiology. J Biol Chem *282*, 33237-33241.

Vance, D.E., and Ridgway, N.D. (1988). The methylation of phosphatidylethanolamine. Prog Lipid Res *27*, 61-79.

Vance, J.E. (1990). Phospholipid synthesis in a membrane fraction associated with mitochondria. J Biol Chem *265*, 7248-7256.

Vance, J.E., and Tasseva, G. (2013). Formation and function of phosphatidylserine and phosphatidylethanolamine in mammalian cells. Biochim Biophys Acta *1831*, 543-554.

Vance, J.E., and Vance, D.E. (1986). Specific pools of phospholipids are used for lipoprotein secretion by cultured rat hepatocytes. J Biol Chem *261*, 4486-4491.

Vance, J.E., and Vance, D.E. (1988). Does rat liver Golgi have the capacity to synthesize phospholipids for lipoprotein secretion? J Biol Chem *263*, 5898-5909.

Varela-Rey, M., Embade, N., Ariz, U., Lu, S.C., Mato, J.M., and Martinez-Chantar, M.L. (2009). Non-alcoholic steatohepatitis and animal models: understanding the human disease. Int J Biochem Cell Biol *41*, 969-976.

Vaughan, C.H., Shrestha, Y.B., and Bartness, T.J. (2011). Characterization of a novel melanocortin receptor-containing node in the SNS outflow circuitry to brown adipose tissue involved in thermogenesis. Brain Res *1411*, 17-27.

Vegiopoulos, A., Muller-Decker, K., Strzoda, D., Schmitt, I., Chichelnitskiy, E., Ostertag, A., Berriel Diaz, M., Rozman, J., Hrabe de Angelis, M., Nusing, R.M.*, et al.* (2010). Cyclooxygenase-2 controls energy homeostasis in mice by de novo recruitment of brown adipocytes. Science *328*, 1158-1161.

Vergnes, L., Chin, R., Young, S.G., and Reue, K. (2011). Heart-type fatty acid-binding protein is essential for efficient brown adipose tissue fatty acid oxidation and cold tolerance. J Biol Chem *286*, 380-390.

Verkade, H.J., Fast, D.G., Rusinol, A.E., Scraba, D.G., and Vance, D.E. (1993). Impaired biosynthesis of phosphatidylcholine causes a decrease in the number of very low density lipoprotein particles in the Golgi but not in the endoplasmic reticulum of rat liver. J Biol Chem *268*, 24990-24996.

Vermeulen, P.S., Lingrell, S., Yao, Z., and Vance, D.E. (1997). Phosphatidylcholine biosynthesis is required for secretion of truncated apolipoprotein Bs from McArdle RH7777 cells only when a neutral lipid core is formed. J Lipid Res *38*, 447-458.

Vetelainen, R., van Vliet, A., Gouma, D.J., and van Gulik, T.M. (2007). Steatosis as a risk factor in liver surgery. Annals of Surgery *245*, 20-30.

Vilatoba, M., Eckstein, C., Bilbao, G., Smyth, C.A., Jenkins, S., Thompson, J.A., Eckhoff, D.E., and Contreras, J.L. (2005). Sodium 4-phenylbutyrate protects against liver ischemia reperfusion injury by inhibition of endoplasmic reticulum-stress mediated apoptosis. Surgery *138*, 342-351.

Virtanen, K.A., Lidell, M.E., Orava, J., Heglind, M., Westergren, R., Niemi, T., Taittonen, M., Laine, J., Savisto, N.J., Enerback, S.*, et al.* (2009). Functional brown adipose tissue in healthy adults. N Engl J Med *360*, 1518-1525.

Vitali, A., Murano, I., Zingaretti, M.C., Frontini, A., Ricquier, D., and Cinti, S. (2012). The adipose organ of obesity-prone C57BL/6J mice is composed of mixed white and brown adipocytes. J Lipid Res *53*, 619-629.

Voelker, D.R. (1984). Phosphatidylserine functions as the major precursor of phosphatidylethanolamine in cultured BHK-21 cells. Proc Natl Acad Sci U S A *81*, 2669-2673.

Voss-Andreae, A., Murphy, J.G., Ellacott, K.L., Stuart, R.C., Nillni, E.A., Cone, R.D., and Fan, W. (2007). Role of the central melanocortin circuitry in adaptive thermogenesis of brown adipose tissue. Endocrinology *148*, 1550-1560.

Wahren, J., and Ekberg, K. (2007). Splanchnic regulation of glucose production. Annu Rev Nutr *27*, 329-345.

Waki, H., and Tontonoz, P. (2007). Endocrine functions of adipose tissue. Annu Rev Pathol *2*, 31-56.

Walden, T.B., Timmons, J.A., Keller, P., Nedergaard, J., and Cannon, B. (2009). Distinct expression of muscle-specific microRNAs (myomirs) in brown adipocytes. J Cell Physiol *218*, 444-449.

Walkey, C.J., Cui, Z., Agellon, L.B., and Vance, D.E. (1996). Characterization of the murine phosphatidylethanolamine N-methyltransferase-2 gene. J Lipid Res *37*, 2341-2350.

Walkey, C.J., Donohue, L.R., Bronson, R., Agellon, L.B., and Vance, D.E. (1997). Disruption of the murine gene encoding phosphatidylethanolamine N-methyltransferase. Proc Natl Acad Sci U S A *94*, 12880-12885.

Walkey, C.J., Shields, D.J., and Vance, D.E. (1999). Identification of three novel cDNAs for human phosphatidylethanolamine N-methyltransferase and localization of the human gene on chromosome 17p11.2. Biochim Biophys Acta *1436*, 405-412.

Walkey, C.J., Yu, L., Agellon, L.B., and Vance, D.E. (1998). Biochemical and evolutionary significance of phospholipid methylation. J Biol Chem *273*, 27043-27046.

Wang, H., Yu, M., Ochani, M., Amella, C.A., Tanovic, M., Susarla, S., Li, J.H., Yang, H., Ulloa, L., Al-Abed, Y.*, et al.* (2003). Nicotinic acetylcholine receptor alpha7 subunit is an essential regulator of inflammation. Nature *421*, 384-388.

Wang, L., Magdaleno, S., Tabas, I., and Jackowski, S. (2005). Early embryonic lethality in mice with targeted deletion of the CTP:phosphocholine cytidylyltransferase alpha gene (Pcyt1a). Mol Cell Biol *25*, 3357-3363.

Wang, P.Y., Caspi, L., Lam, C.K., Chari, M., Li, X., Light, P.E., Gutierrez-Juarez, R., Ang, M., Schwartz, G.J., and Lam, T.K. (2008). Upper intestinal lipids trigger a gut-brain-liver axis to regulate glucose production. Nature *452*, 1012-1016.

Wang, Q.A., Tao, C., Gupta, R.K., and Scherer, P.E. (2013). Tracking adipogenesis during white adipose tissue development, expansion and regeneration. Nat Med *19*, 1338-1344.

Wang, S., Chen, Z., Lam, V., Han, J., Hassler, J., Finck, B.N., Davidson, N.O., and Kaufman, R.J. (2012). IRE1alpha-XBP1s induces PDI expression to increase MTP activity for hepatic VLDL assembly and lipid homeostasis. Cell Metab *16*, 473-486.

Wang, S., and Kaufman, R.J. (2012). The impact of the unfolded protein response on human disease. J Cell Biol *197*, 857-867.

Wang, S.P., Laurin, N., Himms-Hagen, J., Rudnicki, M.A., Levy, E., Robert, M.F., Pan, L., Oligny, L., and Mitchell, G.A. (2001). The adipose tissue phenotype of hormone-sensitive lipase deficiency in mice. Obes Res *9*, 119-128.

Wang, X., Yang, Z., Xue, B., and Shi, H. (2011). Activation of the cholinergic antiinflammatory pathway ameliorates obesity-induced inflammation and insulin resistance. Endocrinology *152*, 836-846.

Wang, Y., Vera, L., Fischer, W.H., and Montminy, M. (2009). The CREB coactivator CRTC2 links hepatic ER stress and fasting gluconeogenesis. Nature *460*, 534-537.

Warne, J.P., Foster, M.T., Horneman, H.F., Pecoraro, N.C., Ginsberg, A.B., Akana, S.F., and Dallman, M.F. (2007). Hepatic branch vagotomy, like insulin replacement, promotes voluntary lard intake in streptozotocin-diabetic rats. Endocrinology *148*, 3288-3298.

Watkins, S.M., Zhu, X., and Zeisel, S.H. (2003). Phosphatidylethanolamine-N-methyltransferase activity and dietary choline regulate liver-plasma lipid flux and essential fatty acid metabolism in mice. The Journal of nutrition *133*, 3386-3391.

Wei, E., Gao, W., and Lehner, R. (2007). Attenuation of adipocyte triacylglycerol hydrolase activity decreases basal fatty acid efflux. J Biol Chem *282*, 8027-8035.

Weisberg, S.P., McCann, D., Desai, M., Rosenbaum, M., Leibel, R.L., and Ferrante, A.W., Jr. (2003). Obesity is associated with macrophage accumulation in adipose tissue. J Clin Invest *112*, 1796-1808.

Wellen, K.E., and Hotamisligil, G.S. (2003). Obesity-induced inflammatory changes in adipose tissue. J Clin Invest *112*, 1785-1788.

Whittle, A.J., Carobbio, S., Martins, L., Slawik, M., Hondares, E., Vazquez, M.J., Morgan, D., Csikasz, R.I., Gallego, R., Rodriguez-Cuenca, S.*, et al.* (2012). BMP8B

increases brown adipose tissue thermogenesis through both central and peripheral actions. Cell *149*, 871-885.

Wiggins, D., and Gibbons, G.F. (1996). Origin of hepatic very-low-density lipoprotein triacylglycerol: the contribution of cellular phospholipid. Biochem J *320 (Pt 2)*, 673-679.

Wikstrom, L., Johansson, C., Salto, C., Barlow, C., Campos Barros, A., Baas, F., Forrest, D., Thoren, P., and Vennstrom, B. (1998). Abnormal heart rate and body temperature in mice lacking thyroid hormone receptor alpha 1. EMBO J *17*, 455-461.

Williams, C.D., Stengel, J., Asike, M.I., Torres, D.M., Shaw, J., Contreras, M., Landt, C.L., and Harrison, S.A. (2011). Prevalence of nonalcoholic fatty liver disease and nonalcoholic steatohepatitis among a largely middle-aged population utilizing ultrasound and liver biopsy: a prospective study. Gastroenterology *140*, 124-131.

Wilton, D.C. (2008). Phospholipases. In Biochemistry of Lipids, Lipoproteins and Membranes, D.E.V.a.J.E. Vance, ed. (Amsterdam, Elsevier), pp. 305-329.

Woods, S.C., Lutz, T.A., Geary, N., and Langhans, W. (2006). Pancreatic signals controlling food intake; insulin, glucagon and amylin. Philos Trans R Soc Lond B Biol Sci *361*, 1219-1235.

Wu, G., Zhang, L., Li, T., Lopaschuk, G., Vance, D.E., and Jacobs, R.L. (2012a). Choline Deficiency Attenuates Body Weight Gain and Improves Glucose Tolerance in ob/ob Mice. J Obes *2012*, 319172.

Wu, G., Zhang, L., Li, T., Zuniga, A., Lopaschuk, G.D., Li, L., Jacobs, R.L., and Vance, D.E. (2013). Choline Supplementation Promotes Hepatic Insulin Resistance in

Phosphatidylethanolamine N-Methyltransferase-deficient Mice via Increased Glucagon Action. J Biol Chem *288*, 837-847.

Wu, J., Bostrom, P., Sparks, L.M., Ye, L., Choi, J.H., Giang, A.H., Khandekar, M., Virtanen, K.A., Nuutila, P., Schaart, G.*, et al.* (2012b). Beige adipocytes are a distinct type of thermogenic fat cell in mouse and human. Cell *150*, 366-376.

Xiao, C., Giacca, A., and Lewis, G.F. (2011). Sodium phenylbutyrate, a drug with known capacity to reduce endoplasmic reticulum stress, partially alleviates lipid-induced insulin resistance and beta-cell dysfunction in humans. Diabetes *60*, 918-924.

Xu, H., Barnes, G.T., Yang, Q., Tan, G., Yang, D., Chou, C.J., Sole, J., Nichols, A., Ross, J.S., Tartaglia, L.A.*, et al.* (2003). Chronic inflammation in fat plays a crucial role in the development of obesity-related insulin resistance. J Clin Invest *112*, 1821-1830.

Yamashita, A., Sugiura, T., and Waku, K. (1997). Acyltransferases and transacylases involved in fatty acid remodeling of phospholipids and metabolism of bioactive lipids in mammalian cells. J Biochem *122*, 1-16.

Yao, C., Sakata, D., Esaki, Y., Li, Y., Matsuoka, T., Kuroiwa, K., Sugimoto, Y., and Narumiya, S. (2009). Prostaglandin E2-EP4 signaling promotes immune inflammation through Th1 cell differentiation and Th17 cell expansion. Nat Med *15*, 633-640.

Yao, Z.M., and Vance, D.E. (1988). The active synthesis of phosphatidylcholine is required for very low density lipoprotein secretion from rat hepatocytes. J Biol Chem *263*, 2998-3004.

Yao, Z.M., and Vance, D.E. (1990). Reduction in VLDL, but not HDL, in plasma of rats deficient in choline. Biochem Cell Biol *68*, 552-558.

Yi, C.X., la Fleur, S.E., Fliers, E., and Kalsbeek, A. (2010). The role of the autonomic nervous liver innervation in the control of energy metabolism. Biochim Biophys Acta *1802*, 416-431.

Yin, H., Pasut, A., Soleimani, V.D., Bentzinger, C.F., Antoun, G., Thorn, S., Seale, P., Fernando, P., van Ijcken, W., Grosveld, F.*, et al.* (2013). MicroRNA-133 controls brown adipose determination in skeletal muscle satellite cells by targeting Prdm16. Cell Metab *17*, 210-224.

Yore, M.M., Syed, I., Moraes-Vieira, P.M., Zhang, T., Herman, M.A., Homan, E.A., Patel, R.T., Lee, J., Chen, S., Peroni, O.D.*, et al.* (2014). Discovery of a class of endogenous mammalian lipids with anti-diabetic and anti-inflammatory effects. Cell *159*, 318-332.

Young, D.L. (1971). Estradiol- and testosterone-induced alterations in phosphatidylcholine and triglyceride synthesis in hepatic endoplasmic reticulum. J Lipid Res *12*, 590-595.

Zborowski, J., Dygas, A., and Wojtczak, L. (1983). Phosphatidylserine decarboxylase is located on the external side of the inner mitochondrial membrane. FEBS Lett *157*, 179-182.

Zechner, R., Kienesberger, P.C., Haemmerle, G., Zimmermann, R., and Lass, A. (2009). Adipose triglyceride lipase and the lipolytic catabolism of cellular fat stores. J Lipid Res *50*, 3-21.

Zechner, R., Strauss, J., Frank, S., Wagner, E., Hofmann, W., Kratky, D., Hiden, M., and Levak-Frank, S. (2000). The role of lipoprotein lipase in adipose tissue development and metabolism. Int J Obes Relat Metab Disord *24 Suppl 4*, S53-56.

Zeisel, S.H. (2006). People with fatty liver are more likely to have the PEMT rs7946 SNP, yet populations with the mutant allele do not have fatty liver. The FASEB Journal *20*, 2181-2182.

Zhang, C., Wang, G., Zheng, Z., Maddipati, K.R., Zhang, X., Dyson, G., Williams, P., Duncan, S.A., Kaufman, R.J., and Zhang, K. (2012). Endoplasmic reticulum-tethered transcription factor cAMP responsive element-binding protein, hepatocyte specific, regulates hepatic lipogenesis, fatty acid oxidation, and lipolysis upon metabolic stress in mice. Hepatology *55*, 1070-1082.

Zhang, K., Shen, X., Wu, J., Sakaki, K., Saunders, T., Rutkowski, D.T., Back, S.H., and Kaufman, R.J. (2006). Endoplasmic reticulum stress activates cleavage of CREBH to induce a systemic inflammatory response. Cell *124*, 587-599.

Zhang, Y., Proenca, R., Maffei, M., Barone, M., Leopold, L., and Friedman, J.M. (1994). Positional cloning of the mouse obese gene and its human homologue. Nature *372*, 425-432.

Zhao, Y., Su, B., Jacobs, R.L., Kennedy, B., Francis, G.A., Waddington, E., Brosnan, J.T., Vance, J.E., and Vance, D.E. (2009). Lack of phosphatidylethanolamine N-methyltransferase alters plasma VLDL phospholipids and attenuates atherosclerosis in mice. Arterioscler Thromb Vasc Biol *29*, 1349-1355.

Zhou, Y., Lee, J., Reno, C.M., Sun, C., Park, S.W., Chung, J., Fisher, S.J., White, M.F., Biddinger, S.B., and Ozcan, U. (2011). Regulation of glucose homeostasis through a XBP-1-FoxO1 interaction. Nat Med *17*, 356-365.

Zhu, X., Mar, M.H., Song, J., and Zeisel, S.H. (2004). Deletion of the Pemt gene increases progenitor cell mitosis, DNA and protein methylation and decreases calretinin expression in embryonic day 17 mouse hippocampus. Brain Res Dev Brain Res *149*, 121-129.

Zhu, X., Song, J., Mar, M.H., Edwards, L.J., and Zeisel, S.H. (2003). Phosphatidylethanolamine N-methyltransferase (PEMT) knockout mice have hepatic steatosis and abnormal hepatic choline metabolite concentrations despite ingesting a recommended dietary intake of choline. Biochem J *370*, 987-993.

Ziegler, D., Zentai, C., Perz, S., Rathmann, W., Haastert, B., Meisinger, C., and Lowel, H. (2006). Selective contribution of diabetes and other cardiovascular risk factors to cardiac autonomic dysfunction in the general population. Exp Clin Endocrinol Diabetes *114*, 153-159.

Zimmermann, R., Strauss, J.G., Haemmerle, G., Schoiswohl, G., Birner-Gruenberger, R., Riederer, M., Lass, A., Neuberger, G., Eisenhaber, F., Hermetter, A.*, et al.* (2004). Fat mobilization in adipose tissue is promoted by adipose triglyceride lipase. Science *306*, 1383-1386.

Zingaretti, M.C., Crosta, F., Vitali, A., Guerrieri, M., Frontini, A., Cannon, B., Nedergaard, J., and Cinti, S. (2009). The presence of UCP1 demonstrates that

metabolically active adipose tissue in the neck of adult humans truly represents brown adipose tissue. FASEB J *23*, 3113-3120.